

LIBRARY

KARST PROCESSES ON CAYMAN BRAC, A SMALL OCEANIC CARBONATE  
ISLAND

**KARST PROCESSES ON CAYMAN BRAC, A SMALL  
OCEANIC CARBONATE ISLAND.**

By

ROZEMARIJN FREDERIKE ANTOINETTE TARHULE-LIPS, LICENCIÉE  
EN SCIENCES GEOGRAPHIQUES, M.Sc.

A Thesis

Submitted to the School of Graduate Studies

in Partial Fulfilment of the Requirements

for the Degree

Doctor of Philosophy

McMaster University

© Copyright by Rozemarijn F.A. Tarhule-Lips, September 1999

DOCTOR OF PHILOSOPHY (1999)

McMaster University

(Geography)

Hamilton, Ontario

TITLE: Karst processes on Cayman Brac, a small oceanic carbonate island.

AUTHOR: Rozemarijn Frederike Antoinette Tarhule-Lips, Licenciée en Sciences Géographiques (Université de Liège, Belgium), M.Sc. (McMaster University)

SUPERVISORS: Dr. D.C. Ford and Dr. H.P. Schwarcz

NUMBER OF PAGES: xvii, 249.

# ABSTRACT

Cayman Brac is a good example of a small oceanic carbonate island which has undergone several periods of submergence and emergence since the Tertiary, resulting in the geological formations being well karstified. This study investigated several karst phenomena on the island including the occurrence and morphology of caves, the water chemistry and microclimate inside the caves, periods of speleothem growth and dissolution, and bell holes.

Caves occur throughout the island at various elevations above sea level. Using elevation as a criterion, the caves were divided into Notch caves, located at, or one - two metres above, the Sangamon Notch, and Upper caves, located at varying elevations above the Notch. Analysis of the morphology, age and the relative abundance of speleothem in the caves further supports this division.

The close proximity of the Notch and the Notch caves is coincidental: speleothem dating by U-series methods shows that the caves predate the Notch. They are believed to have formed between 1400 and 400 ka, whereas a late Tertiary to Early Quaternary age is assigned to the Upper caves.

Speleothem on the island has suffered minor, moderate and major dissolution. Minor dissolution is due to a change in the degree of saturation of the drip water feeding the speleothem, whereas the last two are caused by flooding or condensation corrosion.

Many of the speleothems in fact experienced several episodes of dissolution followed

by regrowth. The latest episode appears to be caused by condensation corrosion rather than flooding. Eleven speleothems containing growth hiatuses were dated by U-series methods. The results indicate that growth cessation did not occur synchronously. Furthermore, the timing of the hiatuses during the Quaternary is not restricted to glacial or interglacial periods.

Oxygen and carbon stable isotope analyses of seven of the samples reveal an apparent shift towards a drier and warmer climate around 120 ka. However, more data and further collaborative evidence is desirable. Of six samples with hiatuses, five show a bi-modal distribution of stable isotope values: before and after the hiatus.

Oxygen isotope analyses of modern drip water found inter-sample variations of over 2 ‰. This is due to cave environmental factors such as evaporation, infiltration velocity and roof thickness. Inside the caves  $\delta^{18}\text{O}$  of drip water decreases with increasing distance from the entrance and thus decreasing external climatic influence. This distance-climatic effect is also reflected in the  $\delta^{18}\text{O}$  calculated for modern calcite: -5.3, -6.5 and -7.6 ‰ VPDB at 3, 10 and 20 m respectively.

The morphology of bell holes, found only in certain Notch caves, was studied in detail. It is proposed that the bell holes are formed by condensation corrosion, probably enhanced by microbiological activity.

The study represents a comprehensive and thorough analyses of karst features on a small oceanic island, and provides information useful for climatic reconstruction during the Quaternary.

# ACKNOWLEDGEMENTS

My deepest gratitude goes to my supervisor Dr. Derek Ford, for his excellent guidance and academic and financial support through the years. I am also grateful to the members of my supervisory committee, Drs. Schwarcz and Rouse, for their contributions to this study. Special thanks to Drs. B.E. Jones and Ian Hunter, University of Alberta, for introducing me to Cayman Brac in the first place.

This study would not have been possible without the logistic support, assistance and cooperation of many people on the Cayman Islands. Deserving special mention are: Karen Lazzari of the Cayman Water Authority; Dr. McLaughlin from the Ministry of Environment of the Cayman Islands; Mr. Banks of the Mosquito Control Unit; Wallace Platt, Chair of the Cayman Brac District Committee of the National Trust and Pedro Lazzari.

I am very grateful to Karen Goodger, Catharina Jager and Nicki Robinson for their friendship and patient guidance in the clean- and mass spectrometry laboratories. U-series dating by  $\alpha$ -spectrometry was done by Nicki Robinson.

All the organisers of the U.S. Geological Survey expeditions to Isla de Mona, especially Dr. Joe Troester, are thanked very much for the opportunity to study this isolated island and for the well organised trips. I am very grateful to Drs. Carol Wicks, Joyce Lundberg, John Mylroie and James Carew for the many fruitful discussions we have had and their friendship over the years.

I thank Mike Bagosy, Craig Malis and Dr. Steve Worthington for their assistance in the field and Dale Boudreau for helping with meteorological instruments and the interpretation of results. All are also thanked for the many discussions and helpful suggestions.

My stay at McMaster was a very pleasant one thanks to the wonderful people of the Geography Department (especially Sue Vajozcki, Joan Parker, Medy Espiritu, Jude Levett, Darlene Watson, Bob Bignell and Patricia Beddows) and Nigerian friends Dr. Daniel Dabi, Dr. Tony Nyong, Rifkatu Yakubu, Dr. Benson and Ada Agi, and Charles Fiki. Ric Hamilton is thanked for the many computer generated figures, Phil van Beynen for the drilling of the stable isotope samples and Martin Knyff for the stable isotope analyses.

The gypsum used in one of the experiments was donated by the Canadian Gypsum Co, Hagersville, Ontario, Canada. This work was supported by a Research Grant to Dr. Ford from the Natural Sciences and Engineering Research Council of Canada. Field work on Isla de Mona was partly supported by the U.S. Geological Survey, Reston, Virginia and San Juan, Puerto Rico Offices, and the Puerto Rico Department of Natural Resources.

Last but not least, I am eternally grateful for the love and support of my husband, Aondover Tarhule, my parents, my sister Marjoleine, and Martin and Mayra. Finally, the love and ever present smile of my son Sesugh kept me going through many difficult moments.

# TABLE OF CONTENT

Abstract .....	iii
Acknowledgements .....	v
Table of Content .....	vii
List of Figures .....	xi
List of Tables .....	xvii
Preface .....	xviii
<b>Chapter One</b>	
Introduction .....	1
1.1. <i>Aspects of the study</i> .....	3
1.2. <i>Organisation of the dissertation.</i> .....	3
<b>Chapter 2   Karstification of Cayman Brac</b> .....	5
Abstract .....	6
2.1 <i>Introduction</i> .....	7
2.1.1. <i>The hydrology of small oceanic islands.</i> .....	8
2.1.2. <i>The Flank Margin model of cave development</i> .....	10
2.2 <i>Study area</i> .....	12
2.2.1. <i>Climate</i> .....	14
2.3 <i>Methods</i> .....	15
2.3.1. <i>Cave plan area and volume calculations</i> .....	15
2.3.2. <i>Cave meteorology</i> .....	16
2.3.3. <i>Water chemistry</i> .....	17
2.3.4. <i>Gypsum tablets</i> .....	18
2.4 <i>Karstification in the Tertiary</i> .....	19
2.4.1. <i>Caymanite.</i> .....	19
2.5. <i>Karstification in the Quaternary</i> .....	22
2.5.1. <i>Karstic features of the surface</i> .....	22
2.5.1.1. <i>Phytokarst</i> .....	22

2.5.1.2.	<i>Soil cover/terra rossa on the plateau</i>	23
2.5.1.3.	<i>Sinkpoints on the plateau</i>	24
2.5.2.	<i>Subsurface karst features</i>	25
2.5.2.1.	<i>Caves and ponds on the coastal platform</i>	25
2.5.2.1.1.	<i>Salinity measurements</i>	26
2.5.2.2.	<i>Caves on the plateau: Bluff Group (Tertiary)</i>	27
2.5.2.2.1.	<i>Notch caves.</i>	28
2.5.2.2.2.	<i>Upper caves.</i>	29
2.5.2.2.3.	<i>Cave geometry and direction.</i>	30
2.5.2.2.4.	<i>Cave sediments</i>	31
2.5.2.2.5.	<i>Speleothem distribution</i>	32
2.5.2.2.6.	<i>Cave micro-climate and condensation corrosion</i>	34
2.5.2.2.7.	<i>Bell holes</i>	36
2.6.	<i>Discussion</i>	37
	<i>Acknowledgements</i>	42
	<i>References</i>	44
	<i>List of Figures</i>	49

<b>Chapter 3</b>	<b>Timing and implications of calcite speleothem growth and hiatuses on Cayman Brac.</b>	65
3.1.	<i>Introduction</i>	65
3.2.	<i>U/Th Thermal ionization mass spectrometry dating of speleothems</i>	68
3.2.1	<i>Problems related to TIMS dating</i>	69
3.3.	<i>Sample Descriptions</i>	71
3.3.1	<i>Cayman Brac</i>	72
3.3.1.1.	<i>Notch</i>	72
3.3.1.2	<i>Notch caves</i>	72
3.3.1.2.1.	<i>Skull Cave</i>	72
3.3.1.2.2.	<i>Bats Cave</i>	73
3.3.1.2.3.	<i>Road Cut Cave</i>	74
3.3.1.2.4.	<i>Great Cave</i>	74
3.3.1.3.	<i>Upper caves</i>	75
3.3.1.3.1.	<i>First Cay Cave</i>	75
3.3.1.3.2.	<i>Tibbetts Turn Cave</i>	77
3.3.1.3.3.	<i>Peter's Cave</i>	78
3.3.1.3.4.	<i>Northeast Cave #5.</i>	79
3.3.2.	<i>Isla de Mona</i>	79
3.3.2.1.	<i>Cueva del Agua at Sardinera</i>	79
3.4.	<i>Hiatuses in the Brac and Mona speleothems.</i>	80
3.4.1.	<i>Dating of hiatuses</i>	82

3.5.	<i>Growth rates</i>	84
3.6.	<i>Discussion of hiatal results</i>	86
3.7.	<i>Stable isotope analyses</i>	91
3.7.1.	<i>Sample description and methods.</i>	95
3.8.	<i>Discussion of stable isotope results</i>	100
3.8.1.	<i>Oxygen isotopic composition</i>	104
3.8.2.	<i>Carbon isotopic composition</i>	106
3.8.3.	<i>Oxygen and carbon records of individual samples</i>	107
3.9.	<i>Conclusion</i>	112
	References	116
	List of Figures	123
	List of Tables	125

#### **Chapter 4    Condensation Corrosion in Caves on Cayman Brac and Isla de**

	<b>Mona.</b>	146
	Abstract	147
4.1.	<i>Introduction</i>	148
4.2.	<i>Study Areas</i>	152
4.3.	<i>Methods of Study</i>	155
4.3.1.	<i>Temperature and relative humidity</i>	155
4.3.2.	<i>Water chemistry</i>	157
4.3.3.	<i>Gypsum tablets</i>	158
4.4.	<i>Results and Discussion</i>	160
4.4.1.	<i>Air Temperature and Relative Humidity</i>	160
4.4.1.1.	<i>Longitudinal profiles.</i>	160
4.4.1.2.	<i>Vertical profiles</i>	160
4.4.2.	<i>Water chemistry</i>	163
4.4.3.	<i>Gypsum tablets</i>	165
4.5.	<i>Conclusions</i>	168
	Acknowledgements	169
	References	171
	List of Figures	174
	List of Tables	176

#### **Chapter 5    Morphometric studies of Bell Hole Development On Cayman Brac.191**

	Abstract	192
5.1.	<i>Introduction</i>	193
5.2.	<i>Hypotheses of Bell Hole Formation</i>	195
5.2.1.	<i>Action of roosting bats</i>	195
5.2.2.	<i>Simple aqueous dissolution</i>	196

5.2.3. <i>Other biogenic or biogenic plus flood origin</i> .....	197
5.3. <i>Cayman Brac</i> .....	198
5.4. <i>Methods of Measurement</i> .....	201
5.5. <i>Results and Analysis</i> .....	202
5.5.1. <i>Location</i> .....	202
5.5.2. <i>Morphometry of individuals</i> .....	203
5.5.3. <i>Compound bell holes</i> .....	206
5.5.4. <i>Bell pits</i> .....	206
5.6. <i>Discussion</i> .....	207
5.6.1. <i>Rates of bell hole formation</i> .....	214
5.7. <i>Conclusions</i> .....	215
Acknowledgements .....	216
References .....	217
List of Figures .....	221
<b>Chapter 6</b> <b>Conclusions</b> .....	<b>242</b>
6.1. <i>Major findings</i> .....	242
6.2. <i>Future Research</i> .....	248

## LIST OF FIGURES

2.1	Geology and location of Cayman Brac and the caves studied. ....	50
2.2	Schematic representation of cave geometric parameters. ....	51
2.3	Location of gypsum tablets in First Cay Cave, a vertical joint type Upper cave.	52
2.4	An example of caymanite from Great Cave. ....	53
2.5	Phytokarst on the coastal platform, NE side of Cayman Brac. ....	54
2.6	Velocity and discharge of incoming and outgoing tide in the Garbage Dump Pond on the south side. ....	55
2.7	Map and profile of B2-Cave, an example of a pit cave on the plateau. ....	56
2.8	Notch caves: <b>a)</b> Skull Cave and <b>b)</b> Great cave. ....	57
2.9	Upper cave: Tibbetts Turn Cave, flank margin type, non fracture-guided. ....	58
2.10	Cave volume and plan area versus distance perpendicular into the cliff for <b>a)</b> Bats Cave, <b>b)</b> Tibbetts Turn Cave and <b>c)</b> First Cay Cave. ....	59
2.11	Cumulative volume of selected Notch caves ( <b>a</b> ) and Upper caves ( <b>b</b> ). ....	60
2.12	Schematic representation of <b>a)</b> major, <b>b)</b> moderate and <b>c)</b> minor speleothem dissolution encountered on Cayman Brac. ....	61
2.13	Saturation Index for dolomite ( $SI_d$ ) versus the Saturation Index for calcite ( $SI_c$ ) for condensation water, May, 1994 and September, 1995. ....	62

2.14	Proposed model of condensation corrosion in coastal caves on small holokarstic oceanic islands with young rocks (Tarhule-Lips & Ford 1998).	63
2.15	Uranium series spectrometric dates (alpha and TIMS) and elevation above mean sea level of speleothem samples on Cayman Brac.	64
3.1	Location of Cayman Brac, Isla de Mona and the caves studied.	125
3.2	a) Sample location in Skull Cave and b) cross section of SC41.	126
3.3	a) Sample location in Bats Cave, sketch (b) and cross section (c) of BC5.	127
3.4	Cross section of RdC2 from Road Cut Cave.	128
3.5	a) Sample location in Great Cave and b) cross section of GC8.	129
3.6	a) Sample location in First Cay Cave; b) schematic profile of the dissolution phases; cross sections of FC1 (c), FC2 (d) and FC3 (e).	130
3.7	a) Sample location in Tibbetts Turn Cave; cross sections of TC12 (b), TC41 (c) and TC42 (d).	131
3.8	a) Sample location in Peters Cave; cross sections of PC2 (b) and PC4 (c).	132
3.9	a) Sample location in Northeast Cave #5 and b) cross section of 5NE1.	133
3.10	a) Sample location in Cueva del Agua, Sardinera, Isla de Mona, and b) cross section of CAS2.	134
3.11	Speleothem growth periods and hiatuses on Cayman Brac.	135
3.12	Proposed model of condensation corrosion in coastal cave on small holokarstic oceanic islands with young rocks (Tarhule-Lips and Ford 1998).	136

3.13	Individual plots of $\delta^{18}\text{O}$ versus $\delta^{13}\text{C}$ of all analysed samples from Cayman Brac and Isla de Mona. Note the distinctly different groupings before and after a hiatus for most of the samples. . . . .	137
3.14	Plot of $\delta^{18}\text{O}$ versus $\delta^{13}\text{C}$ of all analysed samples. Note the separation of the Cayman samples into two groups and the location of the Mona sample. . .	138
3.15	The average $\delta^{18}\text{O}$ versus average $\delta^{13}\text{C}$ of the various samples of Cayman Brac are plotted against each other. The same data is represented in three different ways: <b>a)</b> relative age: $>120$ ka (“old”) versus $< 120$ ka (“young”); <b>b)</b> cave types: Notch versus Upper caves; and <b>c)</b> location within the caves: entrance, mid-cave and deep. . . . .	139
3.16	Oxygen isotope records of the Cayman samples for growth rates of 0.5 and 1.0 mm/ka. . . . .	140
3.17	Carbon isotope records of the Cayman samples for growth rates of 0.5 and 1.0 mm/ka. . . . .	141
3.18	Percentage bedrock carbon and $\text{C}_3$ plants over time for $\text{gr} = 1.0$ mm/ka ( <b>a</b> ) and $\text{gr} = 0.5$ mm/ka ( <b>b</b> ). . . . .	142
4.1	Location of Cayman Brac, Isla de Mona and the caves studied. . . . .	177
4.2	Zonation of speleothem corrosion, meteorological instrument set up, location of gypsum tablets with their surface retreat rates, First Cay Cave, Cayman Brac. . . . .	178

4.3	Temperature <b>(a)</b> and relative humidity <b>(b)</b> profiles in First Cay Cave, Cayman Brac, measured in May 1994. ....	179
4.4	Temperature and relative humidity profiles for September 13, 16, 22, 26 and 28, 1995 in Skull Cave, Cayman Brac. ....	180
4.5	<b>a)</b> Temperature differences between ceiling and floor for all stations, Cueva del Agua Sardinera, Isla de Mona (June, 1994); <b>b)</b> Temperature difference between the ceiling and the floor along selected profiles in the cave; <b>c)</b> Relative humidity difference between ceiling and floor for all stations, Cueva del Agua Sardinera; <b>d)</b> Relative humidity difference between the ceiling and the floor along selected profiles in the cave. ....	181
4.6	Temperature differences between ceiling and floor for all stations in Peter's Cave, Cayman Brac (May, 1994). ....	182
4.7	Relationship between Specific Conductivity and Hardness for drip waters. . .	183
4.8	Saturation Index for dolomite (SI <sub>d</sub> ) versus the Saturation Index for calcite (SI <sub>c</sub> ) for rain, drip and condensation water on Cayman Brac, 1994 and 1995. ....	184
4.9	The change in the Saturation Index for calcite (SI <sub>c</sub> ) of condensation water with distance from the cliff line in three caves on Cayman Brac. ....	185
4.10	Surface retreat of gypsum tablets in First Cay Cave <b>(a)</b> , Peter's Cave <b>(b)</b> , Tibbetts Turn Cave <b>(c)</b> on Cayman Brac and Cueva del Agua <b>(d)</b> on Isla de Mona. ....	186
4.11	Schematic representation of the interaction between the outside and	

	cave environments. ....	187
4.12	Proposed model of condensation corrosion in coastal caves on small holokarstic oceanic islands with young rocks. ....	188
5.1	Natural cross section through a bell hole as a result of ceiling collapse in Rebecca’s Cave. ....	224
5.2	Schematic representation of bell holes. ....	225
5.3	a) Location of Cayman Brac. b) Geology of Cayman Brac and location of caves; c) Profile of Cayman Brac with elevation of the caves. ....	226
5.4	a) Bell hole depth and diameter were measured with graduated wooden dowels. b) Bell hole volume was calculated as a series of stacked cylinders. ....	227
5.5	Location of bell holes (and bell pits) in a) Skull Cave, b) Walk-In Cave, c) Rebecca’s Cave, d) Cross Island Road Cave and e) Charlotte’s Cave. ....	228
5.6	Basal diameter of bell holes in five caves on Cayman Brac versus their straight line distance from the cliff. ....	229
5.7	Cross sectional profiles of all sample bell holes. ....	230
5.8	Frequency distribution of a) depth, b) basal diameter, c) apex diameter and d) volume of bell holes in five caves on Cayman Brac.. ....	231
5.9	Apex diameter versus basal diameter of bell holes.. ....	232
5.10	a) Basal diameter and b) apex diameter versus depth of sample bell holes. ...	233
5.11	Taper angle versus depth of sample bell holes. ....	234
5.12	Volume versus basal diameter of sample bell holes in Charlotte’s Cave ....	235

5.13	Bell pits and associated bell holes in Charlotte's Cave. . . . .	236
5.14	a) Relationship between bell hole diameter and bell pit length/width measurements. b) Relationship between bell hole and bell pit depth. . . . .	237
5.15	Proposed model of condensation corrosion in coastal caves on small holokarstic oceanic islands with young rocks (Tarhule-Lips and Ford 1998). . . . .	238
5.16	Frequency distribution of estimated time (not necessarily continuous) required for the development of bell holes. . . . .	239

## LIST OF TABLES

3.1	Uranium-Thorium activity ratios and ages of 14 speleothem samples from Cayman Brac and one from Isla de Mona. . . . .	143
3.2	Mean speleothem growth rate calculated from four samples from Cayman Brac (this study) and one from Lucayan Cavern, Grand Bahama Island (Lundberg and Ford 1994). . . . .	144
3.3	Oxygen and deuterium stable isotope values for modern rain and drip water on Cayman Brac and calculated oxygen isotopic composition for modern calcite. . . . .	145
4.1	Chemical analyses of different water types on Cayman Brac. . . . .	189
4.2	The gypsum tablet experiment: location, measured surface recession and estimated daily condensation. . . . .	190
5.1	Bell hole sizes reported in the literature. . . . .	240
5.2	Maximum time required for bell hole development. . . . .	241

# PREFACE

This dissertation consists of three papers, which have been published or submitted for publication, and one more conventional analytical chapter that will be modified for one or more publications later. The latter deals with the dating and stable isotope analysis of speleothem.

The central theme of the dissertation is the importance and timing of subaerial dissolution in caves on a small oceanic carbonate island in the Caribbean. The dissertation is presented as follows:

Chapter 1: Introduction

Chapter 2: Tarhule-Lips, R.F.A. and Ford, D.C., 1999 submitted. Karstification of Cayman Brac. *Zeitschrift fur Geomorphologie*.

Chapter 3: Timing and implications of calcite speleothem growth and hiatuses on Cayman Brac.

Chapter 4: Tarhule-Lips, R.F.A. and Ford, D.C., 1998. Condensation corrosion in caves on Cayman Brac and Isla de Mona. *Journal of Cave and Karst Studies*, 60(2): 84-95.

Chapter 5: Tarhule-Lips, R.F.A. and Ford, D.C., 1998. Morphometric studies of bell hole development on Cayman Brac. *Cave and Karst Science*, 25(3): 119-130.

Chapter 6: Conclusions and future research.

Although all the papers have been co-authored by Dr. D.C. Ford, the primary research supervisor, the actual research and writing was done by the first author and candidate. Dr. Ford provided guidance on the research and writing, and critiqued all the papers.

# CHAPTER ONE

## Introduction

Although caves and karst phenomena have attracted the interest of the scientific community since the last century (see Renault 1967, Watson and White 1985, Jennings 1985, White 1988 and Ford and Williams 1989 for reviews), the many small oceanic carbonate islands have largely been ignored. Not until the mid 1970's did scientists finally look at these small closed systems with a more attentive eye (e.g Ollier 1975, Mylroie and Carew 1990, Mylroie *et al.* 1991, Bourrouilh-Le Jan 1992, Wicks 1998). It soon became obvious that models of cave genesis developed in large continental settings could not adequately explain the formation of the caves found in these relatively young, holokarstic systems. A new model was needed. Utilizing information on caves in the Bahamas, Mylroie and Carew (1990) proposed the Flank Margin Model for Cave Development on small oceanic islands. In this area, during periods of sea level high stand only sand dune ridges remained above water. The model postulates that cave development took place under the flanks of the dunes at the margin of the fresh water lens, hence the name "flank margin" caves. This model is described in greater detail in Chapter Two. Though qualitative, it remains the most comprehensive

model to date that deals with cave development on small oceanic carbonate islands. However, more work and verification of the model is required on other islands with similar geologic history and climatic setting. The present study was motivated by the need to test the applicability of the flank margin model to the caves on Cayman Brac.

The second motivation for the study is the widespread occurrence of speleothem dissolution in caves of different elevations and ages in the Caribbean Region; e.g. Netherlands Antilles (Wagenaar Hummelinck 1979), Bahamas (Myroie *et al.* 1991; Myroie Pers. Comm. 1993), Isla de Mona (Frank *et al.* 1998), Grand Cayman Island (Smith 1987) and Cayman Brac (Lips 1993). Cross sections of speleothem samples from Cayman Brac and Isla de Mona revealed that periods of growth cessation and dissolution also occurred in the past, although the exact times of occurrence is not known. This study will attempt to date the periods of growth cessation and dissolution and determine if these periods were coincident in time over the Caribbean Region. At the same time the dates are used to pinpoint the paleoenvironmental and paleoclimatic information that can be obtained from stable isotope analysis of carbon and oxygen. Such information is very important for the reconstruction of the Quaternary geology of the area and could greatly advance the knowledge of glaciations and interglaciations in non-glaciated areas. An oxygen isotope record from speleothems might also be more informative than the existing oxygen isotope record from Foraminifera because of the more precise dating methods available and the fact that the individual data points can measure change in the order of years instead of averaging thousands of years as is the case for marine sediments due to their bioturbation.

1.1. *Aspects of the study*

The main aspects of this study are:

1. The documentation of surface and subsurface karst features on a small oceanic carbonate island and measurements of certain karst processes and rates as a contribution to the further understanding of karstification on such islands.
2. Establishing when, where and why hiatuses in speleothem growth occurred, and the cause of any dissolution at the hiatal surfaces.
3. The collection of paleoclimatic and paleoenvironmental information about the timing and duration of speleothem growth, as a contribution to the Quaternary geology of Cayman Brac in particular and the Caribbean region in general.

1.2. *Organisation of the dissertation.*

Chapter 2 introduces the study area. It provides an overview of the karstification history of the island, timing of important karstifying processes and comprehensively documents all the different karst features on the island.

Chapter 3 investigates the timing and possible causes of periods of growth cessation/dissolution in various speleothems in caves on the island. An attempt is made to reconstruct the paleoclimatic and paleoenvironmental conditions during the periods of speleothem growth.

Chapter 4 analyses the present day microclimatic processes in the caves. It is proposed that the major cause of present day speleothem dissolution is condensation

corrosion.

Chapter 5 examines the phenomenon of bell holes and provides a new hypothesis for their formation: a combination of condensation corrosion and biogenic dissolution.

Finally, the major conclusions and contributions as well as directions for future research are given in Chapter 6. Since the chapters are actually separate journal papers, there is some unavoidable repetition of general background information in certain chapters.

# CHAPTER TWO

## Karstification of Cayman Brac

**Rozemarijn F.A. Tarhule-Lips and Derek C. Ford**

School of Geography and Geology, McMaster University,

Hamilton, Ontario, L8S 4K1, Canada

Submitted: *Zeitschrift für Geomorphologie*.

**Abstract.** Cayman Brac is a typical example of a small oceanic carbonate island which has undergone cyclic periods of submergence and emergence during the Tertiary and Quaternary. During submergence the rocks were dissolved forming cavities of varying sizes, and during emergence these cavities were completely or partially filled in with caymanite, clastic debris and/or calcite. All geological formations on the island are well karstified, both on the surface as well as in the subsurface.

Caves, i.e. cavities that are large enough for human entry, are found all over the island and at all elevations above sea level. Based on the latter, the caves were initially divided into two groups: Notch caves, which are located at or one - two metres above the Sangamon Notch (125 ka), and Upper caves, which have entrances at varying elevations more than two metres above the notch. This study shows that this initial division can also be maintained when looking at morphology, age and speleothem abundance.

The close proximity of the notch and the Notch caves is merely a coincidence. There is no causal relationship between the two. Speleothem dating of two samples taken from two separate Notch caves clearly shows that the Notch caves are much older than the notch. We propose that they are between 1400 and 400 ka old. A late Tertiary to Early Quaternary age is allocated to the Upper caves.

Speleothem dissolution has been found to occur in all caves. It can be divided into three groups: (a) major, (b) moderate and (c) minor dissolution. The latter is due to a change in the degree of saturation of the drip water feeding the speleothem, whereas the first two are caused by either phreatic dissolution or condensation corrosion.

## 2.1 *Introduction*

Until the mid-1970's, little was known about the caves and karst found on small oceanic, carbonate islands. Recently, however, a number of studies (e.g OLLIER 1975, MYLROIE & CAREW 1990, MYLROIE ET AL. 1991, BOURROUILH-LE JAN 1992, WICKS 1998) have shown that there are important differences between karst development on small islands and that of the continents or large islands. The differences arise from the fact that on the small islands there are no allogenic streams and little or no surface runoff occurs on the carbonates due to their high permeability. The water available for bedrock dissolution is provided by direct infiltration from rains and any soil storage, plus saline water underlying the fresh groundwater lens.

Despite the youthful age of the rocks on many of the islands (Tertiary and Quaternary) and the small catchment areas, karstification can be extensive and caves can attain large sizes. For example, several submerged caves in the Bahamas have been explored for many kilometres by divers. On Long Island, Bahamas, Salt Pond Cave contains one chamber with an approximate volume of 14000 m<sup>3</sup>. Based on local geology, it must have developed within a period of 30 ka, which gives an average dissolution rate of about 0.5 m<sup>3</sup> per year (MYLROIE ET AL. 1991). This suggests that the dissolution mechanisms operating in such islands are very effective.

The objectives of the present study were to document surface and subsurface karst features and to measure certain karst processes and rates on Cayman Brac, Cayman Islands, as a contribution to the further understanding of small oceanic carbonate islands.

2.1.1. *The hydrology of small oceanic islands.*

As noted, runoff is insignificant on most small, young carbonate islands and there are no allogenic streams. All rainwater (less evapotranspiration losses) infiltrates into the ground locally and forms a freshwater lens that rests on denser salt water that has invaded from the surrounding seas. The lens drains by broadly radial discharge directly to the sea, or into lakes or low lying swampy areas. The shape and thickness of the lens is determined by several factors including precipitation, porosity and permeability of the bedrock, shape and topography of the island, and sea level fluctuations due to tides, atmospheric pressure, wind action or salinity (VACHER 1978, TARBOX 1986, NG ET AL. 1992). An extensive review of the literature on freshwater lenses is provided by REILLY & GOODMAN (1985).

Mathematically, the shape and thickness of the lens can be approximated by the Badon Ghyben-Herzberg relationship expressed as

$$z = \frac{\rho_f}{\rho_s - \rho_f} h \quad (2.1)$$

where  $z$  is the depth of the halocline (fresh/salt water interface) below mean sea level,  $h$  is the freshwater head above mean sea level,  $\rho_f$  is freshwater density ( $1.000 \text{ kg/m}^3$ ) and  $\rho_s$  is salt water density ( $1.025 \text{ kg/m}^3$ ). The Badon Ghyben-Herzberg principle assumes that the halocline is a sharp boundary between the fresh and saline water under static conditions. Hence, it is depressed 40 m for each metre of freshwater head above mean sea level (i.e. a depth ratio of 1:40). In reality, the halocline in many small carbonate islands is a diffuse and

dynamic zone of transition rather than a sharp, static boundary. Moreover, the halocline does not always intersect the water table precisely at the shoreline as previously believed. Despite these limitations, the ratio of 1:40 gives a good first approximation of the depth to the halocline (BUGG & LLOYD 1976).

During the Quaternary the shape and area of many small islands has varied considerably as a consequence of the glacial cyclic rise and fall of global sea level. BUDD & VACHER (1991) showed that the thickness of a paleo-freshwater lens was a function of the contemporary width of the island, the amount of recharge, and the hydraulic conductivity. On average, the thickness of the lens is about 1% of the width of the island, but this varies with the age and stratigraphy of the rock. Knowledge of the position and thickness of the fresh water lens is important for reconstructing the history of cave development because it indicates where certain modes of development could occur.

The mixing of waters with differing chemical compositions or concentrations is often of great importance in the dissolution of carbonate rocks. BÖGLI (1964 *in* BÖGLI 1980) recognized that when two saturated fresh waters that have equilibrated to different partial CO<sub>2</sub> pressures mix, the resulting water can be undersaturated with respect to calcite and so renew the dissolution (*mischungskorrosion* or mixing corrosion). Dissolution is also enhanced where fresh and saline waters mix (PLUMMER 1975). Preferential mixing zones may occur (a) at or close to the water table, where infiltrating rainwater mixes with static or laterally flowing meteoric groundwater and (b) along the halocline. At the point of discharge (usually along the coast) the water table and halocline intersect, permitting the mixing of

three different types of water (recent rain, longer resident meteoric groundwater, saline ground water) further enhancing carbonate dissolution.

#### 2.1.2. *The Flank Margin model of cave development*

The flank margin model of cave genesis on small oceanic islands is founded on the assumption that the mixing point of the three different types of water provides the most favourable locus for cave formation (MYLROIE & CAREW 1990, RAEISI & MYLROIE 1995). The model is based on observations of caves in the Bahamas, especially on San Salvador Island. These islands are in a tectonically stable region that is subsiding at a rate of 2-3 m/100 ka (MCNEILL ET AL. 1988). Areas above sea level today consist chiefly of Pleistocene carbonate dune ridges (eolianite) up to 60 m high surrounded by low-lying beaches and swamps. Caves that are nowadays about 6 m above mean sea level were formed in Isotope Stage 5e when sea level was higher than at present and only the ridges stood above it. The freshwater lenses in such ridges were of very limited extent and thickness. However, it is believed that the caves were able to form in these small lenses as a result of mixing corrosion, especially at points of discharge of the brackish water along the dune margins, aided by bacterial oxidation and reduction of organic material (RAEISI & MYLROIE 1995). The age of the host rocks is about 150 ka; thus, it is estimated that the caves formed during a maximum time span of no more than 20 ka (i.e the aggregate period during the past 150 ka when the sea level was higher than at present).

Due to inhomogeneities in the bedrock, the flow of the fresh/brackish water is

concentrated along preferential paths, creating dissolution pockets separated by more resistant areas. In time, initial pockets coalesce or enlarge to form bigger chambers filled with brackish water, extending headward into the dune as the increased volume of saline water enhances dissolution. Removal of carbonate rock along any preferential flowpaths leading towards the chambers results in the creation of passages radiating toward the interior where they pinch out or end abruptly. The chambers in flank margin caves tend to be smoothly rounded or ovoid, and oriented parallel to the trend of the ridges. Thin wall partitions and isolated rock pillars are common.

At the type site, San Salvador Island, our personal observation is that certain caves were initiated by the mechanical washout of uncemented carbonate sands behind a thin skin of case hardening on the dune, the "syngenetic cave" model of JENNINGS (1968). When sea level falls, the caves are drained and speleothems (i.e. secondary mineral precipitates) may be deposited. If the sea level rises abruptly, the caves can become flooded and the process of cave development may continue (MYLROIE & CAREW 1990).

OLLIER (1975) also recognized the potential of marine mixing corrosion in his study of the caves of the Trobriand Islands, although he did not use the term explicitly. He noted that "there is no reason why brackish water should not attack limestone to form caves as long as there is some mechanism for occasionally changing the local physico-chemical conditions. The changes in salinity after rain would probably be sufficient to do this" (p. 185). He divided the Trobriand caves into three genetic groups: vadose, water table and phreatic caves, and of the latter suggested that "Cave formation is most likely to occur where

the flow lines converge, and this situation - behind the shoreline and below the level of the cliffs - is precisely where the largest phreatic caves are found" (p. 189). OLLIER did not propose a cave morphogenetic mechanism other than the existing ones based on continental settings but did discuss why these theories did not entirely apply to young coral islands.

At present, the flank margin model is the most comprehensive that has been advanced to explain the formation of caves in small oceanic islands. It is qualitative, giving an explanation for the location and morphology of the caves together with a plausible dissolution mechanism, but makes no quantitative estimates of the rate of dissolution.

## 2.2 *Study area*

Cayman Brac (19° 43'N 79° 47'W) is the most eastern of the three Cayman Islands in the Caribbean Sea (Fig. 2.1). The island is small, 19 km in length and varying from 1.5 to 3.0 km in width. The total area is 44 km<sup>2</sup>. All three islands are situated on separate isolated volcanic blocks that form part of the Cayman Ridge, the northern margin of the Cayman Trench. It has a core of Tertiary strata known as the Bluff Group, fringed by a Pleistocene limestone - the Ironshore Formation (JONES ET AL. 1994a). The bedrock is very pure carbonate with less than 3% insoluble residue; this is due to the distance of the islands from sources of terrigenous or other siliciclastic sediments (LIPS 1993).

As a result of differential tectonic movements, the Bluff Group now forms an inclined plateau with a tilt of 0.5° to the southwest. It descends from a maximum elevation

of 45 m asl at the east end of the island to sea level in the west, where it is overlain by the Ironshore Formation. The boundary of the Bluff strata is a vertical cliff around most of the island, with the Ironshore limestone being deposited on a coastal platform at the cliff foot. The principal shoreline erosional feature is a very strong bio-erosion notch in the cliff at about 6 m above modern sea level. The notch marks the position of the last sea level high stand (isotope stage 5e or Sangamonian, approximately 125 ka) and shows no evidence of tilting. This indicates that the island has been tectonically stable since at least that period (WOODROFFE ET AL. 1983).

The Bluff Group is composed of the Brac, Cayman and Pedro Castle Formations (JONES ET AL. 1994 a & b; Fig. 2.1). The Brac Formation is exposed only in the lower parts of cliffs at the eastern end of the island. On the north side it consists of wackestone to grainstone limestones. Dolostones with pods of skeletal wackestones can be found at various levels on the south side. Foraminifera and  $^{87}\text{Sr}/^{86}\text{Sr}$  ratios from the limestones suggest a late Early Oligocene age (about 28 Ma; JONES ET AL. 1994b).

Most of the island is composed of fabric-retentive dolostones of the Cayman Formation. These are dominated by mudstones and wackestones but beds and lenses of rhodolites, rudstone, packstone and grainstone are also found. Bedding planes are present but difficult to trace for long distances, and marker beds are absent. Leaching of fossils has occurred and fossil-mould vugs are common. Due to the absence of age-determining fossils and disruption of initial  $^{87}\text{Sr}/^{86}\text{Sr}$  ratios by the dolomitization it is not possible to assign a definite age to the formation; a Lower to Middle Miocene age is suspected (JONES ET AL.

1994b).

The Pedro Castle Formation is found over a small area at the western end of the island, where it is overlain by the Ironshore Formation. It consists of dolostones and partially dolomitized limestones. The limestones contain *Stylophora*, a branching coral that became extinct in the Caribbean region towards the end of the Pliocene, and  $^{87}\text{Sr}/^{86}\text{Sr}$  ratios suggest an age of approximately 2 Ma (JONES ET AL. 1994b).

#### 2.2.1. *Climate*

The island has a tropical maritime climate. The mean annual temperature is 26<sup>o</sup> C, with very small seasonal variations; relative humidity is high year round and climatic variations are reflected primarily in the rainfall activity. The Mosquito Control and Research Unit of Cayman Brac maintains eight rain gauges on the island. The longest records have only 23 years of data (1976-1998). The precipitation is concentrated mainly in sporadic storms during the summer months but is bimodal, with a short break in July. Average annual precipitation is 1025 mm but varies from 980 mm in the southwest to 1140 mm in the east, reflecting the NE-SW direction of the rain-bearing trade winds. Actual evapotranspiration from lysimeters attains 90-95% on Cayman Brac (NG & BESWICK 1994); however, we suspect that a high proportion of the rain falling on the karst plateau (below) during storms passes rapidly underground, diminishing evaporative losses there.

### 2.3 *Methods*

The inclined plateau on Cayman Brac is a pitted phytokarst. Three traverses were made across its surface, recording all karst phenomena in sample areas of 1.5 m by 1.5 m at 100 m intervals. Information was collected on soil cover, terra rossa, vegetation, nature and number of sinkpoints. For the purpose of this study, a sinkpoint is defined as any dissolutional depression where water can infiltrate relatively quickly into the bedrock. This very general definition was adopted for the purpose of estimating the density of infiltration points on the surface rather than for a detailed study of the morphology. Cracks in the rock that were of mechanical origin were not included.

The caves were mapped by standard procedures using tape, inclinometer and compass (BCRA grade 5). The distribution and type of all sediments, speleothems, and erosional features such as bell holes were noted on the maps. A special morphometric study of a large sample of the bell holes was undertaken and is described in detail in TARHULE-LIPS & FORD (1998a).

#### 2.3.1. *Cave plan area and volume calculations*

The plan area is the area of the cave calculated from the cave plan as the product of the length and the breadth. To represent the evolution of the plan area from the coast inland, a standard length interval of one metre was chosen (Fig. 2.2). The plan area can thus be calculated as

$$C_i = \sum_{j=1}^n A_{P_j} \quad (2.2)$$

where  $C_i$  is the area of the interval  $i$  metres from the cliff face of cave  $C$ . The quantity on the right hand side of equation (2.2) is the sum of the areas of the  $n$  passages of  $C$  which are in the interval  $i$  m from the cliff face. The total area is then

$$A_C = \sum_{i=1}^L C_i \quad (2.3)$$

where  $A_C$  is the total area of cave  $C$  and  $L$  is the furthest interval distance of  $C$  from the cliff face. The volume of each interval  $i$  is obtained as the sum of the product of the area and the average height of the  $n$  passages that are in this interval. Total volume is then obtained in a similar manner as the total area.

The relationship between area and volume is linearized by taking the natural logs, and it may then be described by a simple regression equation

$$\ln V_C = a + b \ln A_C \quad (2.4)$$

where  $V_C$  is the volume of cave  $C$ ,  $A_C$  is the area of  $C$  and  $a$  and  $b$  are the equation parameters. The first and last metre intervals were often incomplete due to the shape of the caves and their angle with the cliff face.

### 2.3.2. Cave meteorology

Temperature and relative humidity profiles were measured in five sample caves on Cayman Brac (Fig. 2.1, caves FC, PC, TC, GC and SC), traversing from the entrances inward

twice daily (~10:00 hr and ~17:00 hr). Wet and dry bulb temperatures were taken by a T-type thermocouple with a resolution of 0.1 ° F. The measurements were taken at three heights: 5 cm above the floor, midway between floor and ceiling and about 5 cm below the ceiling (in very high rooms, readings were made at 3.5 m above the floors). The Fahrenheit scale was used to increase the precision of calculation of relative humidity and later converted to degrees Celsius. Temperature and relative humidity maps were constructed for FC, PC, SC and GC by using one-time temperature readings at the three heights at sufficient number of points to cover all areas of the caves satisfactorily.

### 2.3.3. *Water chemistry*

Aqueous conductivity was measured with a YSI Model 33 S-C-T (salinity-conductivity-temperature) meter. Measurements were converted to specific conductivity at 25°C using the function

$$\text{SpC}(25^\circ) = 1.81 \text{ SpC}(T) e^{-0.023T} \quad (2.5)$$

where SpC (T) is the measured conductivity at T°C and T is temperature (°C). The equation is derived empirically from karst water data in Pennsylvania and is valid between 0°C to 40°C (WHITE 1988: 133).

pH was determined with an ATC pH meter with a precision of 0.01 pH. The meter was standardised against buffers pH=4.00 and pH=7.00 before each series of measurements. Temperature was taken with a dual-sensor digital thermometer having a resolution of 0.1°C. Alkalinity, calcium and total hardness were measured using a Hach Digital Titrator. The

saturation indices for calcite and dolomite, the partial pressure of CO<sub>2</sub> with which the water would be in equilibrium and ion balance errors were calculated using the program WCHEM3.

On Cayman Brac, the caves are most often quite dry; there are few drip sites and no flowing streams. Only during and immediately after heavy rains were the drip rates fast enough to allow satisfactory water collection; on these occasions samples were collected from as many sites as possible.

Aqueous condensation was induced by chilling the cave air. For condensers, 2 litre plastic bottles filled with water and then frozen solid were used. The condensation water was collected in 250 ml sample bottles, via funnels with small apertures to reduce evaporation. In each sample run three bottles were suspended in the selected cave for a minimum of six hours, by which time all the ice had melted; one was placed close to the entrance, one halfway and one close to the back of the cave. A total of 12 condensation experimental runs were completed in six different caves (B2, CC, GC, PC, SC and TC), including up to three repeat runs at the same positions in a given cave on separate days.

#### 2.3.4. *Gypsum tablets*

Gypsum tablets of known weight were suspended on nylon fishing line away from direct drip sites and walls in four caves on Cayman Brac (B2, FC, PC and TC) for a period of 16 months (May, 1994 to October, 1995). The tablets were dried at 60<sup>o</sup> C in an oven before weighing prior to and after exposure. In each cave they were so located as to form a

profile perpendicular to the cliff, from the entrance inward (Fig. 2.3). One tablet was retained unexposed as reference sample. The gypsum was > 90% pure  $\text{CaSO}_4 \cdot 2\text{H}_2\text{O}$  donated by the Canadian Gypsum Co, Hagersville, Ontario, Canada.

#### 2.4 *Karstification in the Tertiary*

The Tertiary strata were deposited in a series of deposition-erosion cycles. The formations are separated from each other by strong disconformities which “represent weathering surfaces that developed during periods of subaerial exposure” (JONES 1994: 35). During these periods karst developed at the surface and underground. Breccia, calcite and “caymanite” were subsequently deposited in the cavities (JONES 1992, 1994, JONES ET AL. 1994 a&b).

##### 2.4.1. *Caymanite.*

"Caymanite is a multicoloured microcrystalline dolostone with laminae that dip at angles up to 60°" (JONES 1992: 720). The colour can be strong and the layering very distinctive (Fig. 2.4). Caymanite is found only in cavities in the Tertiary strata and was deposited before the dolomitization of the bedrock 2-5 Ma ago. Dolomitization has not destroyed the original sedimentary fabric, structures or pigmentation. The strong colours (red, black and white) are due to pigmenting agents from the source areas of the material forming the caymanite. Red is from iron and black from manganese, both originating in terra rossa, swamps, ponds and/or cave deposits such as guano. The white is from the marine

calcareous muds. These materials were washed into the Tertiary cavities by storms and hurricanes in the early stages of marine transgressions. The sedimentary structures and the angles of deposition of the caymanite are so highly variable because they depend on the points of sediment introduction into the cavities and on the viscosity of the sediment-laden water. Angles steeper than the angle of repose occurred in cavities that were air-filled rather than water-filled at the moment of deposition so that the sediment-laden water could not flow easily. Angles of dip thus cannot be used as indicators of postdepositional tilting (JONES 1992).

On Cayman Brac, caymanite appears to occur mainly in the Brac Formation on the eastern end of the island and more locally in the Cayman Formation. It was observed in the cliffs and in four larger caves (SC, PC, FC and GC), one small cave high up in the cliff on the North East Point of the island and a series of small caves along the beach at Pollard Bay at the southeast end of the island. In the two caves in the Cayman Fm (SC and PC) the caymanite was only present in a few pockets in walls and ceilings. However, in the caves in the Brac Fm (GC, FC and PBC) caymanite can be found in much larger quantities. In First Cay Cave, it was found to a distance of about 30 m into the cave. It forms thin plates and a spongework structure at one location where it appears to have been more resistant to dissolution than the bedrock. In Great Cave and the Pollard Bay Caves, caymanite is found abundantly in the walls and ceiling to a distance of about 15 m from the cliff. Fossil moulds in the bedrock have been filled with caymanite and calcite (Fig. 2.4). At present the caves lie about 20-25 m below the surface but only a few metres below the unconformity

separating the Cayman and the Brac Fms. The small cave high up in the cliff on the North East Point of the island is also situated just underneath the Brac-Cayman unconformity. The caymanite was observed together with calcite in a layer about 0.5 m thick right underneath the flat ceiling formed by the Cayman Fm.

Most of the caymanite in the cliffs have been removed by local people to make jewelry and other souvenirs for tourists. Thus, it is very difficult to properly assess the spatial distribution of the cavities filled with caymanite based on the chance occurrence in the cliffs and the localised position of the caves. One thing is clear however, caymanite occurs far inside the rock, especially when the amount of cliff retreat that must have occurred during the past 2-5 Ma is taken into account. The caymanite in the Brac Fm was deposited before the formation of the Cayman Fm (JONES 1992) and thus the depth under the unconformity needs to be considered rather than the depth under the present day land surface. Unfortunately, it is impossible to tell exactly how deep the caymanite can be found underneath the unconformity because the caves only go to a depth of about 10 m.

It appears that the cavities that were later filled with caymanite were the result of (a) fossil leaching (GC and PBC), (b) dissolution along the halocline, (c) dissolution in a shallow fresh water lens below phytokarst, or (d) phytokarst itself lowered dissolutionally into the halocline cavernous zones. Once this secondary porosity was formed, surface water would have been able to descend readily and fill the cavities during periods of high recharge, as in the situation at present. During marine transgression, storm waters were able to sweep across the low lying, relatively flat island. The infiltrating water carried sediment from the

surface into the subsurface, where it was trapped and deposited in the small cavities (JONES 1992).

## 2.5. *Karstification in the Quaternary*

### 2.5.1. *Karstic features of the surface*

#### 2.5.1.1. *Phytokarst*

The surfaces of the coastal platform and the plateau are both phytokarst, a karst of small but sharp pinnacles separated by dissolutional pits (Fig. 2.5). It is at least partly of organic origin (FOLK ET AL. 1973). In the intertidal zone, *Cyanophyceae* or blue-green algae bore into the rock in search of nutrients and protection from strong sunlight. They thus act as important erosional agents as well as a source of food for grazing marine animals. The depth of boring is believed to be a function of light intensity and may reach 800-900  $\mu\text{m}$  into the rock (TRUDGILL 1985). The bedrock is white except in the spray zone where it is covered with a black/green sheath of algae. According to FOLK ET AL. (1973) the algal acid attacks the limestone, dissolving calcite preferentially over dolomite and even selectively removing calcite from among dolomitised coral septa. Similar karst surfaces have been observed by the second author far from the sea and from dense colonization by marine algae on limestones in Greece, New Mexico, etc, where there is lichen cover but inorganic dissolution in rainwater probably plays the major role in producing the small-scale pitting. Essentially the same forms can also be observed on gypsum and salt surfaces, where there is no algal or lichen contribution.

Soil cover on the island is patchy and thin but the vegetation is thick and continuous because many of the trees root directly on the bedrock. Some roots follow pre-existing joints but many actively bore into the rock on their way to the water table. The pathways created by the roots are of great importance for the drainage of rainwater and the penetration of microorganisms into the subsurface. The effect is greatest near the surface but may reach depths of 10 - 15 m (JONES 1994).

The phytokarst on the Tertiary dolostones of the plateau closely resembles that found on the Pleistocene Ironshore Formation along the coast and, in this instance, is thought to be formed by the same predominant combination of processes: the boring activity of blue-green filamentous algae coupled with rainwater dissolution.

Phytokarst observed on Cayman Brac is light in colour, in contrast to the celebrated “black phytokarst of Hell” described by FOLK ET AL. (1973), which is in a swampy lagoon on Grand Cayman Island. The black pigment there may be a survival mechanism of the algae because it screens out sunlight and thus prevents destruction of the chlorophyll (FRITZ 1907, cited in FOLK ET AL. 1973). On Cayman Brac, it is possible that the dense vegetation cover on the plateau provides adequate protection against the sunlight so that the black pigment is not necessary. BULL & LAVERTY (1982) also observed light coloured phytokarst under dense foliage in cave entrances in Sarawak, Borneo.

#### 2.5.1.2. *Soil cover/terra rossa on the plateau*

Soil cover on the island is shallow and discontinuous and becomes increasingly

more patchy from the east towards the west. The differences reflect the distribution of water on the island. The north, being the windward side experiences higher evapotranspiration. Along the cliff edges, the predominance of stress-release joints and high hydraulic gradient drain water from the surface. The moisture scarcity appears to affect plants that depend for moisture and nutrients on the epikarst. Trees on the other hand have extensive, deep root systems and appear not to be influenced. Consequently, the vegetation is relatively dense despite the shallow soil.

Terra rossa is found in two distinct conditions: as an unconsolidated sediment and as a well indurated, hard rock. The lithified terra rossa is more widespread and probably represents one or more paleosols. Unconsolidated red soil is distributed randomly on the island and is probably the residue of the dissolution of the calcareous cement in the lithified form, plus residues of more recent bedrock dissolution.

#### 2.5.1.3. *Sinkpoints on the plateau*

The size of individual sinkpoints varied from a few centimetres to 1.5 m in diameter and their observed depth from a few centimetres to a few metres. At certain places two or more smaller sinkpoints appeared to have amalgamated into one bigger example, which was counted as one point when sampling for density. Number of sinkpoints counted was related to the amount of bare rock exposed at the sampling stations. In general, sinks were only observed where the soil cover was less than 40%. There was a range of 2-13 per m<sup>2</sup> where more than 95% of the rock was exposed. It is probable that a large number of sinkpoints are

hidden beneath the soil. The arithmetic mean was three sinkpoints per  $\text{m}^2$  on bare rock or  $3 \cdot 10^6$  per  $\text{km}^2$ . As the area of the plateau surface is about  $26 \text{ km}^2$ , it is estimated that it contains approximately  $8 \cdot 10^7$  sinkpoints. Such high number and density precludes surface runoff and reduces evapotranspiration because the sinkpoints are efficient infiltration pathways during intense storms.

### 2.5.2. *Subsurface karst features*

#### 2.5.2.1. *Caves and ponds on the coastal platform*

The authors found no accessible caves in the Ironshore Formation, which composes the coastal platform. However, it rises no more than 4-5 metres above modern sea level. Underground passages certainly exist in it because there are many blowholes and at least one of the lakes on the platform is directly connected to the sea. In some places, underground cavities have collapsed, creating large ponds with overhanging or steep walls. Locally known as “Turtle ponds”, the island residents used them to raise turtles for meat. In the lower, western end of the island GILLAND (1998) describes sinkholes connected to caves. One of these holes, Conch Hole, connects to a 6 m by 15 m room and some underwater passages and is located underneath a road to a quarry. This is the part of the island where the Ironshore Formation overlies the Pedro Castle Formation. The roof of the cave is only 1.5 m thick but nevertheless strong enough to carry the weight of the traffic using the road. Offshore, some underwater caves are said to exist but no information is available on their size, depth below sea level, or geological formation in which they are found. The apparent lack of caves on the

coastal platform reflects marine submergence and/or the dense vegetation that covers much of it.

#### 2.5.2.1.1. *Salinity measurements*

The salinity of 52 ponds (two on the north side and 50 on the south side) located on the Ironshore Formation was taken and the tidal range in a few was measured. The purpose of this study was to form an impression of the salinity of these lakes and thus the salinity of the discharging groundwater. It also provides information on possible mixing corrosion effects and the nature and extent of connection between the ponds and the ocean.

There are four big lakes on the southwest end of the island. They have salinities that are far greater than that of the sea water, ranging from 46‰ to as much as 104‰. By contrast, the measured salinity of sea water ranged from 29‰ to 34.5‰. The hypersalinity is interpreted as the result of limited recharge combined with intense evaporation, indicating that these particular lakes are recharged largely or entirely by rainfall and are not effectively linked to the fresh water aquifer.

The salinity of the smaller ponds ranges from 2‰ to 36‰, and that of one drilled well was 2‰. Taking the well water to represent the salinity of the local fresh water lens, then the salinity of the ponds range from pure fresh water to pure sea water. Percentage sea water was calculated assuming a sea water salinity of 34‰ and a groundwater salinity of 2‰.

Three ponds, the two on the north side and one on the south, have a clear hydraulic

connection to the sea: water levels mimic the rise and fall of the tides. The measured tidal range was 15 cm for the two on the north side and 22.5 cm on the south side. Salinity was between 8.5‰ and 12.5‰ (or 20-30% sea water) in the northern ponds with a reduction of 1-2.5‰ (or an increase of 4-8% fresh water) at low tide. This implies that they are being recharged by less saline water from the interior. The pond on the south side has direct connection to the sea. Figure 2.6 shows the observed velocities and discharge of the turn from outgoing to incoming tide at low tide. These high values indicate that the connection between the pond and the sea is of at least decimetric size. Salinity of the pond at high tide is equal to that of the sea, but slightly lower at low and mid tide indicating that it too is being replenished by some fresh water from the interior.

All this is in agreement with the general observation that fresh water lenses discharge into ponds and low lying areas on the coastal platform, as well as into the sea. The continuous mixing of fresh and saline water in the coastal area promotes dissolution of the bedrock by mixing corrosion.

#### *2.5.2.2. Caves on the plateau: Bluff Group (Tertiary)*

Cave openings can be seen along the entire length of the cliff that rises above the coastal platform around most of the island. A few are at the 6 m Notch itself, but most are scattered at different elevations above it. No extensive cave systems have been entered from the plateau surface behind the cliff. There is much concealment by dense vegetation but numerous big pits have been observed by the authors, some of which give access to small

side chambers containing actively growing speleothems (Fig. 2.7). GILLAND (1998) counted 15 pits within a  $2 \cdot 10^3 \text{ m}^2$  area and determined that they have an average diameter of 6 m and depth of 10 m. At about 7-10 m below the surface there is some dissolutional extension into members of a prominent joint set bearing N60E. Some of the caves continue underwater, where they contain common vadose speleothems such as stalactites, which indicates that they were formerly above the water table and have been back-flooded by the postglacial (and probably earlier) rise of sea level. It is not clear in what formations these caves are located, but they are most likely in the Cayman and/or Pedro Castle strata.

In the cliff face more caves have been found on the south side of the island than on the north due to easier accessibility. At some places the openings are concentrated at particular elevations but it could not be determined if these elevations recurred at the different sites along the faces. On the east end of the island, the unconformity that separates the Brac and Cayman Fms is very prominent and is the principal locus of cave development there.

The caves in the cliffs may be divided into two groups based on their elevation above the Sangamon Notch: (a) "Notch caves" have their entrances at or one-two metres above the Notch, and (b) "Upper caves" with entrances at apparently random elevations more than two metres above the Notch (Fig. 2.1).

#### 2.5.2.2.1. *Notch caves.*

The Notch caves all display a basically similar form. This comprises one or two

large rooms at or close to the entrance, with smaller passages, rooms and recesses radiating off into the interior of the rock mass, where they terminate in blank walls (Fig. 2.8). The form is smoothly rounded with scallop-shaped rather than angular walls and ceilings, and no breakdown except where dissolutional lowering of the plateau surface above has partly intercepted the cave roof. The floor is horizontal but in some cases steps lead to slightly higher parts in the caves. The ceiling in the entrance rooms is up to 4 m high. In them, there are well developed bell holes (e.g. WILFORD 1966, TARHULE-LIPS & FORD 1998a), which are strictly vertical cylinders eroded upwards into the ceiling to heights (depths) as great as 5.5 m. The caves contain little clastic sediment. There are small amounts of calcite speleothem precipitates, tending to be largest and most frequent in the entrance chambers and diminishing further inside; those near the entrances very often display dissolutional faceting.

#### 2.5.2.2.2. *Upper caves.*

The Upper caves are more varied than the Notch caves, displaying several different patterns: (1) vertical joint type (e.g. First Cay Cave, Fig. 2.3; Northeast Cave 5); (2) low angle fissure type (e.g. Peter's Cave) and (3) flank margin type, not fracture-guided (e.g. Tibbetts Turn Cave, Fig. 2.9). The latter resemble the Notch caves morphologically but contain much greater volumes of speleothems, have sloping floors and do not necessarily have the large entrance room. The first two types follow pre-existing joints or fissures sub-parallel or perpendicular to the cliff face.

None of the Upper caves show any signs of vadose dissolution, suggesting they

were formed under phreatic conditions. Water infiltrating down the joints could have mixed with the groundwater at the water table resulting in mixing corrosion. Phreatic groundwater flow was controlled by the fracturing, resulting in preferential dissolution along it. Interplay of these processes plus mixing corrosion at the halocline if it was deeper probably dominated the formation of these caves.

#### 2.5.2.2.3. *Cave geometry and direction.*

A basic premise of the flank margin model (MYLROIE & CAREW 1990) is that the caves form from the coast inland in all directions. If this assertion is true then a decrease in cave volume inland but with lack of preferred orientation would be expected. To test this hypothesis, the plan area, volume and orientation of all the investigated caves were determined.

When the volume and plan area are plotted against distance from the entrance (Fig. 2.10), the caves can be divided into three groups: (a) greatest volume close to the entrance, (b) greatest volume farthest from the entrance and (c) alternating zones of greater and lesser volume parallel to the cliff. All the Notch caves but none of the Upper caves place in the first group. The same distinction between Notch and Upper caves is evident when plotting the cumulative volume (Fig. 2.11). The Notch caves exhibit a greater variation in volume within a short distance of their entrances than the Upper caves.

The taper observed in the Notch caves is due to the occurrence of a large chamber close to the cliff and smaller passages extending inland, as the model predicts. Inland

decrease in volume varies from cave to cave, depending on the number and size of side passages. The Upper caves show a much more gradual increase in volume over the entire length. The sinuosity observed for Peter's Cave and First Cay Cave indicate that the passages are following pre-existing structure parallel to the cliff.

All three parameters confirm that the Notch caves accord with the flank margin model of cave development, whereas most of the Upper caves formed along pre-existing joints. Initial division into Notch and Upper caves was based on height above the notch alone but this study shows that the same division can be based on morphology and speleogenesis. The fact that a few Upper caves resemble the Notch caves indicates that these might have formed under similar, flank marginal conditions. If there ever was a greater population of flank margin caves above the notch, they have been erased by cliff recession.

#### 2.5.2.2.4. *Cave sediments*

The amount of clastic sediment in these caves is very small and often negligible. They are mainly derived from particles liberated as a result of dissolution of the lime mud between grains of the bedrock. The rock over the whole island consists basically of allochthonous dolostones and limestones with less than 10 % of the components being greater than 2 mm in diameter, which is reflected in the dominant grain sizes of the sediments. The coarsest particles appear to be fragments of bedrock and pieces of shells. That most of the sediment consist of bedrock particles is confirmed by the high percentage that is soluble and the grain size of insoluble residues (LIPS 1993).

Organic matter is not very abundant except in caves inhabited by bats and other animals. Iron is present in the majority of the sediments in varying amount. The iron rich material probably derives from the terra rossa at the surface, transported into the cave by seepage water.

Cave entrances in the cliff along the eastern point of the island are open to the direct influence of the sea winds. Sea spray is therefore blown into the caves. This is reflected in the presence of sulphate, chlorine and fluorine amongst the insoluble residues in their sediments (LIPS 1993). During heavy storms and hurricanes seawater might actually be swept into caves low in the cliff. The insoluble sedimentary residues in the other caves consist mainly of clay minerals (alumino-silicates) that were impurities in the carbonate rocks.

#### 2.5.2.2.5. *Speleothem distribution*

Some standard speleothems (stalactites, stalagmites, flowstone and excentrics precipitated in air-filled passages and chambers) are present in all of the caves. As noted, the Upper caves have more which is believed to reflect the fact that they are older than the Notch caves and there has been more time for speleothem deposition.

In all caves examined on Cayman Brac the majority of the speleothems displayed some partial dissolution. Partially dissolved speleothems are also observed on Grand Cayman Island (SMITH 1987), Isla de Mona, Puerto Rico (FRANK ET AL. 1998) and several islands of the Bahamas (MYLROIE ET AL. 1991). Several different mechanisms can

produce this dissolution (or “re-solution”) of precipitates which are usually the youngest features in the cave. A change in the degree of saturation of the feed water depositing the speleothem, from supersaturated to undersaturated with respect to calcite due to some environmental change in the soil, can result in dissolution. Rise in sea level could have flooded the caves, causing dissolution of both bedrock and speleothems. Finally, changes in the physio-chemical atmospheric environment of the cave due to e.g. climatic change, may result in formation of chemically aggressive condensation water with ensuing “condensation corrosion” of both bedrock and speleothem.

Dissolved speleothems on Cayman Brac can be divided into three distinct categories based on the amount of damage they have suffered (Fig. 2.12):

1. Major - the speleothem has been extensively to largely eroded, such that its original depositional shape cannot be recognised. The deposits are preserved as remnants (mainly flowstone) within the curvilinear erosional facets in the walls or ceilings. They are often associated with breccia. In the facet, the transition between bedrock wall, speleothem and/or breccia is so smooth that it is not perceptible to the touch. The speleothem and/or breccia was seemingly attacked at the same time and rate as the bedrock in which it is located. There is no active growth of new calcite.
2. Moderate - the dissolved speleothems still preserve their original shape but, on closer examination, have been reduced considerably in size. Dissolution has often taken place preferentially on one side of the speleothem but the dissolved faces are not necessarily congruous in the individual caves. Active growth has stopped.

3. Minor - there is dissolution along selected faces or edges of the speleothems. The majority of them are still growing on all other parts of their surfaces today.

Extensive dissolution of speleothems is observed in all the caves and an island-wide change (or sequence of changes) in the physio-chemical environment of the caves is suspected. This change in cave environmental parameters probably reflects environmental changes outside the caves as well.

In the Notch caves, major corrosion is limited to flowstones often associated with breccias in small pockets exposed flush with the walls in the modern caves. The breccia and the speleothem must have coexisted. The pockets are completely filled with breccia and/or flowstone and are of small dimensions (less than 0.5 m in diameter). We suppose that these cavities were formed before the caves, but after the caymanite and dolomitization. Cavities filled with flowstone and other material are common in the Tertiary formations on all three Cayman Islands (JONES ET AL. 1994a&b; JONES 1992) which supports the hypothesis that they developed (probably as water table or halocline mixing zone features) before the Upper caves during one or more paleokarst periods.

#### 2.5.2.2.6. *Cave micro-climate and condensation corrosion*

Temperature deep inside the large caves and behind constrictions in passages is 25.5°-26.5°C and relative humidity is maintained at 95-100%. The climate in the small caves and the entrance zones of the larger caves is influenced by fluctuations in the outside weather conditions. In general, temperature near the ceiling is higher than that near the floor,

whereas the relative humidity follows the opposite pattern. During the day, when the temperature outside is higher, cool air drains out along the floor, drawing in warm air at the ceiling. This circulation tends to be weakened or reversed during the night when the cave air is warmer than that outside. But the daytime circulation is often maintained by inertia into the night, cold air enters along the ceiling and convective air circulation is possible (TARHULE-LIPS & FORD 1998b).

Our chemical analyses of condensation water showed that the water can be undersaturated with respect to calcite and/or dolomite (Fig. 2.13). Cooling of the wall rock is needed to sustain the condensation process which, therefore, is most effective in the entrance zones of caves where the air and rock temperature can fluctuate daily. This is the basis for a model of condensation corrosion in small oceanic caves proposed by TARHULE-LIPS & FORD (1998b) and illustrated in Figure 2.14.

From the corrosion of gypsum tablets suspended in the condensation corrosion zones of selected caves the mean condensation corrosion rate for calcite was estimated to be ~24 mm/ka (TARHULE-LIPS & FORD 1998b). BUHMANN & DREYBRODT (1985) developed a model to calculate theoretical dissolution rates. Using the Ca concentrations measured in the induced condensation water, the model predicts a condensation corrosion rate of ~19 mm/ka. The results suggest that the field method gives a good first estimate of the corrosion rate.

The moderate and minor categories of speleothem dissolution in the caves of

Cayman Brac are attributed to this mode of corrosion.

#### 2.5.2.2.7. *Bell holes*

The diagnostic characteristics of bell holes are that they are strictly vertical cylinders of nearly perfect circular cross section seen in the ceilings of caves. The verticality is maintained regardless of lithological variation, stratal dip or the regularity or gradient of the ceiling. On Cayman Brac they were observed only in the entrance zones of Notch caves. Based on depth and diameter, the bell holes of one cave were significantly smaller than those in the other four caves examined: depth ranges from 0.08-1.86 m (average 0.84 m) versus 0.46-5.68 m (average 1.90 m) and diameter ranges from 0.20-0.90 m (average 0.43 m) versus 0.55-1.30 m (average 0.89 m). In some caves there are circular skylights which are believed to be bell holes that were intersected by dissolutional lowering of the surface. TARHULE-LIPS & FORD (1998a) suggest that bell holes were formed by condensation corrosion aided by microbial activity. Colonies of microorganisms (biofilms - JONES 1995) establish themselves in patches on ceilings in the entrance zones, where they obtain moisture from condensing water. Dissolution of the bedrock by these microorganisms initiates a depression in the ceiling. When deep enough, this traps the warmest air, inducing extra condensation in a positive feedback mechanism. The verticality of the holes is attributed to the fact that only the most soluble particles are dissolved by the microorganisms and condensation corrosion; the less soluble carbonate particles (the principal component of clastic sediments in these caves, as noted above) are removed by gravity, which is most effective straight down.

## 2.6. *Discussion*

All the Tertiary formations of Cayman Brac were karstified before dolomitization 2-5 Ma ago. Small cavities were dissolved in the bedrock during periods of submergence and at emergence, two main processes occurred; (a) cavities were in-filled with caymanite before dolomitization and more recently by flowstone and clastic debris, and (b) terra rossa soil was formed. A similar process can be observed at present on the island where phytokarst and pits are being formed in the epikarst layer of the plateau and, to a lesser degree, on the coastal plain.

The shape and other morphological characteristics of the Notch caves are well explained by the flank margin model of cave development; the caves open up in the cliff along the outer rim of the island; each cave has a single large chamber (oval or round) close to the entrance and sub-parallel to the cliff face; passages radiate inland from the chamber and pinch out or end abruptly.

An important point is that the Notch caves must predate the formation of the Notch itself, which is firmly assigned to the last interglacial sea level high stand about 125 ka (WOODROFFE ET AL. 1983). This contention is supported by several direct and indirect evidences.

1. With just two known exception, the caves are developed at least one or more metres above the notch rather than back of it. According to the standard flank-margin model, caves form as a result of mixing corrosion along the halocline and/or water

- table at the point of freshwater discharge. If the caves and the notch were formed at the same time then the point of discharge of the freshwater lens and the elevation of the notch should be at the same altitude, i.e. sea level at the time of formation.
2. The shapes of the principal chambers and the flank-margin model suggest that the caves developed within the rock and were subsequently exposed due to surface erosion and/or cliff retreat. If the notch was formed at the same time as the caves, then its present location should be seaward of the chambers. Instead, it is apparent that the notch has intercepted and exposed the caves.
  3. Perhaps the most convincing evidence that the notch and the caves are of different ages comes from measured ages of speleothems inside two of the caves - Bats Cave and a small cave near Salt Water Point, both on the south side of the island.

The age of speleothems provides a minimum age for the caves because speleothems can be deposited only after the cave has been drained and left relict. Alpha spectrometric U series ages from the youngest part of a 1.4 m high stalagmite in Bats Cave indicated that its growth commenced at the end of the penultimate interglaciation (stage 7; about 200 ka) and terminated during the last interglacial (stage 5e; about 125 ka). The entire stalagmite must be much older. Ages of a drapery from the cave near Salt Water Point were obtained by Thermal Ionisation Mass Spectrometry (TIMS) U series dating (LI ET AL. 1989). It grew, on and off, between >350 ka and 220 ka. Thus the minimum age of this cave is 350 ka.

The dates suggests that the formation of the notch and the cessation of growth in the stalagmite in Bats Cave were coincident. Exposure of the cave to outside air circulation

probably led to the cessation. From the foregoing, it is concluded that the Notch caves formed earlier than the notch. The close proximity of the two is a coincidence. It is most probable that all of the Notch caves formed simultaneously, i.e. in association an earlier high sea stand 2-6 m above the Notch; 6 m is cited as an approximate upper limit to allow for the preserved ceiling heights. The major evidence supporting this contention is the nearly uniform elevation of these caves and their similarity in both form and scale, indicating that the processes responsible for them occurred at the same time, at the same rates and magnitudes.

VÉZINA ET AL. (in press) have determined the elevation and timing of high sea stands for the past four interglacials on Grand Cayman Island: stage 11, >400 ka, sea level high at 5.7 m below present sea level; stage 9, ~346 ka, +0.5 m; stage 7, ~229 ka, +1.1 m; and stage 5, ~131 ka, +6.0 m. The Notch caves are unlikely to be younger than 350 ka. If they developed during stage 11, then the island must have been at least 18 m lower than at present: sea level in stage 11 was about -6 m, the notch is +6 m and to submerge the entirety of the caves another 6 m is necessary above the notch. This would imply that First Cay Cave and Tibbetts Turn Cave amongst the Upper caves were at or slightly above present sea level at the time and could have flooded during the ensuing high stands of stages 9 (+0.5 m asl) and 7 (+1.1 m asl). One speleothem sample from First Cay Cave displays stage 7 growth hiatuses accompanied by clay deposition which appear to be the result of flooding of the cave, which could have happened while the cave was at sea level. Block uplift of Cayman Brac (without tilting) to the modern elevation would then have taken place during stage 6.

No such uplift is recorded on Grand Cayman. It is on a separate tectonic block and could thus have stayed in place while Cayman Brac was raised. However, it is more likely that the caves were created much earlier than stage 11. The stalagmite in Bats Cave grew at a rate of 0.55 mm/ka between 200 ka and 125 ka. If the caves were formed during stage 11 then this stalagmite must have been growing at a rate of 7 mm/ka or more before 200 ka. Although as a generality it can be asserted that growth rates of speleothems tend to vary over time, on Cayman Brac the average growth rate of many dated samples is only 1 mm/ka. At such a rate the 1.4 m high stalagmite in Bats Cave will have required 1.4 Ma to attain its present height. The true age of the stalagmite probably lies somewhere between 400 ka and 1.4 Ma. The Notch caves are probably developed during a high sea stand in that time interval as well. The relatively uniform elevation of these caves above the notch and their horizontality indicates that there has been no differential tectonic movement since their formation.

The Upper caves are older because of the older ages (Fig. 2.15) and greater abundance of their speleothems, implying that there has been more time available for speleothem deposition. Their differing elevations above sea level suggest that several different speleogenetic episodes have occurred. It appears likely that they are late Tertiary-early Quaternary features.

After formation of the caves, speleothems were deposited during periods of emergence. Dating of some samples revealed that speleothem growth was not continuous over time, however. There were periods of growth and of cessation and/or dissolution at

various times in the past. However, these periods are not synchronous for all speleothems in all caves and do not appear to be related to the general glacial-interglacial cyclic rhythm of the Quaternary. Rather, they appear to be dependent on perturbations in the individual caves. Dissolution is most likely the result of either re-establishment of dissolution in the phreatic zone due to a relative rise in sea level, or of condensation corrosion during periods of exceptional exposure of the cave to outside climatic fluctuations. Unfortunately, low thorium yields precluded the dating of some of the hiatuses observed.

Three different degrees of speleothem dissolution have been identified on Cayman Brac. Major dissolution with destruction of speleothem shape in Notch caves is limited to flowstones often associated with breccias in small pockets (less than 0.5 m in diameter) exposed flush with the walls; in the Upper caves, on the other hand, it is more extensive and involves other types of speleothems as well. It appears to be the product of flooding during high sea stands after dolomitization in the late Tertiary or early Quaternary. Moderate dissolution in which the original shape is preserved although 50% or more of the volume has gone is associated with distinct asymmetry in the direction of dissolution and is ascribed to condensation corrosion in vigorously circulating air in entrance zones and mid sections of the caves. Phreatic dissolution cannot be completely ruled out as a possible cause for some of the moderate damage to speleothems. Minor dissolution is due to a change in the saturation state of the drip water, plus possible condensation corrosion effects in the cave interior.

The formation of phytokarst on the Pleistocene Ironshore Formation started as soon

as the rocks became exposed. At the same time cavities were formed in the phreatic zone. At present the fresh water lens discharges in the Ironshore Formation and this is where modern day cave development is taking place. Some of the cavities have collapsed to form ponds with steep or overhanging walls, but most of the caves will only become visible when the sea level falls and surface erosion opens them up.

Karstification is an ongoing process, taking place as long as there is aggressive water and soluble rock. In the case of small oceanic carbonate islands this happens whenever the island is emerged and rainwater can infiltrate to form a fresh water lens above the saline ground water. Cayman Brac is a good example, where there is evidence of both continuous karstification on the plateau and episodic cave genesis and infilling beneath it, from the Tertiary to the present day.

#### *Acknowledgements*

The authors are thankful for the logistic support, assistance and cooperation of many people on the Cayman Islands. Deserving special mention are: Karen Lazzari of the Cayman Water Authority; Dr. McLaughlin from the Ministry of Environment of the Cayman Islands; Mr. Banks of the Mosquito Control Unit; Wallace Platt, Chair of the Cayman Brac District Committee of the National Trust and Pedro Lazzari.

Thanks goes to Dr. Henry Schwarcz for his idea to use ice bottles as condensers for collecting condensation water; to Mike Bagosy, Craig Malis and Dr. Steve Worthington for their assistance in the field and to Dale Boudreau for helping with meteorological

instruments and the interpretation of results. All are also thanked for the many fruitful discussions.

Karen Goodger, Catharina Jager and Nicki Robinson are thanked for helping with the U/Th TIMS dating. U-series dating by alpha spectrometry was done by Nicki Robinson.

A special thanks to Drs. B. Jones and I. Hunter, University of Alberta, for introducing us to the island in the first place.

This work was supported by a Research Grant to Ford from the Natural Sciences and Engineering Research Council of Canada.

### References

- BÖGLI, A. (1980): *Karst Hydrology and Physical Speleology*. Berlin Heidelberg (Springer Verlag), 284 p.
- BOURROUILH-LE JAN, F.G. (1992): Evolution des karsts océaniques (karsts, bauxites et phosphates). *Karstologia*: 31-50.
- BUDD, D.A & H.L. VACHER (1991): Predicting the thickness of fresh-water lenses in carbonate paleo-islands. *J. Sed. Petrol.*, **61**: 43-53.
- BUGG, S.F. & J.W. LLOYD (1976): A study of fresh water lens configuration in the Cayman Islands using resistivity methods. *Q. Jl Engng Geol.*, **9**: 291-302.
- BUHMANN, D. & W. DREYBRODT (1985): The kinetics of calcite dissolution and precipitation in geologically relevant situations of karst areas. 1. Open system. *Chem. Geol.*, **48**: 189-211.
- BULL, P.A. & M. LAVERTY (1982): Observations on phytokarst. *Z. Geomorph. N.F.*, **26**: 437-457.
- FOLK, R.L., H.H. ROBERTS & C.H. MOORE (1973): Black phytokarst from Hell, Cayman Islands, British West Indies. *Geol. Soc. Am. Bull.*, **84**: 2351-2360.
- FRANK, E.F., J.E. MYLROIE, J. TROESTER, JR. E.C. ALEXANDER & J.L. CAREW (1998): Karst development and speleogenesis, Isla de Mona, Puerto Rico. *J. Karst and Cave Studies*, **60 (2)**: 73-83.
- GILLAND, T. (1998): The caves of Cayman Brac. *NSS News*, **July**: 202-207.
- JENNINGS, J.N. (1968): Syngenetic karst in Australia. - In: WILLIAMS, P.W. & J.N.

- JENNINGS (Eds.) *Contributions to the Study of Karst*, Geography Publication G5, Australian National University: 41-110.
- JONES, B. (1988): The influence of plants and micro-organisms on diagenesis in caliche: example from the Pleistocene Ironshore Formation on Cayman Brac, BWI. *Bul. Can. Petrol. Geol.*, **36**: 191-201.
- (1992): Caymanite, a cavity-filling deposit in the Oligocene-Miocene Bluff Formation of the Cayman Islands. *Can. J. Earth Sci.*, **29**: 720-736.
- (1994): Geology of the Cayman Islands. - In: BRUNT, M.A. & J.E. DAVIES (Eds.) *The Cayman Islands: natural history and biogeography*. V.71: Monographiae Biologicae: Dordrecht, The Netherlands (Kluwer Academic Publishers): 13-50.
- (1995): Processes associated with microbial biofilms in the twilight zone of caves: examples from the Cayman Islands. *J. Sed. Res.*, **A65(3)**: 552-560.
- JONES, B., I.G. HUNTER & K. KYSER (1994a): Stratigraphy of the Bluff Formation (Miocene-Pliocene) and the newly defined Brac Formation (Oligocene), Cayman Brac, British West Indies. *Carib. J. Sci.*, **30**: 30-51
- (1994b): Revised stratigraphic nomenclature for Tertiary strata of the Cayman Islands, British West Indies. *Carib. J. Sci.*, **30**: 53-68.
- LI, W-X., J. LUNDBERG, A.P. DICKIN, D.C. FORD, H.P. SCHWARCZ, R. MCNUTT & D. WILLIAMS (1989): High-precision mass-spectrometric uranium-series dating of cave deposits and implications for paleoclimatic studies. *Nature*, **339**: 534-536.
- LIPS, R.F.A. (1993): *Speleogenesis on Cayman Brac, Cayman Islands, British West Indies*.

M.Sc. Thesis, McMaster University, Hamilton, Ontario, Canada, unpublished, 223 p.

MCNEILL, D.F., R.N. GINSBURG, S-B.R. CHANG & J.L. KIRSCHVINK (1988): Magnetostratigraphic dating of shallow-water carbonates from San Salvador, Bahamas. *Geol.*, **16**: 8-12.

MYLROIE, J.E. & J.L. CAREW (1990): The flank margin model for dissolution cave development in carbonate platforms. *Earth Surface Processes and Landforms*, **15**: 413-424.

MYLROIE, J.E., J.L. CAREW, N.E. SEALEY & J.R. MYLROIE (1991): Cave development on New Providence Island and Long Island, Bahamas. *Cave Science*, **18**: 139-151.

NG, K-C., B. JONES & R. BESWICK (1992): Hydrology of Grand Cayman, British West Indies: a karstic dolostone aquifer. *J. Hydrol.*, **134**: 273-295.

NG, K-C. & R. BESWICK (1994): Ground water of the Cayman Islands. - In: BRUNT, M.A. & J.E. DAVIES (Eds.) *The Cayman Islands: natural history and biogeography*. V.71: Monographiae Biologicae: Dordrecht, The Netherlands (Kluwer Academic Publishers): 61-74.

OLLIER, C.D. (1975): Coral island geomorphology. *Z. Geomorph. N.F.*, **19**: 164-190.

PLUMMER, L.N. (1975): Mixing of sea water with calcium carbonate groundwater: quantitative studies in the geological sciences. *Geol. Soc. Am., Memoir* **142**: 219-236.

- RAEISI, E. & J.E. MYLROIE (1995): Hydrodynamic behavior of caves formed in the fresh-water lens of carbonate islands. *Carb. and Evap.*, **10 (2)**: 207-214.
- REILLY, T.E. & A.S. GOODMAN (1985): Quantitative analysis of saltwater-freshwater relationships in groundwater systems - A historical perspective. *J. Hydrol.*, **80**: 125-160.
- SMITH, D.S. (1987): *The speleothemic calcite deposits on Grand Cayman Island, British West Indies*. M.Sc. Thesis, University of Alberta, Edmonton, Alberta, 171 p.
- TARBOX, D.L. (1986): Occurrence and development of water resources in the Bahama Islands. - In: CURRAN, H.A. (ed.) *Proceedings of the 3rd Symposium on the Geology of the Bahamas*, **June 1983**: 139-144.
- TARHULE-LIPS, R.F.A. & D.C. FORD (1998a): Morphometric studies of bell hole development on Cayman Brac. *Cave and Karst Science*, **25(3)**:119-130.
- (1998b): Condensation corrosion in caves on Cayman Brac and Isla de Mona. *J. Cave and Karst Studies*, **60 (2)**: 84-95.
- TRUDGILL, S.T. (1985): *Limestone geomorphology*. (Geomorphology texts, 8). New York (Longman Group Limited), 196 p.
- VACHER, H.L. (1978): Hydrology of small oceanic islands-Influence of atmospheric pressure on the water table. *Ground Water*, **16**: 417-423.
- VÉZINA, J., B. JONES & D.C. FORD (in press): Sea-level highstands over the last 500,000 years: evidence from the Ironshore Formation on Grand Cayman, British West Indies.

WHITE, W.B. (1988): *Geomorphology and hydrology of karst terrains*. New York (Oxford University Press, Inc.), 464 p.

WICKS, C.M. (ed) (1998): Isla de Mona Special Issue. *J. Cave and Karst Studies*, **60 (2)**: 68-125.

WILFORD, C.E. (1966): "Bell Holes" in Sarawak Caves. *N.S.S. Bul.*, **28 (4)**: 179-182.

WOODROFFE, C.D., D.R. STODDART, R.S. HARMON & T. SPENCER (1983): Coastal morphology and late Quaternary history, Cayman Islands, West Indies. *Quat. Res.*, **19**: 64-84.

Address of the authors: School of Geography and Geology, McMaster University, Hamilton, Ontario, L8S 4K1, Canada

### List of Figures

- 2.1 Geology and location of Cayman Brac and the caves studied.
- 2.2 Schematic representation of cave geometric parameters.
- 2.3 Location of gypsum tablets in First Cay Cave, a vertical joint type Upper cave.
- 2.4 An example of caymanite from Great Cave.
- 2.5 Phytokarst on the coastal platform, NE side of Cayman Brac.
- 2.6 Velocity and discharge of incoming and outgoing tide in the Garbage Dump Pond on the south side.
- 2.7 Map and profile of B2-Cave, an example of a pit cave on the plateau.
- 2.8 Notch caves: a) Skull Cave and b) Great cave.
- 2.9 Upper cave: Tibbetts Turn Cave, flank margin type, non fracture-guided.
- 2.10 Cave volume and plan area versus distance perpendicular into the cliff for a) Bats Cave, b) Tibbetts Turn Cave and c) First Cay Cave.
- 2.11 Cumulative volume of selected Notch caves (a) and Upper caves (b).
- 2.12 Schematic representation of a) major, b) moderate and c) minor speleothem dissolution encountered on Cayman Brac.
- 2.13 Saturation Index for dolomite ( $SI_d$ ) versus the Saturation Index for calcite ( $SI_c$ ) for condensation water, May, 1994 and September, 1995.
- 2.14 Proposed model of condensation corrosion in coastal caves on small holokarstic oceanic islands with young rocks (TARHULE-LIPS & FORD 1998b).
- 2.15 Uranium series spectrometric dates (alpha and TIMS) and elevation above mean sea level of speleothem samples on Cayman Brac.

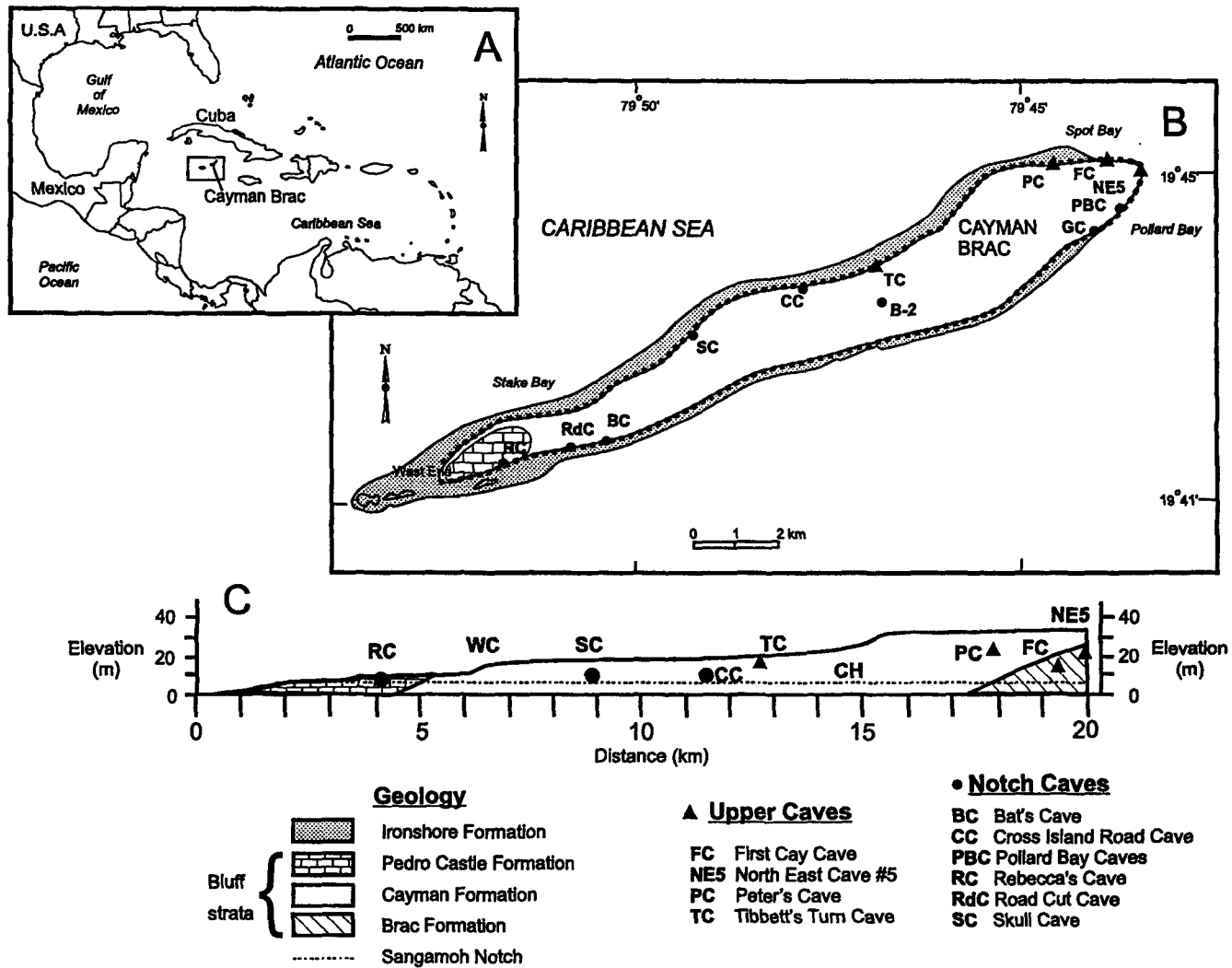


Fig. 2.1 Geology and location of Cayman Brac and the caves studied.

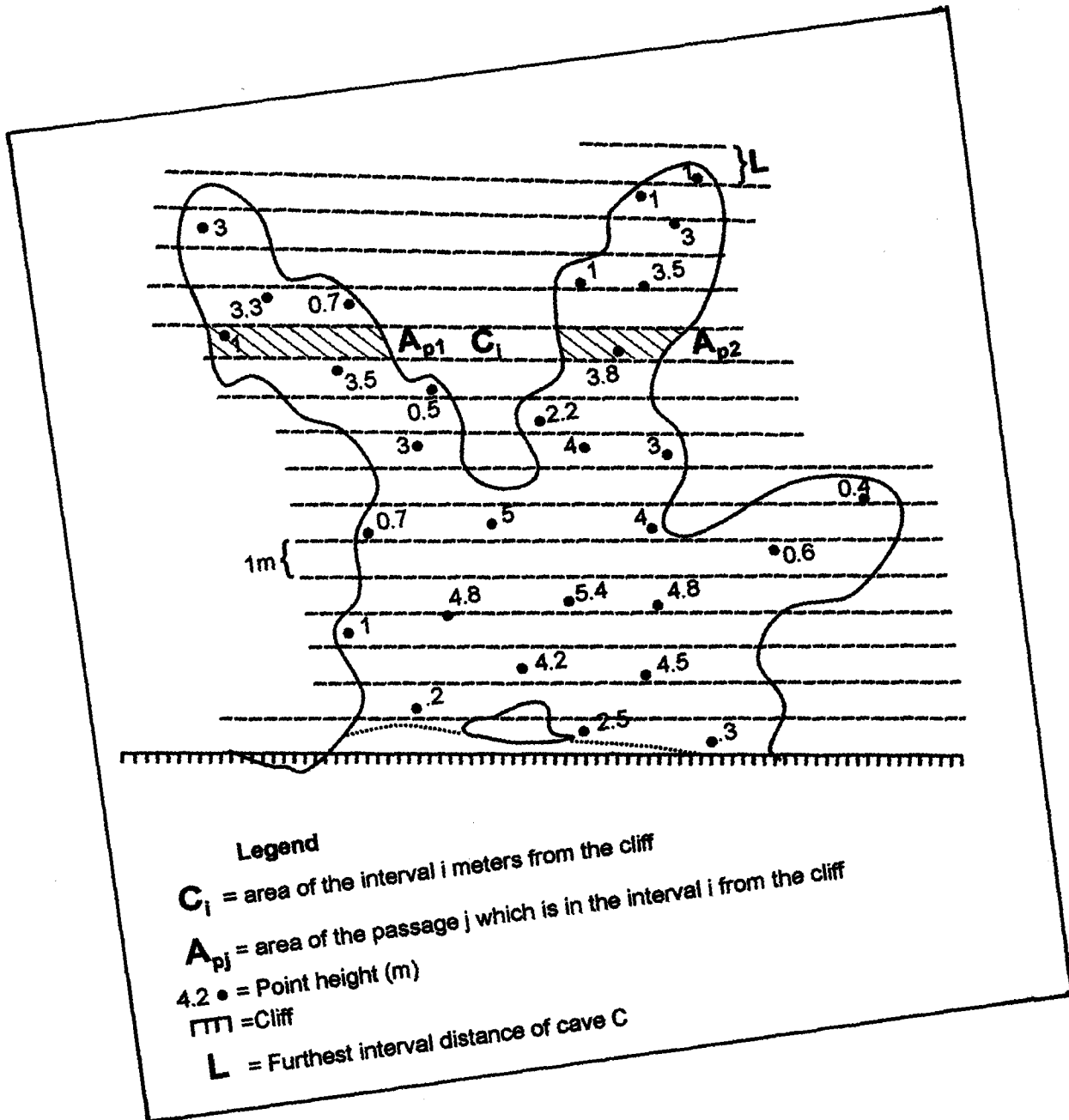


Fig. 2.2 Schematic representation of cave geometric parameters.

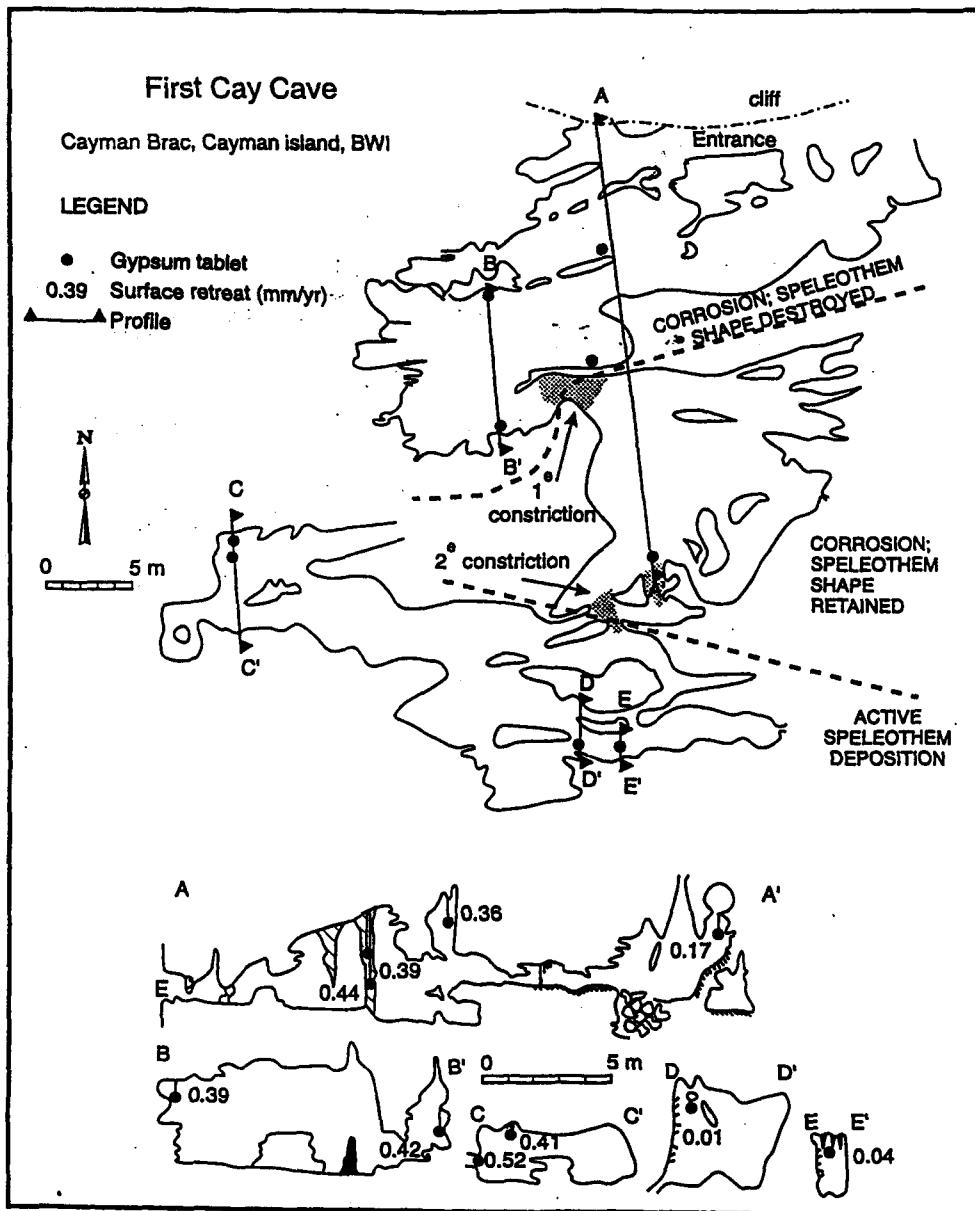


Fig. 2.3 Location of gypsum tablets in First Cay Cave, a vertical joint type Upper Cave.



Fig. 2.4 An example of caymanite from Great Cave.



Fig. 2.5      Phytokarst on the coastal platform, NE side of Cayman Brac.

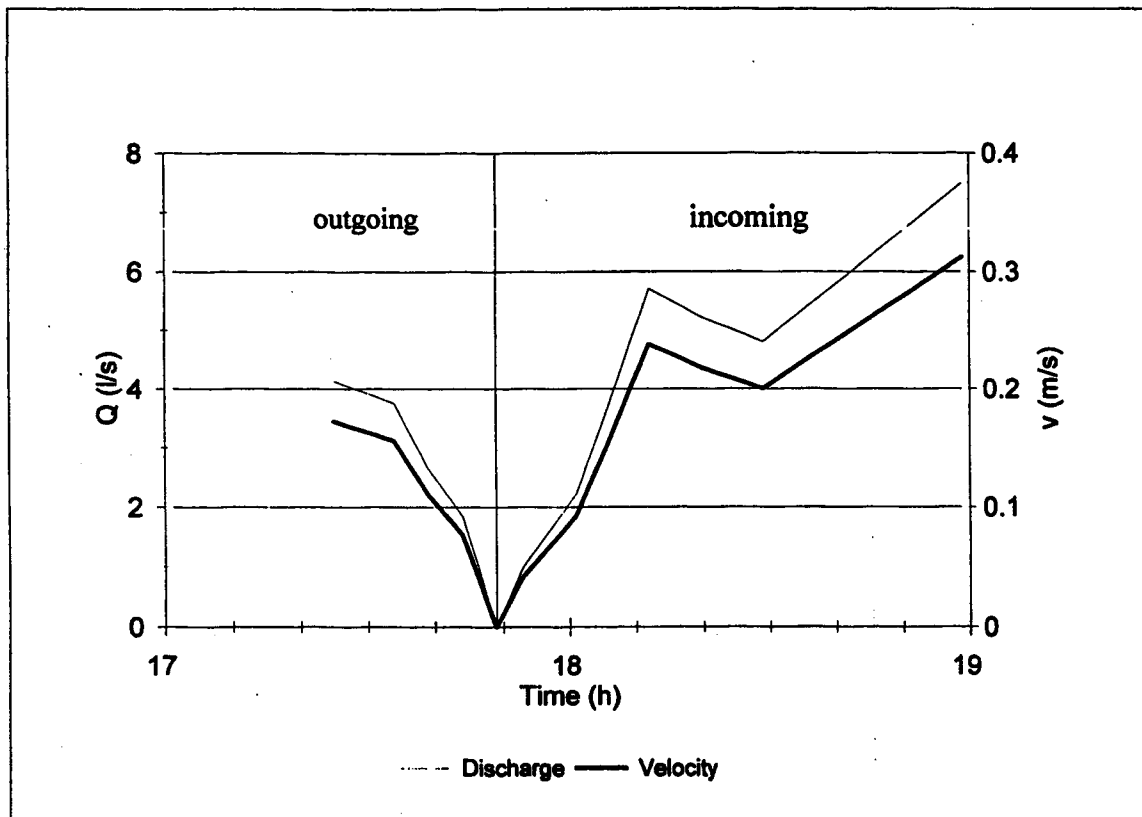


Fig. 2.6 Velocity and discharge of incoming and outgoing tide in the Garbage Dump Pond on the south side.

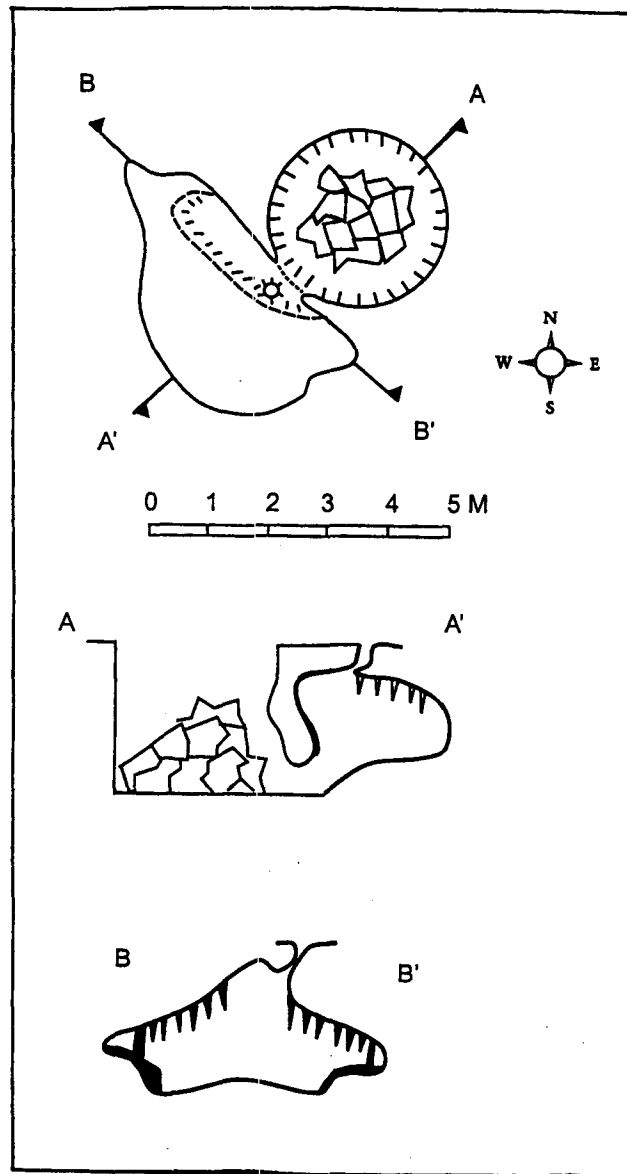


Fig. 2.7 Map and profile of B2-Cave, an example of a pit cave on the plateau.

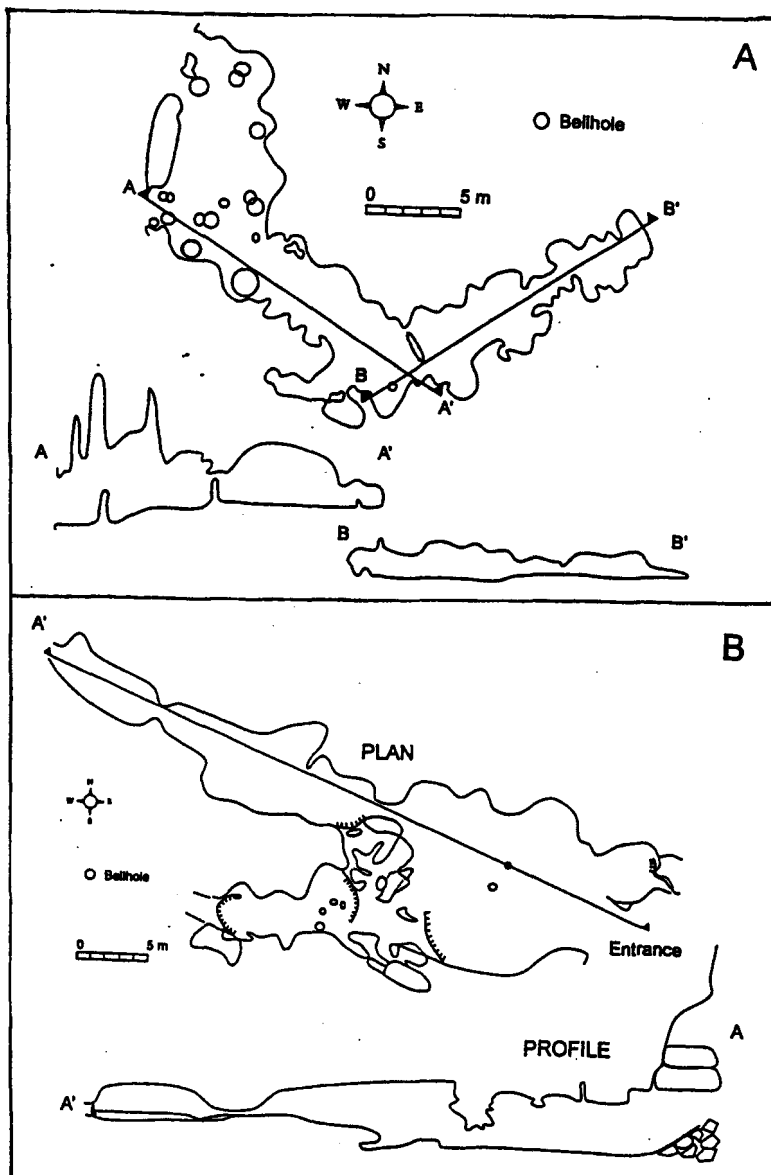


Fig. 2.8 Notch Caves: a) Skull Cave and b) Great cave.

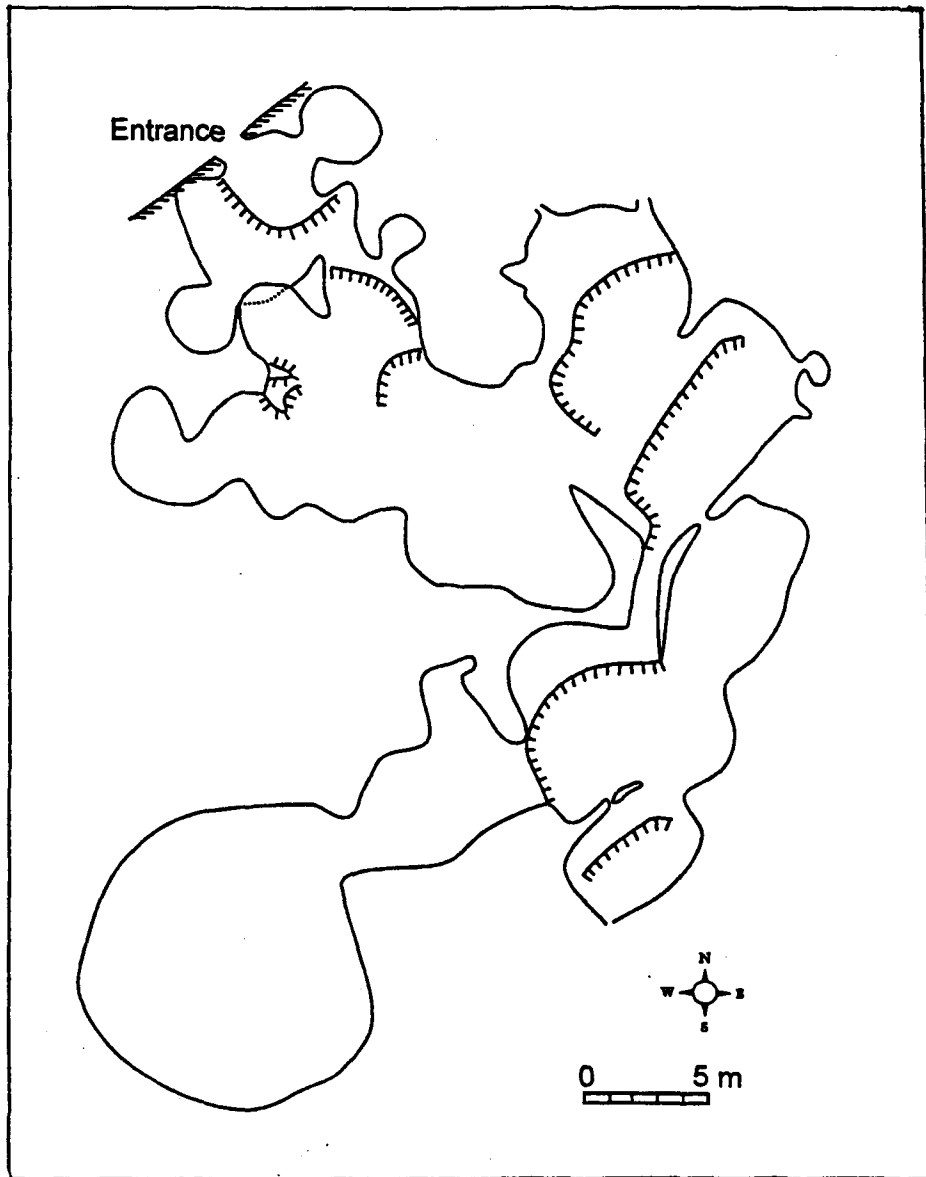


Fig. 2.9 Upper cave: Tibbetts Turn Cave, flank margin type, non fracture-guided.

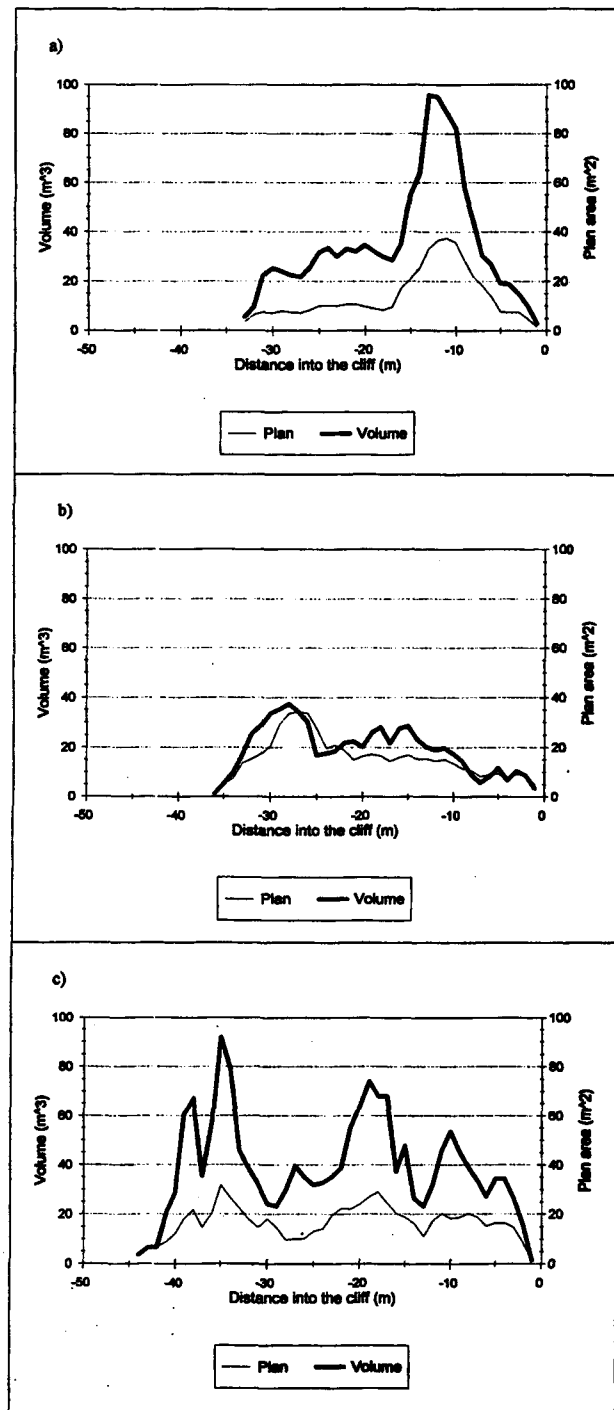


Fig. 2.10 Cave volume and plan area versus distance perpendicular into the cliff for a) Bats Cave, b) Tibbetts Turn Cave and c) First Cay Cave.

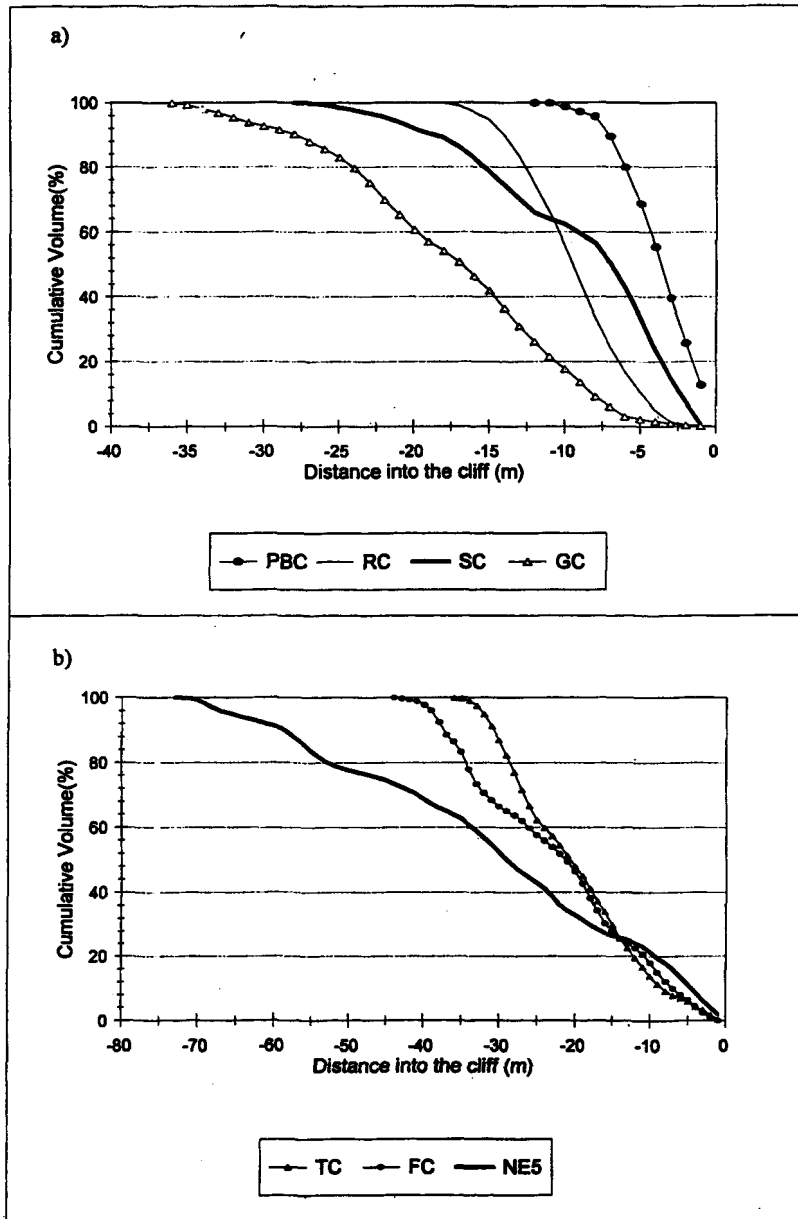


Fig. 2.11 Cumulative volume of selected Notch Caves (a) and Upper Caves (b).

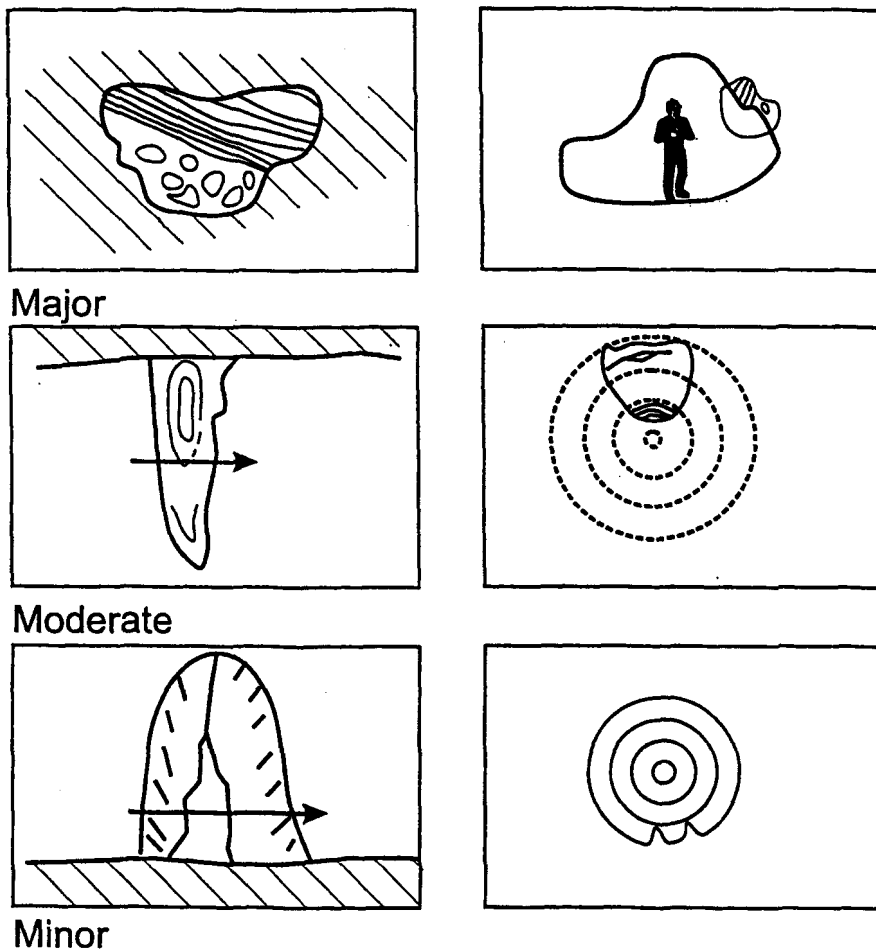


Fig. 2.12 Schematic representation of a) major, b) moderate and c) minor speleothem dissolution encountered on Cayman Brac.

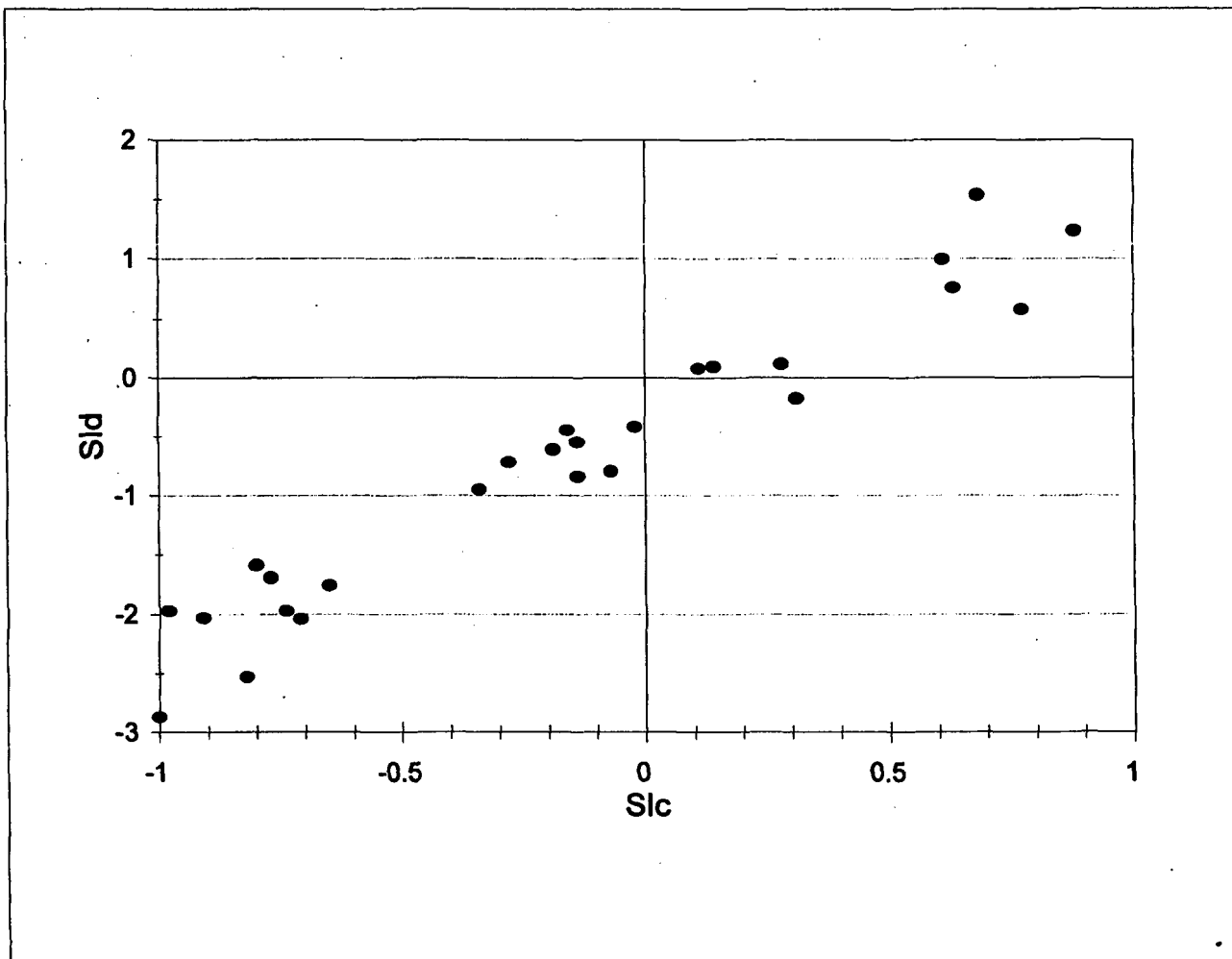


Fig. 2.13 Saturation Index for dolomite (SI<sub>d</sub>) versus the Saturation Index for calcite (SI<sub>c</sub>) for condensation water, May, 1994 and September, 1995.

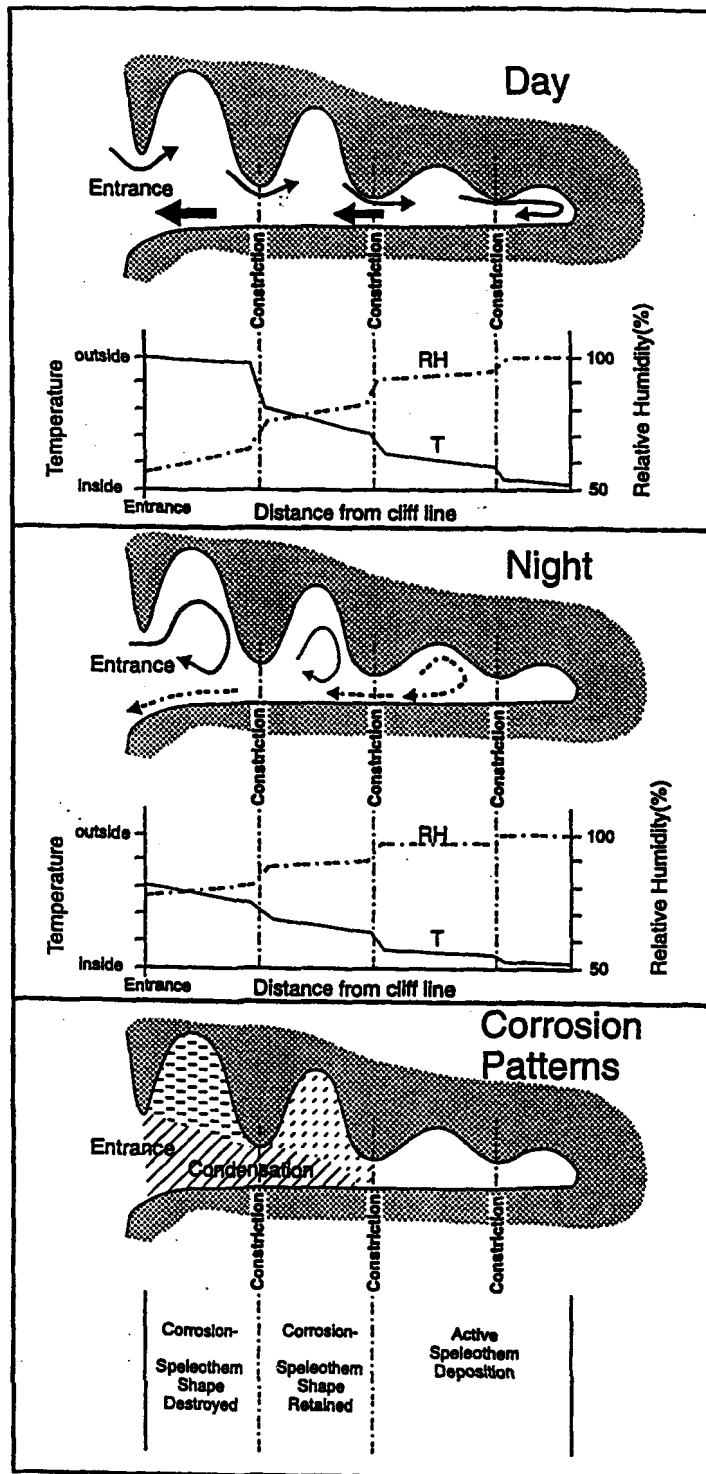


Fig. 2.14 Proposed model of condensation corrosion in coastal caves on small holokarstic oceanic islands with young rocks (Tarhule-Lips and Ford 1998).

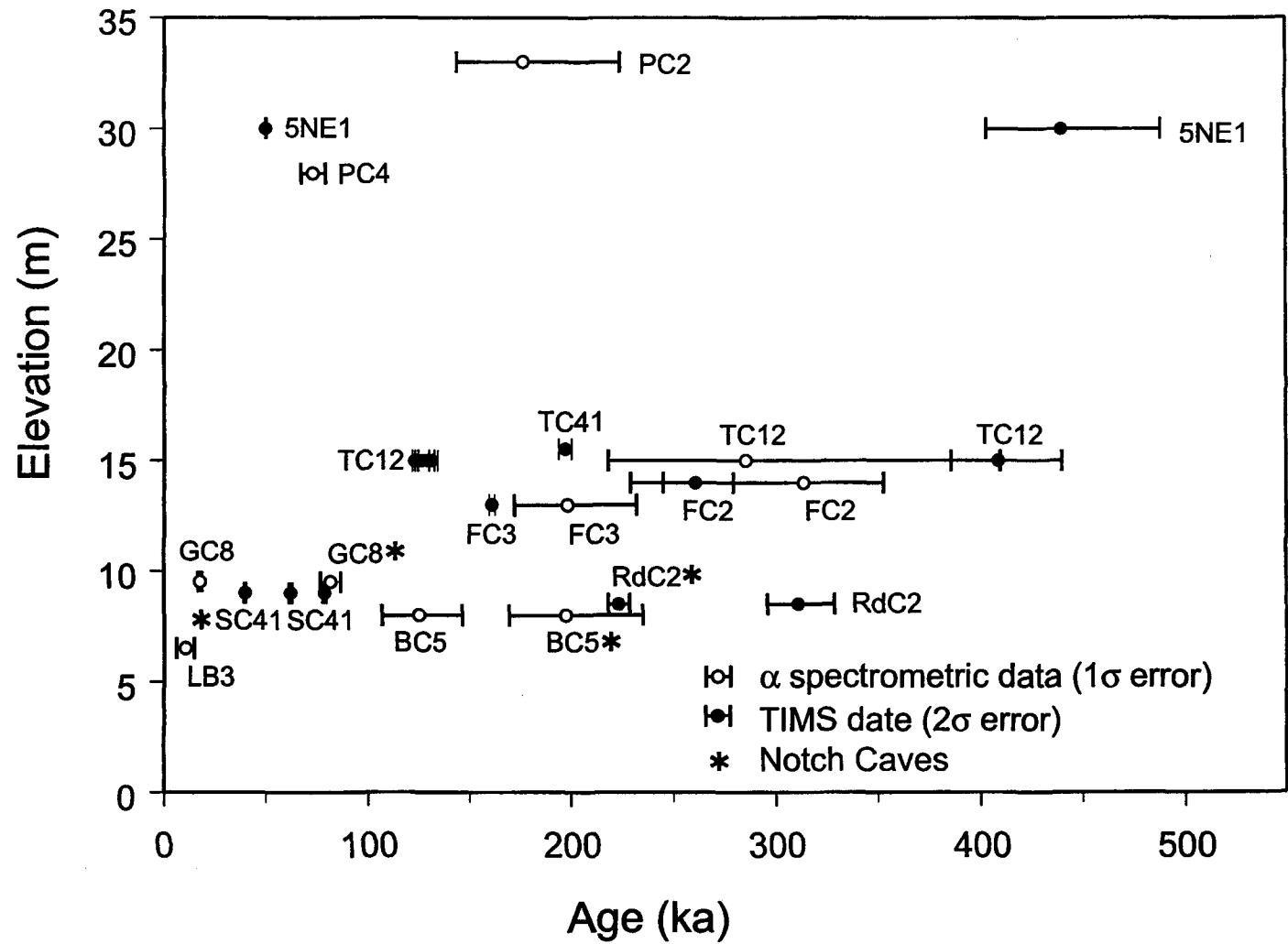


Fig. 2.15 Uranium series spectrometric dates (alpha and TIMS) and elevation above mean sea level of speleothem samples on Cayman Brac.

## CHAPTER THREE

# Timing and implications of calcite speleothem growth and hiatuses on Cayman Brac.

### 3.1. *Introduction*

Many calcite speleothem on Cayman Brac and other islands of the Caribbean display hiatuses in their growth records. The hiatuses are visible as layers of mud or dust, as a difference in calcite texture, or as erosional truncations of calcite growth layers that may or may not be followed by renewed calcite deposition. A hiatus is an indication of a change in the environmental characteristics responsible for the growth of the speleothem. It represents a period in which the speleothem did not grow because it did not receive sufficient drip water. This could be due to (1) the lack of drip water, (2) the cave being flooded by ground water, or (3) the drip water being undersaturated with respect to calcite and causing dissolution rather than deposition of calcite. Since the occurrence of hiatuses is so

widespread and common, it is assumed that they probably result from unfavourable environmental conditions that are equally widespread, rather than from strictly local channel blockage. Knowing the timing and duration of the growth cessation could yield important paleoenvironmental information about the island in question and possibly the Caribbean region as a whole.

The majority of the speleothems in the Brac caves are no longer growing at present and they often show major or moderate speleothem dissolution (Tarhule-Lips and Ford in review, Ch.2). This dissolution is due to changes in the microclimatology of the individual caves, which may result in condensation corrosion (Tarhule-Lips and Ford 1998, Ch. 4).

Speleothem from caves on tropical oceanic islands have great potential for providing a very precise record of climatic and environmental fluctuations of the Quaternary away from the glaciated regions of the earth. Stable isotope records can be pinpointed in time due to the high precision dating technique used on speleothems. In some speleothem, growth layers have been shown to be annual (Shopov *et al.* 1994) and a high sampling density can thus provide data at intervals of a few years instead of the few thousand years of averaging that, due to bioturbation, is the case for the well known Quaternary foraminifera record (Imbrie *et al.* 1984; Martinson *et al.* 1987). The limiting factor for paleoclimatic analyses of speleothems is that the calcite needs to have been deposited in a very stable environment where temperature was constant and relative humidity was close to 100% (Schwarcz 1986). If these conditions are not met the isotope record can be influenced by kinetic fractionation and it will no longer entirely represent the climatic and environmental conditions inside the

cave and at the surface.

At present detailed dated oxygen isotope paleoclimate records covering one or more complete glacial cycles exist from a thermal water calcite vein in Devils Hole, Nevada (Winograd *et al.* 1992, 1997), several selected caves in the USA, Northwestern Europe (Gascoyne 1992) and Tasmania (Goede *et al.* 1986) and from ice cores in Greenland (Dansgaard *et al.* 1993) and Vostok, Antarctica (Jouzel *et al.* 1987). Little has been published on isotope records from tropical speleothem (e.g. Gascoyne 1979 - Jamaica; Harmon 1976 - Mexico). Tropical marine sites such as the Brac are especially interesting because they are in the precipitation source areas for temperate continental records of North America. The present study attempts to provide at least a partial record from such an area.

This study has two objectives:

1. to date growth hiatuses in speleothems to find out when they occurred; if they coincided in time for all samples, this is evidence of the same regional climatic changes, if not, they are caused by other more localised changes in the environment
2. to analyse the stable isotopes of carbon and oxygen in speleothem which might reveal paleoclimatic and paleoenvironmental information during the different growth periods in the past.

This study is the first that concentrates on the timing and significance of growth hiatuses in speleothem in subtropical caves that are above the modern and Sangamon high sea levels. Such hiatuses are not necessarily the result of flooding of the caves by rising sea level during the interglacial periods as was the case in the study by Lundberg (1990),

Lundberg and Ford (1994) of a speleothem that grew at 15 m below the modern tide line.

### 3.2. *U/Th Thermal ionization mass spectrometry dating of speleothems*

At present, uranium series disequilibrium dating by thermal ionization mass spectrometry (TIMS) is the most reliable and precise dating method for speleothem in the age range of 1-600 ka. It is based on the radioactive decay of  $^{238}\text{U}$  and  $^{235}\text{U}$  to stable  $^{206}\text{Pb}$  and  $^{207}\text{Pb}$ . The most common method of dating relies on the build-up of  $^{230}\text{Th}$  over time by radioactive decay of  $^{234}\text{U}$  (itself decayed from  $^{238}\text{U}$ ) in a system where  $^{230}\text{Th}$  is initially absent or at very low levels. In the case of speleothems, uranium present in the feed water is deposited in the crystal lattice of the calcite while the insoluble thorium is left behind in the soil, making it possible to determine the time of deposition.

The activity ratio of  $^{230}\text{Th}/^{234}\text{U}$  is zero at the beginning and reaches equilibrium after about 600 ka (Lundberg 1990). In the interim, the activity ratio can be calculated using the following equation (Schwarcz and Gascoyne 1984):

$$^{230}\text{Th}/^{234}\text{U} = (1 - e^{-\lambda_{230}t}) (^{238}\text{U}/^{234}\text{U}) + [(1 - ^{238}\text{U}/^{234}\text{U}) \times \lambda_{230}/(\lambda_{230} - \lambda_{234})] (1 - e^{-(\lambda_{230} - \lambda_{234})t}) \quad (3.1)$$

where  $t$  is time,  $^{230}\text{Th}/^{234}\text{U}$  and  $^{238}\text{U}/^{234}\text{U}$  refer to the present activity ratios of the isotopes and  $\lambda_{230}$  and  $\lambda_{234}$  are the decay constants of  $^{230}\text{Th}$  and  $^{234}\text{U}$  respectively. To determine the time elapsed since the initiation of the system  $^{230}\text{Th}/^{234}\text{U}$  and  $^{238}\text{U}/^{234}\text{U}$  must be known. With TIMS the isotopes are counted directly due to separation by mass. In alpha spectrometry,

on the other hand, activity ratios are measured by estimating numbers of atoms from their emission of alpha particles at characteristic energy levels.

The precision of a date is expressed as error margins of  $1\sigma$  (68% confidence level; alpha spectrometry) or  $2\sigma$  (95% confidence level; TIMS) on either side of the date. Mass spectrometry is more precise in the measurement of the ratios than alpha spectrometry. Alpha spectrometry has a 1% precision of the measurements of U ratios and 3% of Th ratios, resulting in a cumulative error of about 10% in the estimated date. TIMS however, has errors ranging from 0.04-1.0% ( $2\sigma$ ; Lundberg 1990). Another main advantage of TIMS over alpha spectrometry is the sample size: 20-100 g for alpha spectrometry compared to 0.5-5g for mass spectrometry. Mass spectrometry is thus more precise and more accurate and allows for higher sampling densities.

### 3.2.1 *Problems related to TIMS dating*

The majority of the samples used in this study contain much organic material which is evident from the dirty foam released during sample dissolution. The insoluble residue is removed by centrifuging the sample and the organics are oxidized at the beginning by heating the samples and adding some  $H_2O_2$  before the addition of the spike. The presence of detritus causes the introduction of detrital thorium, i.e. thorium that is attached to detrital material and is not formed by radioactive decay of uranium. The detection of detrital thorium is possible by looking at the presence of  $^{232}Th$  which is not

derived from the decay of  $^{234}\text{U}$  in the calcite. If too much detrital thorium has been introduced the age needs to be corrected for this.

Besides organic matter, most dated subsamples appeared to contain phosphates or high amounts of aluminum. This resulted in difficulty in precipitating uranium and thorium with  $\text{FeCl}_3$  and ammonia. Instead of a uniform red flocculate with a clear supernate, the precipitate was creamy white to orange and the supernate murky. In order to get rid of the phosphates or aluminum the precipitate had to be redissolved in  $\text{HNO}_3$  and be reprecipitated at a pH of 3.4-3.8. The supernate was then discarded and the process repeated until the precipitate became the desired red flocculate with a clear supernate. Some of the sample U and Th can be lost with each precipitation and it was sometimes necessary to use a less than perfect precipitate. It may be noted that this more elaborate extraction procedure is also the common practice for the chemical preparation of tooth enamel samples for dating.

One of the samples (LC2) was difficult to date due to low thorium yields. One of six subsamples gave an age with a relatively large error. Subsamples from some other speleothems had problems with thorium as well and provided no date. Dates obtained on samples TC42 and CAS2 were not in chronological order. Even though their individual dates seemed acceptable they must be used with caution because it is not apparent which of the subsamples gave a correct age. The erroneous ages could have resulted from preferential removal of either uranium or thorium at some point or points in time.

### 3.3. *Sample Descriptions*

Eight speleothem samples from five caves (Northeast Cave #5, Skull Cave, Tibbetts Turn Cave, First Cay Cave and Road Cut Cave) on Cayman Brac (Fig. 3.1) and one from Cueva del Agua, Sardinera, on Isla de Mona (Fig. 3.1) were dated by thermal ionisation mass spectrometry (TIMS). All samples were selected because they displayed one or more hiatuses in deposition. Furthermore, samples were selected by location, in order that all parts of the island were represented in the programme, as well as both types of caves - Notch and Upper caves (Tarhule-Lips and Ford in review, Ch. 2).

In earlier work, seven samples from five caves (Bats Cave, First Cay Cave, Great Cave, Peter's Cave and Tibbetts Turn Cave) and one from the Notch at First Cay Cave were dated by alpha spectrometry (Fig. 3.1; Lips 1993). Three of these have now been dated by both methods and the results clearly show the greater precision of the TIMS technique. Both mass and alpha spectrometry dates are used in this chapter (Table 3.1). From the alpha dating it was clear that the uranium levels in speleothem on Cayman Brac was low (about 0.2 ppm) and relatively large (5-6 g) sample sizes had to be used for TIMS dating. The reliable ages range from about 10 ka to 450 ka.

A brief description of the samples follows. A more detailed description of the caves can be found in Lips (1993).

### 3.3.1 *Cayman Brac*

#### 3.3.1.1. *Notch*

The Notch marks the position of the last sea level high stand at 6 m above present sea level (oxygen isotope stage 5e or Sangamonian, approximately 125 ka). It extends up to 7 m into the cliff, is symmetrical and shows no evidence of tilting after formation, suggesting that the island has been tectonically stable since at least the Sangamonian (Woodroffe *et al.* 1983).

At many locations the Notch contains speleothem that has subsequently been eroded. Sample LB3 was collected from one such site about 50 m west of First Cay Cave. At this location, an eroded speleothem phase was succeeded by a phase of breccia formation, which was then followed by another phase of speleothem formation. LB3 is from that second phase of deposition. No coastal platform is present at this site and continuous wetting by sea spray and breaking of the waves against the speleothem in times of storm cause erosion, even at present.

#### 3.3.1.2 *Notch caves*

##### 3.3.1.2.1. *Skull Cave.*

Skull Cave is in dolostone of the Cayman Fm on the north side of the island. Its floor is about one metre above the Sangamon Notch. It is a typical "Notch cave" (Tarhule-Lips and Ford in review, Ch. 2) with a large room near the entrance and one passage

tapering into the cliff where it ends abruptly (Fig. 3.2). As is common for many of the Notch caves, Skull Cave does not contain much speleothem.

Sample SC41 is a piece of flowstone from the wall of a small side chamber (Fig. 3.2). The sample was selected because it is one of the few speleothem samples collected from Notch caves and it shows at least one, if not two growth hiatuses. Dissolution of the speleothem appears to have taken place during the periods of growth cessation.

#### 3.3.1.2.2. *Bats Cave*

Bats Cave is one of the Notch caves in dolostone of the Cayman Fm on the south side of the island. It consists of a main cave with three radiating passages that end abruptly and one small side cave (Fig. 3.3). The floor of the main cave appears to have collapsed, probably during the formation of the Notch, leaving a big porch at the Notch elevation. It is likely that the formation of the Notch cut into the large entrance room of this cave and that the side cave was also one of the passages radiating from the entrance chamber. BC5 is the top of a stalagmite, 1.4 m high and 0.45 m in diameter, located at the entrance of the small westerly cave (Fig. 3.3). The sample was taken close to the cave wall where the stalagmite was not yet as much eroded as on the side facing the centre of the passage. The base of the stalagmite is about 0.9 m above the centre of the Notch. The sample was selected for alpha spectrometry because it came from a Notch cave and had continuous growth.

#### 3.3.1.2.3. *Road Cut Cave*

This cave was exposed and almost entirely removed when workers made a road up the cliff on the south side of the island, near Salt Water Point. It is located in dolostone of the Cayman Fm and appears to lie about two metres above the Sangamon Notch. The remnant of the cave contains a fair amount of speleothem and RdC2 (Fig. 3.4) is part of one of the draperies. The sample was selected because it shows three hiatuses and is from a Notch cave.

#### 3.3.1.2.4. *Great Cave*

Great Cave is one of the Notch caves on the southeast end of the island in dolostone of the Brac Fm. The entrance is partially blocked by big blocks fallen off the cliff face. It consists of a big room with three passages radiating out, two westward and one eastward (Fig. 3.5). The longest of the westward passages ends in a lake. Sample GC8 was taken from this passage, just before the lake (Fig. 3.5). It is a larger stalactite composed of three smaller stalactites grown together. It was selected because of the occurrence of one hiatus and its location in this southeasterly cave. The hiatus is visible from the difference in calcite structure on either side of it. Growth of the initial three stalactites started before the hiatus and two were joined together at this point in time. The other one was later connected to them by evaporitic calcite. This stalactite is composed of very clear calcite and contained the highest concentrations of uranium observed in any of

the samples analysed. The outside is milky white, resembling weathered calcite.

### 3.3.1.3. *Upper caves*

#### 3.3.1.3.1. *First Cay Cave*

First Cay Cave is located in limestone of the Brac Fm on the northeast end of the island, about 6.5 m above the Notch or 12.5 m asl. The cliff at the foot of the cave descends straight down into the sea and the spray of the breaking waves can be felt at the entrances. The numerous subparallel passages making up the cave have formed along pre-existing vertical joints in the bedrock (Fig. 3.6). Part of the cave has been removed by cliff retreat.

The cave can be divided into three zones based on the degree of speleothem dissolution (Fig. 3.6): zone 1, near the entrances, is an area where the speleothems have undergone major corrosion which completely destroyed their shape; in zone 2 the speleothems have been moderately corroded and the original shape can still be discerned; and zone 3, furthest from the entrance, contains actively growing speleothem and some that have undergone minor corrosion. This is the only cave in which such clear zonation is visible. The zones are separated from each other by narrow constrictions in the cave morphology which have great influence on the cave microclimatology (Tarhule-Lips and Ford 1998, Ch. 4).

Three flowstone samples (FC1,2 and 3) were dated by alpha spectrometry of

which two (FC2 and 3) were repeated by TIMS. They are part of a speleothem section on the floor and ceiling close to the western entrance of the cave (Fig. 3.6). The phases indicated in Figure 3.6 are relative to each other (Phase 1 being the oldest) and Phase 1 on the floor and ceiling may not necessarily represent the same period. FC2 is a sample of ceiling Phase 1, FC1 of floor Phase 1 and FC3 of floor Phase 2. The samples were chosen to find out more about the intriguing sequence of events at this location. Furthermore, FC2 shows five main hiatuses and several less obvious growth interruptions (Fig. 3.6). It also has a layer of evaporitic speleothem below Hiatus 1, but separated from it by a layer of more compact calcite. Hiatus 1 can be recognised by a thin white layer on top of a thin layer of reddish particles which appear to have been deposited together with the calcite. The reddish and white particles are probably dust. The lower layers do not seem to be truncated during this period of growth cessation. The next two hiatuses are clearly visible due to the reddish (hiatus 2) and yellowish (hiatus 3) clay particles. Once again the lower layer does not appear to be truncated by dissolution but this is not completely certain. Hiatus 4 resembles hiatus 1, but the dust particles are more yellowish than reddish. The modern period of dissolution shows a speleothem surface that is clearly sculptured and covered with a greyish dust. Unfortunately, both alpha spectrometry and TIMS dating were hindered by low thorium yields. Only one alpha spectrometry and one TIMS date could be obtained from this important sample.

### 3.3.1.3.2. *Tibbetts Turn Cave*

Tibbetts Turn Cave is one of the Upper caves in dolostone of the Cayman Fm on the north side of the island. It is located near the top of the cliff about 14 m above the Notch or 20 m asl. In morphology this cave resembles the Notch caves more than the other Upper caves, except for the fact that it does not have its largest chamber close to the entrance and the floor is not horizontal. It also contains much more speleothem.

All three samples (TC12, TC41 and TC42) were taken from a room about 31 m inside the cave (Fig. 3.7). They were samples that had been previously broken off and were lying on the floor close to where they once hung on the ceiling. TC41 is a stalactite and the other two are draperies.

TC12 was first dated by alpha spectrometry and later repeated by TIMS. It consists of a light coloured, partially dissolved core with two intact dark parts positioned opposite from each other. The hiatus in TC12 is shown as a thin white layer, clearly indicating weathering of the older core part (Fig. 3.7). The core was preferentially dissolved on one side. The colour difference between the outer and the inner parts indicates a change in the characteristics of the feed water before and after the hiatus. The darker colour is believed to represent more mineral or organic material in the water which would result from a changing vegetative and soil cover on the surface. The colour difference, clear evidence of speleothem dissolution at the time of the hiatus and the location of the sample were the selective criteria for this sample.

TC41 is a stalactite with two hiatuses and some chaotic growth layers near the core. TC42 is a sample of a drapery showing two hiatuses also, and the same colour difference as TC12. Unfortunately the dates obtained from this sample were not in chronological order and thus cannot be used. The oldest part had the youngest date and the youngest part the oldest age. The latter could be a result of leaching of uranium, which is not an uncommon problem in speleothem dating. The former however, would be the result of a removal of thorium or contamination by additional uranium. Removal of thorium, in general, is less likely because it is much more immobile than uranium. Since both the younger and older part appear to have undergone some post depositional alteration of U and Th, it is likely that the rest of the sample was also affected and the age of the middle part should be carefully considered.

#### 3.3.1.3.3. *Peter's Cave*

Peter's Cave is the largest cave known on the island. It consists of two main passages parallel to the cliff and in dolostone of the Cayman Fm. Its main entrance is about 23 m above the Notch, or 29 m asl and there is a second important entrance about 10 m lower and about 25 m westward.

PC4 is a piece of flowstone taken 0.75 m underneath the floor of the main entrance (Fig. 3.8). There is no hiatus visible, only a lightening of the calcite from dark brown at the bottom to white at the top, indicating a change in the characteristics of the

feedwater and probably the vegetation and soil cover. This change in colour and the location of the sample were the reasons for its selection for alpha spectrometry dating.

PC2 is a partially dissolved stalactite from the second main passage (Fig. 3.8). It shows a clear asymmetry in the direction of dissolution and no hiatuses. The sample was chosen to find out the approximate timing of the dissolution causing the asymmetry.

#### 3.3.1.3.4. *Northeast Cave #5.*

Northeast Cave #5 is one of a series of six caves located in the cliff on the northeast point of the island. They are all about 10-15 m underneath the top of the cliff or about 30-35 m above sea level. They are in the Brac Fm and their vertical upward extension was limited by the unconformity separating the Brac and Cayman Fms. Cave #5 goes about 70 m straight into the cliff and the sample 5NE1 was taken from the far end of the cave (Fig. 3.9). It is part of a flowstone on the floor that was dissolved at some point in time and then coated with a new layer of flowstone. The sample was selected because of the high position of the cave and the obvious growth hiatus which was accompanied by speleothem dissolution.

#### 3.3.2. *Isla de Mona*

##### 3.3.2.1. *Cueva del Agua at Sardinera*

Cueva del Agua is located near Playa Sardinera on the southwest corner of Isla

de Mona (Fig. 3.10). It is formed in the Isla de Mona Dolomite (Late Miocene to Early Pliocene). The cave follows the cliff for about 200 m and extends to a maximum distance of 100 m perpendicular to the cliff line (Fig. 3.10). It contains three major chambers and several smaller ones. Sample CAS2 was collected from the floor of the middle chamber (Fig. 3.10) not far from where it had previously been removed by others. It consists of two stalagmites grown together and has a gray dust layer on the outside. At least eight growth hiatuses are visible and the sample was clearly differentially dissolved on one side. The inner part consists of compact calcite while the outer layers have very thin growth layers separated by lots of impurities, which complicated the dating of the sample due to introduction of detrital thorium.

#### 3.4. *Hiatuses in the Brac and Mona speleothems.*

Three different types of hiatuses have been identified in the speleothem samples:

1. Hiatuses without visible weathering or dissolution
2. Hiatuses with weathering but without dissolution
3. Hiatuses with weathering and dissolution.

Besides the hiatuses, which are interruptions in the growth record, many of the speleothems have stopped growing at present and their outer surfaces show weathering, dissolution or nothing at all. It is not known if these speleothems will renew growth at some later date but if they do, then the present would represent a hiatus in their growth

record.

There are several possible causes for hiatuses:

1. Cessation of deposition due to cessation of drip water in a subaerial environment. Dissolution due to condensation corrosion might or might not occur at the same time.
2. Cessation of deposition due to flooding of the cave in a subaqueous environment. Phreatic dissolution is very likely, but not necessarily, to occur during flooding.
3. Rate of corrosion exceeds rate of deposition. In this case the speleothem continues to receive drip water and calcite is deposited but at a lower rate than the removal of calcite by corrosion. This case necessarily occurs in a subaerial environment.

The above causes could be explained by:

1. Changing sea level over time. This could either result in the flooding of the cave (cause 2); or the changing proximity to the ocean could have some climatic effect on the entire island and its water regime, or a local effect at a site such as removal of a screen of trees across a cave mouth as the coastal platform becomes submerged.
2. Recession of the cave due to cliff erosion. This would influence the microclimate inside the cave as can be seen in First Cay Cave (Tarhule-Lips and Ford 1998, Ch. 4). In this case either dissolution (resulting from condensation corrosion) exceeds deposition, or growth has completely stopped and only dissolution is

taking place. One problem with this hypothesis is that regrowth after a period of no growth would appear to be unlikely because the microclimate will presumably remain unfavourable to speleothem growth. A possible countering effect here would be if the relative humidity (RH) inside the cave increases when sea level and the shoreline is closer to the cave and reduces when it is farther away. In the first case the RH in the mid-cave position could increase above a certain level where deposition will start to exceed condensation corrosion and speleothem deposition is again possible: the location of hiatuses at a given site are thus an indicator of relative sea levels in the past.

#### 3.4.1. *Dating of hiatuses*

In a broadly comparable study, Lundberg (1990) found that samples taken from one millimetre either side of a growth hiatus in a Bahamian sample from 15 m below modern sea level resulted in unreliable ages due to leaching of uranium or introduction of detrital thorium. Although care was taken not to sample too closely to growth hiatuses in the Brac and Mona specimens, not all samples gave a usable age. Figure 3.11 plots the elevation above sea level and the age of the hiatuses observed in speleothem on Cayman Brac, with the drowned Bahamian sample for comparison. It is evident from this figure that not all hiatuses occurred at the same time and that some speleothem were growing while others did not. At some periods of growth cessation speleothem was dissolved and

substantial amounts of calcite were removed, thus making it impossible to date the exact start of the hiatus. The hiatuses in the Bahamian sample occur when sea level rose above the elevation of the speleothem at -15 m during the interglacial periods. None of the Cayman samples show the same pattern. Some might have the beginning or end of their hiatus roughly at the same time of one of the hiatuses of the Bahamian sample but the uncertainty in many of the dates could easily change that.

As mentioned above, the present time is a period of growth cessation and probably weak dissolution for the majority of the speleothem on Cayman Brac. Figure 3.11 not only shows that the hiatuses occurred at separate periods in time but also that not all the samples stopped growing at the same time. Some of the samples have undergone dissolution of their outer surface but others did not; e.g. RdC2 stopped growing around 200 ka while 5NE1 stopped around 50 ka and neither of them show any sign of speleothem dissolution of their outer surface.

The actively growing speleothem are mainly located deep inside caves, as can be seen in First Cay Cave (Fig. 3.6). Tarhule and Ford (1998, Ch. 4) have shown that the present day climatic conditions at lesser distances inside the caves are favourable for speleothem dissolution by condensation corrosion (Fig. 3.12). This situation appears to be a good approximation of what happened in the past: some speleothems are growing, some have stopped growing and some are suffering faceting dissolution. At present this mixed situation is the result of the very localised climatic conditions inside the individual caves.

This would suggest that the second explanatory hypothesis advanced above is the correct one. However, the problem of the renewed growth is more complicated than it suggests, because if high sea level were to increase the RH leading to renewed growth then this would coincide with interglacial periods. However, the dates clearly show that this is not necessarily the case.

### 3.5. *Growth rates.*

The rate at which a speleothem grows depends on many factors, such as amount and timing of precipitation, amount of water infiltrating,  $p\text{CO}_2$  of the drip water, difference in  $p\text{CO}_2$  between the drip water and the cave air (e.g. Ford and Williams 1989; Dreybrodt 1988). Therefore, individual speleothems in a particular cave or in caves within one region can grow at different rates. Furthermore, different types of speleothem have different growth rates; e.g. most flowstone will thicken more slowly than nearby stalagmites extend upward. However, in spite of these individual differences, some broad uniformity of growth rates might be expected because the climatic factors play an important role. Especially the amount of rainfall and the rainfall regime are predominant because if there is no water there is no speleothem growth. In principle, the more water there is and the more the water is supersaturated, the faster the speleothem will grow. This would be the case in a humid environment with lots of vegetation, producing high levels of soil  $\text{CO}_2$ .

Growth rates could be extracted from four of the dated samples and are presented in Table 3.2. Samples FC3, BC5 and SC41 grew at rates between 0.5 and 0.9 mm/ka. The oldest part of the drapery from Tibbetts Turn Cave grew at a similar rate, 0.85 mm/ka. However, its two younger parts grew an order of magnitude faster than this, 5.5-7 mm/ka, but for only 9 ka during the last interglacial period. Rapid growth during that time suggests that this period was very favourable for the growth of this particular sample. Other samples, however, stopped growing at about that time, suggesting that the changing climatic conditions were unfavourable for their growth. It is, therefore, essential to investigate more than one sample before attempting any generalising conclusions.

Table 3.2 also presents the results of Lundberg and Ford (1994) for DWBAH, a flowstone sample in Lucayan Caverns, Grand Bahama Island. Except for a few apparent short term growth spurts such as that noted above, speleothem on both islands have mean growth rates between 0.5 and 1 mm/ka. It is hard to accurately link the variations in growth rate to specific climatic conditions because, even for one sample, the growth rate will vary depending on the location of the measurements, due to the irregular shape of the sample.

Matching the oxygen isotope records of samples with the deep sea Foraminifera isotope records (see below) might also be used as an additional aid to determine duration of growth and approximate growth rates of individual samples, because they may have been influenced by the same climatic factors.

### 3.6. *Discussion of hiatal results*

On Cayman Brac speleothems containing hiatuses have been dated back about 500 ka and the caves in which they formed are believed to be of late Tertiary to Mid Quaternary age (Tarhule-Lips and Ford in review, Ch. 2). Dating of these speleothems has shown that growth and growth cessation could have occurred at any time during this period, apparently independent of the global climatic fluctuations that went on at the same time.

Dissolution at the time of growth cessation is a clear indication that the environmental conditions have changed, not only causing the speleothem to stop growing but also to actively dissolve it away. This means that aggressive water must have been in contact with the speleothem, either in a subaerial (condensation water) or a subaqueous (fresh, brackish or saline water) environment. At present three different degrees of dissolution have been identified on Cayman Brac (Tarhule-Lips and Ford in review, Ch. 2): major, moderate and minor. The latter is very site specific whereas the other two require more widespread changes in environmental factors.

Figure 3.11 gives an up-to-date summary of the hiatuses on Cayman Brac; it shows the elevation, age and timing of the hiatuses of the selected samples. Sample DWBAH from Lucayan Cavern (Lundberg and Ford 1994) is also shown for comparison because the hiatuses in this sample indicate when sea level rose above -15 m (the elevation of the sample) during the peaks of the interglacial periods. The highest samples are from

Peter's Cave (PC2 and 4) and Northeast Cave #5 (5NE1). The flowstone sample from the latter cave shows a prolonged period of growth cessation during which time dissolution took place. How much sample was lost and when this period started are unknown, as is the reason for such a long cessation and the sudden start of new growth. From the location of this sample, about 70 m from the entrance (Fig. 3.9), it is more likely that the dissolution resulted from flooding of the cave than from condensation corrosion. If this flood were by sea water then this would mean that all other caves, which are located lower in the cliff, were submerged too at that time and that the island itself was much lower, before the tectonic uplift. However, sample TC12 located about 15 m lower appears to have started growth around 450 ka, excluding this hypothesis. The formation of a freshwater lake or stream would be another possibility which would not require the whole island to be lower or the other caves to be inundated as well. Depending on how much calcite was lost by redissolution, the hiatus probably started between the peak of stage 11 (interglacial), around 400 ka, and the peak of stage 12 (glacial) around 434 ka. The short period of regrowth was before the peak of the stage 3 interstadial.

The other two high elevation samples from Peter's Cave have stopped growing some time ago as well. If both stopped growing at the same time, around 60 ka, PC2 would have lost about 100 ka, or 5-10 cm (depending on what growth rate is being used), worth of calcite to redissolution. The present sample shows a radius of 3 cm and thus the total sample would have had a radius of 8-13 cm or a diameter of 16-26 cm. This is quite

a big size for this part of the cave and it is more likely that either the sample had been growing at a slower rate or that it had stopped growing well before 60 ka. In fact one other sample, FC3, has stopped growing at about 160 ka as well and also shows some signs of dissolution at that time. Around 160 ka was the peak of the stage 6 glacial which might have had some influence on the speleothems and caused them to stop growing and be dissolved. In a same light, 65 ka was about the peak of stage 4 glacial and might have had a similar influence on PC4 as stage 6 had on PC2 and FC3.

The samples from the two other Upper caves, Tibbetts Turn Cave (TC12 and 41) and First Cay Cave (FC2 and 3), also appear to show some correlation between the beginning of a hiatus and the peak of a glacial period. However, it should be kept in mind that better dating could easily eliminate this, especially in the cases where the dates were obtained from alpha spectrometry and have very large error margins.

The location of TC12, 30 m from the entrance, on the ceiling in an Upper cave (Fig. 3.7), suggests that dissolution during the hiatus was caused by flooding, most likely flooding of the entire cave due to a relative rise in sea level. Since the sea level would also have flooded the other caves and DWBAH, the most likely time would have been during stage 7.5 (hiatus 1, 235-232 ka, in DWBAH, Lundberg and Ford 1994). This would mean that about 10 ka or 2.5 mm worth of calcite were lost to dissolution on the side that is still intact today. Since dissolution was asymmetric, much more calcite was lost on the other side. The biggest problem with this hypothesis is that the island would have had to be

about 14 m lower at the time, stage 7 high stand ( $\sim 229$  ka) was at +1.1 m on Grand Cayman, (Vézina *et al.* in press) and the uplift to the present elevation would have had to take place before stage 5e. No such uplift in stage 6 is known from Grand Cayman Island (Vézina *et al.* in press). Although this is no guarantee that Cayman Brac has been stable too during that time (the two islands lie on separate fault block) it does make such a sudden great uplift less likely. The short regrowth of this sample was during the peak of stage 5e interglacial.

The four samples from Notch caves (GC8, SC41, RdC2 and BC5) show less correlation between the beginning of hiatuses and glacial or interglacial periods. Sample BC5 from Bat's Cave appears to have grown for a very long time. The upper 7.5 cm of this 1.4 m tall stalagmite grew from about 225 to 100 ka at a rate of 0.6 mm/ka. If the mean growth rate of 1 mm/ka is used for the entire sample then it would be 1.4 Ma old. It is, however, more likely that the mean growth rate was faster than 1 mm/ka and that the sample is younger. Since only such a small sample of this enormous stalagmite was taken, it is not known if and how many hiatuses are present. The end of growth for this stalagmite was probably caused by cliff retreat and the destruction of the outer part of the cave during the formation of the Notch in the last interglacial, stage 5e.

The small drapery from Road Cut Cave (RdC2) shows three hiatuses, all without redissolution. The age of this sample, together with BC5, has shown conclusively that the Notch caves are older than the last interglacial period as previously was believed to be the

case (Tarhule-Lips and Ford in review, Ch. 2). This sample started growth during stage 10 or 11, had three hiatuses most likely during stage 9, 8 and 7, and stopped growing shortly after that in the middle of stage 7, the penultimate interglacial period. Since no dissolution took place during any of these hiatuses, the growth interruptions simply show that climatic conditions above and/or inside the cave were unfavourable for speleothem deposition. It is impossible to speculate on the exact location of this sample inside the cave since only a very small part of it remains, the rest being destroyed building the road.

The samples from Great Cave (GC8) and Skull Cave (SC41) grew during the last glacial period. Both show one hiatus from about 50-60 ka, the same time period that PC4 stopped growing and the new overgrowth of sample 5NE1 was formed. This again shows that growth conditions can be unfavourable for one sample while they are favourable for another. This period corresponds to the peak of stage 3, an interstadial. Sample GC8 does not appear to have undergone any dissolution while SC41 shows signs of dissolution both during the hiatus and after it stopped growing. This could have been the result of condensation corrosion since the sample is located in a part of the cave where the relative humidity does not reach 100% and temperature fluctuates slightly on a daily basis.

As has been noted above, the hiatuses of the different samples do not coincide in time and show no correlation with those found in DWBAH, which indicate the peaks of the interglacial periods. As a matter of fact, some samples grow straight through the interglacial periods (e.g. PC2, FC3, RdC2) while others grew through the glacial periods

(e.g. GC8, SC41, 5NE1). Some samples even grew through both periods (e.g. TC12 and BC5). This complicates the interpretation of the results. It was therefore decided to consider oxygen and carbon isotopes of suitable specimens from the dating collection to determine if they could cast some light on the problem.

### 3.7 *Stable isotope analyses*

Oxygen and carbon isotope records extracted from speleothem have been successfully used in paleoclimatic and paleoenvironmental studies for the past 30 years (e.g. Hendy and Wilson 1968; Hendy 1971; Thompson *et al.* 1976; Harmon *et al.* 1978a; Gascoyne *et al.* 1981; Goede *et al.* 1986; Müller *et al.* 1986; Schwarcz 1986; Bakalowicz *et al.* 1987; Millen and Dickey 1987; Gascoyne 1992; Talma and Vogel 1992; Coplen *et al.* 1994; Bar-Mathews *et al.* 1997; Berstad *et al.* 1997; Frisia *et al.* 1997; Holmgren *et al.* 1997). The most important criterion for their use is that the calcite from which they are taken must be deposited under conditions of isotopic equilibrium (Hendy 1971). This can be tested by taking several samples from one single growth layer. If all samples have similar  $\delta^{18}\text{O}$  and  $\delta^{13}\text{C}$  values and there is no correlation between the two records, then isotopic equilibrium can be assumed and the records will only be dependent on temperature. If this is not the case, kinetic fractionation of the isotopes will interfere with the temperature dependent record. Isotopic equilibrium is generally reached in the deep interior of humid caves where temperature usually fluctuates by  $< 1\text{ }^{\circ}\text{C}$  over the course

of a year and relative humidity is always close to 100%.

Many studies have also attempted to quantify paleotemperature from the  $\delta^{18}\text{O}$  records (e.g. Hendy and Wilson 1968; Harmon *et al.* 1978c; Gascoyne *et al.* 1981; Goede *et al.* 1986; Millen and Dickey 1987; Talma and Vogel 1992). Several conditions must be met before this can be achieved (Schwarcz 1986; Harmon *et al.* 1978c)

1. The calcite must be precipitated in isotopic equilibrium with the parent drip water.
2. The drip water must represent the local meteoric water.
3. Both the isotopic composition of the calcite and of the parent drip water must be known.
4. The temperature inside the cave must be correlated with surface parameters such as mean annual temperature in a stable manner.
5. The speleothem must not be isotopically altered (e.g. due to recrystallization) after deposition.
6. The time of deposition must be known by dating of the speleothem.

From all the above conditions, number 3, that both the isotopic composition of the drip water and the calcite must be known, is the most difficult to meet since the ancient drip water is no longer available for analyses. In the 1970's and 80's extraction of small amounts of drip water trapped in the crystal lattice of speleothem was believed to provide the solution (e.g. Thompson *et al.* 1976; Harmon *et al.* 1978; Yonge 1982; Schwarcz 1986)

but more recently this method has been judged to be problematic due to analytical difficulties, which are (Gascoyne 1992)

1. All adhering water needs to be removed from a sample before the trapped water can be extracted. The method commonly used requires vacuum drying with gentle heating which carries the potential of premature fluid extraction and, hence, isotopic fractionation of the trapped fluid.
2. The two different methods used to extract fluid inclusions (crushing and gentle heating versus decrepitation at high temperature) appear to give systematically different results.
3. Since oxygen is present in calcite walls of the fluid inclusions, oxygen isotopic alteration is possible due to interaction between the oxygen in the water and in the calcite. As a result  $\delta^2\text{H}$  of the trapped fluid is analysed instead, and the correlated  $\delta^{18}\text{O}$  calculated from the meteoric water line relationship between hydrogen and oxygen (equation 3.2; Clark and Fritz 1997). The problem now lies in the fact that the relationship might have changed over time at a given location and could be different at the same time at different locations.

For these reasons there is a tendency to interpret paleoclimate records in speleothems in terms of warmer/cooler trends rather than actual absolute temperatures.

Talma and Vogel (1992) tried to solve the problem in their study of Cango Caves, Cape Province, South Africa, by estimating drip water composition from water of a

confined and dated groundwater aquifer in the same region as the cave. Although this method seems to have worked in their study, it is not likely that it will be of widespread use since not many caves will have datable old groundwater in the vicinity. As well, it still only provides an approximation of the drip water composition and not an actual analysis of it.

The isotopic composition of rain, drip water and calcite are influenced by several factors (Ford and Williams 1989)

1. Temperature of the cave interior ('Cave temperature effect'). During glacial times the cave interior becomes cooler and the heavier isotopes are preferentially deposited in the calcite; hence a decrease in temperature results in an increase in isotopic values.
2. Temperature of the ocean from which the rain is formed ('Oceanic effect'). During glacial times sea surface temperatures (SST) decrease resulting in a preferential evaporation of the lighter isotopes and thus the formation of rain with a lighter composition; hence a decrease in temperature may result in a decrease in isotopic values in falling rain.
3. At the same time however, the ocean itself has a heavier isotopic composition during glacial times due to the fact that the lighter isotopes are preferentially locked up in the massive glaciers; a decrease in temperature results in an increase in isotopic values.

In most published instances the first and third factors predominate and the interglacial periods are represented as troughs in the oxygen isotopic records. However, oceanic sites appear to be more influenced by the oceanic effect and they show interglacial periods as peaks (Gascoyne 1992). The deep sea oxygen record composed from Foraminifera (Imbrie *et al.* 1984; Martinson *et al.* 1987) shows an inverse relationship with temperature (third factor) and thus with isotopic records from speleothem taken from oceanic locations.

#### 3.7.1. *Sample description and methods.*

For the present study, seven speleothem samples from both cave types (three from Notch caves and four from Upper caves) were analysed for oxygen and carbon isotope ratios. The samples selected had at least one, if not more, reliable dates; had, in general, one or more hiatuses; were of adequate size for a significant run of measurements; and showed clear growth layers in most instances. Since equilibrium deposition is required for reliable isotopic records, the samples were taken from locations that were believed to be of high relative humidity and stable temperature. There were two exceptions to this; one was a flowstone from the entrance to Peter's Cave and another was located a few metres from one of the entrances to First Cay Cave. Both, however, were most likely located further inside at the time of their deposition, because there is strong evidence that the outer part of these caves has been lost to cliff erosion.

Six drip water and one rain water sample were also analysed for their  $^2\text{H}/^1\text{H}$

ratios. Unfortunately, due to technical problems, the samples were never analysed for  $^{18}\text{O}/^{16}\text{O}$ . Instead, oxygen values were calculated using the meteoric water line relationship between deuterium and oxygen (Clark and Fritz 1997:37):

$$\delta^2H = 8.13 \delta^{18}O + 10.8 \quad (3.2)$$

Smith (1987) measured  $\delta^{18}\text{O}$  of similar waters on Grand Cayman. The calculated values for drip water from Cayman Brac are very similar to his mean fresh water value (Table 3.3). Since drip water is water intercepted on its way to the fresh water lens, the drip water and freshwater samples should have similar values and the calculated values are therefore considered to be reliable approximations of the modern day drip water signals on Cayman Brac.

The modern day  $\delta^{18}\text{O}$  of calcite ( $\delta^{18}\text{O}_c$ ) can be calculated using the oxygen ratios from the drip water ( $\delta^{18}\text{O}_w$ ; Ford and Williams 1989: 369)

$$\delta^{18}\text{O}_c = \delta^{18}\text{O}_w + 10^3 \ln \alpha \quad (3.3)$$

where  $10^3 \ln \alpha$  is the equilibrium fractionation factor calculated from (O'Neil *et al.* 1969)

$$10^3 \ln \alpha = 2.78 \cdot 10^6 T_K^{-2} - 2.89 \quad (3.4)$$

where  $T_K$  is temperature in °K. Assuming a constant  $\delta^{18}O_w$  and a temperature range of 20-30°C (subtropical), equation (3.4) implies that for each 1 degree increase in temperature there is about a 0.2 ‰ decrease in  $\delta^{18}O_c$ .

The  $\delta^{18}O_w$  of Cayman Brac shows a positive relationship with temperature ( $R^2 = 0.84$ )

$$\delta^{18}O_w = 1.51 T - 43.78 \quad (3.5)$$

This is typical for oceanic sites where the effect of the temperature dependence of  $\delta^{18}O_p$  outweighs the effects of  $\delta^{18}O_{sw}$  and  $\alpha_{c-w}$  (Gascoyne 1992).

Carbon isotopes can be interpreted in terms of the vegetative cover above the cave (e.g. Talma and Vogel 1992) or variations of the fraction of bedrock carbon in the speleothem  $\delta^{13}C$  (Shopov *et al.* 1997).

Plants can be divided into three groups based on the photosynthetic cycles used (Clark and Fritz 1997):

1. Calvin or  $C_3$  cycle; 85% of plant species; most terrestrial ecosystems, especially temperate and high latitude regions and tropical forests;
2. Hatch-Slack or  $C_4$  cycle; 5% of plant species; hot open ecosystems, e.g. tropical and temperate grass lands;
3. Crassulacean acid metabolism (CAM) cycle, whereby the plants switch from  $C_3$  photosynthesis during the day to  $C_4$  photosynthesis at night; 10% of plant species

(mainly cacti); desert ecosystems.

Uptake of CO<sub>2</sub> by plants is accompanied by a 5-25 ‰ depletion in δ<sup>13</sup>C. The δ<sup>13</sup>C of atmospheric CO<sub>2</sub> is about -7 ‰ VPDB, C<sub>3</sub> plants have δ<sup>13</sup>C between -24 and -30 ‰ VPDB (average -27 ‰ VPDB); δ<sup>13</sup>C of C<sub>4</sub> plants ranges from -10 to -16 ‰ VPDB (average -12.5 ‰ VPDB) and CAM plants can have carbon isotopic compositions which span the whole range of C<sub>3</sub> and C<sub>4</sub> plants, but lie usually somewhere in between. The δ<sup>13</sup>C of the soil will be enriched by about 4 ‰ with respect to the composition of the dominant vegetation due to out gassing of CO<sub>2</sub> during plant decay by aerobic bacteria. Thus soil δ<sup>13</sup>C in a C<sub>3</sub> dominated environment will be about -23 ‰ VPDB, whereas δ<sup>13</sup>C<sub>soil</sub> in a C<sub>4</sub> environment is around -9 ‰ VPDB (Clark and Fritz 1997). Equilibrium isotopic fractionation between soil and calcite then results in δ<sup>13</sup>C<sub>calcite</sub> of ~ -12.8 ‰ VPDB beneath a C<sub>3</sub> dominated environment and ~ +1.2 ‰ VPDB beneath a C<sub>4</sub> vegetative cover (Talma and Vogel 1992). Using these two values and the assumption that

$$\delta^{13}C_{calcite} = x \delta^{13}C_{C_3} + (1-x) \delta^{13}C_{C_4} \quad (3.6)$$

the percentage C<sub>3</sub> plants (x) can be calculated as

$$x = \frac{\delta^{13}C_{calcite} - 1.2}{-14} * 100 \quad (3.7)$$

Shopov *et al.* (1997) note that the "Traditional explanation of δ<sup>13</sup>C variations by

C<sub>3</sub>-C<sub>4</sub> type plants variations...cannot explain the observed temperature dependence of  $\delta^{13}\text{C}$  ... in the speleothems" (p. 65). Instead they argue that all  $\delta^{13}\text{C}$  variations in calcite can be explained by the influence of bedrock  $\delta^{13}\text{C}$  on calcite  $\delta^{13}\text{C}$ . The bedrock fraction in the carbon isotopic composition of calcite varies with climatic conditions and cannot be considered constant over time since climate has not remained constant over time. The carbon isotopic composition of speleothem consists of two components: modern and "dead" (or bedrock) carbon. The percentage modern carbon in speleothem (M) can be calculated as (Shopov *et al.* 1997)

$$M = \frac{\delta^{13}\text{C}_{\text{calcite}} - \delta^{13}\text{C}_{\text{bedrock}}}{\delta^{13}\text{C}_{\text{soil}} - \delta^{13}\text{C}_{\text{bedrock}}} * 100 \quad (3.8)$$

and the bedrock percentage is then  $D = 100 - M$ . The  $\delta^{13}\text{C}_{\text{bedrock}} = +0.6 \text{ ‰ VPDB}$  (Smith 1987: 86) and  $\delta^{13}\text{C}_{\text{soil}}$  can be calculated by (Bottinga 1968)

$$\delta^{13}\text{C}_{\text{soil}} = 10^3 \ln \alpha + \delta^{13}\text{C}_{\text{calcite}} \quad (3.9)$$

where  $10^3 \ln \alpha$  is (Bottinga 1968)

$$10^3 \ln \alpha = -2.988 \cdot 10^6 T_K^{-2} + 7.663 \cdot 10^3 T_K^{-1} - 2.4612 \quad (3.10)$$

where  $T_K$  is temperature in °K. Using equations (3.3) through (3.5)  $T_K$  is calculated from

$$1.51T_K^3 - (\delta^{18}C_{calcite} + 459.15)T_K^2 + 2.78 \cdot 10^6 = 0 \quad (3.11)$$

### 3.8 *Discussion of stable isotope results*

Plots of  $\delta^{18}O$  versus  $\delta^{13}C$  were drawn for all samples (Fig. 3.13). The  $\delta^{18}O$  values range from -1.16 to -7.04 ‰VPDB and  $\delta^{13}C$  from -0.40 to -12.13 ‰VPDB. The modern  $\delta^{18}O_c$  calculated from the drip waters of six caves (Table 3.3) range from -5.33 to -8.08 ‰VPDB. The  $\delta^{18}O_c$  value of -10.24 ‰VPDB from Rebecca's Cave appears to be an outlier probably resulting from rapid throughflow of infiltration water without much exchange with the heavier soil air (see below). The modern values compare with the lighter part of the speleothem samples, suggesting that the latter have undergone either an increase in temperature or kinetic fractionation, or a combination of both.

The  $\delta^{18}O$  and  $\delta^{13}C$  records of samples containing a hiatus are sharply bi-modal in most instances, the two modes placing before and after the hiatus (Fig. 3.13). The only exception to this finding is GC8, a stalactite from Great Cave. PC4 from Peter's Cave does not show a clearly visible hiatus, but rather an abrupt change of colour approximately half way up its growth section. On the  $\delta^{18}O$  versus  $\delta^{13}C$  plot a break is seen at the point of change. Thus, it is probable that the colour change coincides with a growth hiatus here also. Dating is needed to determine if the break in colour and shift in stable isotope signal is an abrupt

change in environmental factors or the result of a growth cessation during which time the climatic/environmental conditions changed more gradually. The darker, older part has higher values of both  $\delta^{18}\text{O}$  and  $\delta^{13}\text{C}$ , suggesting higher temperatures and a greater percentage of drought resistant vegetation ( $\text{C}_4$  plants), hence a warmer, drier climate.

On Figure 3.14 the values of  $\delta^{18}\text{O}$  and  $\delta^{13}\text{C}$  of the selected samples of Cayman Brac and the Mona sample are plotted against each other. The figure clearly shows two groups of values for Cayman Brac and one for Isla de Mona. The mean values and one and two standard deviation envelopes are drawn as well. One of the Cayman groups and the Mona group are very similar and statistically significantly different, both for  $\delta^{18}\text{O}$  and  $\delta^{13}\text{C}$  at  $\alpha = 0.01$  (t-test), from the other Cayman group.

A most important point is that these two groupings distinguish two different time periods (Fig. 3.15a). These are, broadly, before and after 120 ka, although the exact timing of the change is imprecisely established due to the uncertainties in the dating. The mean of  $\delta^{18}\text{O}$  of the “old” group is  $-5.43 \pm 1.01$  ‰VPDB whereas the mean of the “young” group is  $-3.42 \pm 0.84$  ‰VPDB for Cayman Brac and  $-3.12 \pm 0.84$  ‰VPDB for Isla de Mona. The mean  $\delta^{13}\text{C}$  of the “old “ and “young” groups are  $-10.07 \pm 1.13$  ‰VPDB and  $-4.94 \pm 2.40$  ‰VPDB (CB) and  $-3.81 \pm 1.50$  ‰VPDB (Mona) respectively.

For Cayman Brac, the time division also represents a division in the source cave types: the younger isotope analyses are mostly from samples from Notch caves and the older ones from Upper caves (Fig. 3.15b). The exception to this are samples RdC2, an older flowstone from a Notch cave and PC4, a young flowstone from an Upper cave. The

separation into different isotopic behaviour before and after 120 ka appears to be due to factors of location or distance from the cave entrances and, thus, of stability of the microclimatic environment (Fig. 3.15c). The older samples largely derive from locations that were deep inside the caves at time of deposition, where the  $RH > 90\%$  and the temperature is stable. The younger samples tend to come from locations halfway between the entrance and the back of the shorter Notch caves, where  $RH > 80\%$  and the temperature displays some diurnal fluctuation. Again, sample PC4 is an exception to this division, because it was taken from an entrance location, where both RH and temperature presently vary with outside weather conditions. However, as noted, this location was probably much further inside at the time of the calcite deposition and would have experienced a mid-cave (or even a deep cave) climate. The same holds true for FC3 which is located close to the present entrance of the cave, but was most likely formed at a mid-cave location. Samples taken from one growth layer in this sample do not show any variation in both stable isotope values, indicating deposition under equilibrium conditions. The importance of location is that where the RH has not reached 90-100%, evaporation can occur resulting in strong kinetic fractionation of the isotope records. This is then reflected in an increase in the abundance of both  $\delta^{18}\text{O}$  and  $\delta^{13}\text{C}$ .

The modern day samples also show the importance of location. The drip water sample from Rebecca's Cave is almost identical to the rainwater sample (Table 3.3) suggesting that this sample has had very little interaction with the soil air or heavier bedrock ( $\delta^{18}\text{O}_{\text{dolomite}} = +1.6 \text{‰ VPDB}$  and  $\delta^{18}\text{O}_{\text{carbonate}} = -2.6 \text{‰ VPDB}$  for the Bluff Group on Grand

Cayman, Smith 1987: 86) on its way down. This low value appears to result from rapid throughflow and a short travel path because the surviving roof of this cave is very thin, just a few decimeters, and soil cover is thin and patchy above it as it is over most of the island (Tarhule-Lips and Ford in review, Ch.2). Three other samples were taken from approximately 10 m from the cliff where the roofs are much thicker and these samples did show an increase in  $\delta^{18}\text{O}$  as a result of soil gas and bedrock interaction. The increase in Bat's Cave is less than in Skull and Peter's Caves because it still has a thinner roof and faster travel time, leaving less time for interactions. The entrance sample from First Cay Cave is heavier than the sample taken about 20 m away in the same cave, suggesting that some kinetic fractionation due to evaporation has taken place. This effect, however, is far less than the rapid throughflow effect seen in Rebecca's Cave. Excluding the effect of fast travel time, there appears to be a decrease in the  $\delta^{18}\text{O}_w$  with increasing distance from the cliff and decreasing external climatic influence (Table 3.3): -2.7 ‰ VPDB at 3 m; about -3.8 ‰ VPDB at 10 m and -5.1 ‰ VPDB at 20 m. This distance/climatic influence effect is also reflected in the  $\delta^{18}\text{O}$  calculated for modern calcite (Table 3.3): -5.3, -6.5 and -7.6 ‰ VPDB at 3, 10 and 20 m respectively.

An important contributor to any increased evaporation effects in the records is the opening of the caves due to cliff recession at the time of the formation of the Notch during the last interglacial period. In principle, this would have had greater effects on the Notch caves due to their characteristic morphology, a large room close to the cliff. Any slight recession would create a large aperture (entrance) in the outer wall of the chamber. The

Upper caves, on the other hand, do not display the large entrance rooms, so that a slight retreat of the cliff would have only minor influence on the size of the entrance and thus the microclimatic conditions inside the cave.

Considering the Mona sample, all the above characterizations of the Cayman group that it resembles are valid, too: the sample is younger than 120 ka, Cueva del Agua, Sardinera, has the morphology of a typical Notch cave and the sample was taken from what is a mid-cave location.

### 3.8.1 *Oxygen isotopic composition*

The  $\delta^{18}\text{O}$  records for all speleothems are represented in Figure 3.16 together with the deep sea oxygen record of Imbrie *et al.* (1984). The record by Imbrie *et al.* (1984) was chosen in preference to that by Martinson *et al.* (1987) because the latter does not cover the entire period of speleothem growth found on Cayman Brac: also this more precise record would not really contribute more to the interpretation of the results considering the error present in the dating of the Cayman records themselves and the fact that the individual values represent the mean of several hundreds to several thousands of years. Where there is only one date available for a sample, the speleothem records are drawn for the two probable mean growth rates, 0.5 and 1.0 mm/ka, established above.

There is no clear isotopic distinction between glacial and interglacial periods in the speleothem records, regardless of which growth rate is used. This was also found by Gascoyne (1979) and Harmon (1976) for samples from Jamaica and Mexico respectively.

The absence of a distinction between glacial and interglacial is not only obvious when all samples are considered together but also when the samples are looked at individually. In general the older samples ( $> 150$  ka) have a better time fix and a longer record than the younger samples. Both FC3 and the older part of TC12 have two dates fixing them in place and both cross a glacial-interglacial boundary without significant change in their records. FC3 does show a peak at the boundary but the values before and after it are very similar and do not show the same trend as the deep sea record. TC12<sub>old</sub> is even more steady over the entire length of its record, fluctuating by less than 1 ‰ VPDB.

From Figure 3.16 the older samples appear to show an inverse relationship with the deep sea record whereas the relationship between the younger samples and the deep sea record is less clear due to the uncertainties in the dating. As noted above, the inverse relationship is not uncommon for oceanic sites due to the importance of the oceanic effect (Gascoyne 1992). From the deep sea records it is known that there is a 1.5 ‰ increase in  $\delta^{18}\text{O}$  between the peak of an interglacial and the trough of a glacial period (Shackleton 1987). A steady record without such changes between glacial and interglacial periods (e.g. TC12<sub>old</sub>) suggests that there is another effect or effects that counteract this 1.5 ‰ difference. An increase in air temperature of  $7.5^\circ\text{C}$  (equation 3.4) would result in an increase of 1.5 ‰ and could thus theoretically be the counteracting influence. However, such a large temperature difference is not known for the Caribbean (e.g. Mix *et al.* 1999; Norton *et al.* 1997). It should be noted that the intra-sample fluctuations within glacial or interglacial periods often exceed 1.5 ‰ in almost all samples.

The high inter-sample variations in oxygen values for samples of the same age, as is seen in the younger samples, may be explained by factors specific to the cave environments. This is evident in the similar variability in the calculated modern calcite values. It therefore appears that factors like infiltration velocity, roof thickness and evaporation may cause inter-sample variations of 2 ‰ or more at a given time between samples in caves in differing settings. Since these factors are likely to operate in a constant manner over time, however, the resulting isotopic records should still display significant effects of changes in the climatic factors.

### 3.8.2 *Carbon isotopic composition*

The  $\delta^{13}\text{C}$  records over time of all samples are represented in Figure 3.17 for both growth rates. As has been noted above, there is a sharp change in the carbon isotopic composition around 120 ka. The inter-sample variations found in the oxygen records are also visible in the carbon records, but are less pronounced, e.g. the great variation between  $\delta^{18}\text{O}$  of  $\text{RdC2}_{\text{old}}$  and  $\text{TC12}_{\text{old}}$  is not found in the carbon record. Figure 3.18 shows the same records in terms of bedrock carbon fraction in speleothem calcite and percentage  $\text{C}_3$  vegetation. In general terms, an increase in the amount of bedrock carbon implies a shift towards a drier and warmer climate as does a decrease in percentage of  $\text{C}_3$  plants. Thus the two records show an inverse relationship with each other, as can be clearly seen from Figure 3.18.

The older samples show a relatively constant bedrock contribution of about 50%, indicative of a tropical humid environment, whereas the younger samples show a much

greater variation with bedrock contributions ranging from 50-90%, i.e. humid to desert-like environments (Shopov *et al.* 1997). The percentage of C<sub>3</sub> plants for the older samples varies from about 50-90% whereas the younger samples show values as low as 10%. These observations would suggest that the climate on Cayman Brac was relatively constant from about 450 ka to 120 ka, namely warm and wet, and that it changed to a drier climate with more CAM and C<sub>4</sub> plants following the last interglacial. No such sudden shift in climate since the last interglacial is known from other areas of the Caribbean. It is therefore believed to be a result of more localised effects, such as location within the cave and the resulting microclimatic effect specific for that cave.

### 3.8.3 *Oxygen and carbon records of individual samples*

Results in Figures 3.16 ( $\delta^{18}\text{O}$ ), 3.17 ( $\delta^{13}\text{C}$ ) and 3.18 (percentage bedrock carbon and C<sub>3</sub> plants) may be analysed sample by sample, from old to young (i.e. 5NE1 to SC41). Some direct correlation between  $\delta^{18}\text{O}$  and temperature is assumed and the above remarks on inter-sample variability should be kept in mind.

5NE1. The older part of this flowstone shows a bimodal distribution in the oxygen record indicating, within stage 12, a warmer period and the peak of this cold stage. There is approximately a 4 ‰ difference between these two groupings. The carbon record, on the other hand, does not show any such distribution and no hiatus or clear colour change can be seen at the break of the oxygen record. Assuming that the oxygen record indeed shows a sudden shift towards lower temperatures, this change did not

appear to have an effect on the vegetative cover or the factors responsible for a change in bedrock contribution. This would suggest that precipitation remained high enough to support a  $C_3$  dominated vegetation.

The younger overgrowth falls in stage 3, just after the peak of this particular interstadial. It shows an increase in oxygen values, which would suggest, according to our assumptions, that there is an increase in temperature. In the carbon record there is a sudden increase followed by a sharp decrease for the same time period. It appears to be changing from a humid to a desert like environment. This trend towards a drier warmer climate contradicts the trend of the deep sea record which is moving towards the peak of stage 2 and suggests a decrease in temperature. Either the timing or our assumptions are in error for this particular sample.

RdC2. The older part of this drapery shows a very steady oxygen and carbon record during stages 11 and 10 (or stage 10 only, depending on the growth rate considered) and a wave during stage 9. The oxygen record ends with a sharp decrease because the last value is much lower than the rest. It was taken from the outer, red layer of this part, just before the hiatus. In the carbon record this same point is almost identical to the previous point and shows no indication of being an outlier. Ignoring the final oxygen value, this sample indicates that the environmental changes of stage 9 had a greater influence on the calcite composition than the changes during stage 10/11. The younger part falls in the middle of stage 7, the penultimate interglacial period and has oxygen values much closer to the modern day values than those of the older

part.

TC12. The older part of TC12 covers most of the time period of the older part of RdC2 and also shows oxygen values much closer to the modern day values. The carbon records for the same samples over the same time period are very close. This suggests that during stages 9-10/11 some local environmental factor(s) influenced the oxygen isotopic composition for RdC2 and TC12 in a different manner without doing same for carbon.

The younger part of TC12 represents the peak of the last interglacial, stage 5e. The entire sample has an oxygen isotopic composition close to that calculated for modern calcite, although the older part does have lower values and a greater variability. The zig-zag pattern in the oxygen record of the younger part is not found in the smoother deep sea record. This could be due to the greater resolution of the former. The similarity of TC12 and the younger part of RdC2 to modern values may imply that the temperature during the previous interglacial periods, and likely during part of the glacial periods, was similar to that of today, about 26.5°C, and that there have been few temperature fluctuations. The carbon isotopic composition of the younger part is the lowest of all samples and is about 1‰ lower than that of the older part. Unfortunately no modern carbon isotopic composition is available and thus a similar comparison between old and modern environments can not be made on the basis of carbon.

FC3. This flowstone from First Cay Cave grew during the later part of stage 7 and the

first half of stage 6. There are rapid fluctuations in its oxygen and carbon records which could represent frequent climatic/environmental changes. There is no clear difference in either record between the interglacial half and the glacial half. Better dating of the upper limit of this sample might stretch the record towards a greater age, making the peaks and troughs of the oxygen record more closely related to the fluctuations of the deep sea record. The one high value in both records at the boundary between stages 7 and 6 could be an outlier or more likely is a valid point indicative of some environmental change influencing both carbon and oxygen.

PC4. On all three figures the darker, older part of PC4 is represented directly following the younger part. However, as mentioned above, there is probably a growth hiatus between the darker and the lighter parts which would shift the darker part towards greater ages. Because of the uncertainty in the timing of this part of the sample it will not be considered further.

The lighter part of the record has grown during the later half of stage 5 and all of stage 4. The oxygen record remained steady during stage 4 and showed a dip and rise during stage 5 which was either in direct correlation ( $gr = 1.0 \text{ mm/ka}$ ) or inverse correlation ( $gr = 0.5 \text{ mm/ka}$ ) with the deep sea record. The carbon record shows the same dip at the end of stage 5 and a more cyclic (zig-zag) pattern during stage 4.

GC8. This sample was dated by alpha spectrometry which is reflected in the poor time fix and big difference between the records at the two different growth rates. It has the highest oxygen values and the largest intra-sample variation. Also, the records for

oxygen and carbon follow each other closely, showing the same ups and downs. All this hints at vigorous kinetic fractionation of the record which seems to be confirmed by the fact that part of the calcite has the appearance of surficial or cave entrance evaporitic calcite. Considering the evaporation effect a constant, the fluctuations should still reflect some overall climatic fluctuations of environmental factors. The older part, which grew during the same time period as the lighter part of PC4, shows a similar dip and rise as PC4, only there is a peak before and after this section rather than the steady values found in the PC4 records. The younger part grew during stage 2 and possible during parts of stages 1 and 3 as well. The sharp dip in its oxygen record corresponds with the peak of stage 2.

- SC41. This sample too shows a peak at about the same time as PC4 and GC8, around 75-80 ka, after which it decreases, showing an inverse relationship between its oxygen record and the deep sea record. The two other parts of this sample suggest that the temperature increased from stage 4 to the middle of stage 3. The carbon record on the other hand suggests that the climate was desert like in the middle of stage 4, became more humid at the beginning of stage 3 after which it returned to a desert like environment at the peak of stage 3.

In general, better dating of the younger samples will improve the interpretation of the isotopic records. Taking young samples from the interior of Upper caves should also help clarify the observed changes around 120 ka in both isotopic records.

### 3.9. *Conclusion*

Throughout the Caribbean Region, growth hiatuses and partial dissolution have been observed in speleothem samples (Tarhule-Lips and Ford in review, Ch. 2). The hiatuses are evidence of interruption of the water supply to the speleothem, either due to loss of drip water, or to the flooding of the cave, as a result of a relative rise in sea level or to a situation in which corrosion exceeds deposition. Dissolution at the time of growth cessation indicates that the speleothems have come into contact with aggressive water either in the form of floodwater (subaqueous environment) or condensation water (subaerial environment).

Dating of the hiatuses shows that their timing in a given sample does not necessarily coincide with the timing of hiatuses in other samples. There does appear to be a tendency for the older, higher samples to have the beginning of a hiatus during a glacial period. At present, the majority of the speleothems located above sea level on Cayman Brac and Isla de Mona, the islands of interest to this study, are no longer growing. As with the hiatuses there is no time coincidence for when the samples stopped growing. Also, some display dissolution while others have stayed intact both during hiatuses and after the samples stopped growing all together.

Modern day speleothem growth and cessation appears to be dominated by the microclimatic conditions within the cave in question rather than the regional climatic conditions (Tarhule-Lips and Ford 1998, Ch. 4). Since it has been shown in this chapter that what was happening in the past was similar, it would be easy to suggest that all hiatuses were results of local microclimatic fluctuations within the caves themselves. However, if this were

invariably the case then the samples would not be likely to start to grow again after some period of time because the climatic conditions (entrance zone and evaporitic) should still be unfavourable for speleothem growth. One plausible solution was that rise in sea level would increase the relative humidity (RH) permitting at least the mid-cave positions to reach RH levels that would again favour net deposition over corrosion. In this case the renewed growth would coincide with interglacial periods, which, as has been shown before, is not necessarily the case. Hence, it is not possible to simply look at the present to find out what happened in the past, even though the situations appear to be similar.

Analyses of carbon and oxygen isotopic records do not reveal a distinction between glacial and interglacial periods either. The individual oxygen isotopic records seem to show an inverse relationship with the deep sea oxygen record, especially for the older samples. This inverse relationship can also be seen in the calculated modern day calcite values.

The plots of  $\delta^{13}\text{C}$  versus  $\delta^{18}\text{O}$  of individual samples clearly show bi-modal distribution where the sample has a hiatus, the modes placing before and after it. Plotting the values of all samples on one figure reveals that the samples can be grouped into two statistically different (t-test,  $\alpha = 0.01$ ) groups. These two groups can be characterised in terms of time, “young” (<120 ka) and “old” (>120 ka); or cave type, Notch and Upper caves; or location within the cave, entrance, mid-cave (RH > 80%, some diurnal temperature fluctuations) and deep cave (RH > 90%, stable temperature) position. The sample of Isla de Mona falls into the “young” group and displays the same characteristics: <120 ka, Notch cave morphology and mid-cave position.

It therefore appears that the hiatuses separate different local climatic conditions/periods; depositional conditions before and after the hiatus are not similar as would be expected if the hiatuses corresponded with the glacial periods, and the growth of speleothem with the interglacial periods or *vice versa*.

Modern calcite values for oxygen in the calcite were calculated from the drip water values and correspond with the speleothem values found during the previous interglacials and some glacials. This suggests that the climatic/environmental conditions have not changed much over time. They also show that there can be great inter-sample variation between different cave environments. It appears that a very thin roof and fast throughflow result in drip water oxygen compositions close to that of rain water and that evaporation also plays a role, though less than the throughflow effect in our case, resulting in higher  $\delta^{18}\text{O}$  values due to kinetic fractionation. Excluding the throughflow effect, there appears to be a decrease in the  $\delta^{18}\text{O}_w$  with increasing distance from the cliff and decreasing external climatic influence: -2.7 ‰VPDB at 3 m; about -3.8 ‰VPDB at 10 m and -5.1 ‰VPDB at 20 m. This distance/climatic influence effect is also reflected in the  $\delta^{18}\text{O}$  calculated for modern calcite (Table 3.3): -5.3, -6.5 and -7.6 ‰VPDB at 3, 10 and 20 m respectively.

The inter-sample variations calculated for modern calcite were more than 2 ‰. This helps to explain the great inter-sample variations found in the ancient speleothems, especially in the younger isotopic records. Supposing that the temperature and climatic conditions changed little in tropical marine regions over the Quaternary, the calculated modern day range of oxygen isotopic composition of calcite can be used as a basis for comparison with

the speleothems. It then appears that samples GC8, the dark part of PC4, the older part of RdC2 and the latest part of 5NE1 all must have undergone more localised environmental influences like evaporation (e.g. GC8) or extremely slow throughflow (e.g. PC4 and RdC2). Unfortunately no modern day  $\delta^{13}\text{C}$  values are known and a similar comparison, which would have given us more insight into the vegetative cover, is not possible for this isotope.

The carbon records indicate that the climate over the period 450-120 ka has been relatively stable: tropical and wet, dominated by  $\text{C}_3$  type plants. Since the last interglacial period the carbon record shows the same large fluctuations observed in the oxygen records which could be interpreted as changes between tropical and desert like environments, dominated by  $\text{C}_3$  and a combination of  $\text{C}_4$  and CAM type plants respectively. However, such drastic change in climate has not been reported from other parts of the Caribbean and could be the result of more localised effects.

It is clear from the above observations that a more detailed study needs to be undertaken to address the apparent climate change at about 120 ka. Young samples from deep inside Upper caves and better dating of the younger samples, as well as more detailed isotope sampling are needed.

## References

- Bakalowicz, M.J., Ford, D.C., Miller, T.E., Palmer, A.N. and Palmer, M.V. (1987) Thermal genesis of dissolution caves in the Black Hills, South Dakota. *Geological Society of America Bulletin*, 99: 729-738.
- Bar-Matthews, M., Ayalon, A. and Kaufman, A. (1997). Late Quaternary paleoclimate in the Eastern Mediterranean Region from stable isotope analysis of speleothems at Soreq Cave, Israel. *Quaternary Research*, 47: 155-168.
- Berstad, I.M., Einevoll, S. and Lauritzen, S.E. (1997). U-series dating and stable isotope analysis of some last interglacial speleothems from north Norway. *Proceedings of the 12<sup>th</sup> International Congress of Speleology, Switzerland*, Vol. 1: 53-54.
- Bottinga, Y. (1968). Calculated fractionation factors for carbon and oxygen in the system calcite - carbon dioxide - water. *Journal of Physical Chemistry*, 72: 800-808.
- Clark, I.D. and Fritz, P. (1997). *Environmental isotopes in hydrogeology*. New York (Lewis Publishers), 328 p.
- Coplen, T.B., Winograd, I.J., Landwehr, J.M. and Riggs, A.C. (1994). 500,000-year stable carbon isotopic record from Devils Hole, Nevada. *Science*, 263: 361-365.
- Dansgaard, W., Johnsen, S.J., Clausen, H.B., Dahl-Jensen, D., Gundestrup, N.S., Hammer, C.U., Hvidberg C.S., Steffensen, J.P., Sveinbjörnsdottir, A.E., Jouzel, J. and Bond, G. (1993). Evidence for general instability of past climate from 250-kyr ice-core record, *Nature*, 364: 218-220.

- Dreybrodt, W. (1988). *Processes in karst systems: physics, chemistry, and geology*. Berlin (Springer), 288 p.
- Ford, D.C. and Williams, P.W. (1989). *Karst geomorphology and hydrology*. London (Unwin Hyman), 601 p.
- Frisia, S., Borsato, A., Spiro, B., Heaton, T., Huang, Y., McDermott, F. and Dalmeri, G. (1997). Holocene paleoclimatic fluctuations recorded by stalagmites: Grotta di Ernesto (northeastern Italy). *Proceedings of the 12<sup>th</sup> International Congress of Speleology, Switzerland*, Vol. 1: 77-80.
- Gascoyne, M. (1979). *Pleistocene climates determined from stable isotope and geochronologic studies of speleothem*. Ph.D. Thesis, McMaster University, Hamilton, Ontario, Canada, unpublished, 433 p.
- Gascoyne, M. (1992). Palaeoclimate determination from cave calcite deposits. *Quaternary Science Reviews*, 11: 609-632.
- Gascoyne, M., Ford, D.C. and Schwarcz, H.P. (1981). Late Pleistocene chronology and paleoclimate of Vancouver Island determined from cave deposits. *Canadian Journal of Earth Sciences*, 18: 1643-1652.
- Goede, A., Green, D.C. and Harmon, R.S. (1986). Late Pleistocene palaeotemperature record from a Tasmanian speleothem. *Australian Journal of Earth Science*, 33: 333-342.
- Harmon, R.S. (1976). *Late Pleistocene paleoclimates in North America as inferred from isotopic variations in speleothems*. Ph.D. Thesis, McMaster University, Hamilton, Ontario, Canada, unpublished.

- Harmon, R.S., Thompson, P., Schwarcz, H.P. and Ford, D.C. (1978a) Late Pleistocene paleoclimates of North America as inferred from stable isotope studies of speleothems. *Quaternary Research*, 9: 54-70.
- Harmon, R.S., Schwarcz, H.P. and O'Neil, J.R. (1978b). D/H ratios in speleothem fluid inclusions: a guide to variations in the isotopic composition of meteoric precipitation? *Earth and Planetary Science Letters*, 42: 254-266.
- Harmon, R.S., Schwarcz, H.P. and Ford, D.C. (1978c). Stable isotope geochemistry of speleothems and cave waters from Flint Ridge-Mammoth Cave system, Kentucky: implications for terrestrial climate change during the period 230,000 to 100,000 years B.P. *Journal of Geology*, 86: 373-384.
- Hendy, C.H. (1971) The isotopic geochemistry of speleothem I. The calculation of the effect of different modes of formation on the isotopic composition of speleothem and their applicability as paleoclimatic indicators. *Geochim Cosmochim Acta*, 35: 801-824.
- Hendy, C.H. and Wilson, A.T. (1968) Paleoclimatic data from speleothems. *Nature*, 216: 48-51.
- Holmgren, K., Karlén, W., Lauritzen, S.E., Lee-Thorp, J., Partridge, T.C., Shaw, P.A. and Tyson, P.D. (1997) Spleochronology, stable isotopes and laminae analysis of stalagmites from southern Africa. *Proceedings of the 12<sup>th</sup> International Congress of Speleology, Switzerland*, Vol. 1: 55-56
- Imbrie, J., Hays, J.D., Martinson, D.G., McIntyre, A., Mix, A.C., Morley, J.J., Pisias, N.G., Prell, W.L. and Shackleton, N.J. (1984). The orbital theory of Pleistocene climate:

- support from a revised chronology of the marine  $^{18}\text{O}$  record. *in: A.L. Berger et al.* (eds.) *Milankovitch and climate*. Dordrecht (Reidel): 269-305.
- Jouzel, J., Lorius, C., Petit, J.R., Genthon, C., Barkov, N.I., Kotlyakov, V.M. and Petrov, V.M. (1987). Vostok ice core: a continuous isotope temperature record over the last climatic cycle (160,000 years), *Nature*, 329: 403-408.
- Lips, R.F.A. (1993). *Speleogenesis on Cayman Brac, Cayman Islands, British West Indies*. M.Sc. Thesis, McMaster University, Hamilton, Ontario, Canada, unpublished, 223 p.
- Lundberg, J. (1990). *U-series dating of carbonates by Mass Spectrometry with examples of speleothem, coral and shell*. PhD Thesis, McMaster University, Hamilton, Ontario, Canada, unpublished 271 p.
- Lundberg, J. and Ford, D.C. (1994). Late Pleistocene sea level change in the Bahamas from Mass Spectrometric U-series dating of submerged speleothem. *Quaternary Science Reviews*, 13: 1-14.
- Martinson, D.G., Pisias, N.G., Hays, J.D., Imbrie, J., Moore, T.C., Jr., and Shackleton, N.J. (1987). Age dating and the orbital theory of the Ice Ages: development of a high-resolution 0 to 300,000-year chronostratigraphy. *Quaternary Research*, 27: 1-29.
- Millen, T.M. and Dickey, D.N., Jr. (1987). A stable isotopic investigation of waters and speleothems in Wind Cave, South Dakota: an application of isotope paleothermometry. *NSS Bulletin*, 49: 10-14.
- Mix, A.C., Morey, A.E. and Pisias, N.G. (1999). Foraminiferal faunal estimates of

- paleotemperature: circumventing the no-analog problem yields cool ice age tropics. *Paleoceanography*, 14(3): 350-359.
- Müller, G., Botz, R. and Linz, E. (1986). Oxygen and carbon isotope composition of calcareous tufa and speleothems from the Schwäbische Alb, SW Germany. *N. Jb. Miner. Mh.*, 7: 289-296.
- Norton III, F.L., Hausman, E.D. and McElroy, M.B. (1997). Hydrospheric transports, the oxygen isotope record, and tropical sea surface temperatures during the last glacial maximum. *Paleoceanography*, 12(1): 15-22.
- O'Neil, J.R., Clayton, R.N. and Mayeda, T.K. (1969). Oxygen isotope fractionation in divalent metal carbonates. *Journal of Chemical Physics*, 51: 5547-5558.
- Schwarcz, H.P. (1986). Ch. 7. Geochronology and isotope geochemistry of speleothems. In: Fritz, P. and Fontes, J.Ch. (Eds) *Handbook of environmental isotope geochemistry*, Vol 2 (The terrestrial Environment, B). New York (Elsevier), 557 p.: 271-303.
- Schwarcz, H.P. and Gascoyne, M. (1984). Uranium series dating of Quaternary deposits. In: Mahaney, W.C. (ed.) *Quaternary dating methods*. Amsterdam (Elsevier): 33-51.
- Shackleton, N.J. (1987). Oxygen isotopes, ice volume and sea level. *Quaternary Science Reviews*, 6: 183-190.
- Shopov, Y.Y., Ford, D.C. and Schwarcz, H.P. (1994). Luminescent microbanding in speleothems: high-resolution chronology and paleoclimate. *Geology*, 22: 407-410.
- Shopov, Y.Y., Tsankov, L.T., Yonge, C.J., Krouse, H.P.R. and Jull, A.J.T. (1997). Influence of the bedrock CO<sub>2</sub> on stable isotope records in cave calcites. *Proceedings of the*

12<sup>th</sup> International Congress of Speleology, Switzerland, Vol. 1: 65-68.

Smith, D.S. (1987). *The speleothemic calcite deposits on Grand Cayman Island, British West Indies*. M.Sc. Thesis, University of Alberta, Edmonton, Alberta, 171 p.

Talma, A.S. and Vogel, J.C. (1992). Late Quaternary paleotemperatures derived from a speleothem from Cango Caves, Cape Province, South Africa, *Quaternary Research*, 37: 203-213.

Tarhule-Lips, R.F.A. & D.C. Ford (1998). Condensation corrosion in caves on Cayman Brac and Isla de Mona. *Journal of Cave and Karst Studies*, 60 (2): 84-95.

Tarhule-Lips, R.F.A. & D.C. Ford (in review). Karstification of Cayman Brac. *Zeitschrift für Geomorphologie*.

Thompson, P., Schwarcz, H.P. and Ford, D.C. (1976). Stable isotope geochemistry, geothermometry, and geochronology of speleothems from West Virginia. *Geological Society of America Bulletin*, 87: 1730-1738.

Vézina, J., Jones, B. and Ford, D.C. (in press). Sea-level highstands over the last 500,000 years: evidence from the Ironshore Formation on Grand Cayman, British West Indies.

Winograd, I.J., Landwehr, J.M., Ludwig, K.R., Coplen, T.B. and Riggs, A.C. (1997). Duration and structure of the past four interglaciations. *Quaternary Research*, 48: 141-154.

Winograd, I.J., Coplen, T.B., Landwehr, J.M., Riggs, A.C., Ludwig, K.R., Szabo, B.J., Kolesar, P.T. and Revesz, K.M. (1992). Continuous 500,000-year climate record

from vein calcite in Devils Hole, Nevada. *Science*, 258: 255-260.

Woodroffe, C.D., Stoddart, D.R., Harmon, R.S. and Spencer, T. (1983). Coastal morphology and late Quaternary history, Cayman Islands, West Indies. *Quaternary Research*, 19: 64-84.

### List of Figures

- 3.1 Location of Cayman Brac, Isla de Mona and the caves studied.
- 3.2 **a)** Sample location in Skull Cave and **b)** cross section of SC41.
- 3.3 **a)** Sample location in Bats Cave, sketch **(b)** and cross section **(c)** of BC5.
- 3.4 Cross section of RdC2 from Road Cut Cave.
- 3.5 **a)** Sample location in Great Cave and **b)** cross section of GC8.
- 3.6 **a)** Sample location in First Cay Cave; **b)** schematic profile of the dissolution phases; cross sections of FC1 **(c)**, FC2 **(d)** and FC3 **(e)**.
- 3.7 **a)** Sample location in Tibbetts Turn Cave; cross sections of TC12 **(b)**, TC41 **(c)** and TC42 **(d)**.
- 3.8 **a)** Sample location in Peters Cave; cross sections of PC2 **(b)** and PC4 **(c)**.
- 3.9 **a)** Sample location in Northeast Cave #5 and **b)** cross section of 5NE1.
- 3.10 **a)** Sample location in Cueva del Agua, Sardinera, Isla de Mona, and **b)** cross section of CAS2.
- 3.11 Speleothem growth periods and hiatuses on Cayman Brac. Sample DWBAH from Lucayan Cavern, Grand Bahama Island (Lundberg and Ford 1994) is given for comparison. The vertical lines separate deep sea isotope stages (Martinson *et al.* 1987; Imbrie *et al.* 1984).
- 3.12 Proposed model of condensation corrosion in coastal cave on small holokarstic oceanic islands with young rocks (Tarhule-Lips and Ford 1998)
- 3.13 Plots of  $\delta^{18}\text{O}$  versus  $\delta^{13}\text{C}$  of all analysed samples from Cayman Brac and Isla de Mona. Note the distinctly different groupings before and after a hiatus for most of the samples.
- 3.14 Plot of  $\delta^{18}\text{O}$  versus  $\delta^{13}\text{C}$  of all analysed samples. Note the separation of the Cayman samples into two groups and the location of the Mona sample. Indicated are also the average values of each of the three groups with one and two standard deviation envelopes.
- 3.15 The average  $\delta^{18}\text{O}$  versus average  $\delta^{13}\text{C}$  of the various samples of Cayman Brac are plotted against each other. For those samples with hiatuses there are two, one for before and one for after the hiatus. The same data is represented in three different ways: **a)** relative age: >120 ka (“old”) versus < 120 ka (“young”); **b)** cave types: Notch versus Upper caves; and **c)** location within the caves: entrance, mid-cave and deep.
- 3.16 Oxygen isotope records of the Cayman samples for growth rates of 0.5 and 1.0 mm/ka. The deep sea record according to Imbrie *et al.* (1984) is also drawn for comparison.
- 3.17 Carbon isotope records of the Cayman samples for growth rates of 0.5 and 1.0 mm/ka.
- 3.18 Percentage bedrock carbon and  $\text{C}_3$  plants over time for  $gr = 1.0$  mm/ka **(a)** and  $gr$

= 0.5 mm/ka (b). Note: an increase in bedrock carbon and a decrease in C<sub>3</sub> plants indicates a trend towards a drier and warmer climate.

### **List of Tables**

- 3.1 Uranium-Thorium activity ratios and ages of 14 speleothem samples from Cayman Brac and one from Isla de Mona.
- 3.2 Mean speleothem growth rate calculated from four samples from Cayman Brac (this study) and one from Lucayan Cavern, Grand Bahama Island (Lundberg and Ford 1994).
- 3.3 Oxygen and deuterium stable isotope values for modern rain and drip water on Cayman Brac and calculated oxygen isotopic composition for modern calcite.

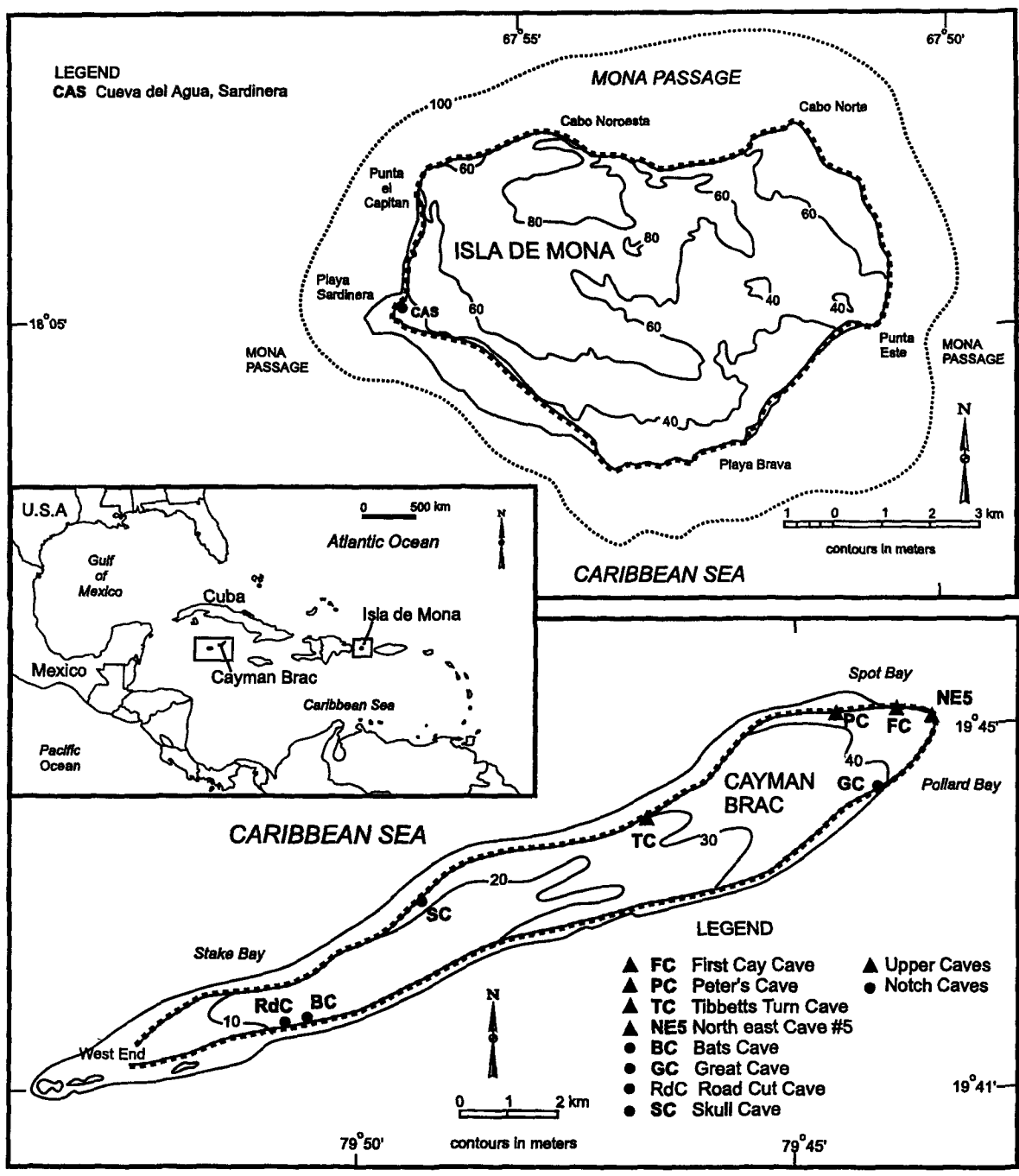


Fig. 3.1 Location of Cayman Brac, Isla de Mona and the caves studied.

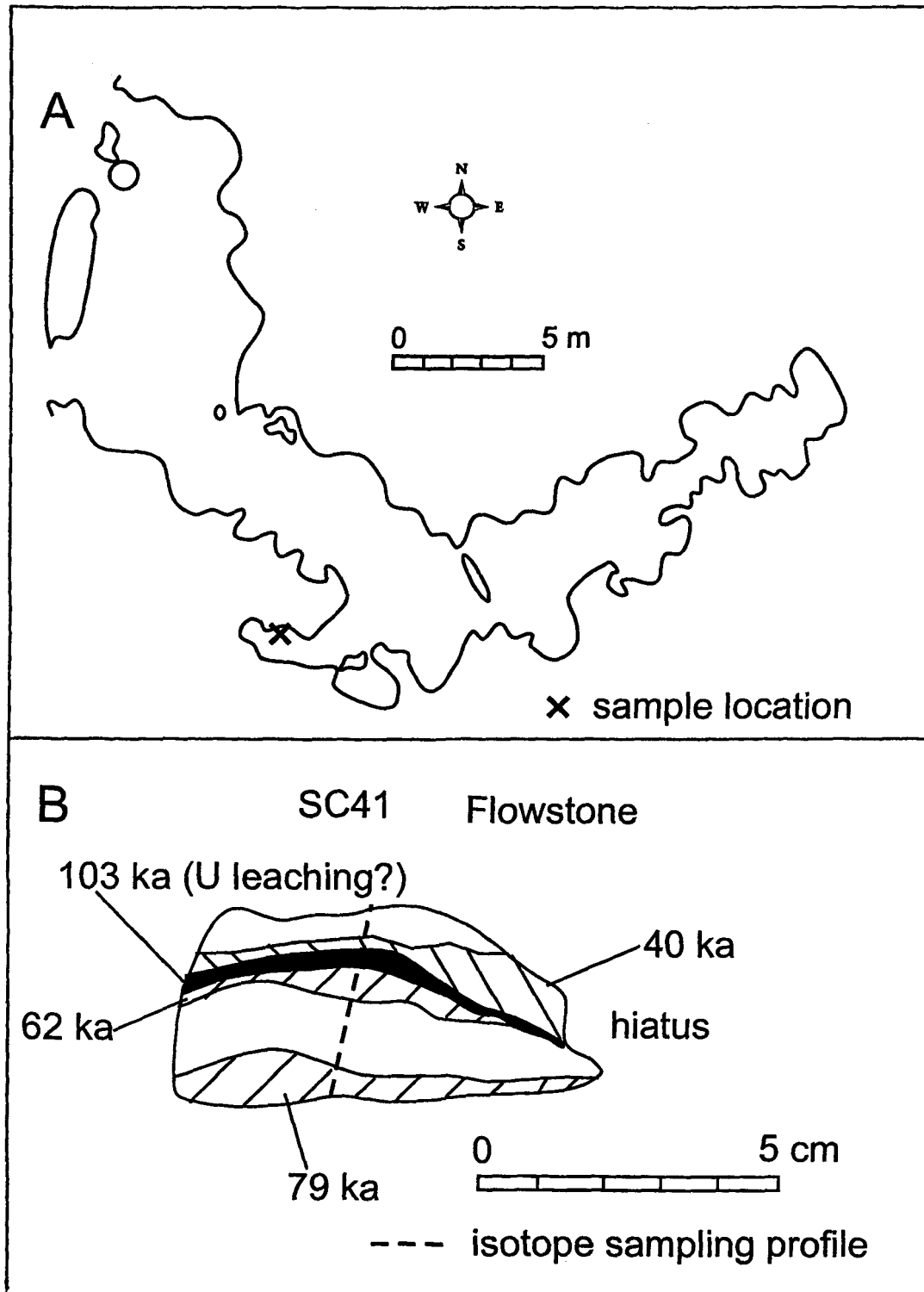


Fig. 3.2

a) Sample location in Skull Cave and b) cross section of SC41.

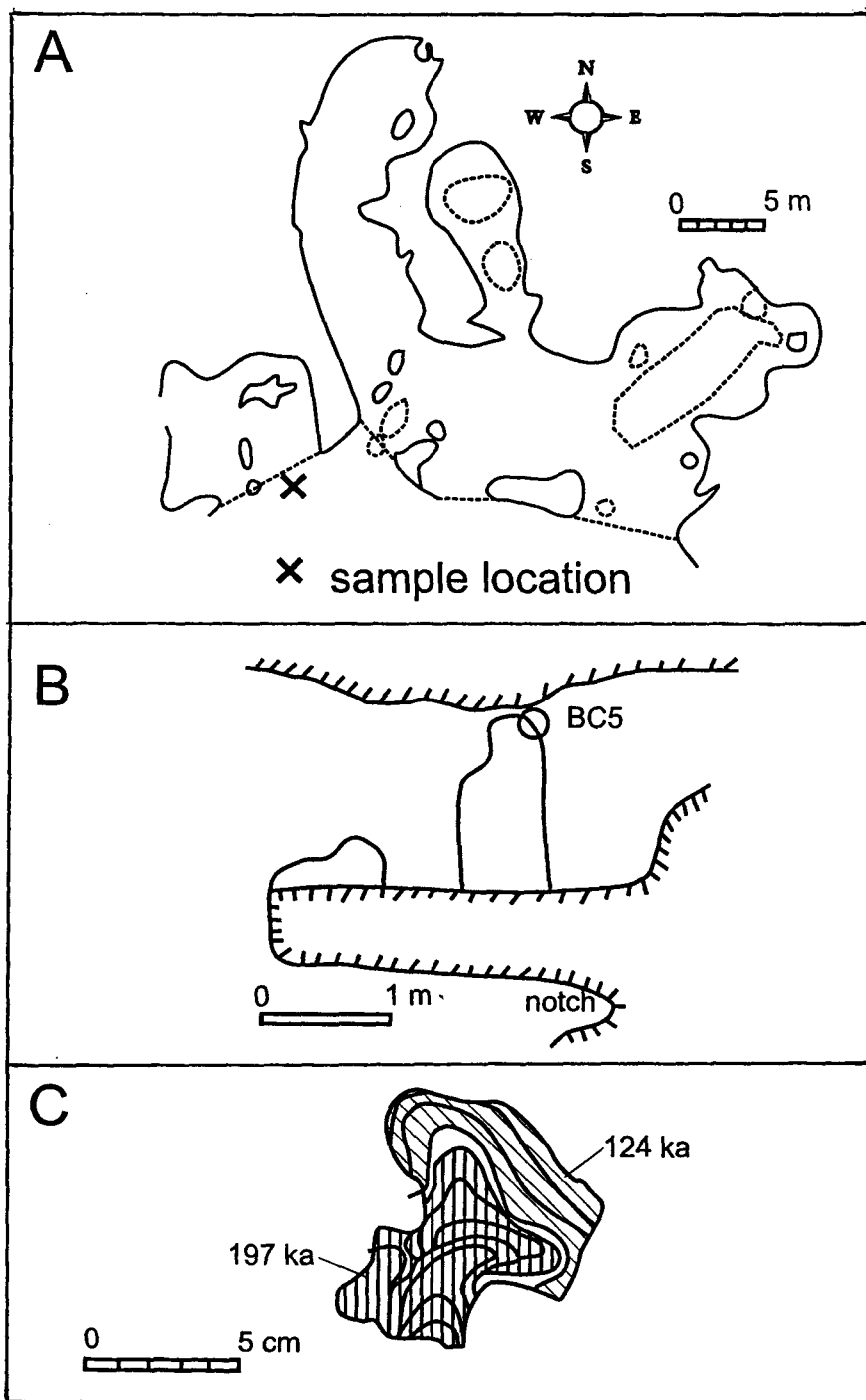


Fig. 3.3

a) Sample location in Bats Cave, sketch (b) and cross section (c) of BC5.

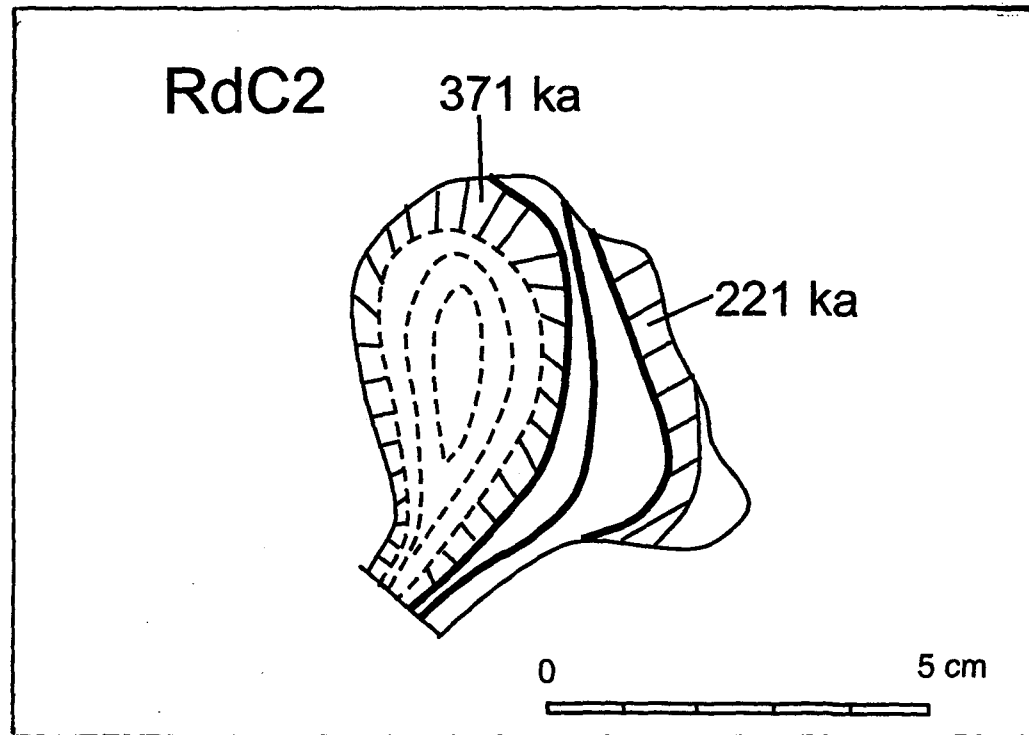


Fig. 3.4 Cross section of RdC2 from Road Cut Cave.

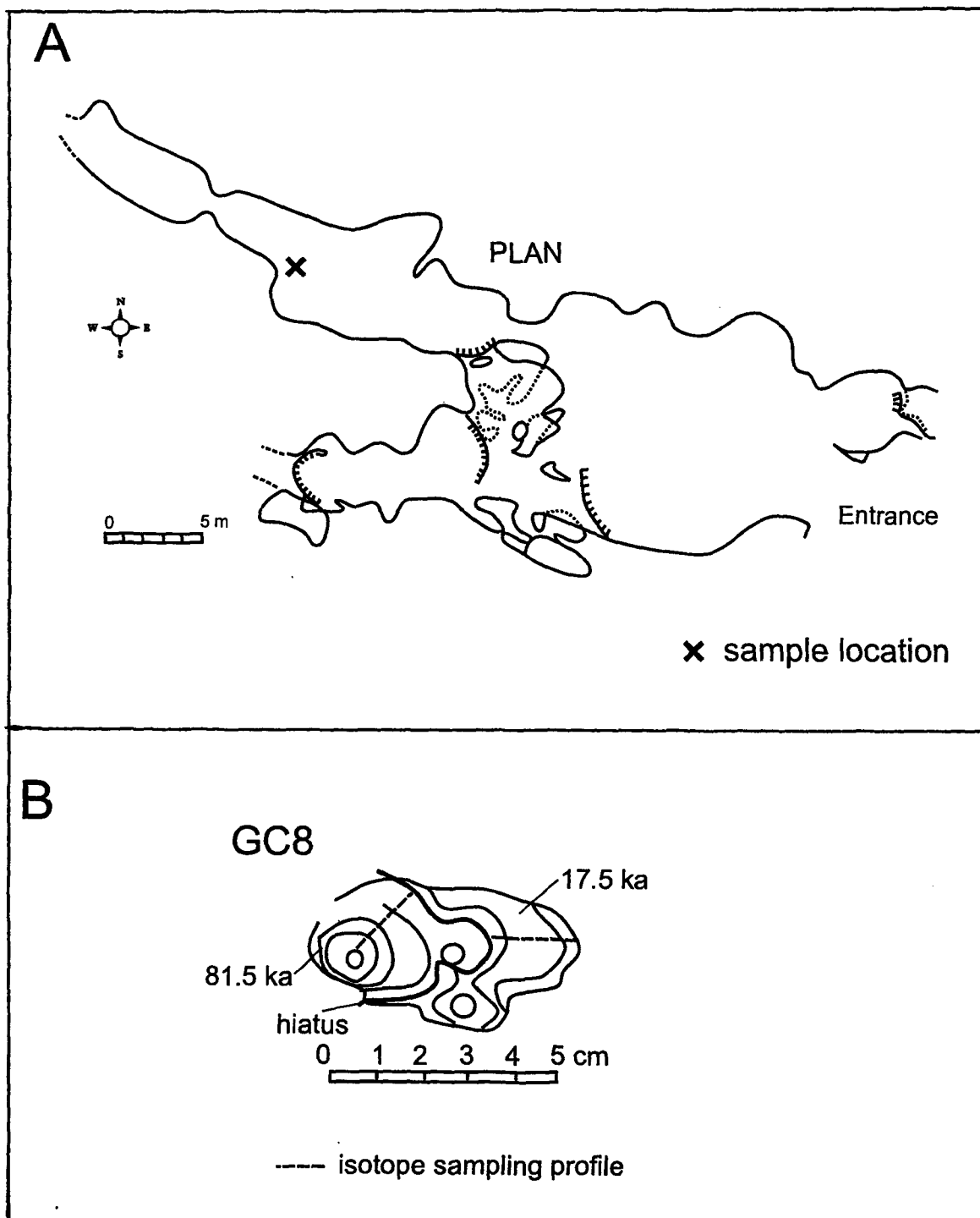


Fig. 3.5 a) Sample location in Great Cave and b) cross section of GC8.

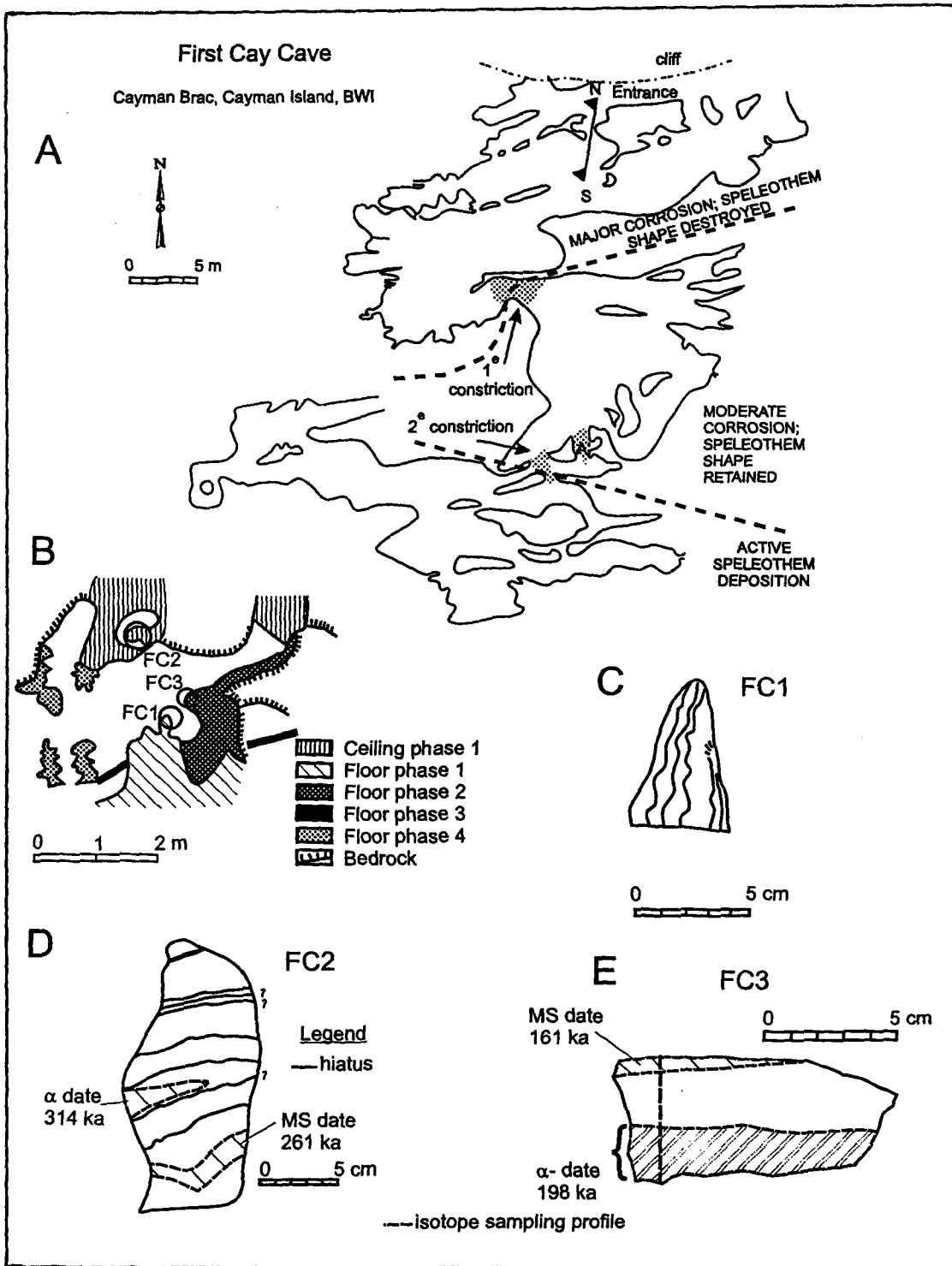


Fig. 3.6 a) Sample location in First Cay Cave; b) schematic profile of the dissolution phases; cross sections of FC1 (c), FC2 (d) and FC3 (e).

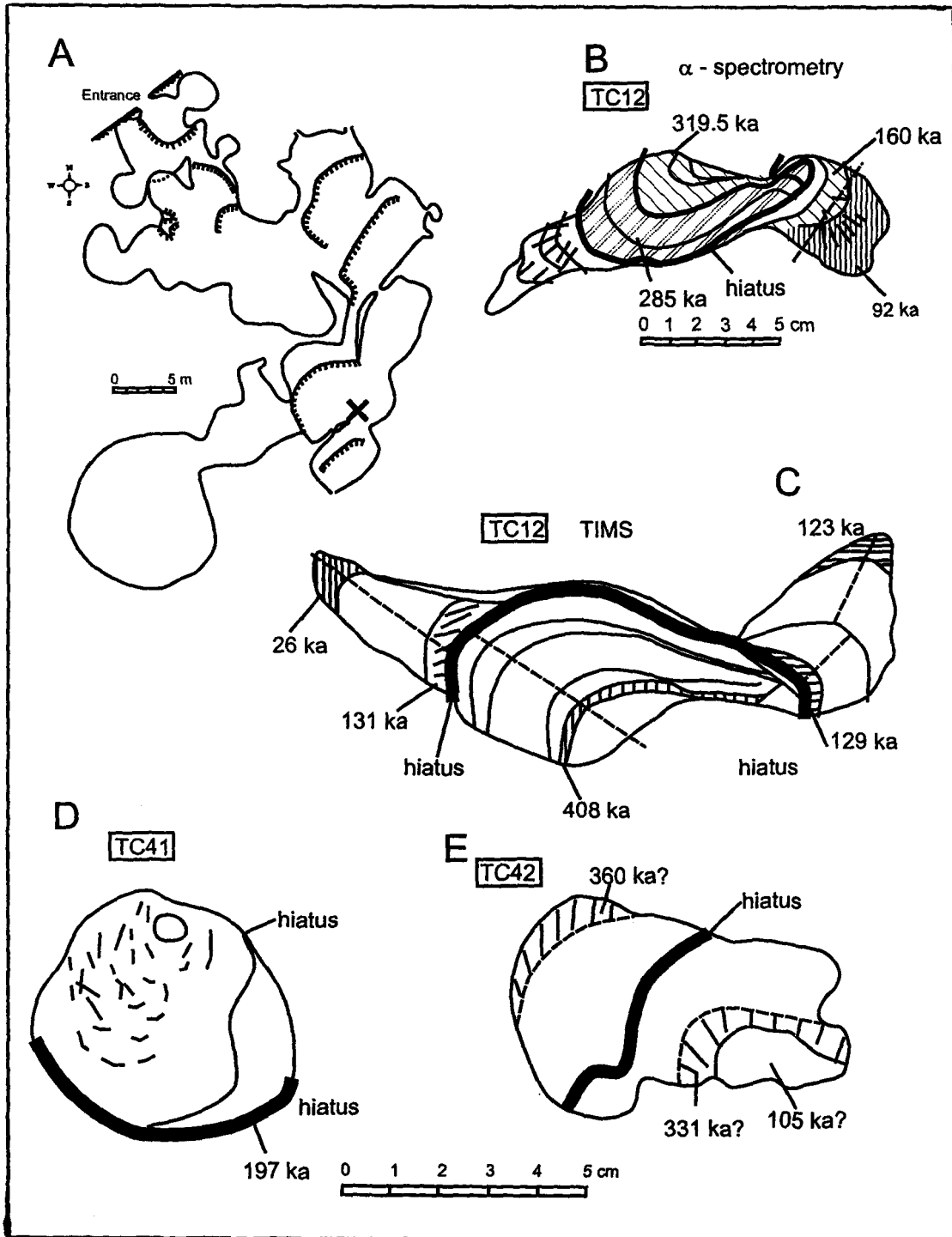


Fig. 3.7 a) Sample location in Tibbetts Turn Cave; cross sections of TC12 (b), TC41 (c) and TC42 (d).

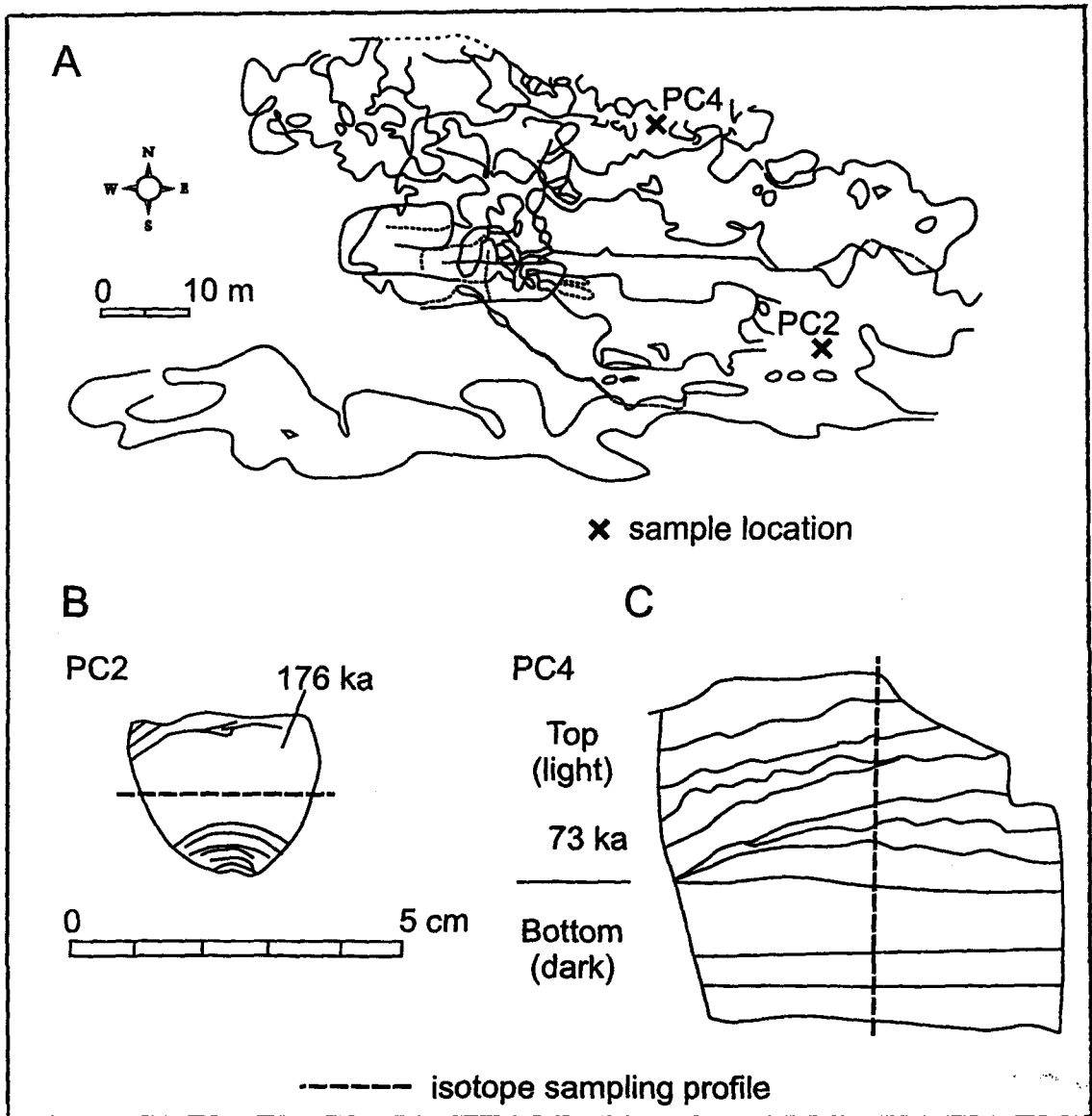


Fig. 3.8 a) Sample location in Peters Cave; cross sections of PC2 (b) and PC4 (c).

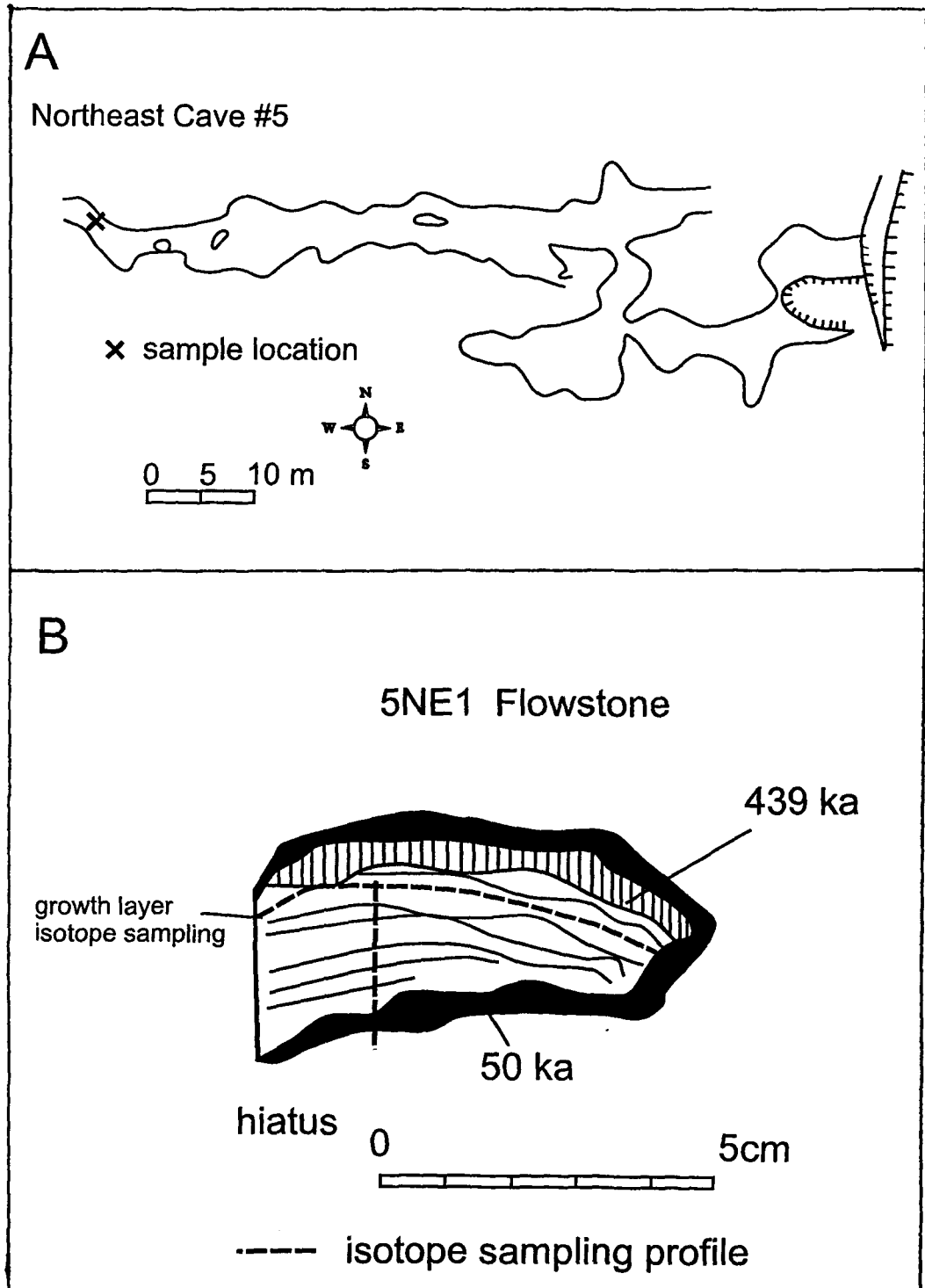


Fig. 3.9

a) Sample location in NorthEast Cave #5 and b) cross section of 5NE1.

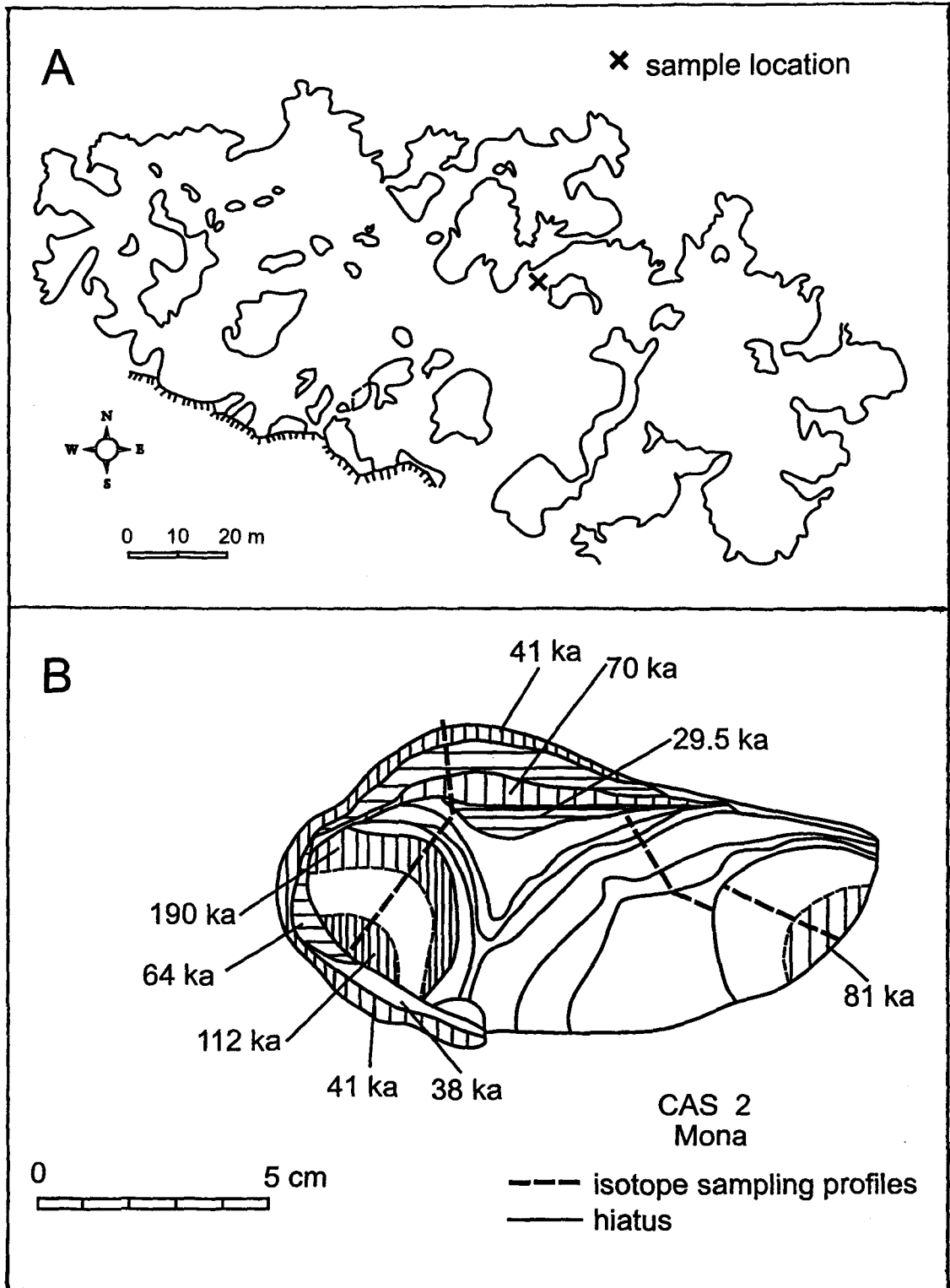
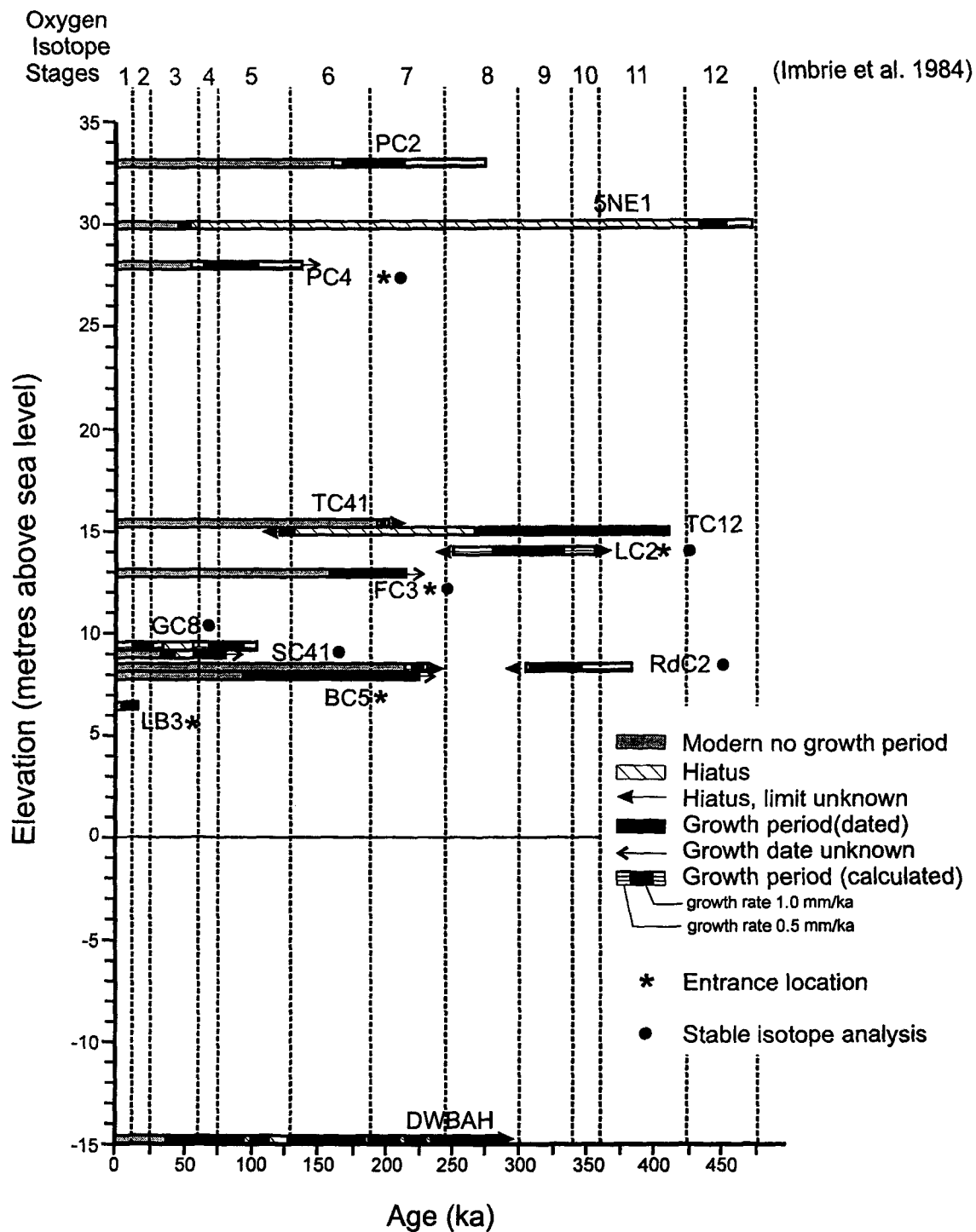


Fig. 3.10 a) Sample location in Cueva del Agua, Sardinera, Isla de Mona, and b) cross section of CAS2.



- 3.11 Speleothem growth periods and hiatuses on Cayman Brac. Sample DWBAH from Lucayan Cavern, Grand Bahama Island (Lundberg and Ford 1994) is given for comparison. The vertical lines separate deep sea isotope stages (Martinson *et al.* 1987; Imbrie *et al.* 1984).

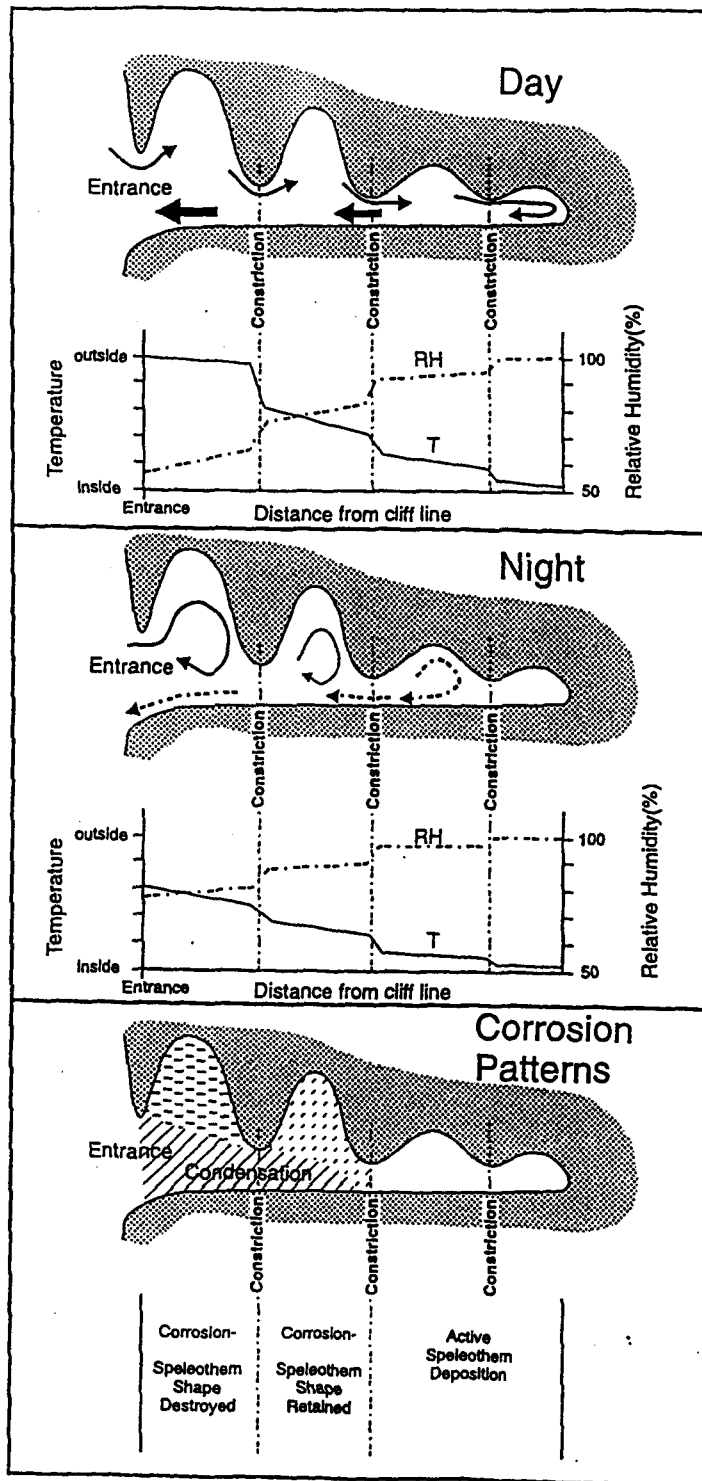


Fig. 3.12 Proposed model of condensation corrosion in coastal caves on small holokarstic oceanic islands with young rocks (Tarhule-Lips and Ford 1998).

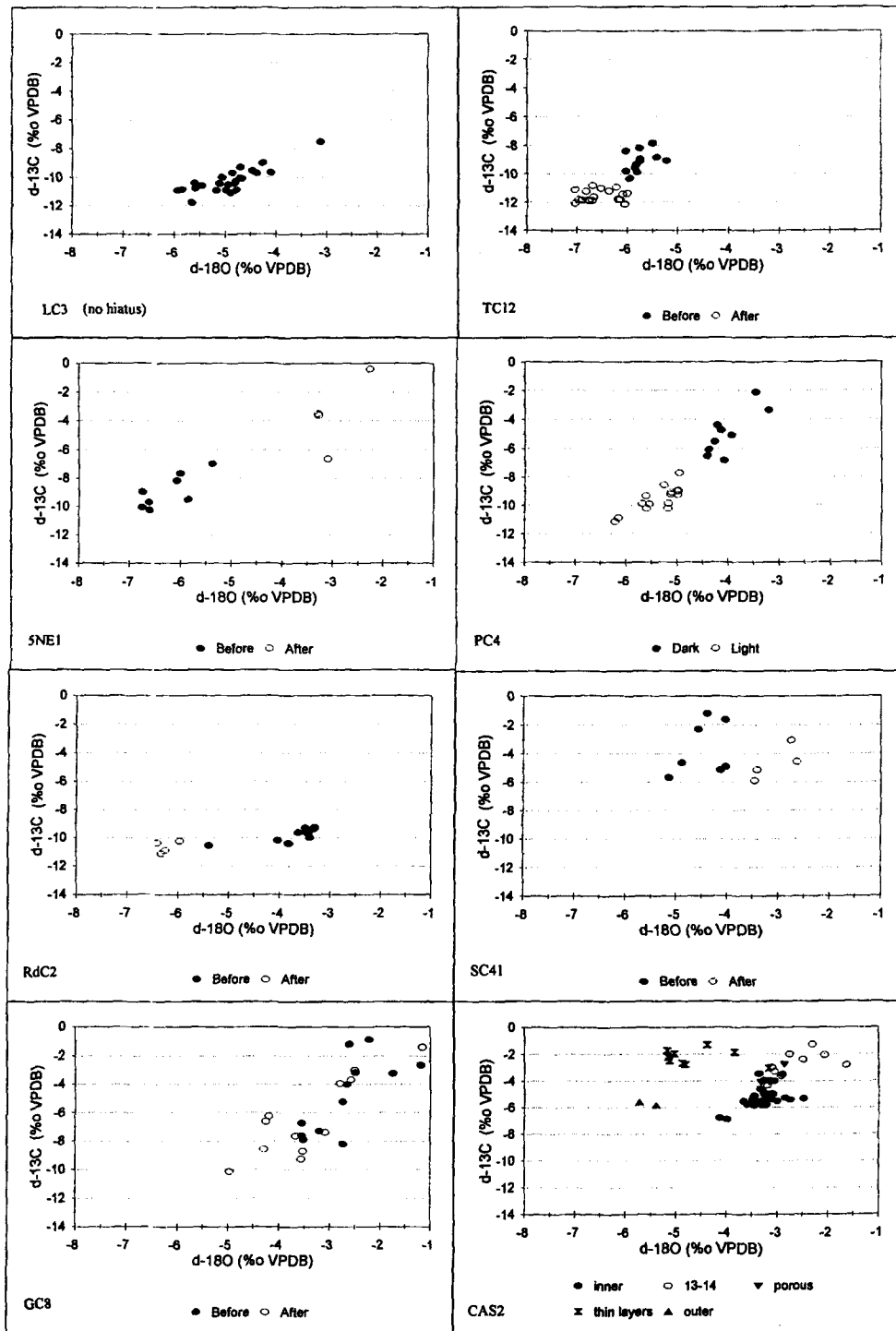


Fig. 3.13 Plots of  $\delta^{18}\text{O}$  versus  $\delta^{13}\text{C}$  of all analysed samples from Cayman Brac and Isla de Mona. Note the distinctly different groupings before and after a hiatus for most of the samples.

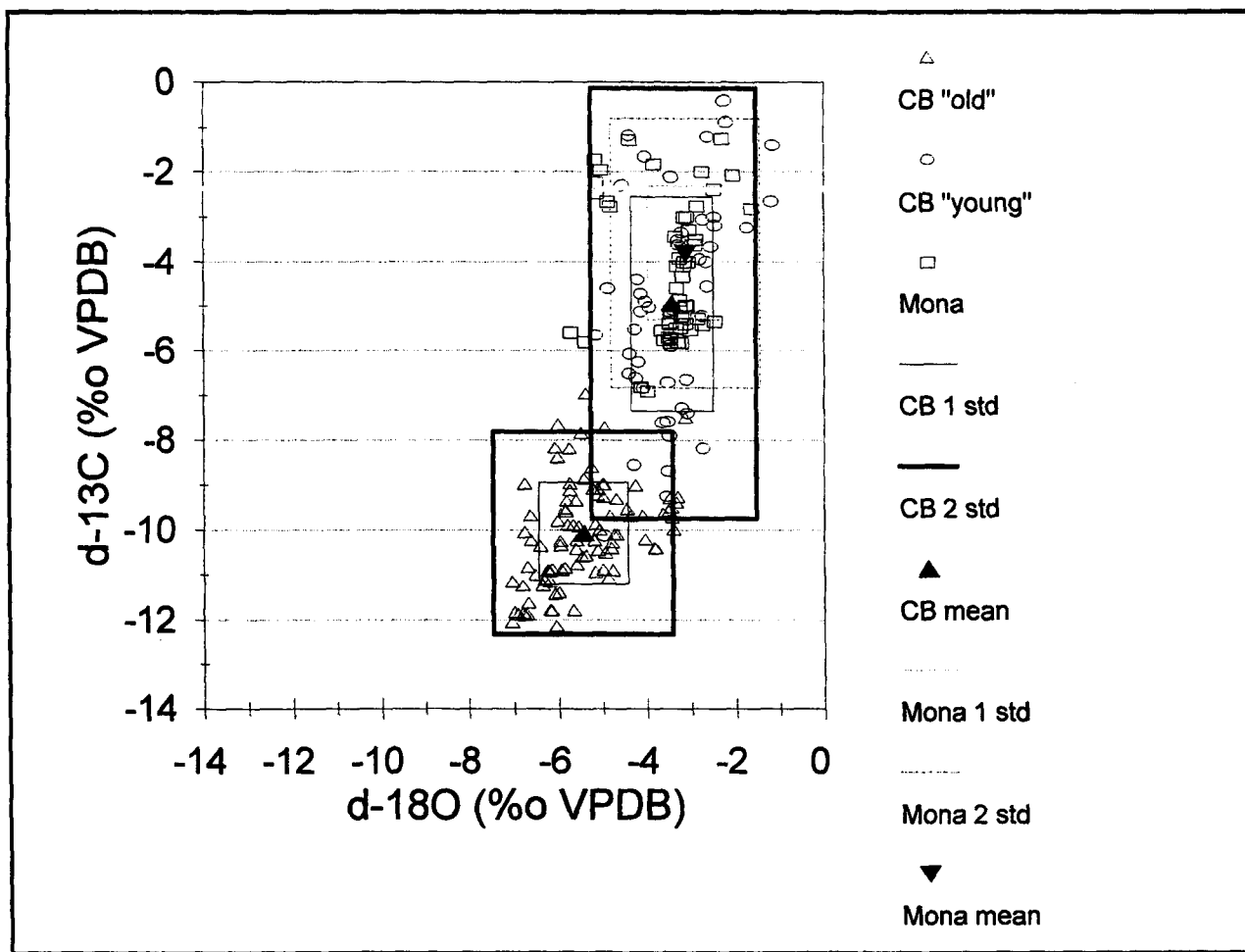


Fig. 3.14 Plot of  $\delta^{18}\text{O}$  versus  $\delta^{13}\text{C}$  of all analysed samples. Note the separation of the Cayman samples into two groups and the location of the Mona sample. Indicated are also the average values of each of the three groups with one and two standard deviation envelopes.

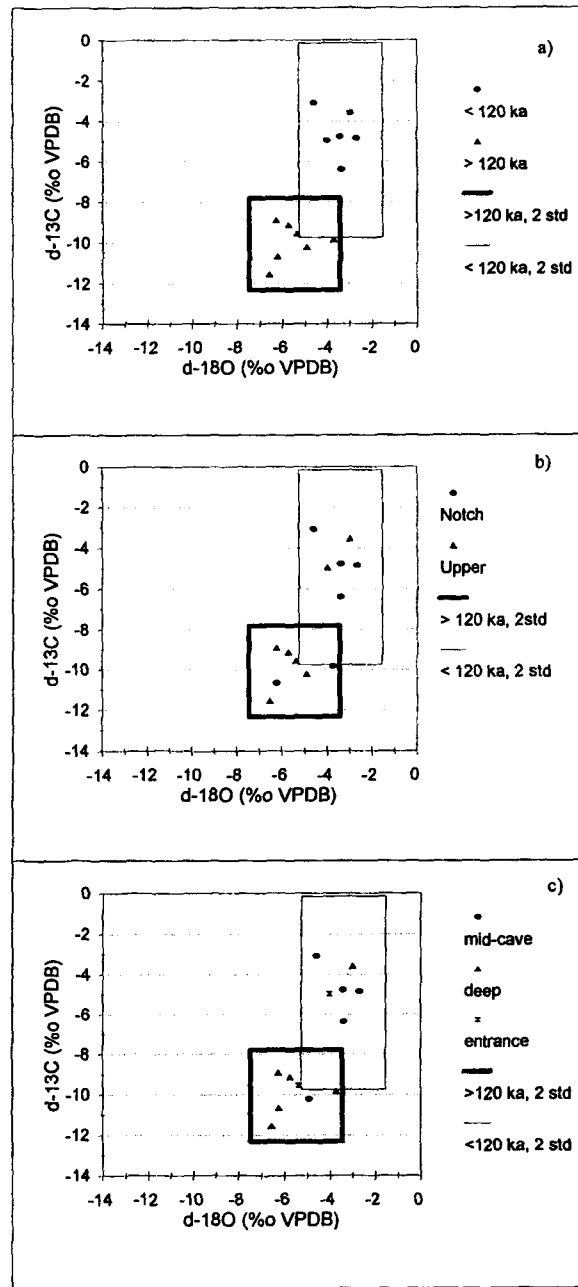


Fig. 3.15

The average  $\delta^{18}\text{O}$  versus average  $\delta^{13}\text{C}$  of the various samples of Cayman Brac are plotted against each other. For those samples with hiatuses there are two, one for before and one for after the hiatus. The same data is represented in three different ways: a) relative age: >120 ka ("old") versus < 120 ka ("young"); b) cave types: Notch versus Upper caves; and c) location within the caves: entrance, mid-cave and deep.

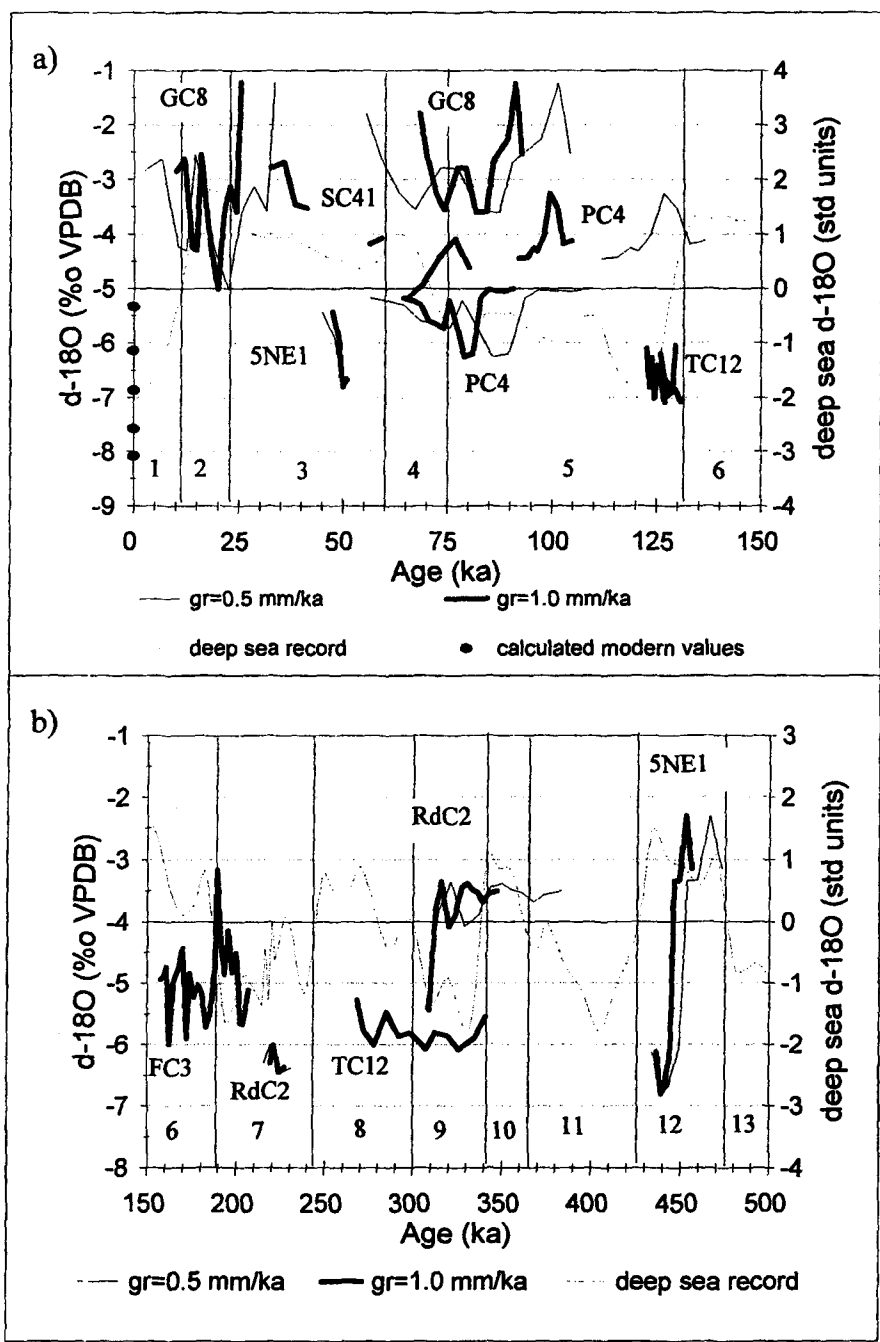


Fig. 3.16 Oxygen isotope records of the Cayman samples for growth rates of 0.5 and 1.0 mm/ka. The deep sea record according to Imbrie at al. (1984) is also drawn for comparison.

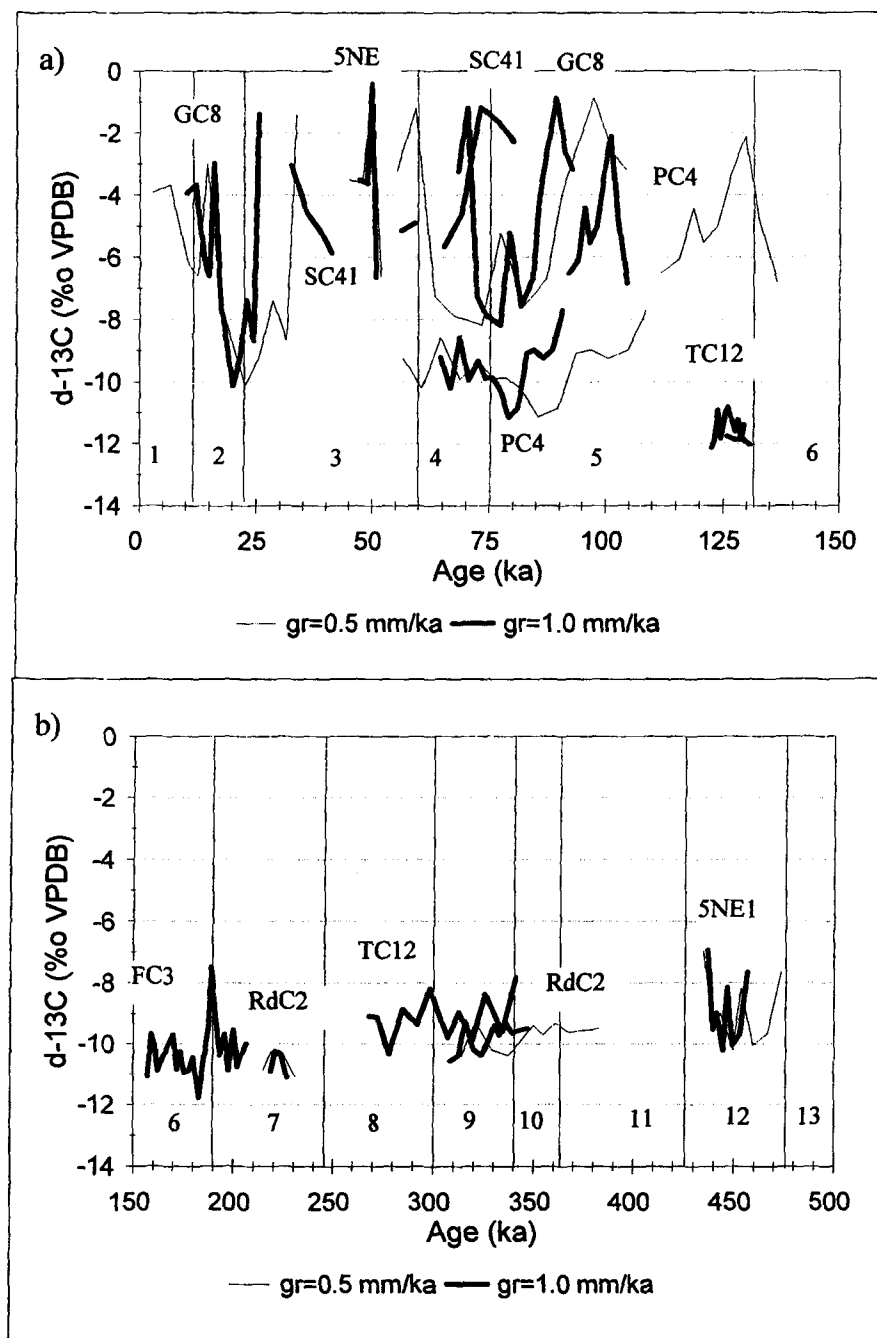


Fig. 3.17 Carbon isotope records of the Cayman samples for growth rates of 0.5 and 1.0 mm/ka.

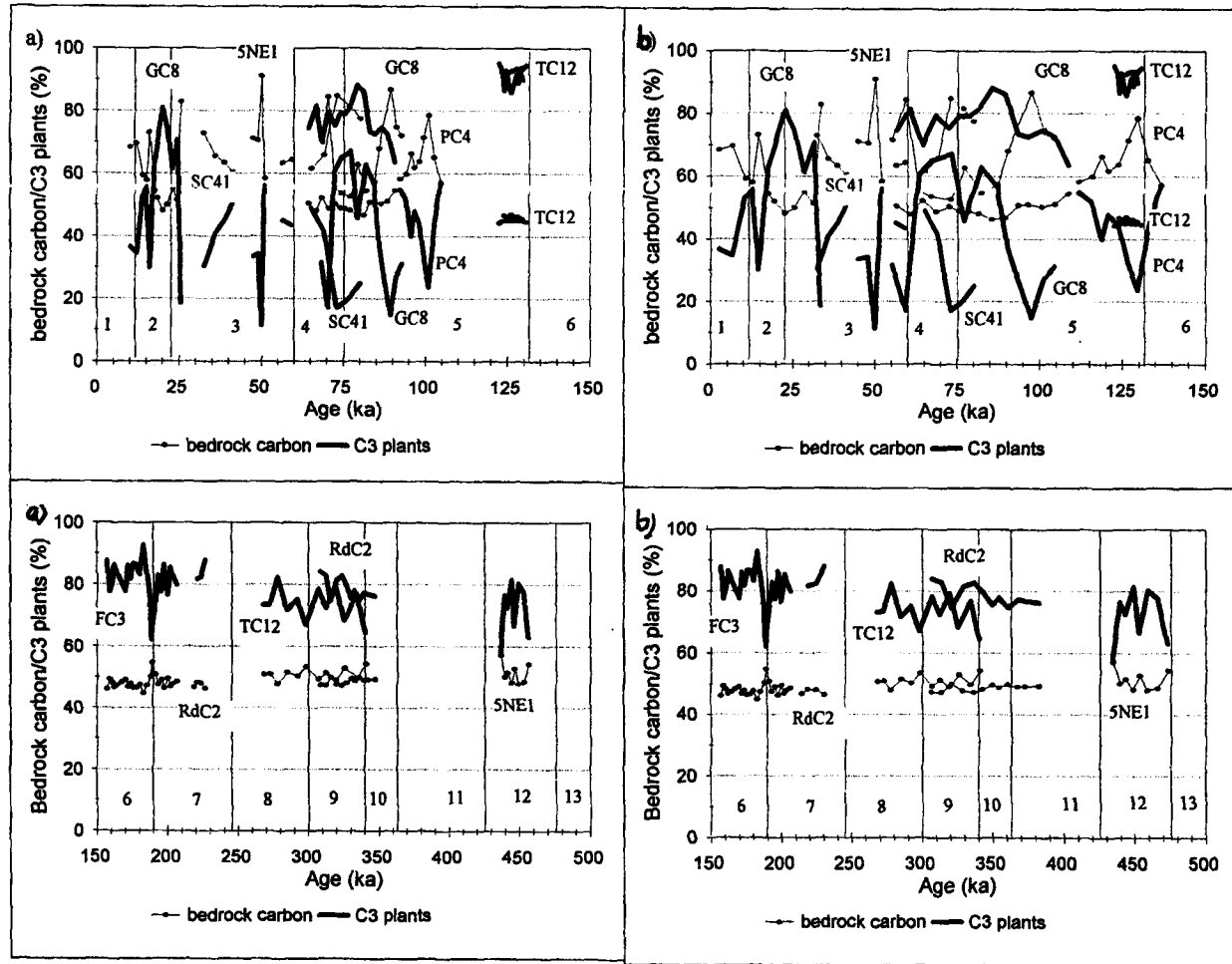


Fig. 3.18 Percentage bedrock carbon and C<sub>3</sub> plants over time for gr = 1.0 mm/ka (a) and gr = 0.5 mm/ka (b). Note: an increase in bedrock carbon and a decrease in C<sub>3</sub> plants indicates a trend towards a drier and warmer climate.

Table 3.1 Uranium and thorium activity ratios and ages of 14 speleothem samples from Cayman Brac and one from Isla de Mona.

Cave	Sample	Elevation (m)	Dating method *	Age ** (ka)		Mass spec. +2 sig. -2 sig. (ka)		Alpha spec. +1 sig. -1 sig. (ka)		234U/238U	230Th/234U	230Th/232Th	234U/238U	U conc. (ppm)
				uncorr	corr					Actual	Actual	Actual	Initial	
Bats Cave	BC5 (core)	8	A	197.2				37.5	27.9	1.01	0.84	87	1.03	0.16
	BC5 (out)	8	A	124.7				21.6	19.1	1.15	0.70	161	1.22	0.17
First Cay Cave	LC1	13	A	>350						0.94	1.09	55		0.09
First Cay Cave	LC2 (middle)	14	A	313.8				39.1	84.9	1.04	0.96	43	1.09	0.11
First Cay Cave	LC2-BC	14	MS	260.5		18.4	15.8			1.09	0.93	1861	1.19	
	LC3 (top)	13	A	125.1				14.6	12.9	1.09	0.69	58	1.13	0.14
	LC3 (bottom)	13	A	197.9				33.9	26.0	1.05	0.85	36	1.09	0.21
	LC3-A	13	MS	160.8		1.5	1.5			1.07	0.78	200	1.11	
				160.2		1.5	1.5							
Notch at First Cay Cave	LB3 (out)	6	A	10.4				4.4	4.3	1.04	0.11	8	1.04	0.82
				12.3				3.0	2.9					
Great Cave	GC8 (core)	9.5	A	81.4				5.0	4.8	1.02	0.53	81	1.02	0.84
	GC8 (out)	9.5	A	17.6				0.9	0.9	1.07	0.15	101	1.07	0.82
NE Cliff Cave #5	SNE1-A	30	MS	50.0		0.3	0.3			1.02	0.37	573	1.02	0.25
	SNE1-B	30	MS	439.5		48.8	36.6			1.01	0.96	860	1.03	0.31
Peter's Cave	HRC4 (top)	28	A	72.7				6.0	5.7	1.05	0.49	100	1.08	0.26
Peter's Cave	HRC2 (out)	33	A	176.0				47.2	32.8	1.02	0.81	165	1.03	0.17
Skull Cave	HC41-A	9	MS	103.4		22.0	17.2			1.01	0.81	38	1.02	0.57
				100.4		21.2	16.7							
	HC41-B	9	MS	39.7		0.3	0.3			1.04	0.31	779	1.04	0.83
	HC41-C	9	MS	62.0		0.6	0.6			1.01	0.44	20	1.01	0.30
	HC41-D	9	MS	78.6		0.7	0.7			1.02	0.52	9	1.03	0.09
				68.3		0.6	0.6							
Tibbitts Turn Cave	TC12-A (out)	15	MS	125.9		3.4	3.2			1.01	0.69	763	1.02	0.22
	TC12-B	15	MS	130.9		1.3	1.3			1.02	0.70	359	1.02	0.22
				130.5		1.3	1.3							
	TC12-D (core)	15	MS	408.5		31.0	23.1			1.04	0.99	838	1.11	0.17
	TC12-H	15	MS	129.0		4.8	4.6			1.01	0.70	301	1.01	0.29
	TC12-I (out)	15	MS	122.6		1.3	1.2			1.01	0.68	266	1.01	0.34
				122.2		1.3	1.2							
Tibbitts Turn Cave	TC12 A (core)	15	A	319.7				165.0	96.5	1.00	0.95	252	1.00	0.14
	TC12 B	15	A	285.1				124.2	67.4	1.05	0.94	106	1.12	0.15
	TC12 C	15	A	160.2				31.9	24.5	0.96	0.77	83	0.83	0.21
	TC12 D (out)	15	A	92.6				15.0	13.2	1.12	0.58	94	1.16	0.24
Tibbitts Turn Cave	TC41-A	15.5	MS	196.9		3.2	3.1			1.02	0.84	203	1.04	0.42
				196.1		3.1	3.0							
Tibbitts Turn Cave	TC42-A	15	MS	105.4		0.8	0.8			1.01	0.62	2054	1.01	0.26
	TC42-B	15	MS	331.0		15.9	13.8			1.00	0.95	2616	1.01	0.20
	TC42-E	15	MS	360.2		36.3	26.9			1.02	0.97	6313	1.05	0.14
Road-cut Cave	RdC2-A	8.5	MS	223.0		5.5	5.2			1.08	0.89	83	1.15	0.08
				221.2		5.4	5.1							
	RdC2-D	8.5	MS	311.0		17.7	15.2			1.07	0.96	13	1.17	0.05
				299.0		15.7	13.7							
Cueva del Agua	CAS2-A		MS	42.4		0.3	0.3			1.08	0.32	74	1.09	0.19
				41.6		0.3	0.3							
	CAS2-C1		MS	39.9		0.2	0.2			1.08	0.31	45	1.09	0.33
				38.7		0.2	0.2							
	CAS2-C2		MS	71.1		0.8	0.7			1.09	0.48	88	1.10	0.31
				70.1		0.7	0.7							
	CAS2-D		MS	65.0		0.6	0.6			1.09	0.45	66	1.11	0.55
				63.8		0.6	0.6							
CAS2-E		MS	30.5		0.2	0.2			1.10	0.25	46	1.11	0.52	
			29.5		0.2	0.2								
CAS2-H		MS	190.2		3.8	3.7			1.06	0.84	1032	1.10	0.15	
CAS2-I		MS	112.3		1.8	1.8			1.05	0.65	1941	1.07	0.19	
CAS2-K		MS	80.9		0.8	0.8			1.06	0.53	1281	1.08	0.21	

Notes

\* A = Alpha spectrometry; MS = Mass spectrometry

\*\* Uncorr = uncorrected; corr = corrected

Table 3.2. Mean speleothem growth rates, calculated from four samples from Cayman Brac (this study) and one from Lucayan Cavern, Grand Bahama (Lundberg and Ford 1994)

Cave	Name	Type	Dating	Growth period (ka)		Isotope stage	Mean Growth rate (mm/ka)
		*	**	from	to	***	
Tibbetts Turn Cave, Cayman Brac	TC12	D	MS, A	408	285	11.3**** - 8.5	0.3
Lucayan Cavern, Grand Bahama	DWBAH	F	MS	280	235	8.4 - 7.4	0.3
Lucayan Cavern, Grand Bahama	DWBAH	F	MS	230	220	7.4	1.5
Lucayan Cavern, Grand Bahama	DWBAH	F	MS	212	133	7.2 - 6	0.6
First Cay Cave, Cayman Brac	FC3	F	A, MS	198	161	7.1 - 6.41	0.8
Bats Cave, Cayman Brac	BC5	S	A	197	125	7.1 - 5.5	0.5
Tibbetts Turn Cave, Cayman Brac	TC12	D	MS	131	126	6.0 - 5.5	7.0
Tibbetts Turn Cave, Cayman Brac	TC12	D	MS	129	122	6.0 - 5.5	5.5
Lucayan Cavern, Grand Bahama	DWBAH	F	MS	97	30	5.3 - 3.1	0.5
Skull Cave, Cayman Brac	SC41	F	MS	79	62	5.1 - 4	0.8

\* D = draperie; F = flowstone; S = stalagmite

\*\* A = Alpha Spectrometry; MS = Mass Spectrometry

\*\*\* Martinson et al. 1987

\*\*\*\* Imbrie et al. 1984

Table 3.3 Deuterium and Oxygen isotope values for modern rain and drip water on Cayman Brac (this study) and for DWBAH, Grand Bahama Island (Lundberg and Ford 1994).

Sample	Distance from cliff (m)	Temperature (deg C) (measured)	d-2H (‰ VSMOW) (measured)	d-18O (‰ VSMOW) (Calculated from meteoric water line) (1)	d-18O (‰ VSMOW) (Calculated from temperature) (2)	d-18O difference (‰ VSMOW) (3)	eta (c-w) ‰ (4)	d-18O calcite (‰ VSMOW) (calculated) (5)	d-18O calcite (‰ VPDB) (calculated) (6)
<b>Cayman Brac</b>									
Drip water									
Rebecca's Cave	11	26.7	-51.85	-7.71	-3.44	-4.26	28.06	20.36	-10.24
Bats Cave	10	25.5	-35.82	-5.73	-5.26	-0.48	28.31	22.58	-8.08
Skull Cave	10	26.7	-17.60	-3.49	-3.52	0.02	28.07	24.58	-6.14
Peter's Cave	10	26.4	-24.03	-4.28	-3.90	-0.39	28.12	23.84	-6.86
First Cay Cave (entrance)	3	26.4	-11.21	-2.71	-3.90	1.19	28.12	25.42	-5.33
First Cay Cave ("dome")	20	26.0	-30.70	-5.10	-4.50	-0.61	28.21	23.10	-7.57
Rain		23.9	-49.34	-7.40	-7.67				
Drip water (average)		26.3	-28.53	-4.84	-4.08		28.15	23.31	-7.37
Drip water (average without RC)		26.2	-23.87	-4.26	-4.21		28.17	23.90	-6.79
<b>Grand Cayman (Smith 1987: 87)</b>									
Fresh Water (temperature p. 92)		27 - 31		-4.27					
Brackish Water				-4.09					
Sea water				1.44 - 1.48					

Notes

- (1)  $d-2H = 8.13 d-18O + 10.8$  (Clark & Fritz 1997: 37)
- (2)  $d-18O = 1.511 T - 43.786$  (this study)
- (3) difference between  $d-18O_{mwl}$  and  $d-18O_t$  (Column (1) - (2))
- (4)  $\eta = 2.78 \cdot (10^6 / (T + 273)^2) - 2.89$  (O'Neil et al. 1969)
- (5)  $d-18O_c = d-18O_w + \eta$  (Ford & Williams 1989: 369)
- (6)  $d-18O_{pdb} = 0.97002 d-18O_{smow} - 29.98$  (Clark & Fritz 1997: 10)

## **CHAPTER FOUR**

# **Condensation Corrosion in Caves on Cayman Brac and Isla de Mona.**

**Rozemarijn F.A. Tarhule-Lips and Derek C. Ford**

School of Geography and Geology, McMaster University,

Hamilton, Ontario, L8S 4K1, Canada

Published: *Journal of Cave and Karst Studies*, 60(2): 84-95.

**Abstract** Many speleothems in caves on Cayman Brac and Isla de Mona have suffered considerable dissolution. It is suggested that this is a consequence of condensation corrosion rather than of aqueous flooding of the entire cave. A program of temperature and relative humidity measurements during the rainy seasons showed that the entrance zones are areas of comparatively large diurnal variation where condensation from warm air onto cooler walls may occur. Artificial condensation was induced using ice bottles: chemical analysis of the condensation waters determined that they were generally undersaturated with respect to calcite and/or dolomite but that this changes over space and time. Gypsum tablets were suspended inside three sample caves on Cayman Brac and one on Isla de Mona for 16 and 13 months respectively. At the end of this period tablets close to the entrances and to the floor were found to have undergone considerable dissolution; this could only have been the result of condensation corrosion.

#### 4.1. *Introduction*

Where water condensing onto cave walls in soluble rocks is undersaturated with respect to the mineral (calcite, dolomite, gypsum, etc.), the potential exists for dissolution to occur; the process is termed “condensation corrosion” (Ford and Williams 1989: 309). It may create some characteristic speleogen features. The most widespread are “air scallops” (Hill 1987: 89), shallow, rounded recesses on walls and ceilings, with lengths ranging from decimeters to several metres. Less common are corrosion channels in ceilings or furrows in floors where condensation water has dripped from above. “Punk rock” (Hill 1987: 89; cavernous weathering with some decomposition of the inter-cavern partitions) may be seen where particularly corrosive air attacks bedrock of heterogeneous solubility. In hydrothermal caves, such speleogens are often large and easily recognized; this is because of the large temperature differences between the thermal water sources of vapour and the bedrock, and also because of greater  $\text{CO}_2$  partial pressure and/or the formation of  $\text{H}_2\text{SO}_4$  from discharged  $\text{H}_2\text{S}$ , both of which will increase the aggressivity of the condensation water. In other categories of caves condensation water is normally less abundant and probably also less aggressive: the resulting speleogens are readily confused with those caused by other processes, primarily phreatic dissolution (Cigna and Forti 1986). This has led to much misinterpretation in some past cave genetic studies.

Small holokarstic oceanic islands in young rocks are ideal sites to study the development of condensation corrosion features. They constitute closed systems without strong external influences: the only fresh water derives from condensation or infiltrating rain

because areas above the caves are too small to support surface streams, and the comparatively high primary porosity of the rock dampens the amplitude of any rain floods underground. As a consequence, prolonged flooding (establishing or re-establishing phreatic hydrodynamic conditions) will only be the result of a relative rise in sea level that is due to eustatic or tectonic effects.

The climate in caves is often described as being constant but in reality this is found only in deep interiors where there is minimal interaction between the cave and the outside environment. Condensation will occur where the air is cooled below its dew-point temperature by mixing with colder air or through contact with colder walls. Condensation should be negligible in cave interiors which have stable temperatures close to the mean annual exterior temperatures of their region and, in humid regions, relative humidity of ~100%. However, it might be observed in the entrance or transition zones. For nearly horizontal caves with single entrances (broadly, the conditions found on Cayman Brac and Isla de Mona) the climate model available is one developed by Wigley and Brown (1971). They modelled the entrance and transition zone for three seasonal conditions - summer, winter and transitional periods (fall or spring) - in humid temperate and alpine climates (i.e. those with warm summers and cold winters). The longitudinal temperature distribution was calculated by

$$T_{mean} = T_a + (T_0 - T_a) e^{-X} + (L/c) (q_0 - q_a) X e^{-X} \quad (4.1)$$

where  $T_{mean}$  is the mean temperature of the air in the cave ( $^{\circ}\text{C}$ ),  $T_a$  is the wall temperature ( $^{\circ}\text{C}$ ),  $T_0$  is the temperature of the air entering the cave ( $^{\circ}\text{C}$ ),  $L$  is the latent heat of vaporization provided that the thermal diffusivity of the wall is much less than that of the air ( $\text{J/kg}$ ),  $c$  is the specific heat (at constant pressure) of the air ( $\text{J/kg/K}$ ),  $q_0$  is the specific humidity of the air entering the cave ( $\text{g/kg}$ ),  $q_a$  is the specific humidity at the wall ( $\text{g/kg}$ ) and  $X$  is a non-dimensional length defined by

$$X = \frac{x}{x_0} \quad (4.2)$$

where  $x$  is the distance measured from the entrance (m). In caves external temperature and humidity fluctuations decay with increasing penetration distance into a cave. This decay, or damping of specific humidity/temperature in the absence of moisture is characterized by a relaxation length (or “e-folding” length),  $x_0$ . The latter is determined by the Prandtl, Reynolds and Nusselt numbers, which are non-dimensional groups frequently used in heat transfer and fluid mechanics. Eventually,  $x_0$  only depends on the radius of the cave and the flow velocity as defined by (Wigley and Brown 1971)

$$x_0 = 36.44 a^{1.2} V^{0.2} \quad (4.3)$$

Accordingly, the longitudinal humidity distribution was calculated by

$$q_{mean} = q_a + (q_0 - q_a) e^{-X} \quad (4.4)$$

Wigley and Brown (1971) suggest that equilibrium is reached in about  $5x_0$  to  $6x_0$  from the entrance of the cave. This model is for the most ideally simple case: a pipe of circular cross-section and fixed radius. Where the cross-section is tapered or irregular with many constrictions, the relaxation length remains  $x_0$  but it is no longer a constant. Most coastal caves show either taper or irregularities with constrictions or both, and will thus have a changing  $x_0$ .

During the winter and the transition seasons evaporative cooling will occur for all  $x$  where  $T_a$  is greater than the outside dew-point temperature. In the summer months the situation is reversed and condensation occurs on the cave walls, increasing the air temperature (Wigley and Brown 1971).

The Caribbean region has a tropical marine climate where seasonal temperature variations are small compared to the diurnal variations that occur. This permits measurement of the Wigley-Brown parameters within a short period of time: daytime corresponds with the summer situation and nighttime with the winter situation. The configuration of the caves on Cayman Brac and Isla de Mona is also relatively simple: large entrances give access to large rooms close to coastal cliff faces, from which smaller passages radiate modest distances into the rock. The caves show many of the types of speleogens associated with condensation corrosion. They are also richly decorated with vadose speleothems, many of which are dry and show signs of dissolution, indicating that they are no longer growing. Often a corrosion pocket will cut across both bedrock and speleothem in a uniform facet. Since many caves are well above sea level at present, flooding is unlikely to have occurred. Condensation corrosion

is believed to have been the cause of the later phases of dissolution of the cave walls and speleothems. Analysis of the cave microclimate can help establish whether the present-day conditions are suitable for condensation corrosion and if the process is still continuing.

The objectives of the study reported in this paper were to investigate the microclimatology and water chemistry of selected caves on Cayman Brac and Isla de Mona to determine whether significant condensation corrosion could be occurring there at present.

#### 4.2. *Study Areas*

Cayman Brac (19°43'N 79°47'W) and Isla de Mona (18°05'N 67°55'W) are very similar in appearance, size and geology (Fig. 4.1). Both islands have cores of Tertiary (mainly Miocene) carbonates. Their coastlines are vertical cliffs partially fringed by narrow coastal plains of Pleistocene limestones. The bedrock is very pure because the islands are located far from any mainland or continental shelves where rivers might supply clays or sands. The Tertiary strata are extensively dolomitized and have been tectonically uplifted in the past, tilting the islands. Isla de Mona was uplifted 20 m in the south, increasing to 90 m in the north. Cayman Brac displays zero uplift in the west, rising steadily to 45 m at the east end. The presence of horizontal Pleistocene coastal plains and marine erosional notches in the cliffs above them indicates that both islands have been tectonically stable since at least the last interglacial period (oxygen isotope substage 5e, 125,000 years BP; Woodroffe *et al.* 1983; Taggart and González 1994; Frank *et al.* 1998).

Hydrological conditions on both islands are similar and relatively simple. There are

no stream channels. Infiltrating rain water creates shallow freshwater lenses which float on top of denser saline water.

The majority of the cave entrances are in the coastal cliffs. The caves are confined to narrow zones behind them, extending inland no more than 50 m from the cliffs on Cayman Brac and 250 m on Isla de Mona. This suggests that the caves developed around the edges of the islands and were opened up by cliff recession. There are two spatially distinct groups of caves on Cayman Brac: Notch caves which are located at or one to two metres above the +6 m, stage 5e marine notch, and Upper caves with entrances at irregular elevations more than two metres above the notch. The caves of Isla de Mona and the Notch caves on Cayman Brac fit the flank margin cave development model, according to which caves form at the discharging margins of the freshwater lens prior to uplift (Myroie *et al.* 1994; Myroie and Carew 1990). The Upper caves on Cayman Brac are also believed to have formed in the phreatic zone around the margins of the island, but they appear to have been influenced by pre-existing structures in the bedrock to a greater extent. The caves on Isla de Mona are bigger than those of Cayman Brac, which might be partially due to the different configuration of the islands; Isla de Mona is larger in area and quite circular in shape, whereas Cayman Brac is very elongated. Island shape greatly influences the extent and thickness of the freshwater lenses and, thus, the magnitude of the formation of flanking caves. On the plateaus above them the karst features are limited to dissolution pits, sometimes associated with small cave chambers or shafts.

The sample caves on Cayman Brac include First Cay Cave (FC), Peter's Cave (PC),

Tibbetts Turn Cave (TC), Cross Island Road Cave (CC) and Skull Cave (SC) located on the North side of the island, Great Cave (GC) on the South side and B2-Cave (B2) on the plateau (Fig. 4.1). FC and GC are developed in the Brac Formation (late Early Oligocene) - FC being in limestone and GC in dolostone: all other caves in the sample are formed in dolostones of the Cayman Formation (Lower to Middle Miocene; Jones *et al.* 1994). CC, SC and GC are Notch caves. They have less speleothem growth than the Upper caves. In general, the speleothems far inside the caves are still growing, whereas those closer to the entrances show increasing amounts of corrosion. In FC speleothem dissolution is very clearly zonal: in the entrance, speleothems have been corroded to the point where their original shape can no longer be recognized; this is succeeded by a zone of corroded speleothems with still recognizable shapes and finally, deep inside the caves, there are actively growing speleothems (Fig. 4.2). Because of its greater size and this very clear zonation FC was studied in more detail than the other caves.

On Mona, Cueva del Agua, Sardinera (CAS), is located in the Isla de Mona Dolostone (Late Miocene to Early Pliocene) in the southwest corner of the island (Fig. 4.1). Cueva del Agua, Playa Brava (CAP), is at the southeast corner (Fig. 4.1) and has a more complicated geologic history. Initially, a large cave developed in Lirio Limestone (Miocene) which was then filled with reef rubble of Pleistocene age that became lithified. A relative sea level change submerged the site and the present day cave was dissolved in both the Pleistocene rubble and the Miocene limestone (Frank 1993).

The climate on the islands is of the tropical marine type with very small seasonal

temperature variations. Annual precipitation averages 1025 mm on Cayman Brac and 800 mm on Isla de Mona and is concentrated mainly in the summer months. Proximity to the sea causes comparatively high relative humidity at all times in the caves.

#### 4.3. *Methods of Study*

Field measurements were taken during two rainy season months (May, 1994 and September, 1995) in seven caves on Cayman Brac, and in June 1994 in two caves on Isla de Mona (Fig. 4.1).

##### 4.3.1. *Temperature and relative humidity*

Temperature and relative humidity profiles were taken at five caves on Cayman Brac (FC, PC, TC, GC and SC) from the entrances inward, twice daily (~10:00 hr and ~17:00 hr). Wet and dry bulb temperatures were measured with a T-type thermocouple to a resolution of 0.1 °F. The measurements were taken at three heights: 5 cm above the floor, midway between floor and ceiling and about 5 cm below the ceiling (in very high rooms, readings were made at 3.5 m above the floors). The Fahrenheit scale was used to increase the precision of calculation of relative humidity and later converted to degrees Celsius.

Temperature and relative humidity maps were constructed for FC, PC, SC and GC using one-time temperature readings at the three heights at sufficient points to cover all areas of the caves satisfactorily. Due to time limitations only simpler line (transect) profiles could be constructed for CAS and CAP on Isla de Mona.

In First Cay Cave a more elaborate system was installed, consisting of two anemometers, two wind vanes, and two sets of dry bulb - wet bulb thermocouples connected to a datalogger (Fig. 4.2). This permitted continuous measurements during the period, September 12 - October 5, 1995. The wind measurements were taken at the two main entrances to the cave, and the psychrometric temperature measurements at 2 m (entrance) and 8 m (middle of the entrance room) inward from the cliff line.

Relative humidity was calculated from the equation:

$$RH = \frac{m \cdot \exp\left(\frac{aT_w}{T_w + b}\right) - 6.6 \cdot 10^{-4}(1 + 1.5 \cdot 10^{-3}T_w) \cdot P \cdot (T_d - T_w)}{m \cdot \exp\left(\frac{aT_d}{T_d + b}\right)} \cdot 100 \quad (4.5)$$

where RH is relative humidity (%),  $T_w$  is wet bulb temperature ( $^{\circ}\text{F}$ ),  $T_d$  is dry bulb temperature ( $^{\circ}\text{F}$ ),  $P$  is barometric pressure (kPa), and  $m$ ,  $a$  and  $b$  are empirically-derived coefficients optimized for the 0 to 50  $^{\circ}\text{C}$  temperature range ( $m = 0.61121$ ,  $a = 17.368$  and  $b = 238.88$ ; Boudreau 1993).

Air density was calculated by the formula of Cigna and Forti (1986)

$$k = \frac{3.484 (P - RH \cdot P_w)}{273.15 + T} + RH \cdot k_w \quad (4.6)$$

where  $k$  is air density ( $\text{kg}/\text{m}^3$ ),  $P$  is atmospheric pressure reduced at  $0^{\circ}\text{C}$  (kPa), RH is relative

humidity ( $h =$  for 100%),  $P_w$  is vapour partial pressure reduced to 0°C (kPa),  $T$  is air temperature (°C) and  $k_w$  is the vapour density (kg/m<sup>3</sup>).

#### 4.3.2. *Water chemistry*

Conductivity was measured with a YSI Model 33 S-C-T (salinity-conductivity-temperature) meter. Measurements were converted to specific conductivity at 25°C using the function

$$SpC(25^\circ) = 1.81 * SpC(T) * e^{-0.023T} \quad (4.7)$$

where  $SpC(T)$  is the measured conductivity at  $T^\circ\text{C}$ ,  $T$  is the temperature (°C). The equation is derived empirically from karst water data in Pennsylvania and is valid between 0 to 40°C (White, 1988).

pH was determined with an ATC pH meter with an accuracy of 0.01 pH. The meter was standardised against buffers pH = 4.00 and pH = 7.00 before each series of measurements. Temperature was taken with a dual-sensor digital thermometer having a resolution of 0.1 °C and an accuracy of  $\pm 1.0$  °C in the range -10 to + 50 °C. Alkalinity, calcium and total hardness were measured using a Hach Digital Titrator. The saturation indices for calcite and dolomite, the partial pressure of CO<sub>2</sub> with which the water would be in equilibrium and ion balance errors were calculated using the program WCHEM3.

No water analyses were made on Isla de Mona. On Cayman Brac, the caves are quite dry in general and there are few drip sites. Only during heavy rains were the drip rates

fast enough to allow satisfactory water collection; on these occasions samples were collected from as many sites as possible.

Condensation was induced by chilling the cave air. Half-gallon plastic milk containers that had been filled with water and then frozen solid were used as condensers. The condensation water was collected in 250 ml sample bottles, via funnels with small apertures to reduce evaporation. In each sample run three bottles were suspended in the selected cave for a minimum of six hours, by which time all the ice had melted; one was placed close to the entrance, one halfway and one close to the back of the cave. A total of 12 condensation experimental runs were completed in six different caves (B2, CC, GC, PC, SC and TC), including up to three repeat runs at the same positions in a given cave on separate days.

#### 4.3.3. *Gypsum tablets*

Gypsum tablets of known weight were suspended on nylon fishing line away from direct drip sites and walls for 16.5 months (May, 1994 to October, 1995) in four caves on Cayman Brac (B2, FC, PC and TC) and for 13 months (June, 1994 to July, 1995) in CAS, Isla de Mona. The tablets were dried overnight at 60°C in an oven before weighing prior to and after exposure. In each cave they were so located as to form a profile perpendicular to the cliff, from the entrance inward (Fig. 4.2). On each island one sample was retained unexposed to be used as a reference sample. The gypsum was > 90% pure  $\text{CaSO}_4 \cdot 2\text{H}_2\text{O}$  donated by the Canadian Gypsum Co, Hagersville, Ontario, Canada. Assuming that the moisture reaches equilibrium before dripping off, the surface retreat rates were calculated by

$$r = s * 10^{-3} * \rho^{-1} * \epsilon * 365 \quad (4.8)$$

where  $r$  is surface retreat rate (mm/a),  $s$  is solubility of gypsum (2.5 g/l),  $\rho$  is density of gypsum (2.35 g/cm<sup>3</sup>) and  $\epsilon$  is the amount of condensation water accumulated on the surface in one day, expressed as the water film thickness this amount of condensation water would form on the surface of the tablet (mm/day), given by

$$\epsilon = W * (At)^{-1} * 10 \quad (4.9)$$

where  $A$  is surface area of the gypsum tablet (cm<sup>2</sup>),  $t$  is duration of exposure (days) and  $W$  is amount of water in thermodynamic equilibrium with gypsum that is needed to dissolve the observed weight loss (cm<sup>3</sup>) i.e.

$$W = (w_1 - w_2) * s^{-1} * 10^3 \quad (4.10)$$

where  $w_1$  and  $w_2$  are weight before and after exposure respectively. The minimum amount of condensation water needed per day ( $C$ ) to dissolve the observed weight loss is thus

$$C = W/t = \epsilon * 10^3 * A \quad (4.11)$$

#### 4.4. *Results and Discussion*

##### 4.4.1. *Air Temperature and Relative Humidity*

###### 4.4.1.1. *Longitudinal profiles.*

A constant climate with a temperature of 25.5 to 26.5 °C on Cayman Brac and 25 to 25.5 °C on Isla de Mona and a relative humidity of 95% to 100% was reached deep inside the larger caves and behind constrictions (Fig. 4.3). In the smaller caves, the relative humidity did not reach its stable level, but rather remained between 90% and 95% even behind some constrictions (Fig. 4.4). Both on maps and profiles, it is clear that quite short constrictions in cave passages can substantially reduce the penetration of outside climatic effects.

The entrance zone was the area most affected by the outside climate. The penetration of external influences was greatest near the ceiling and varied with the cave configuration and the temperature and relative humidity differences between the two environments (Fig. 4.4).

###### 4.4.1.2. *Vertical profiles*

On most occasions, the temperature near the ceiling was greater than the floor temperature. This temperature difference was highest in the entrance zones, which usually consist of large rooms where the air can circulate most readily (Fig. 4.4 and 4.5).

During the periods of study, outside daytime temperatures were higher than the inside temperature. Air was drawn into the caves along the ceilings, was cooled down in the

interiors and drained out again along the floors. Because warmer air can contain more water vapour, the air along the ceilings had lower relative humidities than that at the floors (Fig. 4.5). In areas with poor air exchange (e.g. deep inside the cave or behind constrictions), the relative humidity was either stable up the vertical profile or increased slightly from the floor to the ceiling.

According to the Wigley-Brown model temperature and relative humidity equilibrium will be attained after  $5x_0$  to  $6x_0$ ; thus,  $x_0$  was calculated by dividing the distance required to arrive at equilibrium in the sample caves by six. On Cayman Brac average  $x_0 = 5$  m; however, because of the changing cross-section of the passages in these caves, it varies with distance from the entrance, as illustrated in detail in Figure 4.4. As noted, the Wigley-Brown model was developed for a simple pipe of constant radius. The configuration of the caves on Cayman Brac and Mona is that of series of chambers/high passages separated by constrictions. This configuration is an extreme test of the Wigley-Brown model. Values of  $x_0$  for these caves calculated according to the model are at least one order of magnitude higher than the actual measured average. This discrepancy is most likely explained by the presence of the constrictions. The implication is that the basic Wigley-Brown model needs to be considerably modified into a "chamber-constriction-chamber" model - which was not the objective of this paper.

A quite different pattern of air circulation can be established in these caves by convective processes. Convection may occur if denser air can accumulate initially at the ceilings rather than at the floors and then settle downwards, setting up a vertical cellular

circulation. In general this will correspond to cooler air flowing along the ceilings. This pattern is not expected to occur in every cave and is temporary and superimposed on the general circulation described above. In First Cay Cave this situation tended to occur during the nights and early mornings and was recorded at distances up to 30 m from the entrance. It is a consequence of the daytime "hot" general circulation in at the ceiling and out along the floor being sustained into the night by inertia. In Peter's Cave one fifth of the stations used for the temperature and relative humidity maps recorded such temperature inversions (Fig. 4.6). Convection cells could form at these locations. They were distributed throughout the cave, indicating that the process occurs only on a small scale but it is likely to be of local significance.

As noted in the introduction, the climate on Cayman Brac and Isla de Mona is dominated by diurnal rather than seasonal variations and this permits measurement of the Wigley-Brown parameters within a short period of time. Daytime corresponds with the summer situation, when the wall temperature is less than the outside dew-point temperature and condensation occurs on the walls. At night the situation is similar to the winter condition and inside temperature is greater than the outside dew-point temperature resulting in evaporation. This diurnal variation between condensation and evaporation will be greatest in the area of greatest diurnal temperature and relative humidity differences, i.e. the entrance zones. It is very likely that this alternation plays a major role in condensation corrosion because energy is needed to evaporate water and this will cool the walls. No droplets or sheet flow were observed to occur on the walls, indicating that the condensation water was not

substantial enough to form droplets or water films thick enough to overcome the surface tension and flow down, removing dissolved material in the process. During evaporation some material might be removed in the vapour phase, which would explain the high concentrations of calcium and magnesium observed in the condensation waters. At the same time, dissolved material could crystallize as small individual particles when evaporation is fast enough to prevent molecules of the dissolved material from rejoining the crystalline structure of the bedrock. As such, they can then be removed as aerosols by gravity, dislodgment by air circulation or some other process.

#### 4.4.2. *Water chemistry*

The chemical characteristics of water samples collected on Cayman Brac are presented in Table 4.1. Drip water could be collected only on rainy days when the drip rates were high. Relative humidity was then close to 100% and thus evaporation, which would increase mineral concentrations in the water, was assumed to be negligible.

Figure 4.7 compares the specific conductivity (SpC) of the drip waters with their total hardness. The solid line is the relationship between these two parameters that has been established for bicarbonate waters of Pennsylvania by White (1988). The drip waters fall mainly above the bicarbonate water line, indicating that they have a higher SpC due to the presence of significant quantities of ions other than calcium and magnesium. These foreign ions are believed to have come from sea salt particles in the air or deposited on vegetation.

Two different factors each divide the drip waters into distinct groups. First, samples

from rains of May 1994 and September 26 1995 have in general greater hardness and lower specific conductivity than the samples of October 3 and 4 1995 (Fig. 4.7a). The difference is attributed to different rainfall intensities, duration and amounts. During the night of September 25 - 26 as well as part of the day it rained steadily, resulting in a mean rainfall of 65 mm for the island. On October 3 the heaviest downpour of the entire study period was experienced due to the influence of Hurricane Opal. Rain fell all day; mean precipitation for the island was 95 mm, varying from 50 mm at the west end to 135 mm in the middle. With a steady rain the amount of water is less and takes longer to penetrate the rock, giving it more time to dissolve the bedrock and thus a greater hardness. Heavy downpours will be able to penetrate the bedrock faster and they will flush all the foreign ions through the system as well, increasing the SpC but keeping the hardness relatively low.

As a second effect, these differentiated storm waters also divide in two subgroups according to location within the cave. Waters from the entrance zone have higher SpC for a given hardness than those deep inside, indicating that there is a higher foreign ion content close to the entrances (Fig. 4.7b). This is in agreement with the temperature and relative humidity observations, which indicated that the entrance zone is most influenced by outside climate. The inflowing air not only conveys heat and moisture into the cave but also sea salt aerosols. Sea salt aerosols are very hygroscopic and can initiate aqueous condensation at relative humidities as low as 80% (Wells 1986). The presence of these particles may therefore cause condensation in the air, increasing the amount of condensation water and the likelihood of condensation corrosion.

Figure 4.8 displays the saturation index values of the different water samples with respect to calcite ( $SI_c$ ) and dolomite ( $SI_d$ ). It is seen that the induced condensation waters are similar to the intense storm drip waters of October 3 and 4, 1995. Condensation waters were undersaturated with respect to both minerals in 75% of the cases and supersaturated in 25%. The calcite index values are the most significant in this study. Their range was from -1.06 to +0.88, the former representing a water capable of dissolving a speleothem quite rapidly and the latter one that would deposit new calcite upon it.

Some measured relationships between the  $SI_c$  of sample condensation waters and their distances from cave entrances are shown in Figure 4.9. They are quite complex, varying between caves and at different dates in the same cave. To generalise, however, a majority of the traverses detected little change in the  $SI_c$  state on a given day at distances up to 25 m from the cliff lines but Tibbetts Turn Cave (TC) gave quite aberrant results. Two traverses deeper than 25 m in Great Cave measured significant increases in  $SI_c$ , the waters becoming slightly supersaturated. The need for more research here is evident.

#### 4.4.3. *Gypsum tablets*

The calculated losses by surface retreat on the gypsum, the condensation film thicknesses and minimum quantities of condensation water needed to achieve those losses are given in Table 4.2. The two reference samples did not display any loss of material. All other tablets recorded losses, which can be represented as surface retreat rates of up to 0.5 mm/a. There was no correlation between the surface areas of the different gypsum tablets and

their retreat rates.

With some exceptions, gypsum tablets that were suspended close to the entrances suffered more dissolution than those further inside the caves. Tablets close to the floors were more affected than those close to the ceilings (Fig. 4.10). Condensation corrosion is the only feasible mechanism for this dissolution: the gypsum tablet experiments reinforce the conclusion from the meteorological work - that condensation occurs preferentially in entrance zones and close to the floors.

The greatest number of tablets were placed in First Cay Cave. The amount of surface retreat decreased rapidly beyond a distance of 30 m from the cliff (second constriction; Fig. 4.10a). Beyond the first constriction at 17 m the temperature became nearly invariant and the relative humidity stabilised at around 99 % (Figs. 4.2 and 4.3). Almost no dissolution occurred on tablets where the relative humidity exceeded 95 % and remained constant over time. Substantial dissolution was observed at relative humidities less than 95 %, i.e. in the entrance areas. These are the zones with the greatest diurnal climatic variations and where alternation of condensation and evaporation is believed to occur. As noted above this cycle of condensation and evaporation might enhance condensation corrosion.

In Peter's Cave the tablets suspended near the ceiling and near the floor displayed similar retreat rates (Fig. 4.10b). This is believed to be the result of a more homogeneous air mass than in the other caves. The tablets were suspended in the second and third principal passages, which are parallel to the cliff line and in direct contact with the first (or outer) principal passage by an aperture of about 20 cm diameter. The gypsum tablet profile follows

a downward slope between the second and third passage. The temperature and relative humidity measurements indicate that convection cells form on a very localised scale in these passages, which might enhance the homogenisation of the air mass.

In Cueva del Agua, Sardinera, the highest surface retreat was found on a sample 92 m from the entrance and close to the ceiling (Fig. 4.10d). A local convection cell might explain this anomaly also, but temperature and relative humidity measurements indicate this was not occurring on the day these measurements were taken. Another possibility might be that the sample was located under or close to an aggressive drip site that was not active at the time of the field measurements.

Excluding the reference samples, the mean surface retreat on the gypsum tablets was 0.36 mm/a. If a ratio of 10 : 1 is assumed for the ratio of gypsum solubility to calcite solubility (Ford and Williams 1989), the calculated mean calcite (limestone and speleothem) corrosion is 0.036 mm/a or 36 mm/ka. This must be reduced by a measure that takes into account the greater porosity of gypsum: 33% would seem a likely maximum for this effect, giving a corrosion rate of ~24 mm/ka for calcites with porosities below ~5%. This remains a considerable loss rate.

Theoretical condensation corrosion rates were also calculated, using

$$R = \alpha(c_{eq} - c) \quad (4.12)$$

where  $R$  is the dissolution rate in  $\text{mmol}/\text{cm}^2\text{s}$ ,  $\alpha$  is the kinetic constant in  $\text{cm}/\text{s}$ ,  $c$  is the Ca-concentration in the water film and  $c_{eq}$  is the equilibrium concentration of calcium in  $\text{mol}/\text{l}$

(= mmol/cm<sup>3</sup>) with respect to calcite (Buhmann and Dreybrodt 1985; Baker *et al.* in prep.). An average value of 19 mm/ka was obtained using the Ca-concentrations measured in the induced condensation waters. This corresponds very well with the rates calculated from the gypsum tablet experiments, indicating that (although the methods were crude and the time spans short) the results of the field experiments appear to be meaningful. U-series dating has determined that the growth rates of some larger speleothems on Cayman Brac can be up to 7 mm/ka but are generally < 1 mm/ka (Lips 1993). These are far below the corrosion rates that can prevail: thus, for instance, a flowstone 10 cm thick will require about 100,000 years to form and can be dissolved away again in only 4000 - 5000 years.

#### 4.5. *Conclusions*

Condensation corrosion occurs at present in the entrance zones of caves where the atmospheric variables fluctuate on a daily basis and are highly influenced by the outside climate. The relationships are complicated, however; Figure 4.11 schematically outlines how they and other environmental variables will contribute to the formation of condensation water and the condensation corrosion inside caves that is a consequence. The climatic variables have both short and long term influences on the climate inside the caves, whereas sea level fluctuations are only of long term importance. The latter influence the size of the entrance, the configuration of the cave and the distance between the sea and the cave.

The physical model for condensation corrosion that is suggested by this investigation is depicted in Figure 4.12. The typical coastal caves consist of a series of

chambers and constrictions. The latter inhibit the free flow of air and dampen the external climatic influences substantially.

The mean condensation corrosion rate was estimated to be ~24 mm/ka. This corresponds well with a theoretical rate of ~19 mm/ka that can be calculated from the model of Buhmann and Dreybrodt (1985).

#### *Acknowledgements*

First of all the authors would like to thank Dr. Henry Schwarcz for his idea to use ice bottles as condensers for collecting condensation water; Karen Lazzari of the Water Authority for the ever important logistical support on Cayman Brac; Dr. Ashley McLaughlin from the Ministry of Environment of the Cayman Islands for the meteorological data and the permission to collect samples of everything we needed; Mr. Floyd Banks of the Mosquito Control unit of Cayman Brac for the meteorological data during the period of study; Pedro Lazzari for showing us the island from a fisherman's point of view; and everybody else on Cayman Brac who helped us in our study of the caves of their island. Very special thanks go to Dale Boudreau for his enormous help with the meteorological equipment and the interpretation of the climatology data. Mike Bagosy, Craig Malis and Dr. Steve Worthington are thanked for being the field assistants and for their helpful discussions. A special thank you to Dr. Brian Jones for introducing us to Cayman Brac. Thanks also go to the anonymous reviewer of this paper for valuable comments and suggestions.

All the organisers of the Isla de Mona expeditions, especially Joe Troester, are

thanked very much for the opportunity to study this desolated island and for the well organised trips.

U-series dating by  $\alpha$ - spectrometry was done by Nicki Robinson. Karen Goodger and Catharina Jager were very patient teaching the first author the mass spectrometric dating procedures.

The gypsum was donated by the Canadian Gypsum Co, Hagersville, Ontario, Canada.

This work was supported by a Research Grant to Ford from the Natural Sciences and Engineering Research Council of Canada.

### References

- Baker, A., Genty, D., Dreybrodt, W., Barnes, W.L., Mockler, N.J. and Grapes, J. (in prep.)  
Testing theoretically predicted stalagmite growth rates with recent annually laminated samples: implications for past stalagmite deposition.
- Boudreau, L.D. (1993). *The energy and water balance of a high subarctic wetland underlain by permafrost*. M.Sc. Thesis, McMaster University, Hamilton, Ontario, Canada, 205 p.
- Buhmann, D. and Dreybrodt, W. (1985) The kinetics of calcite dissolution and precipitation in geologically relevant situations of karst areas. 1. Open system. *Chemical Geology*, 48: 189-211.
- Cigna, A.A. and Forti, P. (1986). The speleogenetic role of air flow caused by convection. First contribution. *International Journal of Speleology*, 15: 41-52.
- Ford, D.C. and Williams, P.W. (1989). *Karst geomorphology and hydrology*. London (Unwin Hyman), 601 p.
- Frank, E.F. (1993). *Aspects of karst development and speleogenesis, Isla de Mona, Puerto Rico: an analogue for Pleistocene speleogenesis in the Bahamas*. M.Sc. Thesis, Mississippi State University, Starkville, Mississippi, USA, 288 p.
- Frank, E.F., Wicks, C.M., Mylroie, J.E., Troester, J.W., Alexander, E.C. Jr. and Carew J.L., (1998), Karst development and speleogenesis, Isla de Mona, Puerto Rico. *Journal of Cave and Karst Studies*, Journal of Cave and Karst studies, 60(2): 73-83.
- Hill, C.A. (1987). Geology of Carlsbad Cavern and other caves in the Guadalupe Mountains,

- New Mexico and Texas. *New Mexico Bureau of Mines and Mineral Resources, Bulletin 117*, 150 p.
- Jones, B., Hunter, I.G. and Kyser, K., 1994, Revised stratigraphic nomenclature for Tertiary strata of the Cayman Islands, British West Indies. *Caribbean Journal of Sciences*, 30: 53-68.
- Myloie, J.E. and Carew, J.L. (1990). The flank margin model for dissolution cave development in carbonate platforms. *Earth Surface Processes and Landforms*, 15: 413-424.
- Myloie, J.E., Carew, J.L., Frank, E.F., Panuska, B.C., Taggart, B.E., Troester, J.W. and Carrasquillo, R. (1994). Comparison of flank margin cave development on San Salvador Island, Bahamas and Isla de Mona, Puerto Rico. *San Salvador, Bahamas, 7th Symposium on the geology of the Bahamas, June 16-20, 1994*.
- Taggart, B.E. and González, L.A. (1994). Quaternary geology of Isla de Mona, Puerto Rico: San Juan, Puerto Rico. *Presented at the XX Simposio de los Recursos Naturales, November 16-17, 1994, Puerto Rico Department of Natural and Environmental Resources*.
- Wells, N. (1986). *The atmosphere and ocean: a physical introduction*. London (Taylor & Francis), 347 p.
- White, W.B. (1988). *Geomorphology and hydrology of karst terrains*. New York (Oxford University Press, Inc.), 464 p.
- Wigley, T.M.L. and Brown, M.C. (1971). Geophysical applications of heat and mass transfer

in turbulent pipe flow. *Boundary-Layer Meteorology*, 1: 300-320.

Woodroffe, C.D., Stoddart, D.R., Harmon, R.S. and Spencer, T. (1983). Coastal morphology and late Quaternary history, Cayman Islands, West Indies. *Quaternary Research*, 19: 64-84.

### List of Figures

- 4.1 Location of Cayman Brac, Isla de Mona and the caves studied.
- 4.2 Zonation of speleothem corrosion, meteorological instrument set up, location of gypsum tablets with their surface retreat rates, First Cay Cave, Cayman Brac.
- 4.3 Temperature **(a)** and relative humidity **(b)** profiles in First Cay Cave, Cayman Brac, measured in May 1994.
- 4.4 Temperature and relative humidity profiles for September 13, 16, 22, 26 and 28, 1995 in Skull Cave, Cayman Brac. The relaxation lengths,  $x_0$ , are indicated along the top of each profile. Note the varying length of  $x_0$  with distance away from the entrance as a result of the cave configuration. Arrows indicate the location of constrictions. **a)** Morning temperature profile along the floor; **b)** Morning temperature profile along the ceiling; **c)** Morning relative humidity profile along the floor; **d)** Morning relative humidity profile along the ceiling; **e)** Afternoon temperature profile along the floor; **f)** Afternoon temperature profile along the ceiling; **g)** Afternoon relative humidity profile along the floor; **h)** Afternoon relative humidity profile along the ceiling.
- 4.5 **a)** Temperature differences between ceiling and floor for all stations, Cueva del Agua Sardinera, Isla de Mona (June, 1994); **b)** Temperature difference between the ceiling and the floor along selected profiles in the cave. Three transects were made NNE-SSW, one in the western end (west), one in the eastern end (east) and one midway between the two (mid). One transect was almost perpendicular to the

previous three transects (SE-NW) and transect East 2 first goes SSW-NNE and then turns SE-NW to join the eastern transect; **c**) Relative humidity difference between ceiling and floor for all stations, Cueva del Agua Sardinera; **d**) Relative humidity difference between the ceiling and the floor along selected profiles in the cave (transect location see 5b).

- 4.6 Temperature differences between ceiling and floor for all stations in Peter's Cave, Cayman Brac (May, 1994).
- 4.7 Relationship between Specific Conductivity and Hardness for drip waters. **a**) Drip waters by cave; closed symbols indicate drip waters from heavy downpours (October 3 and 4, 1995) and open symbols drip waters from steady rain (May 1994 and September 26, 1995); **b**) Drip waters at the entrances and deep inside caves (Sept-Oct, 1995). The solid line is the Pennsylvania water line for inland bicarbonate waters given by White (1988, p. 137).
- 4.8 Saturation Index for dolomite (SI<sub>d</sub>) versus the Saturation Index for calcite (SI<sub>c</sub>) for rain, drip and condensation water on Cayman Brac, 1994 and 1995.
- 4.9 The change in the Saturation Index for calcite (SI<sub>c</sub>) of condensation water with distance from the cliff line in three caves on Cayman Brac for September 15, 18, 22, 26, 27, 28 and 30, 1995.
- 4.10 Surface retreat of gypsum tablets in First Cay Cave (**a**), Peter's Cave (**b**), Tibbetts Turn Cave (**c**) on Cayman Brac and Cueva del Agua (**d**) on Isla de Mona.
- 4.11 Schematic representation of the interaction between the outside and cave

environments.

- 4.12 Proposed model of condensation corrosion in coastal caves on small holokarstic oceanic islands with young rocks.

### **List of Tables**

- 4.1 Chemical analyses of different water types on Cayman Brac.
- 4.2 The gypsum tablet experiment: location, measured surface recession and estimated daily condensation.

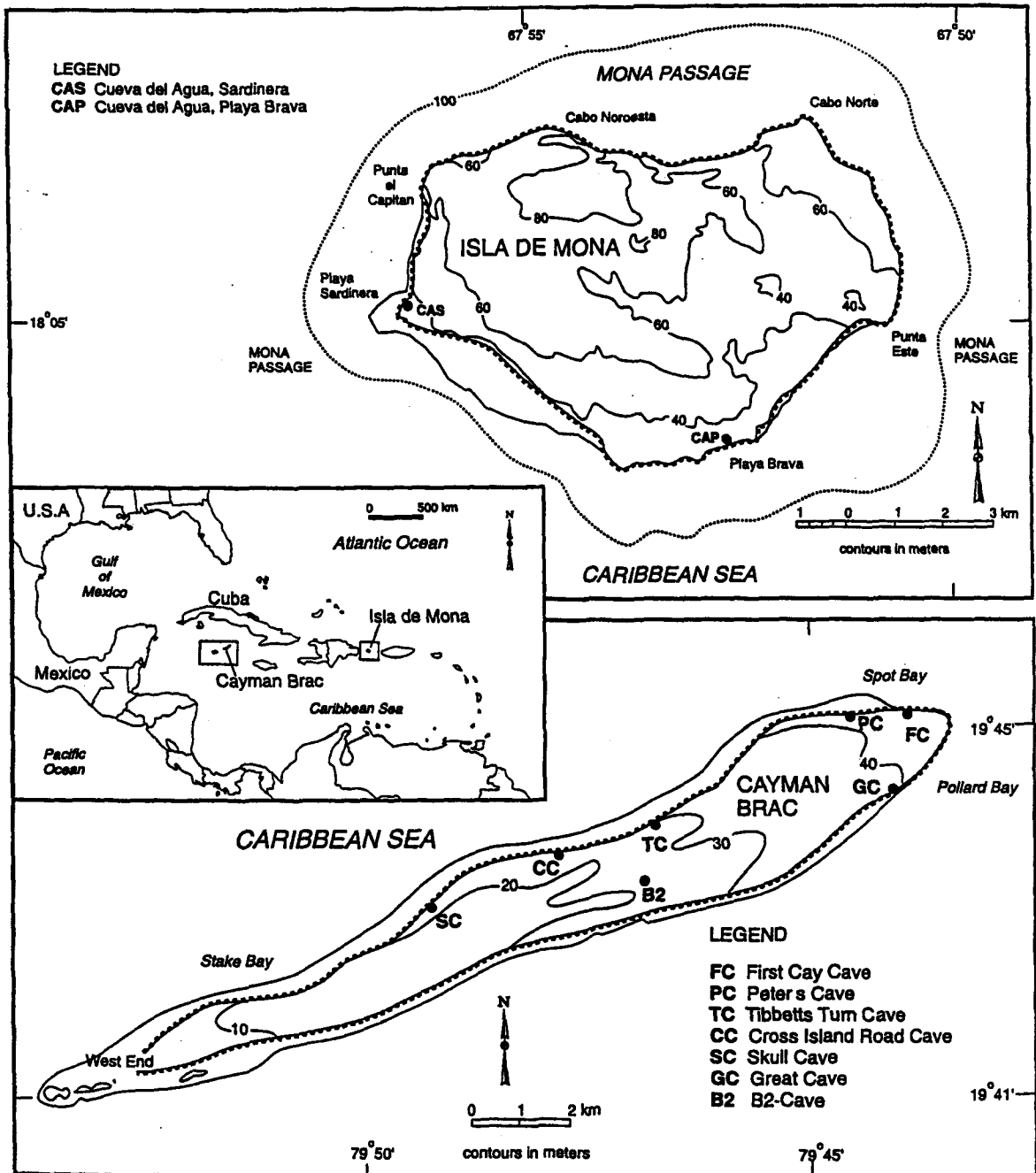


Fig. 4.1 Location of Cayman Brac, Isla de Mona and the caves studied.

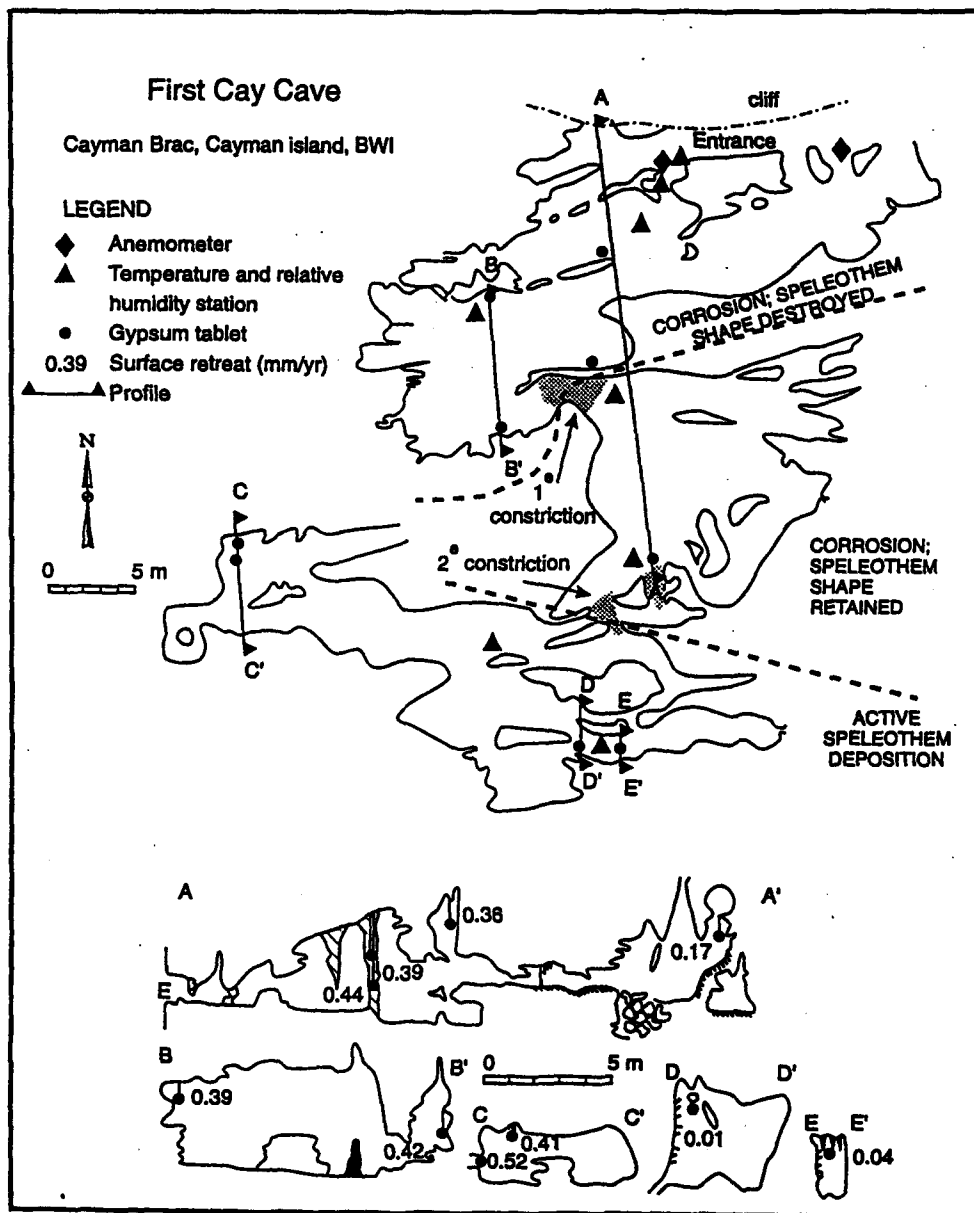


Fig. 4.2 Zonation of speleothem corrosion, meteorological instrument set up, location of gypsum tablets with their surface retreat rates, First Cay Cave, Cayman Brac.

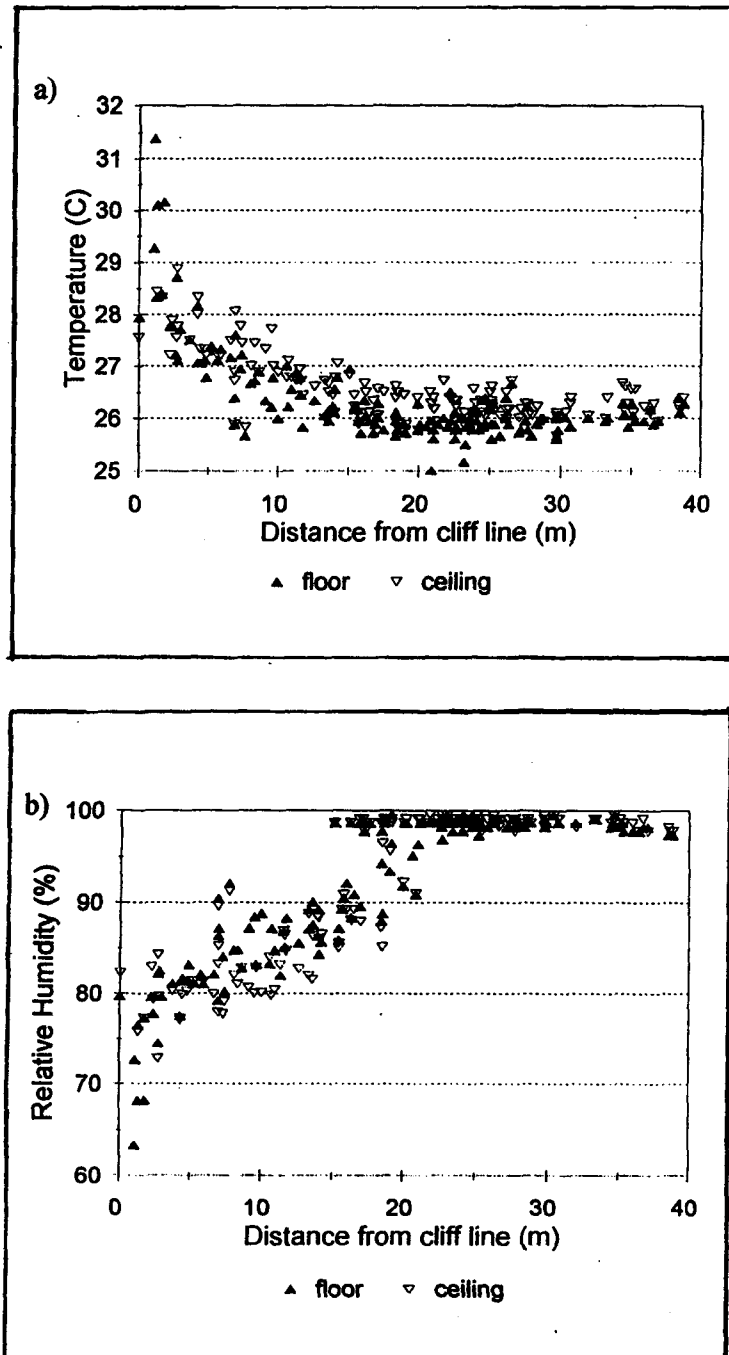


Fig. 4.3 Temperature (a) and relative humidity (b) profiles in First Cay Cave, Cayman Brac, measured in May 1994.

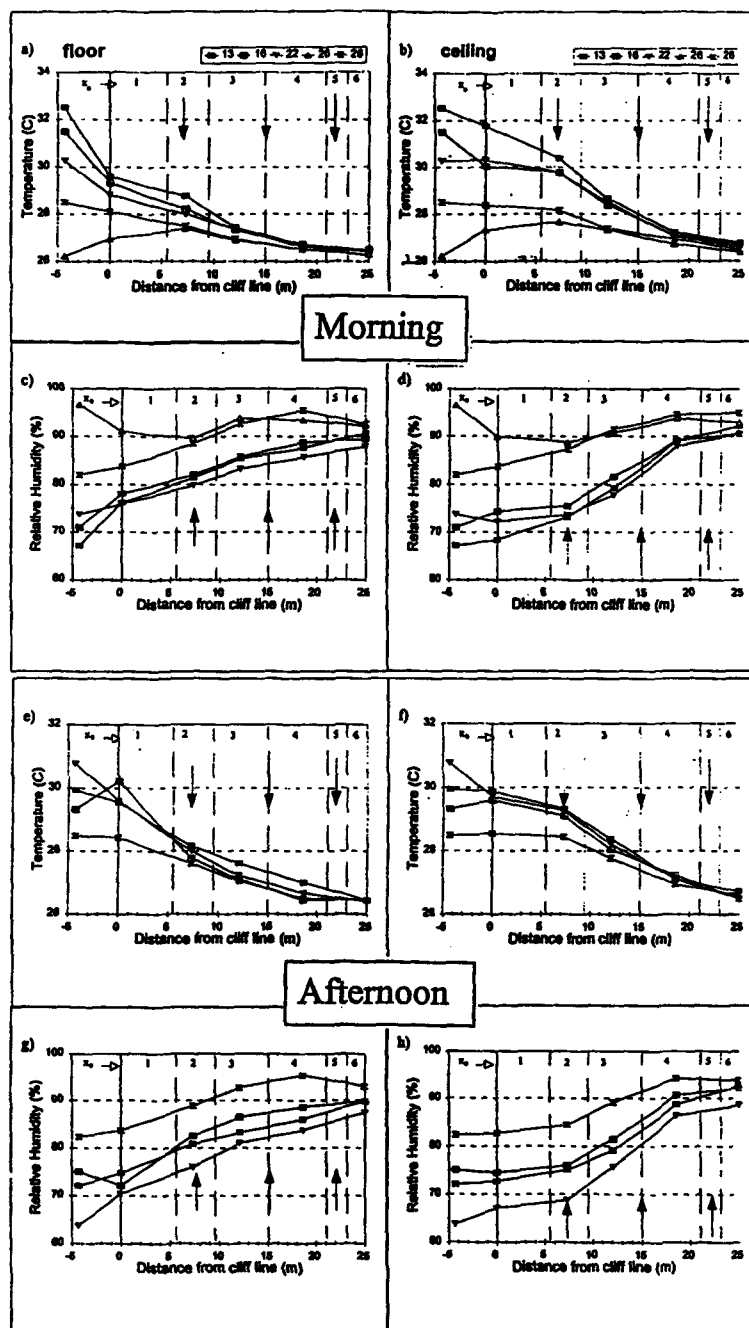


Fig. 4.4 Temperature and relative humidity profiles for September 13, 16, 22, 26 and 28, 1995 in Skull Cave, Cayman Brac. The relaxation lengths,  $x_0$ , are indicated along the top of each profile. Note the varying length of  $x_0$  with distance away from the entrance as a result of the cave configuration. Arrows indicate the location of constrictions. a) Morning temperature profile along the floor; b) Morning temperature profile along the ceiling; c) Morning relative humidity profile along the floor; d) Morning relative humidity profile along the ceiling; e) Afternoon temperature profile along the floor; f) Afternoon temperature profile along the ceiling; g) Afternoon relative humidity profile along the floor; h) Afternoon relative humidity profile along the ceiling.

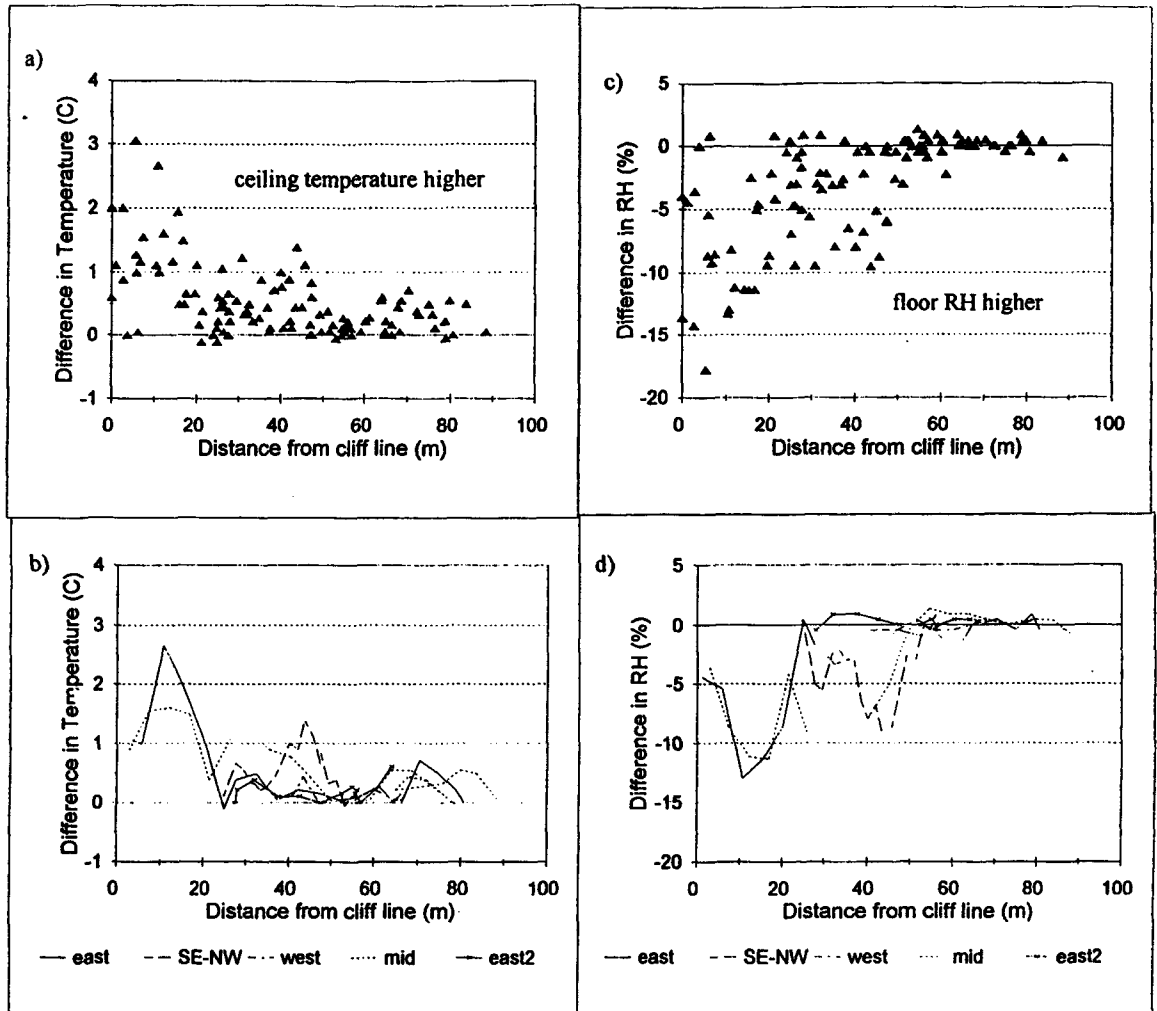


Fig. 4.5 **a)** Temperature differences between ceiling and floor for all stations, Cueva del Agua Sardinera, Isla de Mona (June, 1994); **b)** Temperature difference between the ceiling and the floor along selected profiles in the cave. Three transects were made NNE-SSW, one in the western end (west), one in the eastern end (east) and one midway between the two (mid). One transect was almost perpendicular to the previous three transects (SE-NW) and transect East2 first goes SSW-NNE and then turns SE-NW to join the eastern transect; **c)** Relative humidity difference between ceiling and floor for all stations, Cueva del Agua Sardinera; **d)** Relative humidity difference between the ceiling and the floor along selected profiles in the cave (transect location see 5b).

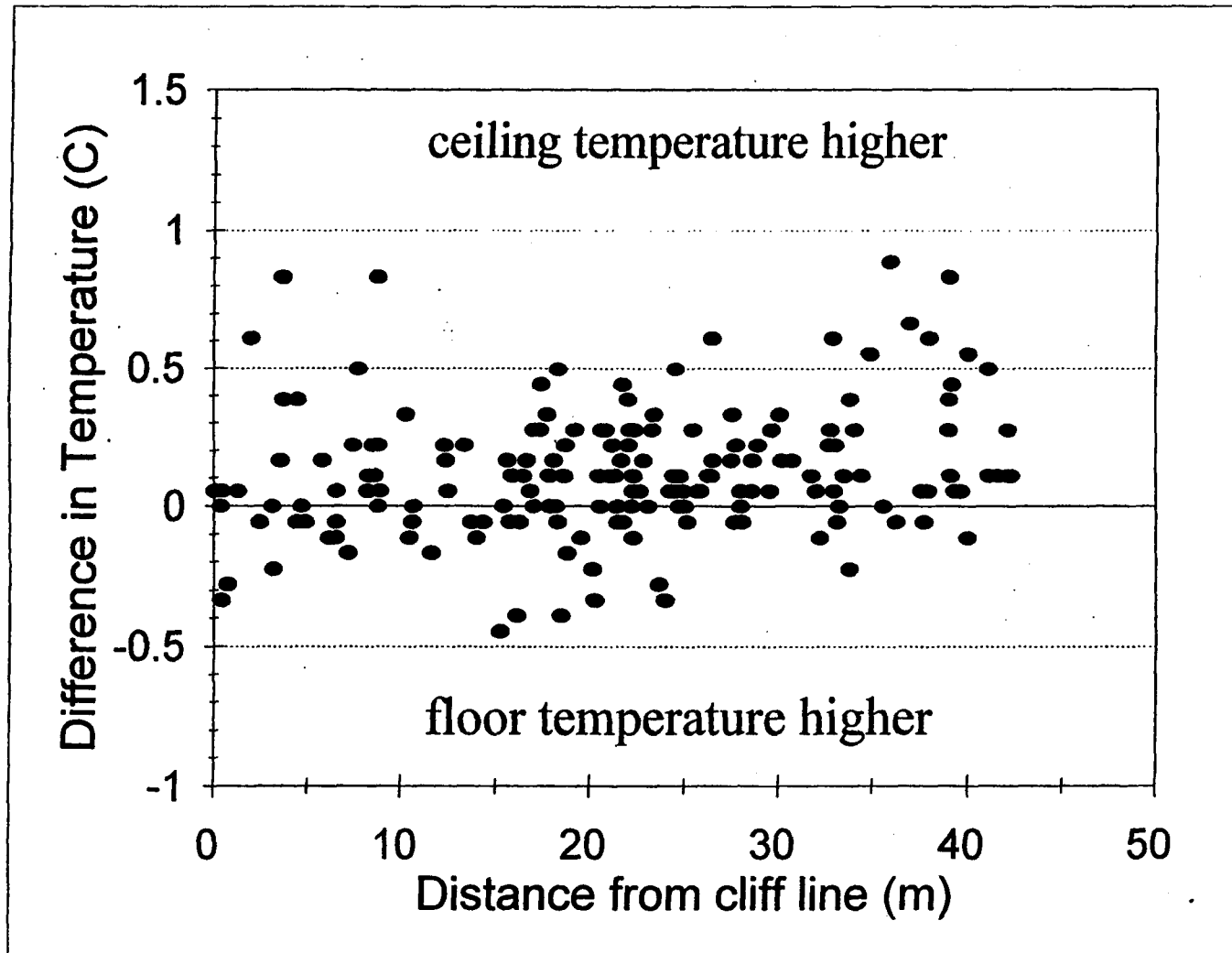


Fig. 4.6 Temperature differences between ceiling and floor for all stations in Peter's Cave, Cayman Brac (May, 1994).

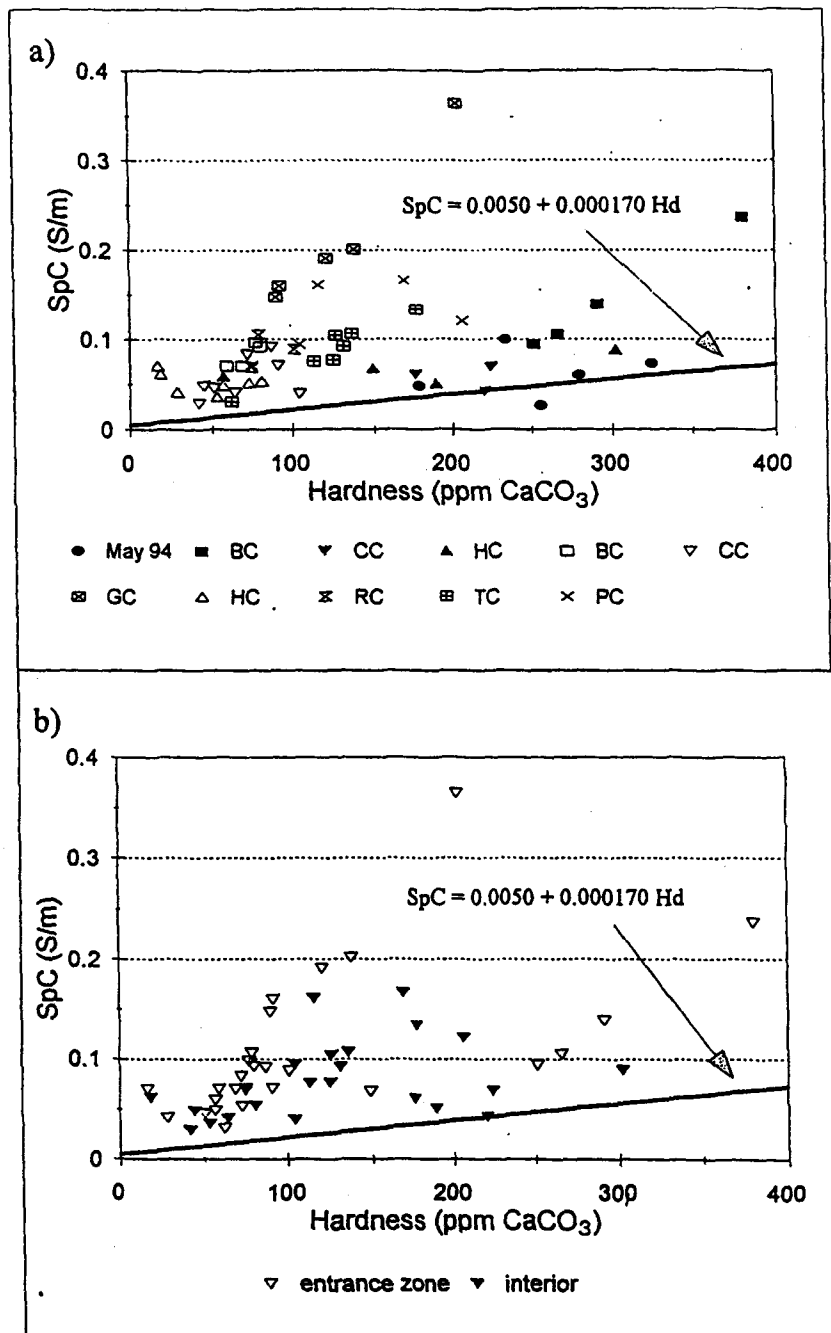


Fig. 4.7 Relationship between Specific Conductivity and Hardness for drip waters. a) Drip waters by cave; closed symbols indicate drip waters from heavy downpours (October 3 and 4, 1995) and open symbols drip waters from steady rain (May 1994 and September 26, 1995); b) Drip waters at the entrances and deep inside caves (Sept-Oct, 1995). The solid line is the Pennsylvania water line for inland bicarbonate waters given by White (1988, p. 137).

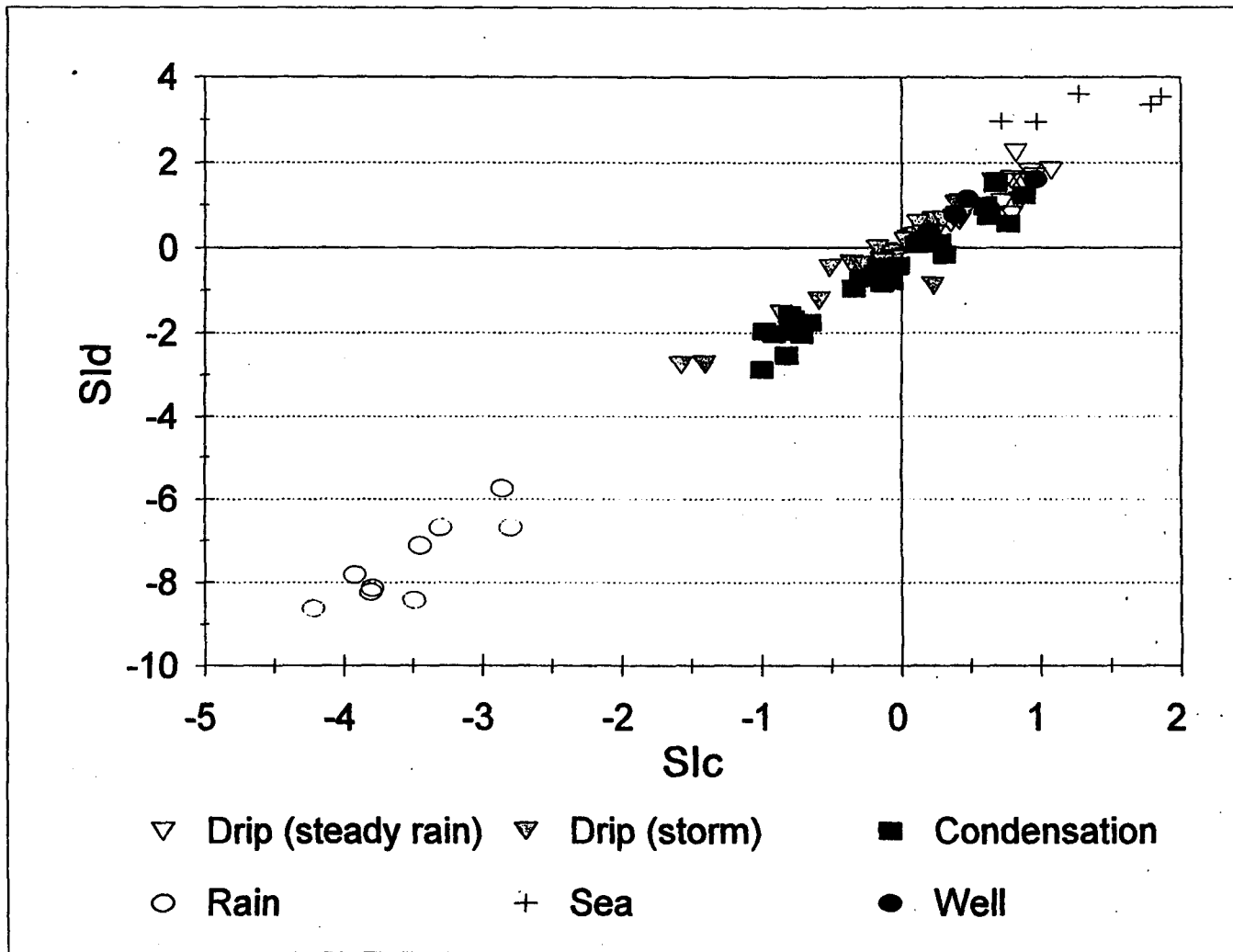


Fig. 4.8 Saturation Index for dolomite (SI<sub>d</sub>) versus the Saturation Index for calcite (SI<sub>c</sub>) for rain, drip and condensation water on Cayman Brac, 1994 and 1995.

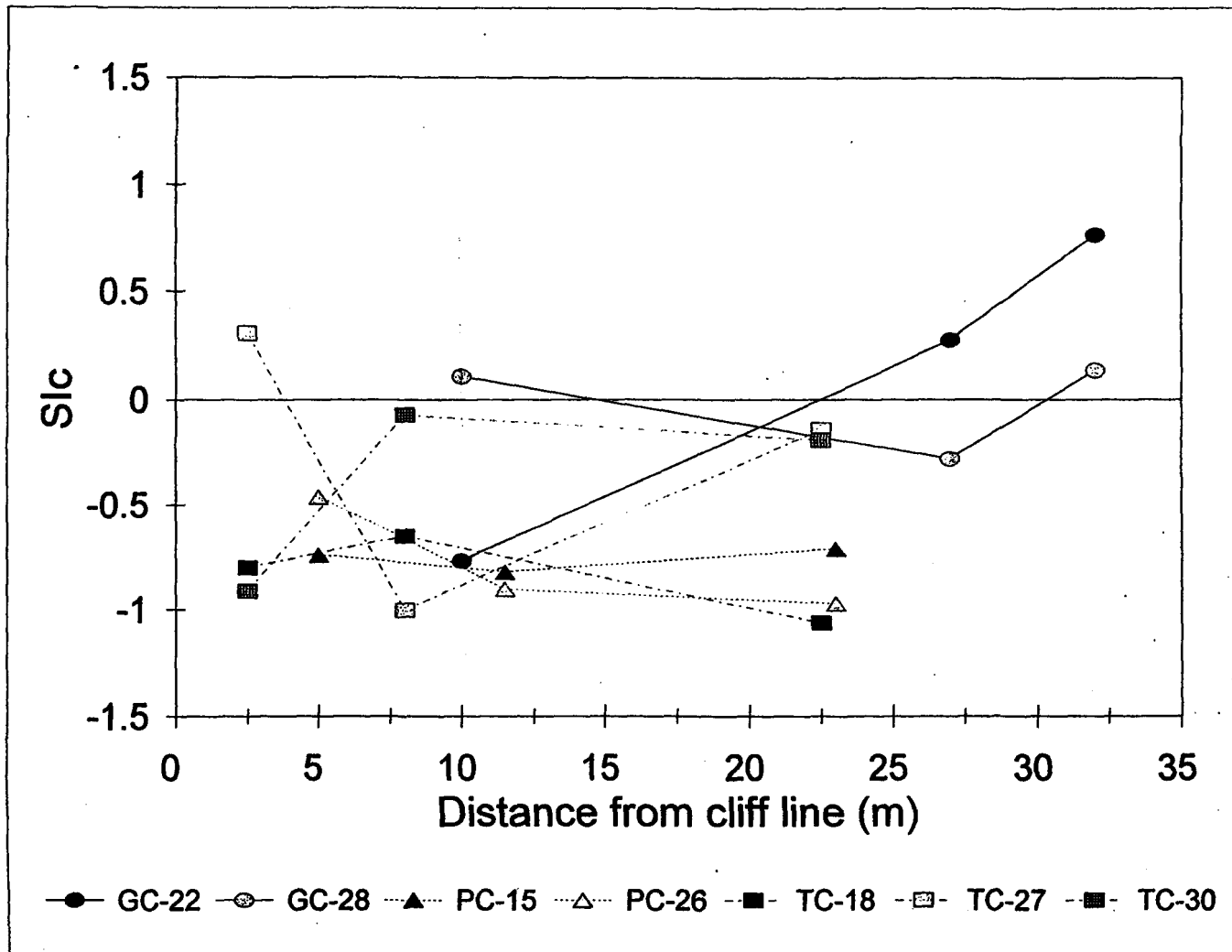


Fig. 4.9 The change in the Saturation Index for calcite (SIc) of condensation water with distance from the cliff line in three caves on Cayman Brac for September 15, 18, 22, 26, 27, 28 and 30, 1995.

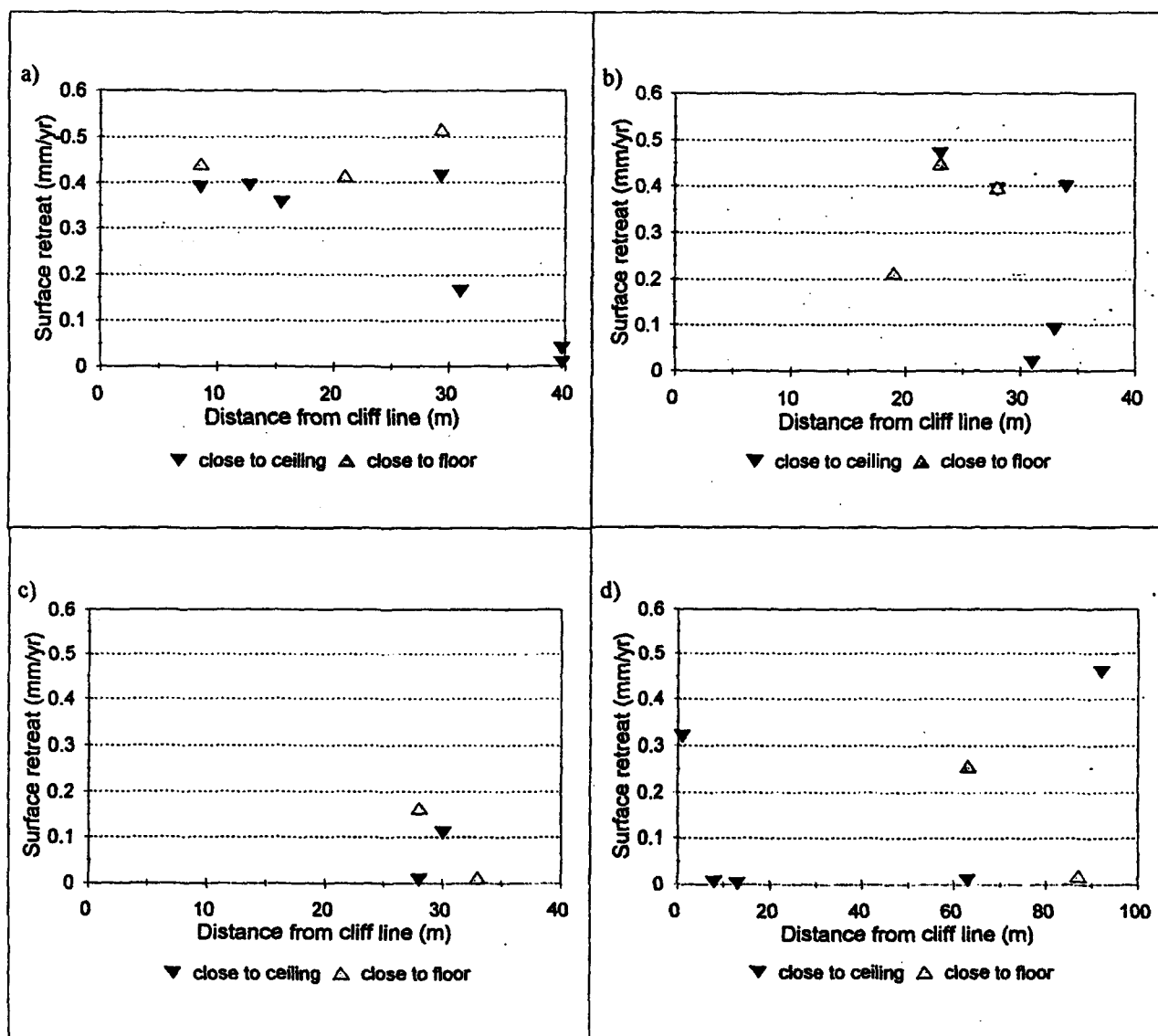


Fig. 4.10 Surface retreat of gypsum tablets in First Cay Cave (a), Peter's Cave (b), Tibbetts Turn Cave (c) on Cayman Brac and Cueva del Agua (d) on Isla de Mona.

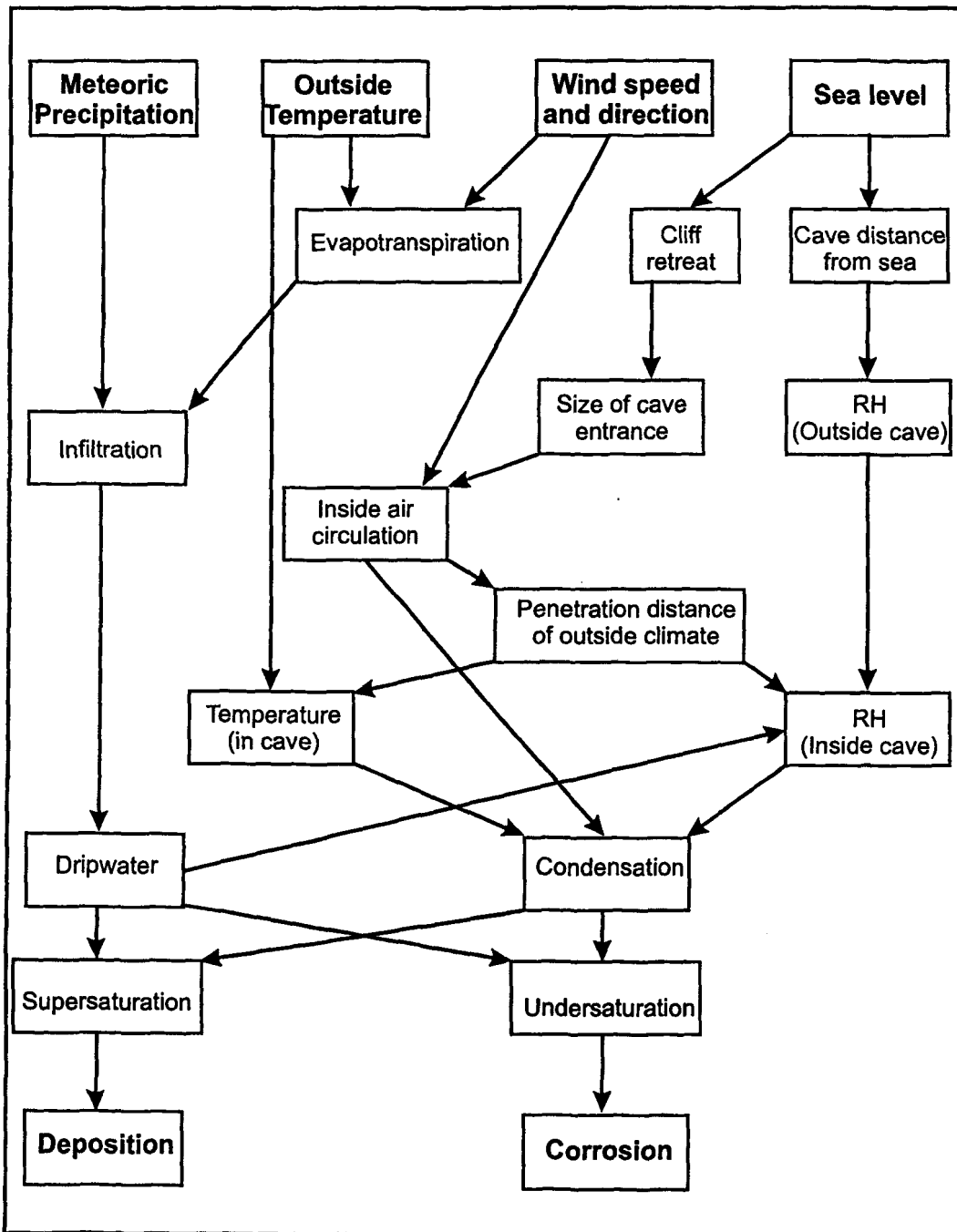


Fig. 4.11 Schematic representation of the interaction between the outside and cave environments.

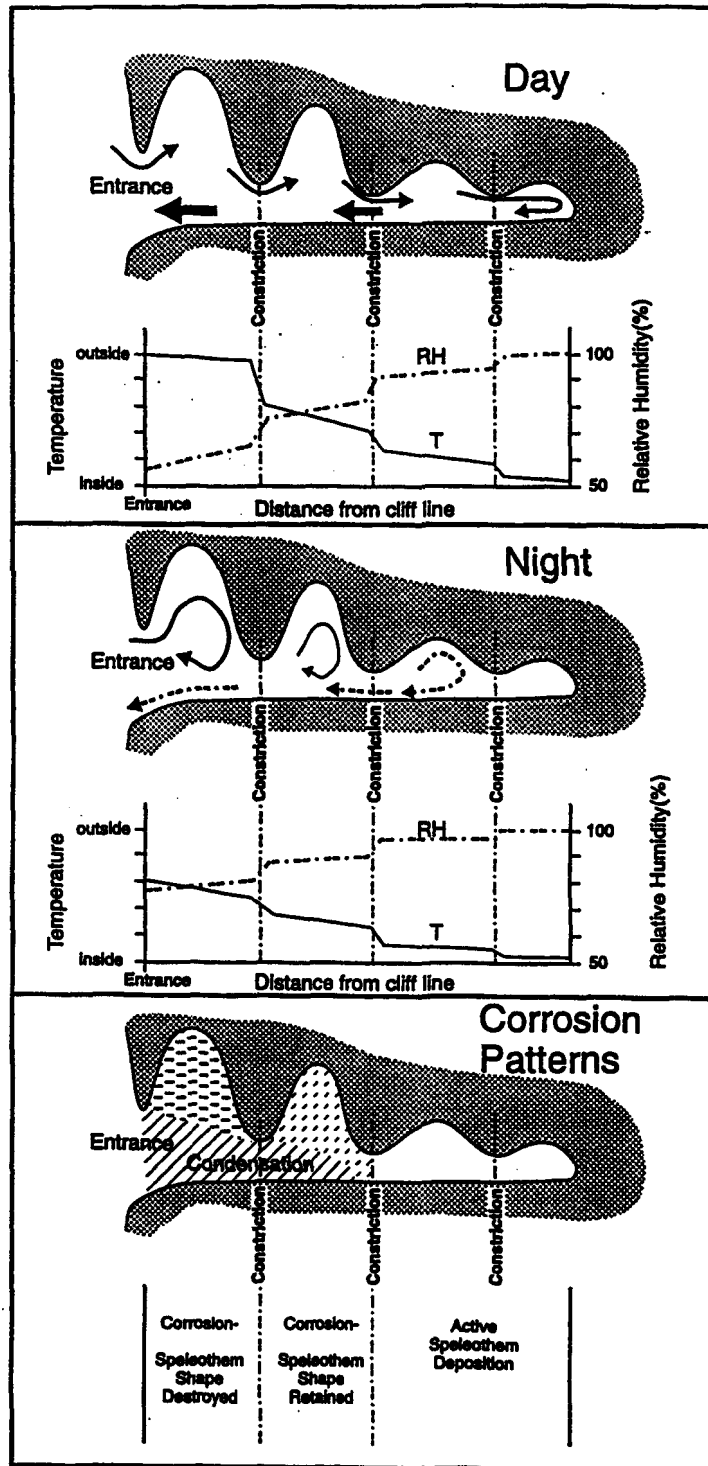


Fig. 4.12 Proposed model of condensation corrosion in coastal caves on small holokarstic oceanic islands with young rocks.

Table 4.1 Chemical analyses of different water types on Cayman Brac.

	SpC ( $\mu\text{S}/\text{cm}$ )			Ca tot ( $\text{mmol/l}$ )			Mg tot ( $\text{mmol/l}$ )			Sic			Std		
	max	min	mean	max	min	mean	max	min	mean	max	min	mean	max	min	mean
<b>Cayman Brac, May 1994</b>															
Sea	56000	46000	51660	148.13	104.91	116.73	648.56	0.50	265.98	1.86	0.72	1.32	3.62	2.96	3.30
Well	2180	210	1576	8.52	2.55	4.11	4.79	1.51	2.48	0.96	0.20	0.51	1.62	0.40	1.00
Rain	60	24	42	0.05	0.02	0.04	0.03	0.01	0.02	-2.88	-3.92	-3.38	-5.73	-7.81	-6.84
Drip	1000	270	616	1.75	0.96	1.23	2.52	0.81	1.42	0.82	0.43	0.69	2.25	1.08	1.62
Condensation	200	20	103	2.76	0.16	1.11	0.98	0.00	0.31	0.88	-0.96	0.05	1.54	-1.97	0.02
<b>Cayman Brac, Sept-Oct 1995</b>															
Rain	20	9	15	0.04	0.01	0.03	0.01	0.00	0.00	-2.80	-4.22	-3.59	-6.68	-6.62	-6.68
Drip	3646	292	945	2.87	0.07	0.84	1.19	0.00	0.41	1.07	-1.58	0.10	1.83	-2.76	0.10
Condensation	116	27	50	3.32	0.24	0.98	0.46	0.00	0.19	0.77	-1.06	-0.42	0.58	-2.67	-0.89
<b>Drip water for sample caves</b>															
Peters Cave	1664	718	1231	1.24	0.46	0.76	0.86	0.30	0.60	0.30	-0.27	-0.02	0.67	-0.50	0.11
Tibbets Tum Cave	1337	310	887	1.15	0.48	0.85	0.65	0.14	0.41	0.46	-0.13	0.17	0.88	-0.51	0.23
Cross Island Road Cave	917	292	565	2.09	0.23	0.76	0.71	0.14	0.34	0.95	-0.51	0.12	1.67	-0.47	0.19
Skull Cave	889	358	575	2.01	0.07	0.65	1.12	0.00	0.31	1.05	-1.58	-0.22	1.79	-2.76	-0.56
Rebecas Cave	1060	694	880	0.74	0.66	0.71	0.29	0.02	0.15	0.42	-0.06	0.19	0.64	-0.89	-0.30
Bats Cave	2367	703	1132	2.67	0.42	1.38	1.19	0.17	0.50	1.07	-0.11	0.46	1.83	-0.43	0.71
Great Cave	3646	1476	2130	1.04	0.56	0.73	1.03	0.33	0.58	0.40	0.06	0.19	1.04	0.18	0.49
<b>Condensation water for sample caves</b>															
Peters Cave	45	27	31	0.55	0.24	0.43	0.08	0.00	0.03	-0.46	-0.97	-0.77	-1.97	-2.53	-1.09
Tibbets Tum cave	116	29	59	2.94	0.41	1.16	0.42	0.00	0.22	0.31	-1.06	0.50	-0.17	-2.87	-1.18
Great Cave	107	38	56	3.32	0.44	1.25	0.46	0.16	0.30	0.77	-0.77	0.04	0.58	-1.69	-0.26

Table 4.2 The gypsum tablet experiment: location, measured surface recession and estimated daily condensation.

Cave	Shortest distance to cliff (m)	Measured surface recession (mm/yr)		Estimated aqueous condensation (mm/day)	
		H*	L*	H*	L*
<b>Reference samples</b>					
PC	19	0.01		0.02	
CAS	87	0.00		0.00	
<b>Cayman Brac</b>					
B2-Cave	1	0.37		0.94	
	2		0.08		0.22
First Cay Cave	9	0.39	0.44	1.00	1.14
	13	0.39		1.01	
	16	0.36		0.92	
	21		0.42		1.07
	29	0.41	0.52	1.07	1.33
	31	0.17		0.43	
	40	0.01		0.02	
	40	0.04		0.10	
Peters Cave	19		0.21		0.55
	23	0.47	0.45	1.21	1.16
	28	0.39	0.40	1.01	1.02
	31	0.02		0.05	
	33	0.09		0.23	
	34	0.40		1.03	
Tibbetts Turn Cave	28	0.01	0.16	0.02	0.42
	30	0.11		0.28	
	33		0.01		0.03
maximum		0.47	0.52	1.21	1.33
minimum		0.01	0.01	0.02	0.03
mean		0.24	0.30	0.62	0.77
<b>Isla de Mona</b>					
Cueva del Agua	1	0.32		0.82	
	6	0.01		0.02	
	13	0.00		0.00	
	63				
	83	0.01	0.26	0.03	0.66
	87		0.02		0.05
	92	0.46		1.18	
maximum		0.46	0.26	1.18	0.66
minimum		0.00	0.02	0.00	0.05
mean		0.16	0.14	0.41	0.36

H\* = close to ceiling; L\* = close to floor

## **CHAPTER FIVE**

# **Morphometric studies of Bell Hole Development On Cayman Brac.**

**Rozemarijn F.A. Tarhule-Lips and Derek C. Ford**

School of Geography and Geology, McMaster University,

Hamilton, Ontario, L8S 4K1, Canada

Published: *Cave and Karst Science*, 25(3): 119-130.

**Abstract** Bell holes are cylindrical cavities that extend vertically upwards into ceilings of caves. They have been reported only in the humid tropics. The processes responsible for their formation are not fully identified; different hypotheses have suggested mechanical, chemical or biological action but none of these appear to explain the holes satisfactorily.

On the Caribbean island of Cayman Brac bell holes appear to be distributed at random in the entrance zones of certain caves. The environment in which these holes formed and developed is subaerial rather than subaqueous. Fifty-five bell holes from five sample caves were measured in detail with a graduated gauge; profiles were drawn and volumes calculated for each. Bell holes in four of the caves displayed similar morphometry whereas the holes in the fifth cave were significantly different in size but not shape. All appear to be dissolutional rather than erosional features. Dissolution, enhanced or not by microbiological activity, is thought to take place in a thin film of condensation water.

### 5.1. *Introduction*

Bell holes are cylindrical or saucer-shaped cavities occurring in the ceilings of certain caves (Fig. 5.1). Their long axes are always vertical. Diameter and depth are variable but, in general, are less than one metre and two metres respectively (Table 5.1). Bell holes appear to be developed with complete disregard for any bedrock controls such as stratal dip or the ceiling geometry (horizontal or inclined, planar or curving, etc.; Fig. 5.2). They may form in rock without fractures or any other apparent feedwater inputs at their apex. In some instances two or more holes have merged to create a compound form.

As far as we are aware bell holes have been reported only from caves located in humid tropical settings, e.g. Trinidad (King-Webster and Kenny 1958), Sarawak (Wilford 1966), Trobriand Islands (Ollier 1975), Netherlands Antilles (Wagenaar Hummelinck 1979), Belize (Miller 1981), Cayman Islands, BWI (Lips 1993), Isla de Mona, Puerto Rico, and Bahamas (Lauritzen *et al.* 1997), Yucatan, Mexico (Beddows pers. comm. 1998) and in most of the circum-Caribbean lowland cave areas (Miller pers. comm. 1997). Six of these locations are islands and one a peninsula (Yucatan), where the caves are at or close to the coast but the Sarawak and Belizean examples are far inland. Table 5.1 presents the range of bell hole depths and diameters reported by these authors.

Bell holes differ from the most common type of ceiling solution pockets, observed in caves in all environments (tropical, temperate and arctic/alpine) because of their more limited form, cylindrical and strictly vertical. Conventional ceiling pockets are, in general, associated with fissures, joints or bedding planes in the ceiling (Slabe 1995; Dreybrodt and

Franke 1994; Ford and Williams 1989; Quinif 1973; Bretz 1942). Several different explanations have been offered for their origin and development. Bretz (1942) suggested that wall and ceiling pockets are formed in a phreatic environment with “an absence of definite current” (p.711). He also discussed ceiling tubes and half-tubes which he believed to be phreatic features formed when a slow hydraulic circulation utilizes the intersection of a bedding plane and a joint. Quinif (1973) and Ford and Williams (1989) also consider that the majority of conventional ceiling pockets develop under phreatic conditions and suggest that their preferential dissolution may be initiated by enhanced chemical aggressivity where groundwater flow in the principal conduit mixes with infiltration water descending along joints.

In contrast, Dreybrodt and Franke (1994) contend that ceiling solution pockets form in a vadose environment when infiltration water entering a cave through a fracture is undersaturated with respect to calcite, resulting in bedrock dissolution. If surface water with a  $p\text{CO}_2 < 5 \cdot 10^{-3}$  atm enters a joint and dissolves limestone on its way down under closed system conditions it will have a lower  $p\text{CO}_2$  than the cave air and it will absorb  $\text{CO}_2$  from the cave air, thus increasing its aggressiveness and dissolving more limestone. Following Lange (1968), these authors describe ceiling solution pockets as “negative copies of stalagmites” (p. 241) because the principles of the formation of both features are the same except that stalagmites are formed by nett precipitation and ceiling pockets by nett dissolution of material.

A distinctive feature of bell holes that must be emphasised is that they appear to lack any point of entry for infiltration waters from above. This would indicate that the process or processes responsible act from within the cave environment and that they are formed from the base upwards; simple dissolution or mixing corrosion involving drainage from overhead fissures is not an option. This was also stressed by Wilford (1966) for the bell holes of Sarawak.

## 5.2. *Hypotheses of Bell Hole Formation*

The origin and development of bell holes remains poorly understood. Previous authors have invoked a variety of mechanical, chemical and biological processes to explain their development.

### 5.2.1. *Action of roosting bats*

Early on it was suggested that the action of bats might be central to the process. King-Webster and Kenny (1958) proposed that bell holes were excavated by the claws of generations of roosting bats jostling for the centre position in a chance indentation in the cave ceiling. Over time this caused erosion of the soft granular rock. The slight widening that causes taper upwards in most examples was attributed to bats climbing the sides to get to the apex when the cavity becomes too deep to fly into directly. Miller (1981) also observed bell holes only where there were bats and suggested that their urine might be an active agent because its acidity will increase limestone dissolution.

The fact that bats and bell holes are often associated does not necessarily mean that the bats are responsible for the holes, however: the explanation may be as straightforward as the fact that bats look for protected places to roost and bell holes are ideal for this purpose. Moreover, the nearly perfect cylindrical forms and the absence of any claw-marks on the walls of the bell holes that we have observed cast doubt on this hypothesis. A major role for urine also seems problematic since it would require the bats to urinate upwards at the top; it could more likely contribute to the widening but the bell holes we have seen have very smooth and regular walls, rather than streaked, channelled or fluted by acidic trickles. Black spots have been observed in some bell holes occupied by bats but these could be explained equally well by dirty claws or body fat.

### 5.2.2. *Simple aqueous dissolution*

Wilford (1966) suggested that bell holes are aqueous dissolution features formed in the same manner as potholes, being "produced by eddies in fairly fast flowing water, the turbulence locally increasing the potential aggressiveness of the water" (p. 180). However, bell holes are often observed in parts of caves where such rapid flow is very unlikely or impossible, which led even Wilford to question his hypothesis. In addition, potholes are generated, at least in part, by one or more grinding rocks that are trapped inside them and spun by the force of the water, thus eroding mechanically down and outwards. This is clearly infeasible in the case of bell holes, where rocks could never be trapped or spun around to erode the ceiling. Furthermore, the precise verticality of the bell holes despite the frequent

occurrence of inclined structures militates against this hypothesis.

Ollier (1975) suggested that bell holes may be formed by slowly flowing waters in the phreatic zone, where dissolution can occur equally well in all directions. But if so, they would also be expected to occur in the cave walls. This was not found to be the case on Cayman Brac and is not reported from the other sites described in the literature. Once again, the strictly vertical long axes are difficult to explain in any simple phreatic situation. In addition, Miller (1981) observed bell holes in Belize “above relatively recent collapse in old phreatic chambers, where it is obvious they postdate the phreatic activity” (p.77). Lauritzen *et al.* (1997) and Lauritzen and Lundberg (in press) also argue for a vadose rather than a phreatic origin for bell holes on San Salvador Island, Bahamas, because of the association of bell holes with depressions on the floor directly underneath them and the fact that both appear to intersect vadose speleothems such as stalagmites at some locations.

### 5.2.3. *Other biogenic or biogenic plus flood origin*

In addition to bats, cyanobacteria, algae and the decay of larger plant material might, in theory, play a role in bell hole development through increase of limestone dissolution as a consequence of CO<sub>2</sub> liberation and production of other acidic compounds, etc. There have been no field studies or modelling of any effects, as yet.

Plant material is usually introduced into caves by rivers but none of the caves on Cayman Brac have or have had flowing rivers. Occasionally, hurricanes might have been able to flood some of them, thus introducing organic material. The development of bell holes

probably takes much time, however, and this mechanism would require that plant material always be deposited at the same few locations and that there be no equivalent dissolution of the remainder of the ceiling. This seems unlikely.

All of the genetic proposals summarised above seem incomplete or otherwise unsatisfactory at present. Despite the simple, striking form of bell holes there have been no previous attempts to measure them in detail. Therefore, the objectives of the field study reported below were to measure bell hole morphology and distribution by precise techniques, in the hope that this might reveal quantitative relationships more strongly indicative of the genetic mechanism(s).

### 5.3. *Cayman Brac*

Cayman Brac ( $19^{\circ}43'N$   $79^{\circ}47'W$ ) is the most eastern of the three Cayman Islands in the Caribbean Sea (Fig. 5.3). The islands lie on isolated volcanic blocks forming part of the Cayman Ridge, the northern margin of the Cayman Trench. They have cores of Tertiary strata - the Bluff Group (Jones *et al.* 1994a) which are fringed by a Pleistocene limestone - the Ironshore Formation.

Cayman Brac is a tilted island 19 km long and 1.5 to 3 km wide. The Bluff Group forms an inclined plateau descending from +45 m at the east end to sea level in the west, where it is overlain by the Ironshore Formation. The dip or tilt is due to differential tectonic movements of the island. The Bluff strata are cliffed around most of the island, with the

Ironshore limestone forming a coastal platform at the cliff foot. The principal shoreline erosional feature is a very strong bioerosion notch in the cliff at +6 m above modern sea level. This does not show any evidence of tilting, which indicates that there has been tectonic stability since at least the last sea level high stand (stage 5e or Sangamonian, 125,000 years BP; Woodroffe *et al.* 1983).

The Bluff Group consists of the Brac, Cayman and Pedro Castle formations (Fig. 5.3). The Brac Formation is exposed only in lower parts of cliffs at the eastern end of the island. On the north side it consists of wackestone to grainstone limestones. There are dolostones with pods of skeletal wackestones at various levels on the south side. Foraminiferal fauna and  $^{87}\text{Sr}/^{86}\text{Sr}$  ratios from the limestones indicate a late Early Oligocene (about 28 Ma) age (Jones *et al.* 1994b).

Most of the island is composed of fabric-retentive dolostones of the Cayman Formation. These are dominated by mudstones and wackestones but beds and lenses of rhodolites, rudstone, packstone and grainstone are also present. Bedding planes are difficult to trace from one end of the island to the other and marker beds are absent. Leaching of fossils has occurred and fossil-moulded vugs are visible. Due to the absence of age-determining fossils and disruption of initial  $^{87}\text{Sr}/^{86}\text{Sr}$  ratios by dolomitization it is not possible to assign a definite age to the formation; a Lower to Middle Miocene age is suspected (Jones *et al.* 1994b).

The Pedro Castle Formation (Jones *et al.* 1994a) is found only over a small area at the west end of the island where the Bluff Group is overlain by the Ironshore Formation. It

consists of dolostones and partially dolomitised limestones. The presence of *Stylophora*, a branching coral that became extinct in the Caribbean region towards the end of the Pliocene, and an average  $^{87}\text{Sr}/^{86}\text{Sr}$  ratio of 0.70912 from the limestones, suggesting a minimum age of approximately 2 million years, are good indicators of the Pliocene age of this formation (Jones *et al.* 1994b).

The known caves on the island are between 5 and 450 m in length and are situated in the cliff all around the island and on the plateau. The caves in the cliff have entrances between one and 23 m above the Sangamon +6 m Notch and may be divided into two groups: “Notch” caves which have their entrances only one to two metres above the Sangamon level, and “Upper” caves with entrances at irregular intervals more than two metres above the Notch. Although the former are close to the Notch this does not necessarily imply that the two features are genetically linked and have the same age. Four of the five sample caves that were used for this study are located in dolostones of the Cayman Formation (Charlotte's Cave, Skull Cave, Cross Island Road Cave and Walk-in Cave). Rebecca's Cave is formed in partially dolomitised limestone of the Pedro Castle Formation.

The morphologies of the two types of caves differ substantially. The “Notch” caves are good examples of the flank margin or coastal water mixing zone caves described by Mylroie and Carew (1990): horizontal cavities with rounded walls, characterised by large rooms close to the cliff that are backed by blind passages radiating inwards, and with few speleothems. They are relatively short on Cayman Brac, being less than 100 m in aggregate passage length, even when small lateral tubes or niches are measured separately. The

“Upper” caves do not display such common features. They have multiple passages, are longer (>100 m) and their formation has been influenced by structural features such as joints and bedding planes.

The bell holes are limited almost entirely to the entrance zones of the Notch caves. Circular skylights observed in certain caves (e.g. Rebecca's Cave and Bats Cave) are believed to have originated as bell holes, but subsequently have been intersected by dissolutional lowering of the land surface overhead.

Cayman Brac is an ideal site in which to study bell holes because of its physical simplicity. The island is small (44 km<sup>2</sup>), contains only one short stream (as far as we know) and has a relatively simple hydrological system: infiltrating rain water forms a freshwater lens which floats on top of the heavier saline water. The bedrock is very pure, with less than 3% insoluble residue, because the island is located far from any mainland or shelves where rivers might bring clays and sands into the sea. The climate is of a tropical marine type. The mean annual temperature is 26°C with very small seasonal temperature variations. Average precipitation is 1025 mm, concentrated mainly in the summer months and reflecting the NE-SW direction of the rain-bearing trade winds. The proximity of the sea maintains a quite high relative humidity at all times.

#### 5.4. *Methods of Measurement*

The caves were mapped at BCRA Grade 5 by standard procedures, with the locations of all bell holes plotted precisely upon them.

The depth and diameter of 55 sample bell holes in five caves were measured using graduated wooden dowels (Figs. 5.2 and 5.4a). The horizontal bars of the T-shaped device were of known lengths in 5 cm intervals. The vertical section consisted of dowels with adjustable linkage, graduated in one cm intervals. Standard procedure was to measure the height of the ceiling and the diameter of the bell hole at ceiling level (basal diameter), then to measure diameter up the hole in steps of 5 or 10 cm, reading off the distance to the floor at each step. Bell hole profiles were drawn by subtracting the floor-ceiling distance from these measurements. Bell hole volumes were calculated as series of stacked cylinders because the diameter does not always decrease gradually from base to apex (Fig. 5.4b).

## 5.5. *Results and Analysis*

For this study ten bell holes in Skull Cave, four in Walk-in Cave, six in Rebecca's Cave, eleven in Cross Island Road Cave and 24 in Charlotte's Cave were used (Fig. 5.5). All bell holes extend vertically into the ceiling regardless of its angle and display smooth walls without any vertical fluting or other kinds of grooves. Sometimes two or more bell holes intersect each other (e.g. in Skull Cave) to form a compound bell hole.

### 5.5.1. *Location*

Bell holes on Cayman Brac appear to be limited to the entrance zones of the Notch caves. In most instances these contain the largest and highest rooms in these caves and receive some measure of daylight. Bell hole distribution within the entrance zones appears

to be random, however, although in some cases they are found in clusters. Also, within this zone, there is no relationship between the distance from the entrance and the depth, basal diameter or volume of the bell holes (Fig. 5.6). It can be concluded that whatever process(es) are responsible for the formation of the holes, they operate rather uniformly over the areas in which they are found.

Charlotte's Cave is an exception because 8 of its 24 bell holes follow two lines intersecting at an angle of  $90^\circ$ , one line being parallel to the cliff and the other perpendicular to it (Fig. 5.6e). There did not appear to be any lithological or structural reason for this alignment. However, at the same place there is an abrupt step of about 2 m in the floor that is roughly parallel to the cliff, while the ceiling slopes upwards, into the cave and normal to it; therefore, the alignment might be due to some, as yet unknown, topographical influence on bell hole formation.

#### 5.5.2. *Morphometry of individuals*

Figure 5.8 depicts the measured sections of all sample bell holes, which are drawn at the same scale to emphasise the variety of their depth and diameter in the different caves. The bell holes of Charlotte's Cave look like miniature versions of the range of shapes and proportions measured in the other four caves. This might be an indication that the developmental process in this cave is slower or working under less than ideal situations. It might also be that the bedrock at this particular location is more resistant to the process because of its composition, e.g. more coral-rich.

Bell holes RC1, RC2 and CH3 are examples of the perfect vertical long axis occurring where the ceiling is steeply inclined. Some holes have a broad, nearly flat apex (e.g. SC10 and CC7) whereas others are more pointed (e.g. CC9, WC1 and CH5). Several holes display drastic reduction in diameter near the apex (e.g. CC6, CH11 and CH20). Others show a more stepped taper (e.g. SC4, CC8 and CH2). WC2 is exceptional in that it first widens and then narrows again along its mid-section. These changes in diameter most likely are indicative of changes in the parameters governing the developmental process, e.g. change in environmental conditions. SC5 has the most atypical bell hole shape; it is narrow at the bottom and widens towards the apex. It is one of three bell holes which have merged to form a compound feature and this might have caused its unusual form.

The depth of bell holes varies from as shallow as 0.2 m to as deep as 5.7 m, but the majority do not exceed three metres (Fig. 5.8a). The deepest bell holes are limited to Skull Cave and Cross Island Road Cave. Bell holes in Walk-in Cave and Rebecca's Cave, plus four from Skull Cave, are very similar in depth, between 1.0 m and 1.5 m. The majority of the holes found in Charlotte's Cave are much shallower and narrower.

Diameters measured at the base of individual bell holes range from 0.25 m to 1.3 m (Fig. 5.8b). In spite of this range the basic shape of the holes is very similar, with a depth to diameter ratio  $\geq 1$  for the vast majority. Almost all of them display taper upwards: the taper angle ranges from  $2.5^\circ$  to  $30.5^\circ$ , with an average of  $10^\circ$ . The apex diameter can be taken to represent the bell hole as a perfect cylinder, while the basal diameter indicates its widening away from the perfect form. The apex diameter (indicated by a dash near the apex

of bell holes on Fig. 5.7) never exceeds 0.7 m and is generally between 0.3 m and 0.5 m. (Fig. 5.8c). Plotting the two diameters against each other produces a very poor relationship, especially if the Charlotte's Cave data are not drawn (Fig. 5.9). This suggests that any subsequent widening is not related to the initial diameter alone. Relationships between depth and either apex or basal diameter are very poor as well (Fig. 5.10). Instead there does seem to be a relationship between depth and taper angle; the latter appears to decrease exponentially with increasing depth, suggesting that widening of the bell holes slows as they become deeper (Fig. 5.11).

The volume of bell holes is very varied, ranging from 0.002 m<sup>3</sup> to 2.55 m<sup>3</sup>. The smaller volumes were found in Charlotte's Cave and the largest ones in Skull Cave and Cross Island Road Cave (Fig. 5.8d).

In general, the bell holes in Charlotte's Cave differ from those in the other caves because of their smaller size and high depth to diameter ratio (Fig. 5.8). Mean diameters, depths and volumes form a class of their own on the lower side of the scale, differing at a 95% probability level (Student t-test) from the other four caves. Volume of the bell holes in Charlotte's Cave is more strongly correlated with the basal diameter ( $r^2 = 0.80$ ; Fig. 5.12) than in the other four caves. Charlotte's Cave is in the same dolostone formation as three of the other caves, suggesting that these pronounced differences are not related to the bedrock composition or texture in any very simple manner. The entrance of Charlotte's Cave is much smaller than any of the others, however, resulting in a darker environment with fewer hours of light per day. If photosynthetic biological activity is (partly) responsible for the initiation

and development of bell holes (as will be discussed later) then this might result in a less ideal growth situation for the organisms and, consequently, smaller bell hole sizes.

### 5.5.3. *Compound bell holes*

From time to time, two or more bell holes merge to form a more complex feature, referred to as a compound bell hole. The majority of bell holes noted in caves on Trinidad by King-Webster and Kenny (1958) were compound. On Cayman Brac there are four pairs and one triplet in Skull Cave and two pairs in Charlotte's Cave.

Even in these compound features it is possible to identify the individual bell holes quite clearly. This suggests that there is simultaneous expansion outwards and upwards of individual bell holes after connection has been established. This could occur either in a water-filled passage or when there is dissolution from a thin water film on the walls, as might be expected if condensation corrosion played a role.

### 5.5.4. *Bell pits*

Bell pits (Lauritzen *et al.* 1997; Lauritzen and Lundberg in press) are circular to oval floor depressions that are often found directly underneath bell holes or may occur on their own. On Cayman Brac they were only observed in Charlotte's Cave.

Although in Lighthouse Cave, San Salvador Island, Bahamas, "almost every bell hole is associated with a paired bell pit in the floor" (Lauritzen and Lundberg in press) only nine of the 24 measured bell holes in Charlotte's Cave had such a relationship (Figs. 5.6 and

5.13). There were also four bell pits that did not have a bell hole in the ceiling above them. Each bell pit in Lighthouse Cave had a slightly larger diameter than its associated bell hole and none were quite as deep as the hole (Lauritzen *et al.* 1997; Lauritzen and Lundberg in press). In Charlotte's Cave two pits had slightly greater diameters than the bell holes above them, another two were about the same and five were smaller (Fig. 5.14a); two bell pits were deeper even than the holes above them (Fig. 5.14b). Of the 13 bell pits in the cave, seven had a circular cross section and six were oval. This is distinctly different from bell holes, which are almost always circular in cross section.

## 5.6. Discussion

There are three alternative environments in which bell holes might have formed: a) subaqueous, b) sporadic flooding and c) subaerial. In the subaqueous environment bell hole development would most likely take place according to the mechanisms proposed by Ollier (1975). The Notch caves were formed in phreatic zones at the margins of a freshwater lens in conditions of slow water flow. As noted, the bell holes appear to have formed from the base upward and outward. In the case of dissolution in a water-filled passage, bell hole-like shapes should also occur in the walls and floors of the passages. Further, the sharp rims between individual bell holes in compound examples should gradually round out and then disappear as dissolution enlarges the voids. The rims in all compound cases on Cayman Brac are still clearly visible and sharply inflected, strongly suggesting a subaerial rather than a subaqueous environment.

Since no rivers or evidence of past rivers are observed inside the caves, sporadic flooding could only have occurred when sea level was higher than at present or, perhaps, during hurricanes. The islanders use the caves for shelter during hurricanes today suggesting that, if they flood at all under modern conditions, it is extremely rare. The last period when sea level was close to the entrances of the caves was when the Notch formed during the last (Sangamon) interglacial, 125,000 years ago. If complete flooding of each bell hole cave occurred during the Sangamon, then the caves were older and open to the outside at that time. Sea level must have risen a further 6 m or more above the +6 m notch on occasion (2 m to the typical entrance and another 4+ m to reach the ceilings). Flooding might also have been the result of very high and intensive wave action during this period of high sea level. However, the entrances to Skull Cave, Rebecca's Cave and Charlotte's Cave are (very) small, implying that wave action will have been drastically dampened inside the caves. As with phreatic submergence of the caves, a periodic flooding mechanism does not appear to offer a satisfactory explanation for the development of the bell holes.

All bell holes on Cayman Brac are in the entrance zones of the caves, as are those studied by Lauritzen and Lundberg (1997) on San Salvador Island. In Belize, Miller (per. comm. 1997) observed a few bell holes far inside one river cave, but most examples were also near to the entrances. This apparent preference for entrance zones would suggest that certain conditions exist here that favour their formation. On Cayman Brac, all are found in areas which receive some amount of natural light and where significant aqueous condensation occurs (Tarhule-Lips and Ford 1998). Condensation is prevalent in the entrance

areas and quickly decreases inwards from the cliff (Fig. 5.15). Water condenses as thin films on walls and ceilings when warmer, humid air flows along cooler surfaces. Heat released by condensation eventually warms the rock surface to the ambient air temperature, thereby inhibiting further condensation. For it to be renewed, cooling of the surface is thus required. This is achieved either when cooler air flows over the rock or when water evaporates from it. Both cases will occur during the night on Cayman Brac, when the outside dew point temperature falls below that in the caves. The process is thus sustained by a regular alternation of warmer and cooler (day and night) airflow, which can only take place when the cave is open to effective outside air circulation (Fig. 5.15).

Condensation corrosion is the dissolution of soluble rock by condensation water. Condensation water which is undersaturated with respect to carbonate bedrock has been observed in many different karst areas of Eurasia (see Dublyansky and Dublyansky 1998 for a review). It is believed to be active primarily in the cave entrance zones on Cayman Brac, (both at and above the Notch), where it can be seen to have dissolved both bedrock and speleothem (Tarhule-Lips and Ford 1998).

Air exchange in the bell holes will likely be less dynamic than the general cave air exchange but still can occur on a daily basis. M.J.Simms (review comment 1998) suggests that "When warm air flows into the cave during the day the air in the bell holes, which will have cooled gradually during the night, will sink to be replaced by rising warm humid air. The water in this humid air will then condense on the, by then slightly cooled, walls of the bell holes and so cause dissolution. The air in the bell holes will be fairly static and, being

slightly warmer than the night-time air, will remain there during the night when cooler air flows into the cave below. Only when warmer air flows into the cave again during the day will the, by then slightly cooler and drier, air in the bell hole be replaced by more warm humid air. The static nature of the air in the bell hole may be the controlling factor in producing the remarkable symmetry of these dissolutional karst forms, while the regular daily replacement of cool dry air by warm humid air by the mechanism outlined above will ensure the continued upward growth of these features. The deeper bell holes will provide a more stable environment for static air and hence will favour their continued formation in a positive feedback mechanism”.

The initiation of bell holes remains a stumbling block for this proposed mechanism, as it does in general terms for all of the alternatives reviewed above. For preferred condensation, it is necessary to have an initial indentation into the ceiling that is deep enough to prevent the general air circulation from exchanging the air inside the hole with great frequency. We suspect that favourable patches on the ceiling rock surface or within its skin, and/or favourable illumination, wetting and drying on patches attracts microorganisms capable of enhancing bedrock dissolution. Queen (1994) has concluded that the systematic redistribution of water, heat, atmospheric gases and solutes by thermal convection in a cave influences “the physical environments which control the nature and distribution of cave macro- and microbiota” (Queen 1994: 62).

Cunningham *et al.* (1994: 13) reported heterotrophic bacteria and probably also autotrophic bacteria in “ceiling-bound deposits of supposedly abiogenic condensation-

corrosion residues” (p. 13). The ceiling deposits were often associated with floor deposits of “talc-like, porous, white to buff coloured material” which was derived from the surrounding bedrock. The autotrophic bacteria were believed to utilize trace elements (iron, manganese or sulphur) in the bedrock to “mechanically (and possibly biochemically) erode the limestone bedrock to produce the residual floor deposits”. Bedrock can also be dissolved by liquid acidic compounds released by microorganisms or by carbonic acid formed from water plus the CO<sub>2</sub> that they produce.

Jones (1995) investigated microbial biofilms on cave walls in the twilight zone in Skull Cave and Bats Cave on Cayman Brac and Old Man Village Cave on Grand Cayman. The bell holes in Bats cave were not selected for this study. The cave has mainly circular skylights that are believed to have been bell holes that were intersected by surface erosion (Lips, 1993). He concluded that all microbes had an epilithic life mode. The biofilms were 100-200 µm thick and “incorporate an abundant, diverse community of microbes and mucus that mediate a wide array of destructive and constructive processes” (Jones 1995: 559), the destructive processes being more common than the constructive ones. Calcite and dolomite were attacked by irregular etching, leaving small (< 4 µm) residual particles of the two minerals. There was “relatively little evidence of detrital grains being trapped and bound” by the filamentous microbes (p. 556), leading us to suppose that the solid particles are carried away from the local system. The dissolved calcite and dolomite can be reprecipitated (calcification) or can also leave the system. Calcification was found to be limited and to be controlled by environmental factors rather than by the microbes themselves. Merz (1992,

cited in Jones 1995: 559) “noted that calcification takes place only if the associated waters are supersaturated with respect to calcite, if there is bicarbonate uptake by cyanobacteria, and if the sheath is suitable for precipitation”. If the water used by the microorganisms derives from condensation, (as we believe), lack of calcification is due to the fact that the condensation water on Cayman Brac is generally undersaturated, not supersaturated, with respect to calcite and/or dolomite (Tarhule-Lips and Ford 1998).

In order to better understand the role of fungi in carbonate diagenesis, Jones and Pemberton (1987 a&b) placed 20 different species onto crystals of Iceland spar calcite in Pyrex vessels, where they were kept moist and at a constant temperature for 253 days. At the end of the period a samples of the calcite crystals was examined with a scanning electron microscope and found to be extensively damaged by dissolution. Although they had taken great care not to put any moisture directly onto the crystals and fungi, Jones and Pemberton (1987a) noted that some of the water condensing on the inside of the vessels had dripped onto the calcite, washing silt size particles from them to form accumulations on the bottoms of the dishes.

From these findings, we suggest that bell holes may be initiated where colonies of microorganisms are able to establish themselves at certain locations within a cave that are wetted by condensation water. Microbial activity is at its optimum in the well lit - twilight entrance zones of caves, although it is not precluded deeper inside. Enhanced dissolution beneath thicker biofilms on preferred patches of a ceiling cause them to recede faster than the remainder, resulting in an indentation. The strict circularity of the bell holes and their

characteristic maximum diameter at the apex suggest that regular microbial colonies with dominant species are at work. Daily cycles of condensation and evaporation are also at their optimum in the entrance zones, as shown above. During the condensation period there is wetting of the film plus simple (inorganic) dissolution, while desiccation during the evaporative phase permits any detrital particles that have been liberated to fall away.

The strict verticality of the bell holes strongly suggests to us that the formative process (initiating and maintaining the cylinder) is gravity-dependent. Removal of residual particulate matter (such as Jones and Pemberton (1987a,b) observe in their experiments) is most effective where it can fall freely downwards. The particles released are likely to be very small ( $< 4 \mu\text{m}$ ; Jones 1995) and, because no heaps of sediments were noted directly underneath the Cayman bell holes, it may be supposed that they are dispersed as aerosols. Regulation of growth by the detachment and fall of micro-particles explains why bell holes become deeper more rapidly than they become wider, resulting in the typical bell shape. Once a cylinder is formed, water condensing on the walls will flow away as a very thin film in which dissolution capacity is progressively reduced towards the base because saturated water flowing down from above dilutes any undersaturated water condensing on the lower parts. This may explain the exponential decrease in degree of taper with increasing depth in the Cayman bell holes (Fig. 5.11). As they become deeper, film flow at the base is increasingly dominated by transfer of saturated water from above, reducing rates of dissolution in these lower parts whereas they remain the same near the apex.

Lauritzen *et al.* (1997) ascribed the bell pits underneath bell holes in Lighthouse

Cave, San Salvador Island, to chemically aggressive drip water from the bell holes. This implies that the film flow retains some dissolutional competence at the base of the bell hole, at least at certain times of the year. We would add that some of the bell pits observed in Charlotte's Cave, Cayman Brac, are cut into steeply inclined slopes, supporting the proposition that they must be formed by aggressive drip water. Miller (1981) also described bell pits underneath some bell holes in Belize and thought that they might have been formed by "films of aggressive water as suggested by re-solution of some nearby stalagmites" (p. 77). Many of the bell pits in Belize were filled with bat guano, which might have enhanced dissolution through its acidity. None of the pits in Charlotte's Cave contain guano at present but it is possible that they did so in the past.

#### 5.6.1. *Rates of bell hole formation*

From recession rates measured on gypsum tablets suspended in four caves on Cayman Brac, mean condensation corrosion rates of ~24 mm per 1000 years have been estimated for calcite (Tarhule-Lips and Ford 1998). If we consider only the vertical recession of the bell holes and attribute that to dissolution by condensation water alone, (neglecting any microbial enhancement) then the calculated time required to form them ranges from ~2000 years for the smallest individuals to ~90,000 years for the deepest; excepting Charlotte's Cave, the mean age is ~35,500 years (Fig. 5.16; Table 5.2). From the dated speleothem record on Cayman Brac (Tarhule-Lips and Ford 1997) it is clear that vigorous dissolution by condensation corrosion in cave entrance zones has occurred during distinct periods in the

past but not continuously. If condensation corrosion and bell hole formation are linked, then it is most likely that bell hole formation has not been continuous, either: our estimates give a crude idea of the amount of corrosion time that may be required to form these bell holes, but do not necessarily indicate the age of their initiation. Discontinuous formation might also explain some of the more abrupt changes in the shapes of certain bell holes (e.g. CC6, CC8, WC2, SC2, SC4, CH2, CH16 and CH19 in Fig. 5.7).

#### 5.7. *Conclusions*

Bell holes are generated from the base upwards in the illuminated entrance zones of Notch caves on Cayman Brac. They have obtained their typical bell shape as a result of simultaneous upward and outward expansion, where the upward expansion is more rapid. From the degree of taper it is concluded that the outward expansion slows down as the bell hole grows deeper. The most likely environment for bell hole development is subaerial rather than subaqueous because the perfect vertical long axis and the location are difficult to explain in fully flooded or intermittently flooded situations. We suspect that they develop as a result of a combination of microbiological activity and condensation corrosion. The most soluble particles are removed first, discharged in the film flow. Their loss permits the residual grains to fall away. Simple gravitational fall makes a most important contribution to bell hole deepening, we suggest; it explains the precise verticality of the long axis.

Estimates of the time necessary to create the deepest examples range up to 90,000 years but are probably overestimates because biocorrosion is not included. However, in the

deeper cases, bell hole growth was probably periodic rather than continuous.

We suggest that further research into the role of condensation and of microbiological activity is needed. The walls and apices of bell holes should be sampled for the presence of biofilms. Detailed microclimatological studies inside the bell holes might help to establish the patterns of air exchange in them but will be difficult to carry out: computer modelling is probably an easier option. The amounts and chemical composition of their condensation water should also be looked at in detail.

#### *Acknowledgements*

The authors would like to thank Karen Lazzari of the Cayman Water Authority for logistical support; Dr. McLaughlin from the Ministry of Environment of the Cayman Islands for permission to study the caves and collect samples; Mr. Banks of the Mosquito Control Unit for meteorological data during the period of study; Pedro Lazzari for showing us the island from a fisherman's point of view; and everybody else on Cayman Brac who helped and kept us company during our stay on the island. Thanks goes to Mike Bagosy, Craig Malis and Dr. Steve Worthington for their assistance in the field and to Dale Boudreau for helping with meteorological instruments and the interpretation of results. All are also thanked for the many fruitful discussions. A special thanks to Dr. B.E. Jones, University of Alberta, for introducing us to the geology and people of the island.

This paper has greatly benefited from the helpful comments and suggestions of the reviewers, S.-E. Lauritzen and M.J. Simms.

This work was supported by a Research Grant to Ford from the Natural Sciences and Engineering Research Council of Canada.

### References

- Bretz, J.H., 1942. Vadose and phreatic features of limestone caverns. *J. Geol.*, 50 (6): 675-811.
- Cunningham, K.I., Northup, D.E., Pollastro, R.M., Wright, W.G. and LaRock, E.J., 1994. Bacterial and fungal habitation in Lechuguilla Cave, Carlsbad Caverns National Park, New Mexico - Possible biologic origin of condensation-corrosion residues. In: Sasowski, I.D. and Palmer, M.V. (Ed.). Breakthroughs in Karst Geomicrobiology and Redox Geochemistry, Abstracts and field-trip guide for the symposium held February 16 through 19, 1994, Colorado Springs, Colorado, *Karst water Institute, Special Publication 1*, 111 p.: 13-14
- Dreybrodt, W. and Franke, H.W., 1994. Joint controlled solution pockets (Laugungskolke) in ceilings of limestone caves: a model of their genesis, growth rates and diameters. *Z. Geomorph. N.F.*, 38 (2): 239-245.
- Dublyansky, V.N. and Dublyansky, Y.V., 1998. The problem of condensation in karst studies. *J. Cave and Karst Studies*, 60(1): 3-17.
- Ford, D.C. and Williams, P.W., 1989. *Karst geomorphology and Hydrology*. London (Chapman and Hall), 601 p.
- Jones, B., 1995. Processes associated with microbial biofilms in the twilight zone of caves: examples from the Cayman Islands. *J. Sed. Res.*, A65(3): 552-560.
- Jones, B. and Pemberton, S.G., 1987a. The role of fungi in the diagenetic alteration of spar calcite. *Can. J. Earth Sci.*, 24: 903-914.

- Jones, B. and Pemberton, S.G., 1987b. Experimental formation of spiky calcite through organically mediated dissolution. *J. Sed. Petrol.*, 57(4): 687-694.
- Jones, B., Hunter, I.G. and Kyser, K., 1994a. Revised stratigraphic nomenclature for Tertiary strata of the Cayman Islands, British West Indies. *Carib. J. Sci.*, 30: 53-68.
- Jones, B., Hunter, I.G. and Kyser, K., 1994b. Stratigraphy of the Bluff Formation (Miocene-Pliocene) and the newly defined Brac Formation (Oligocene), Cayman Brac, British West Indies. *Carib. J. Sci.*, 30: 30-51.
- King-Webster, W.A. and Kenny, J.S., 1958. Bat erosion as a factor in cave formation. *Nature*, 181: 1813.
- Lange, A.L., 1968. The changing geometry of cave structures. *Cave Notes*, 10(1-3): 1-10, 13-19, 26-27, 29-32.
- Lauritzen, S.-E. and Lundberg, J., in press. Chapter 6. Meso- and micromorphology of caves. 6.1 Solutional and erosional morphology. In: Klimchouk, A. (Ed.) *Speleogenesis*. Huntsville, Alabama; National Speleological Society of America.
- Lauritzen, S.-E., Lundberg, J., Mylroie, J.E. and Dogwiler, T. , 1997. Bell hole morphology of a flank margin cave and possible genetic models: Lighthouse Cave, San Salvador, The Bahamas. in: Jeannin, P.-Y. (ed.) *Proceedings of the 12<sup>th</sup> International Congress of Speleology*, La Chaux-de-Fonds, Switzerland, August 10-17, 1997, V.1: 178.
- Lips, R.F.A., 1993. *Speleogenesis on Cayman Brac, Cayman Islands, British West Indies*. M.Sc. Thesis, McMaster University, Hamilton, Ontario, Canada, 223 p.

- Miller, T., 1981. *Hydrochemistry, hydrology, and morphology of the Caves Branch Karst, Belize*. PhD Thesis, McMaster University, Hamilton, Ontario, Canada, 280 p.
- Myroie, J.E. and Carew, J.L., 1990. The flank margin model for dissolution cave development in carbonate platforms. *Earth Surface Processes and Landforms*, 15: 413-424.
- Ollier, C.D., 1975. Coral island geomorphology. *Z. Geomorph. N.F.*, 19: 164-190.
- Queen, J.M., 1994. Influence of thermal atmospheric convection on the nature and distribution of microbiota in cave environments. In: Sasowski, I.D. and Palmer, M.V. (Ed.), 1994. Breakthroughs in Karst Geomicrobiology and Redox Geochemistry, Abstracts and field-trip guide for the symposium held February 16 through 19, 1994, Colorado Springs, Colorado, *Karst water Institute, Special Publication 1*, 111 p.: 62-63.
- Quinif, Y., 1973. Contribution a l'étude morphologique des coupoles, *Ann. Spéléol.*, 28: 565-573.
- Slabe, T., 1995. *Cave rocky relief and its speleogenetical significance*. Ljubljana (Znanstvenoraziskovalni Center SAZU) Zbirka ZRC, 10, 128 p.
- Tarhule-Lips, R.F.A. and Ford, D.C., 1998. Condensation corrosion in caves on Cayman Brac and Isla de Mona. *J. Cave and Karst Studies*, 60 (2): 84-95.
- Tarhule-Lips, R.F.A. and Ford, D.C., 1997. Studies of speleothem dissolution on Cayman Brac and Isla de Mona, in: Jeannin, P.-Y. (ed.) *Proceedings of the 12<sup>th</sup> International Congress of Speleology*, La Chaux-de-Fonds, Switzerland, August 10-17, 1997,

V.1: 261.

Wagenaar Hummelinck, P., 1979. *Caves of the Netherlands Antilles*. Uitgaven van de Natuurwetenschappelijke Studiekring voor Suriname en de Nederlandse Antillen,

97, Natuurhistorische Reeks, No. 1, 176 p.

Wilford, C.E., 1966. "Bell Holes" in Sarawak Caves. *N.S.S. Bull.*, 28 (4): 179-182.

Woodroffe, C.D., Stoddart, D.R., Harmon, R.S. and Spencer, T., 1983. Coastal morphology and late Quaternary history, Cayman Islands, West Indies. *Quat. Res.*, 19: 64-84.

### List of Figures

- 5.1 Natural cross section through a bell hole as a result of ceiling collapse in Rebecca's Cave.
- 5.2 Schematic representation of bell holes. Note the strictly vertical long axis and the complete disregard for any bedrock controls such as stratal dip or for the ceiling geometry.
- 5.3 a) Location of Cayman Brac. b) Geology of Cayman Brac and location of caves; caves discussed in this paper are indicated by letters. c) Profile of Cayman Brac with elevation of the caves.
- 5.4 a) Bell hole depth and diameter were measured with graduated wooden dowels. The ceiling height was measured to a precision of one cm and was subtracted from the measured height, thus giving the bell hole depth. The diameter was measured with dowels of known length that varied, allowing diameter measurements between 5 and 150 cm to be measured, with a precision of five cm. b) Bell hole volume was calculated as a series of stacked cylinders.
- 5.5 Location of bell holes (and bell pits) in a) Skull Cave, b) Walk-In Cave, c) Rebecca's Cave, d) Cross Island Road Cave and e) Charlotte's Cave. Approximate location of well-lit, twilight and dark zones is indicated on each cave plan.
- 5.6 Basal diameter of bell holes in five caves on Cayman Brac versus their straight line distance from the cliff.
- 5.7 Cross sectional profiles of all sample bell holes. The horizontal check marks near

the apex of each bell hole indicate where the apex diameter was measured. Bell holes that formed compound bell holes could not be measured where they were joined to another bell hole and their lower limits are indicated with dotted lines to show the approximate shape.

- 5.8 Frequency distribution of a) depth, b) basal diameter, c) apex diameter and d) volume of bell holes in five caves on Cayman Brac. Note the distinct distribution of Charlotte's Cave when compared with the other four caves.
- 5.9 Apex diameter versus basal diameter of bell holes. The solid line indicates a one-to-one relationship between the two parameters.
- 5.10 a) Basal diameter and b) apex diameter versus depth of sample bell holes.
- 5.11 Taper angle versus depth of sample bell holes.
- 5.12 Volume versus basal diameter of sample bell holes in Charlotte's Cave; solid line is the line of best fit.
- 5.13 Bell pits and associated bell holes in Charlotte's Cave.
- 5.14 a) Relationship between bell hole diameter and bell pit length/width measurements.  
b) Relationship between bell hole and bell pit depth.
- 5.15 Proposed model of condensation corrosion in coastal caves on small holokarstic oceanic islands with young rocks (Tarhule-Lips and Ford 1998).
- 5.16 Frequency distribution of estimated time (not necessarily continuous) required for the development of bell holes.

### List of Tables

- 5.1 Bell hole sizes reported in the literature.
- 5.2 Maximum time required for bell hole development.

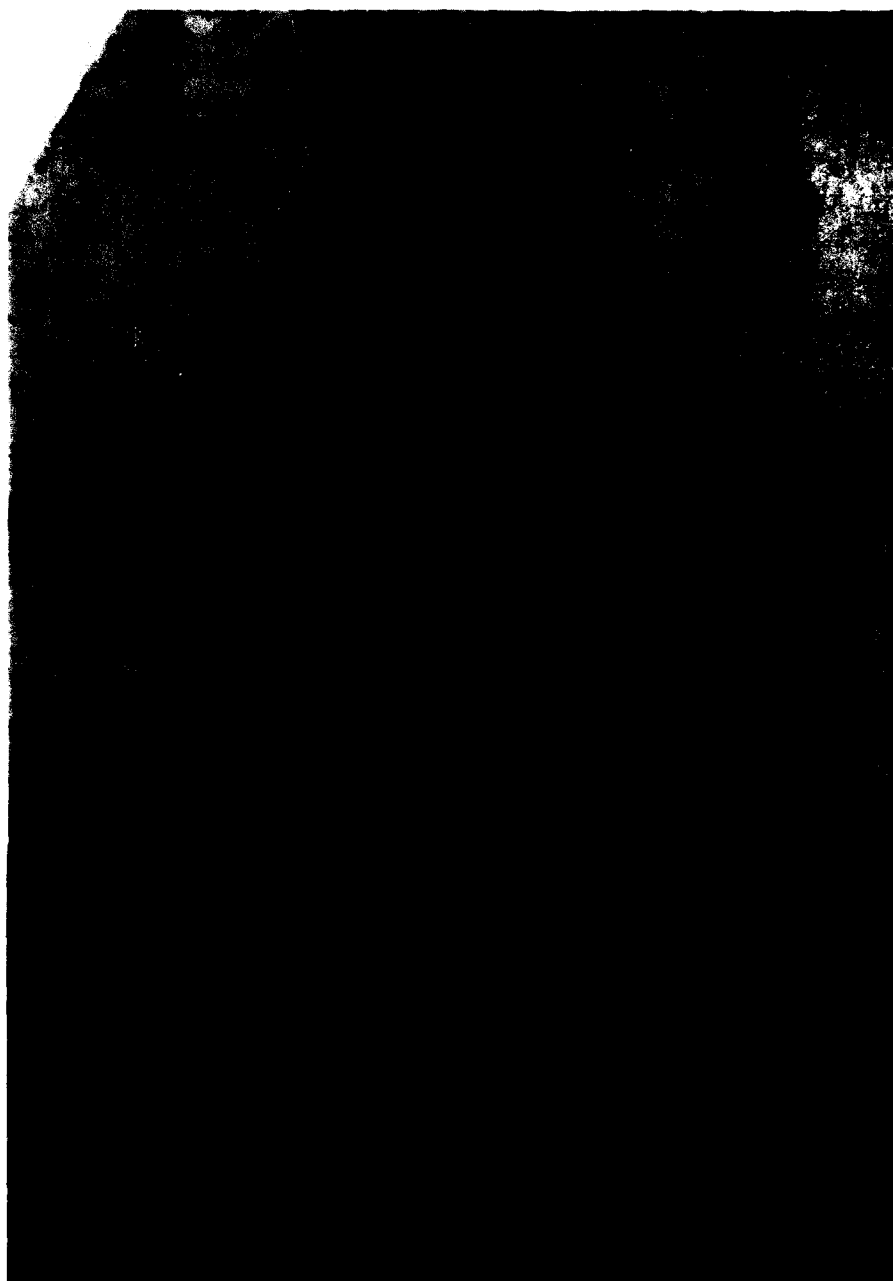
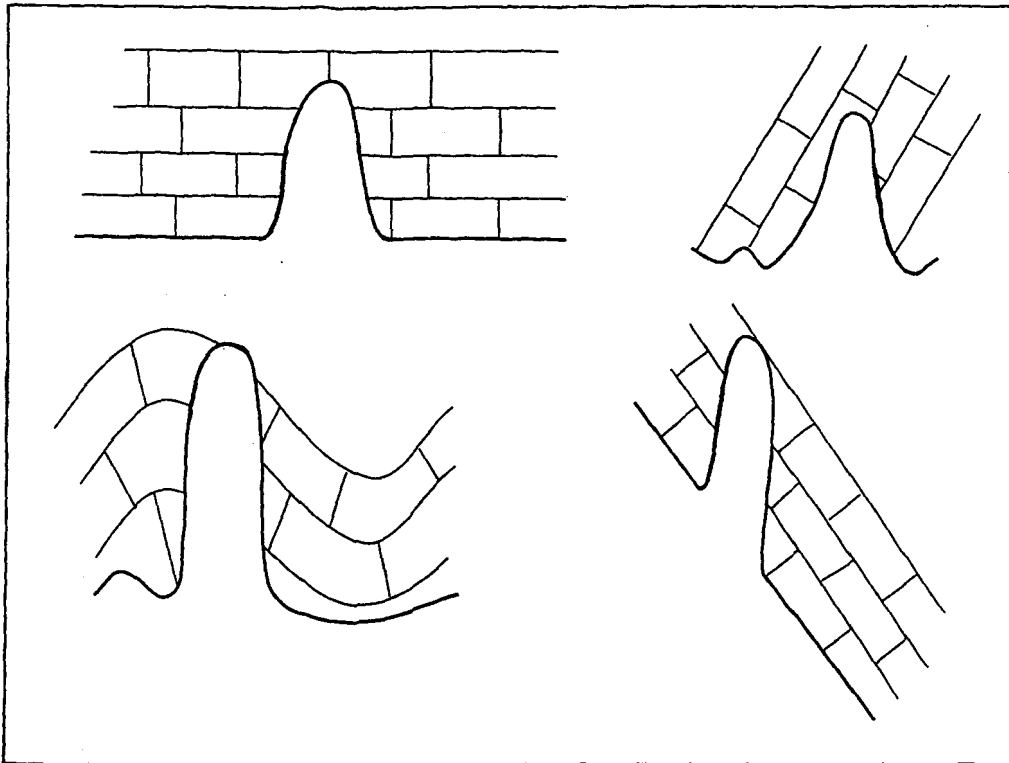
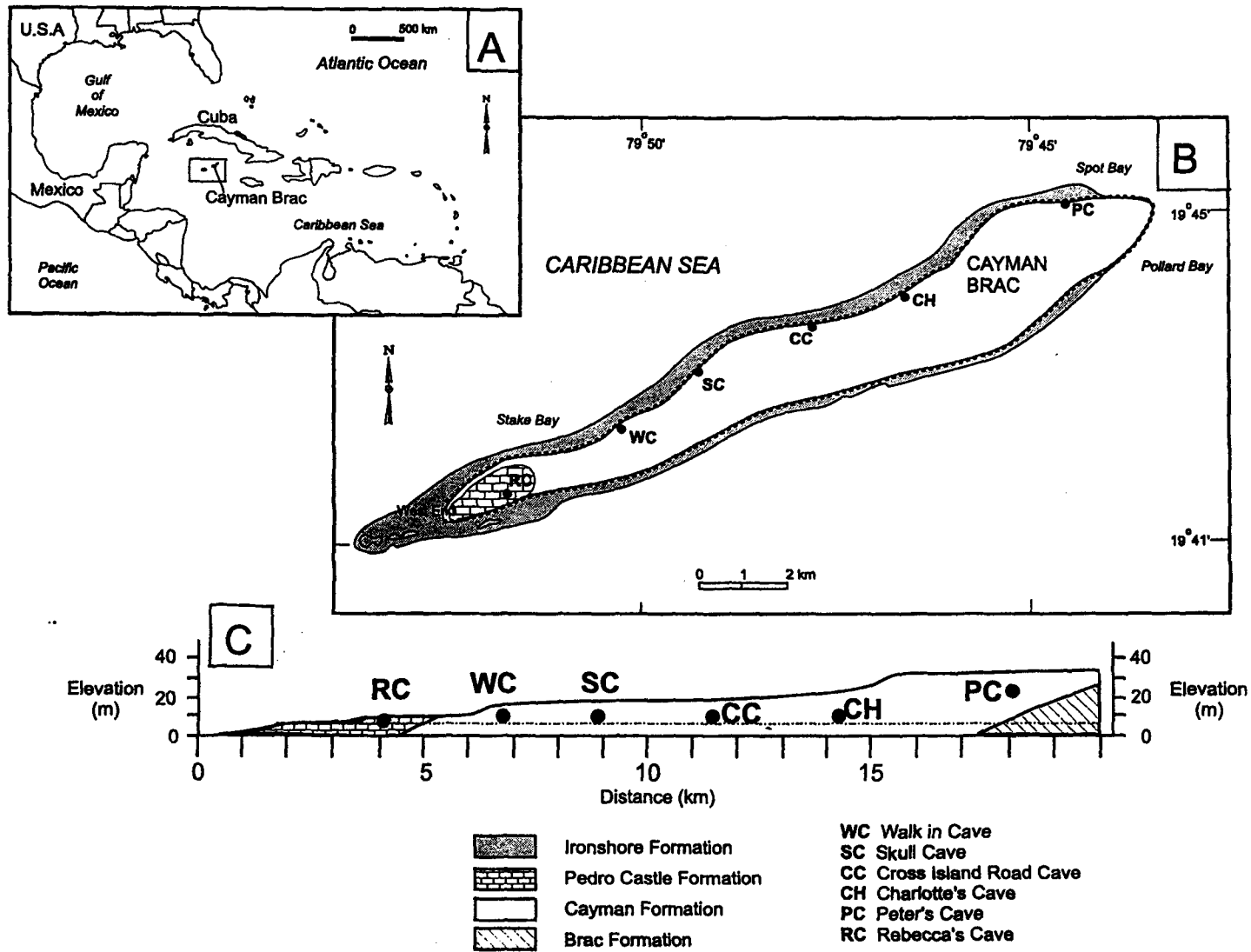


Fig. 5.1. Natural cross section through a bell hole as a result of ceiling collapse in Rebecca's Cave.



**Fig. 5.2** Schematic representation of bell holes. Note the strictly vertical long axis and the complete disregard for any bedrock controls such as stratal dip or for the ceiling geometry.



**Fig. 5.3** a) Location of Cayman Brac. b) Geology of Cayman Brac and location of caves; caves discussed in this paper are indicated by letters. c) Profile of Cayman Brac with elevation of the caves.

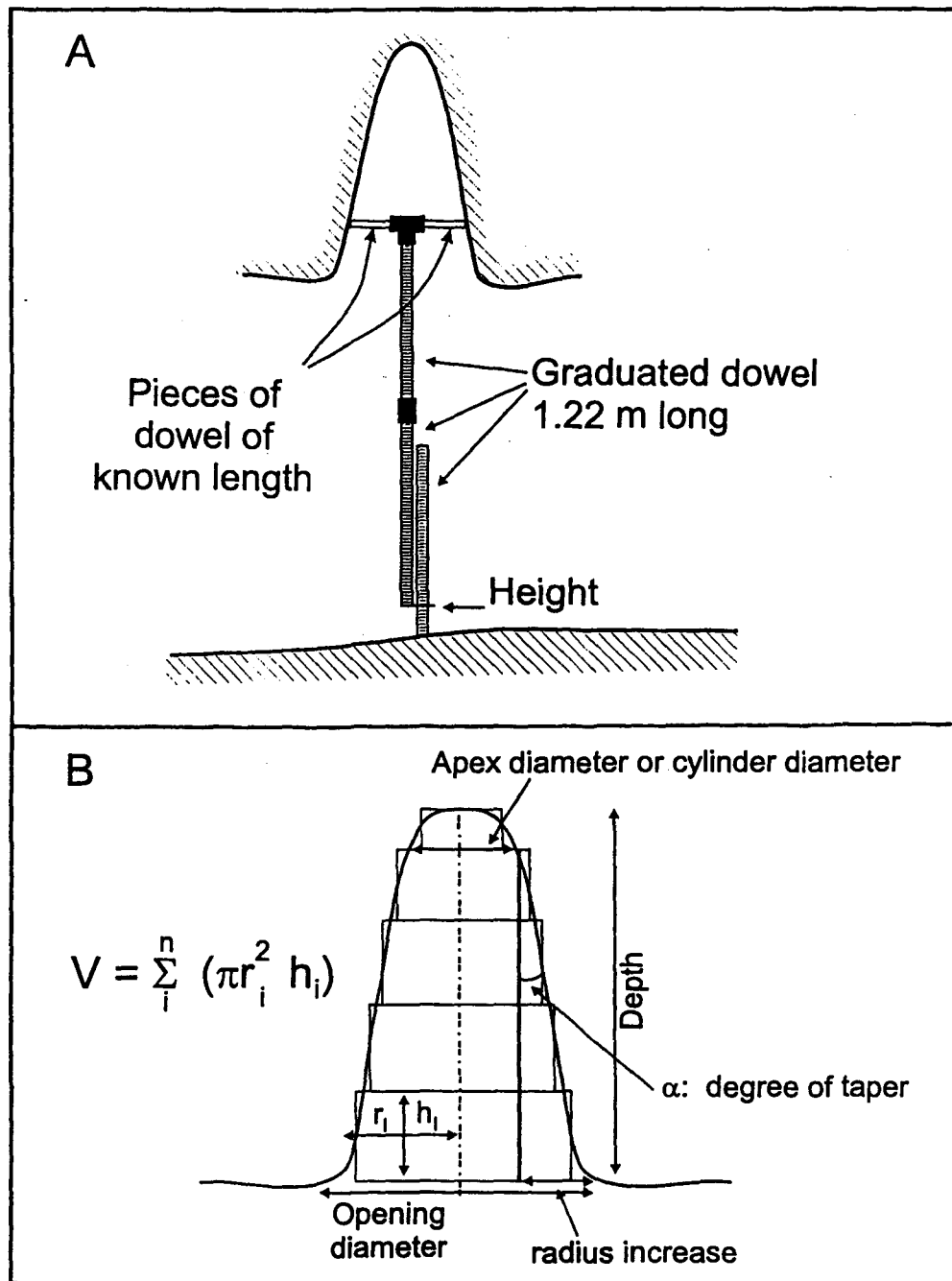
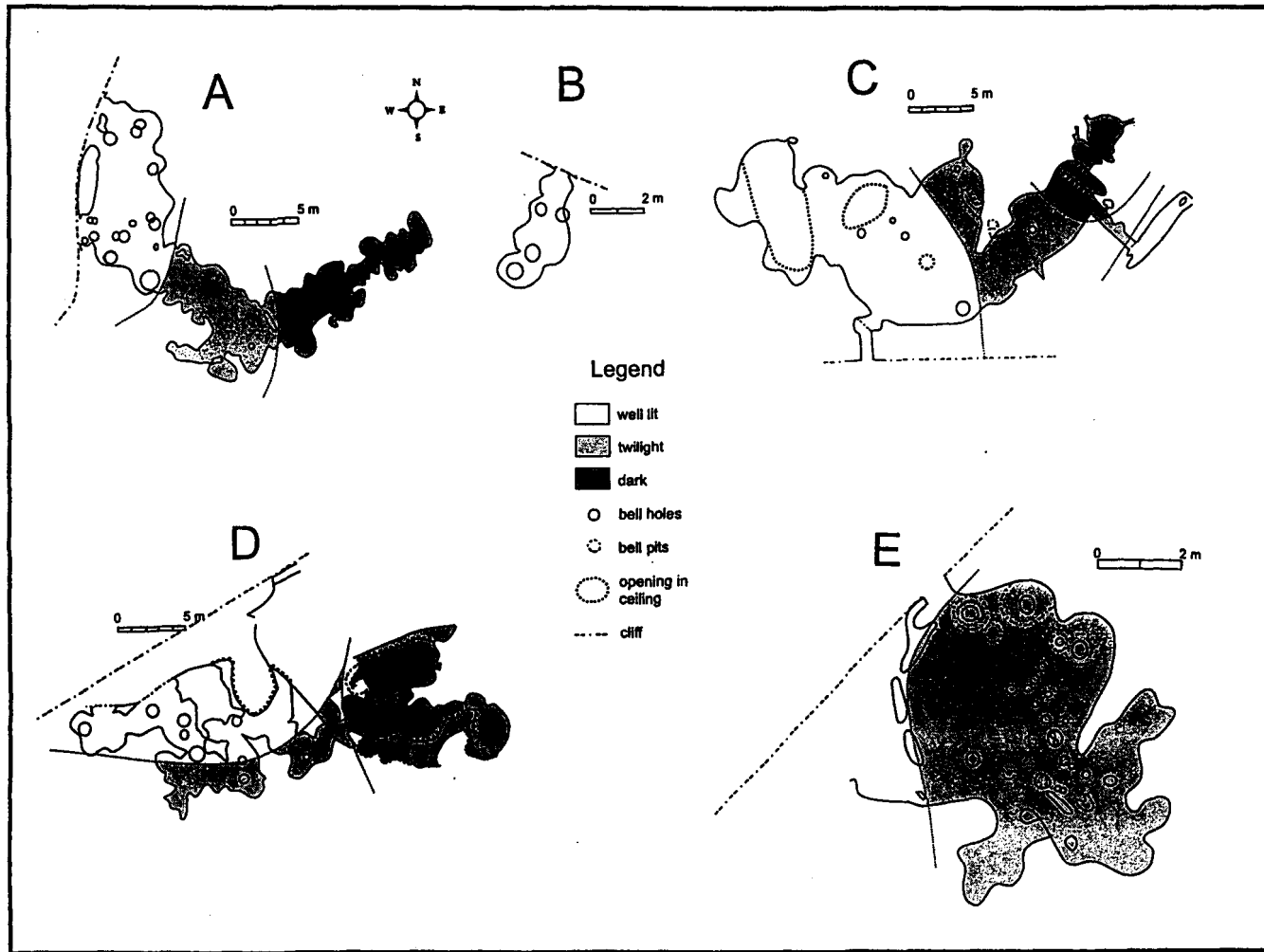


Fig. 5.4 a) Bell hole depth and diameter were measured with graduated wooden dowels. The ceiling height was measured to a precision of one cm and was subtracted from the measured height, thus giving the bell hole depth. The diameter was measured with dowels of known length that varied, allowing diameter measurements between 5 and 150 cm to be measured, with a precision of five cm. b) Bell hole volume was calculated as a series of stacked cylinders.



**Fig. 5.5** Location of bell holes (and bell pits) in **a) Skull Cave, b) Walk-In Cave, c) Rebecca's Cave, d) Cross Island Road Cave and e) Charlotte's Cave.** Approximate location of well-lit, twilight and dark zones is indicated on each cave plan.

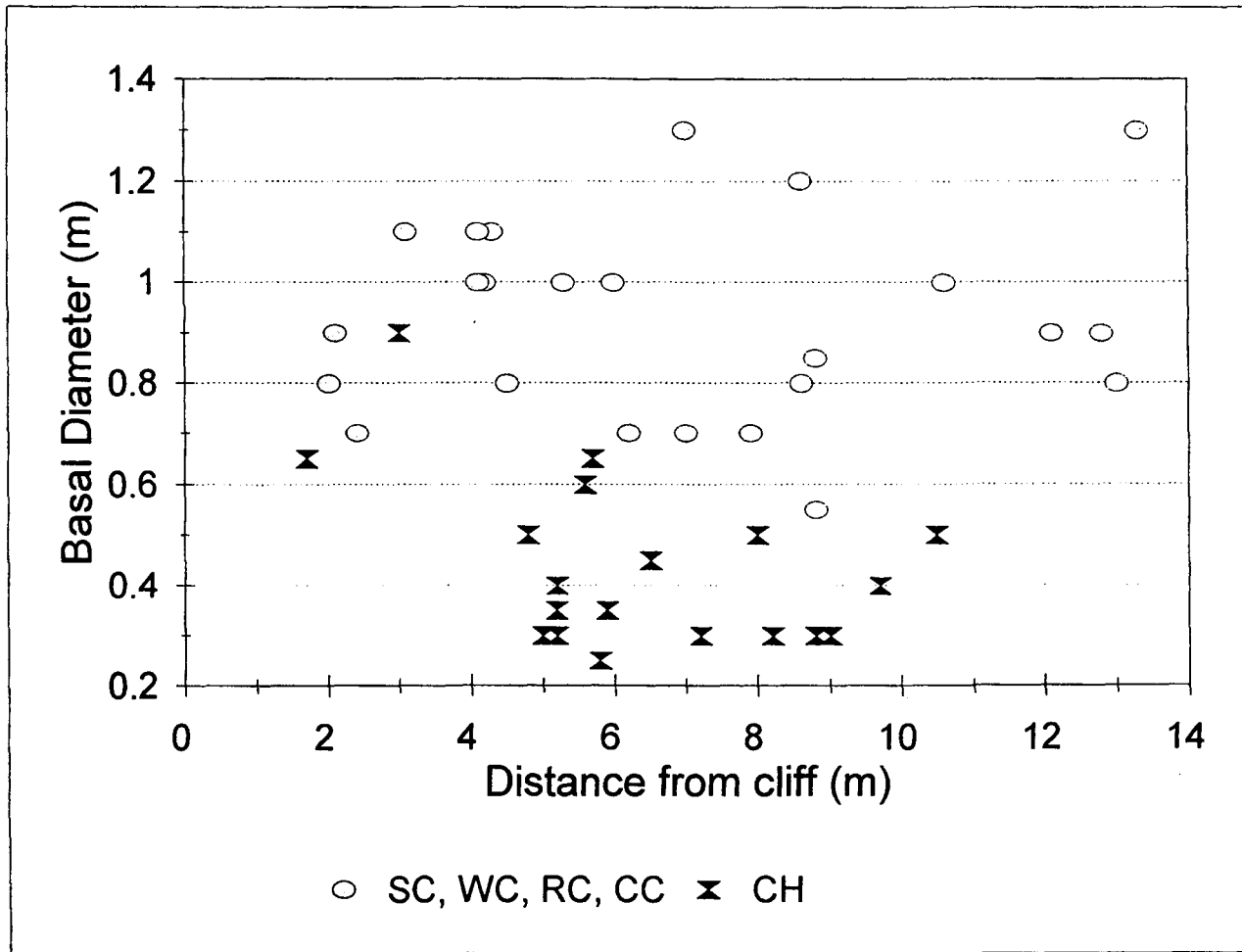
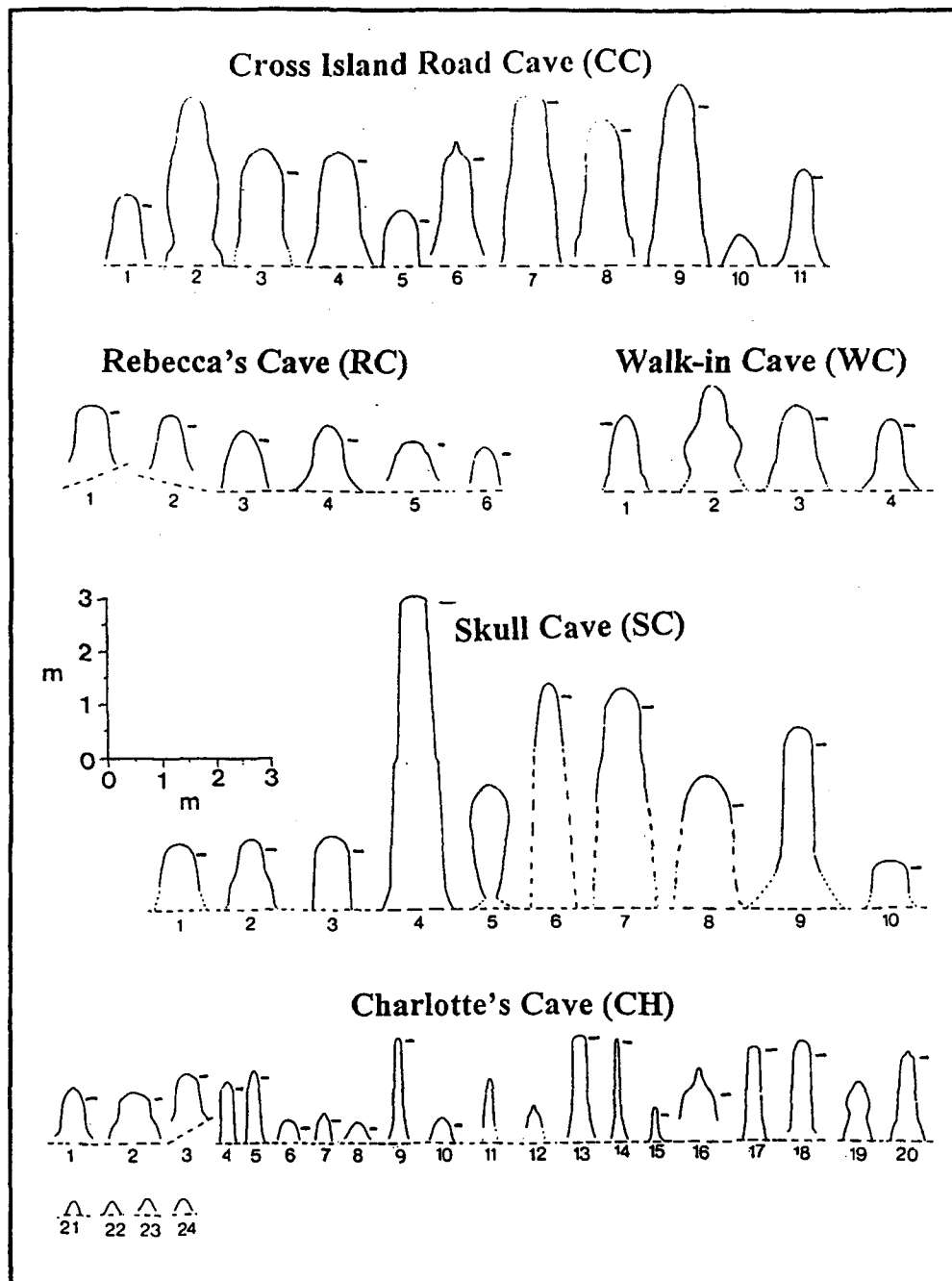
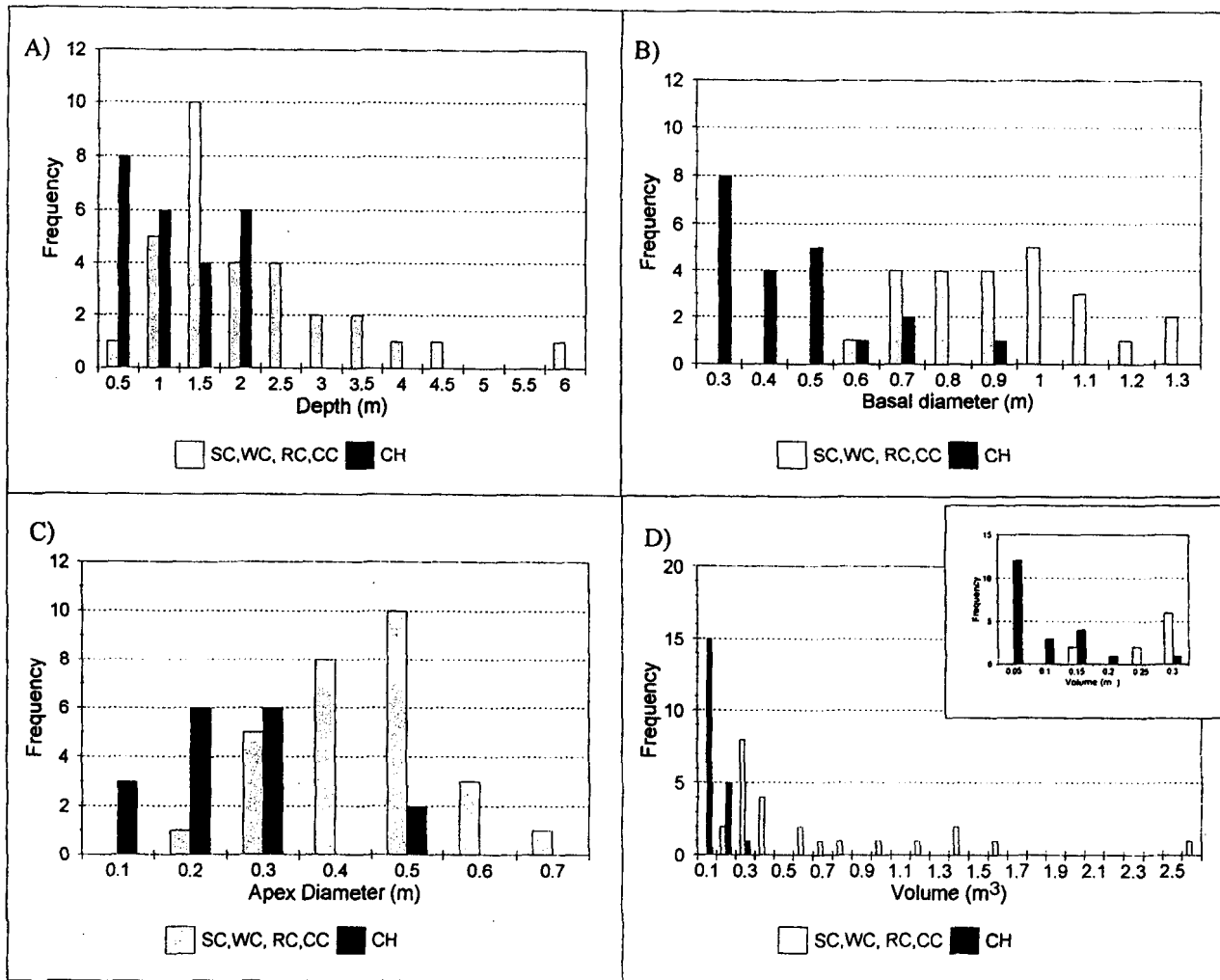


Fig. 5.6 Basal diameter of bell holes in five caves on Cayman Brac versus their straight line distance from the cliff.



**Fig. 5.7** Cross sectional profiles of all sample bell holes. The horizontal check marks near the apex of each bell hole indicate where the apex diameter was measured. Bell holes that formed compound bell holes could not be measured where they were joined to another bell hole and their lower limits are indicated with dotted lines to show the approximate shape.



**Fig. 5.8** Frequency distribution of a) depth, b) basal diameter, c) apex diameter and d) volume of bell holes in five caves on Cayman Brac. Note the distinct distribution of Charlotte's Cave when compared with the other four caves.

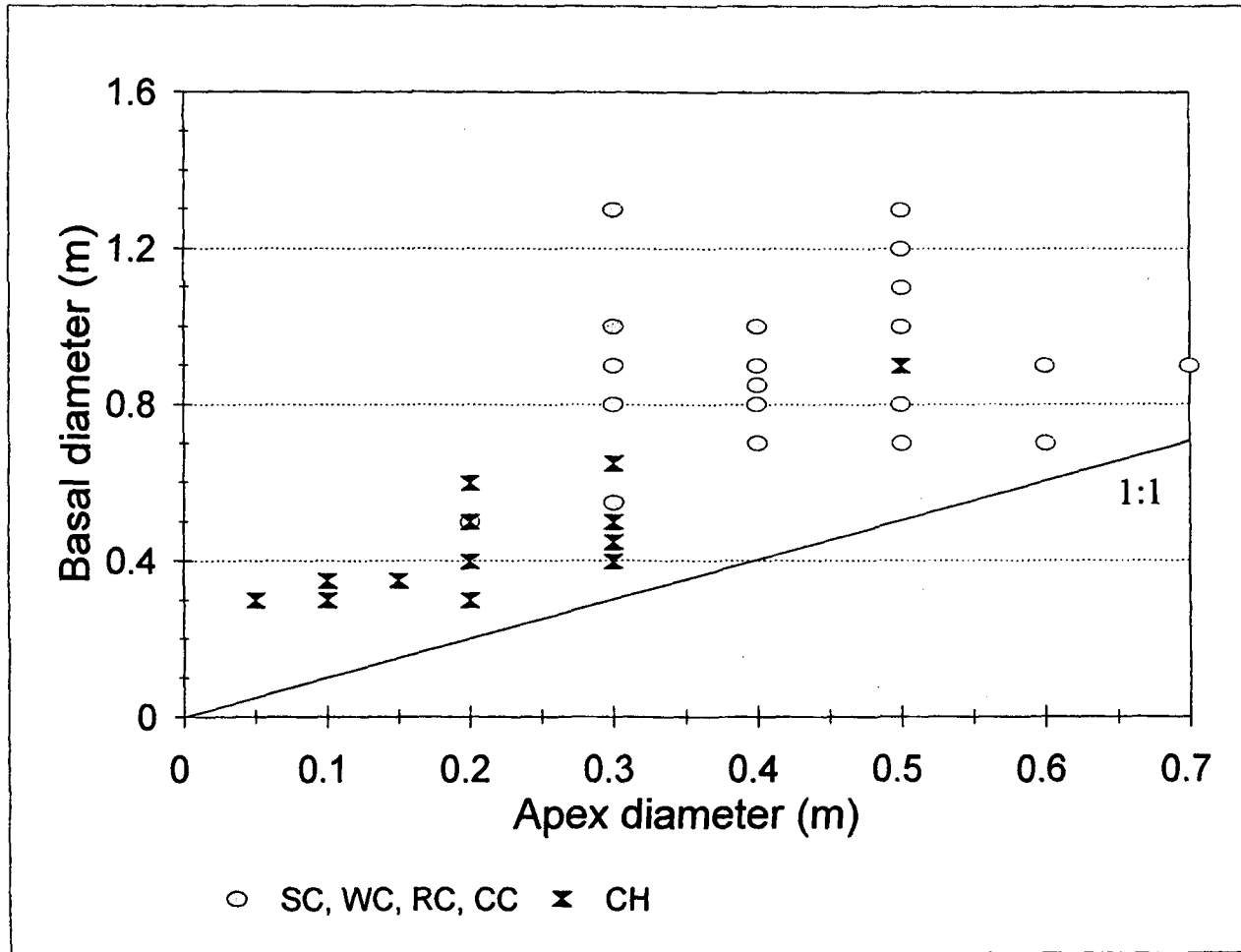


Fig. 5.9 Apex diameter versus basal diameter of bell holes. The solid line indicates a one-to-one relationship between the two parameters.

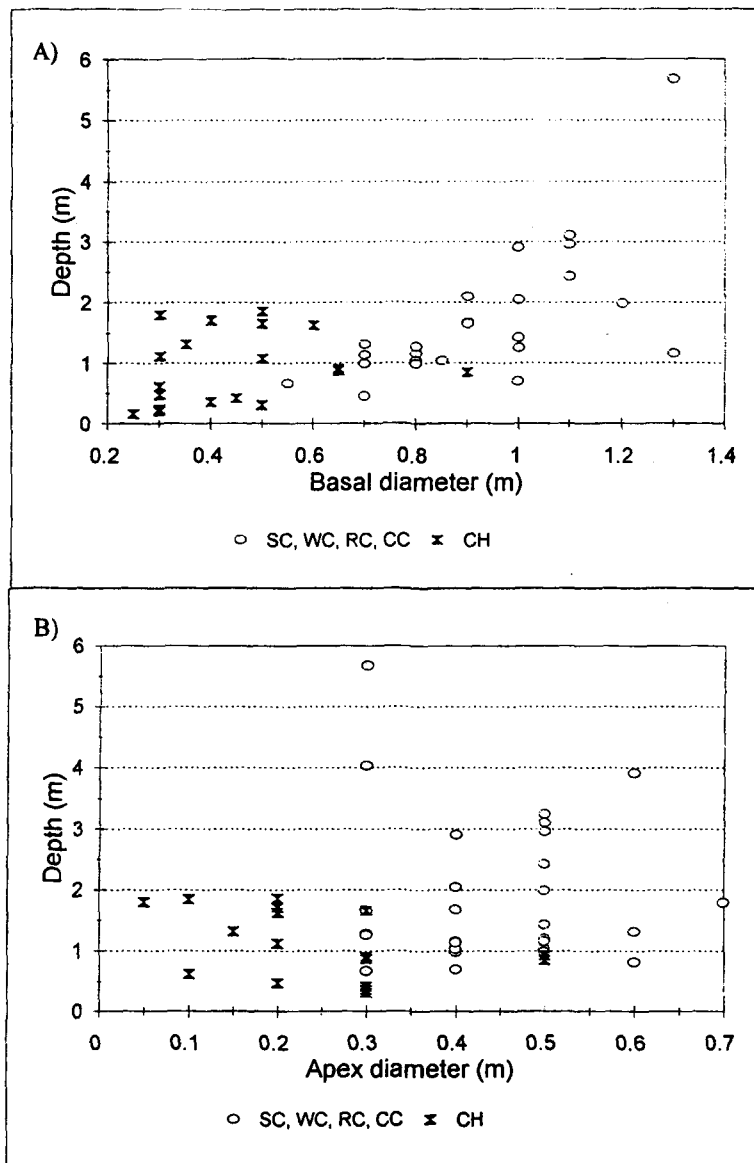


Fig. 5.10 a) Basal diameter and b) apex diameter versus depth of sample bell holes.

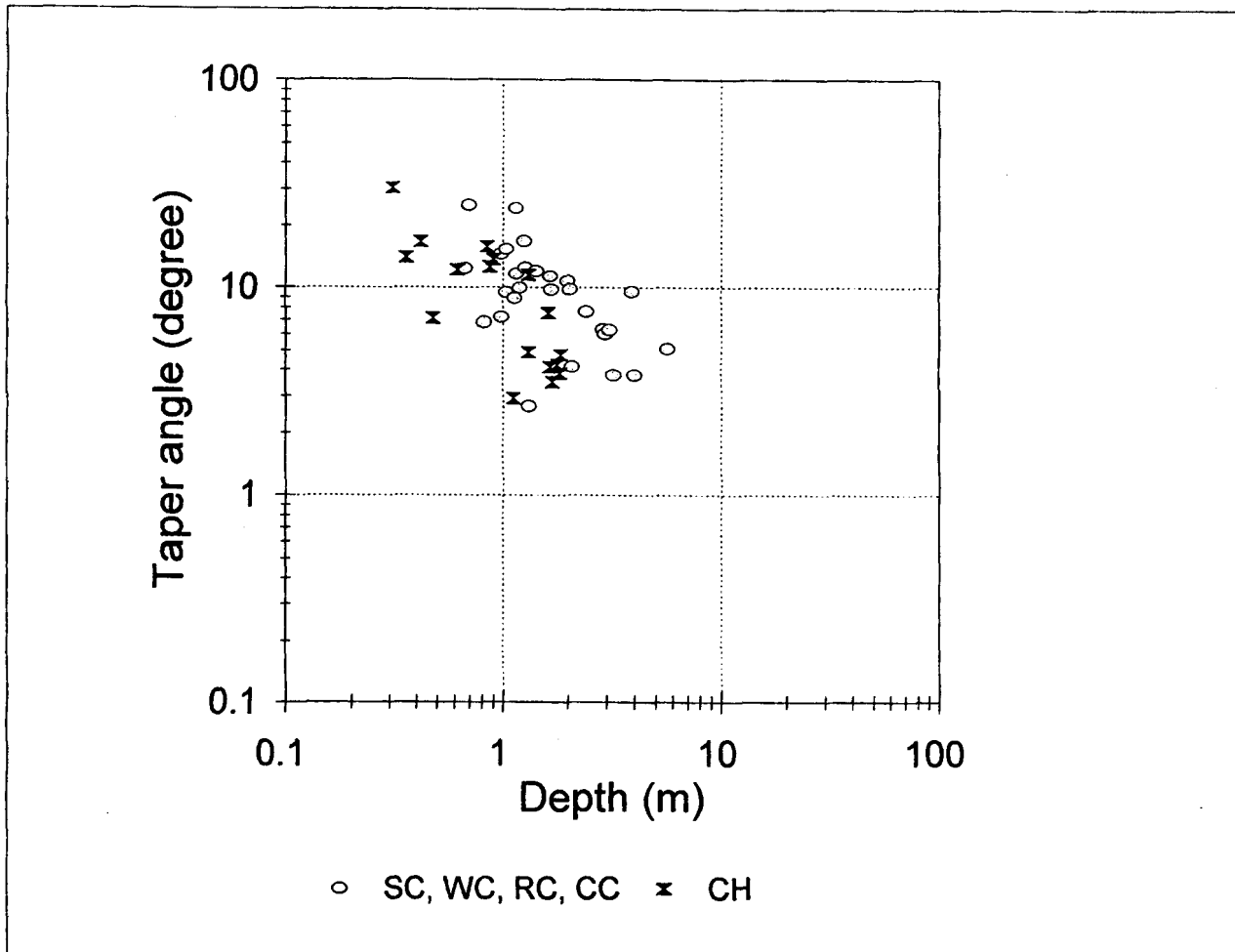


Fig. 5.11 Taper angle versus depth of sample bell holes.

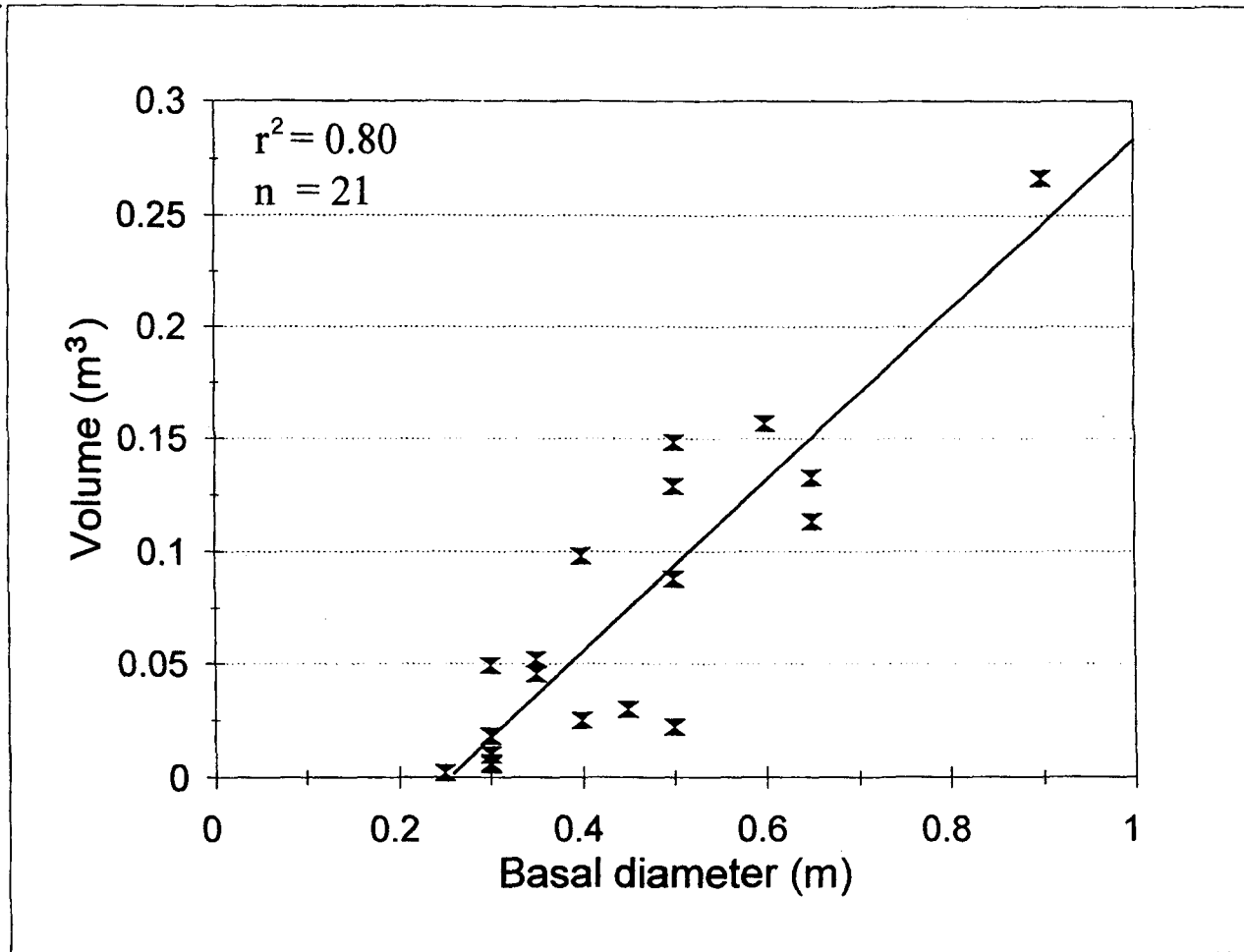


Fig. 5.12 Volume versus basal diameter of sample bell holes in Charlotte's Cave; solid line is the line of best fit.

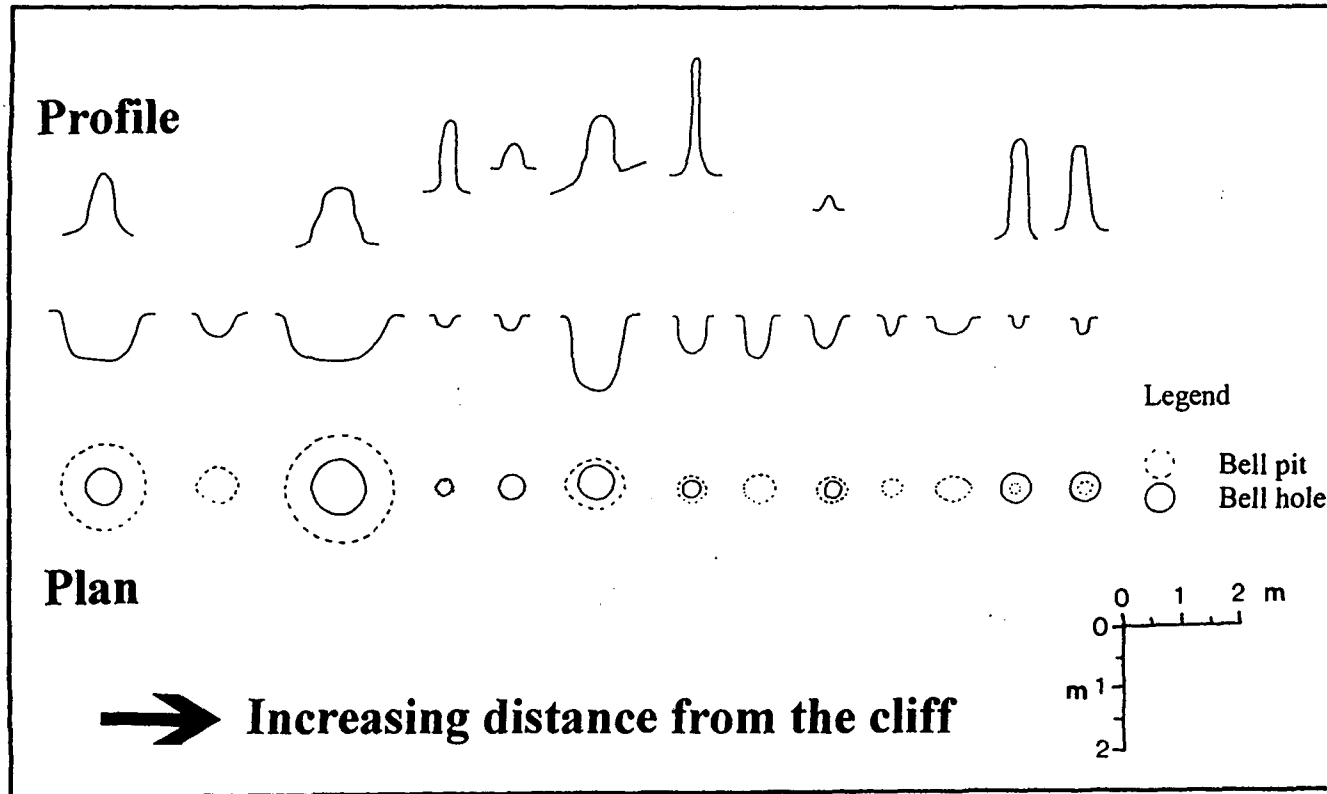


Fig. 5.13 Bell pits and associated bell holes in Charlotte's Cave.

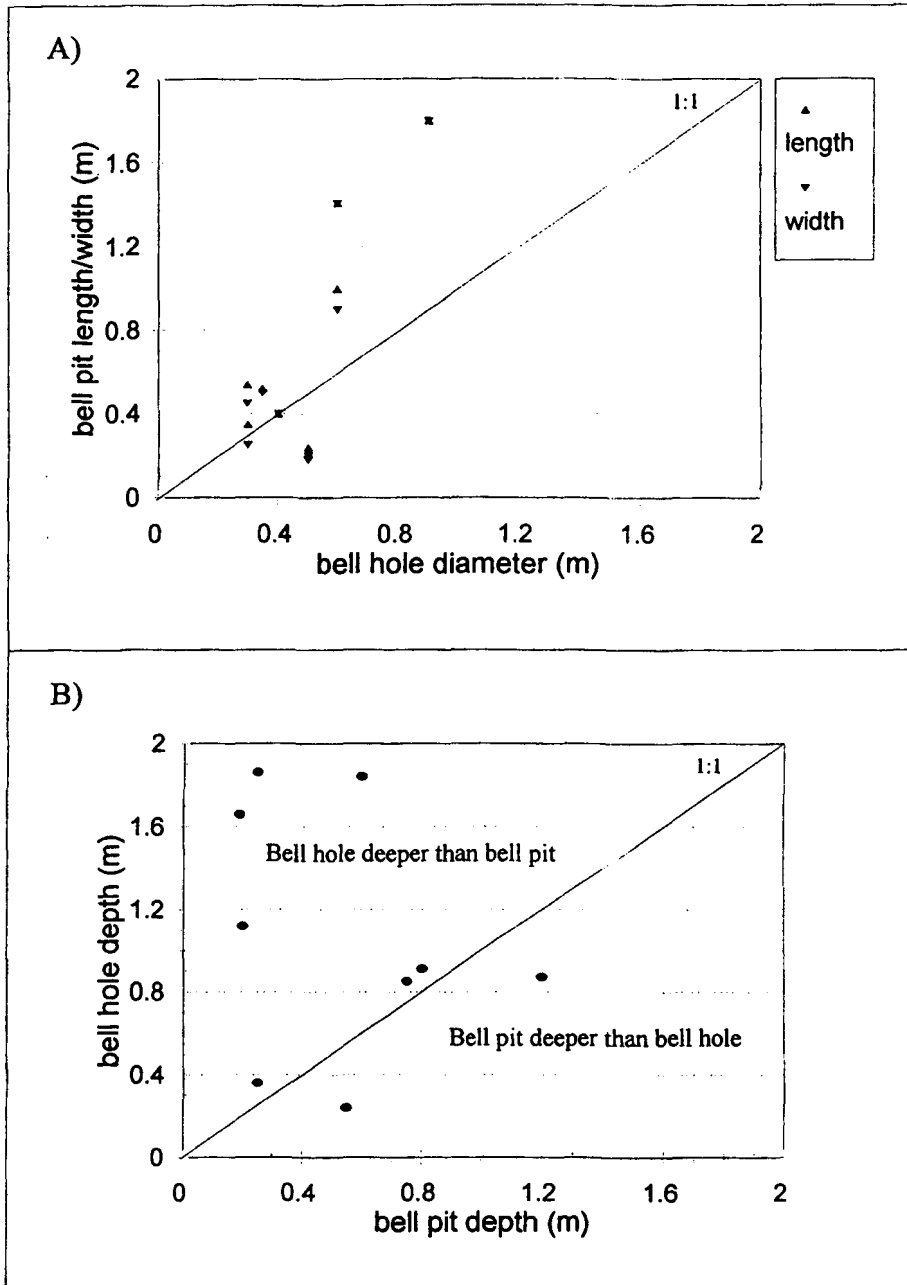


Fig. 5.14 a) Relationship between bell hole diameter and bell pit length/width measurements. b) Relationship between bell hole and bell pit depth.

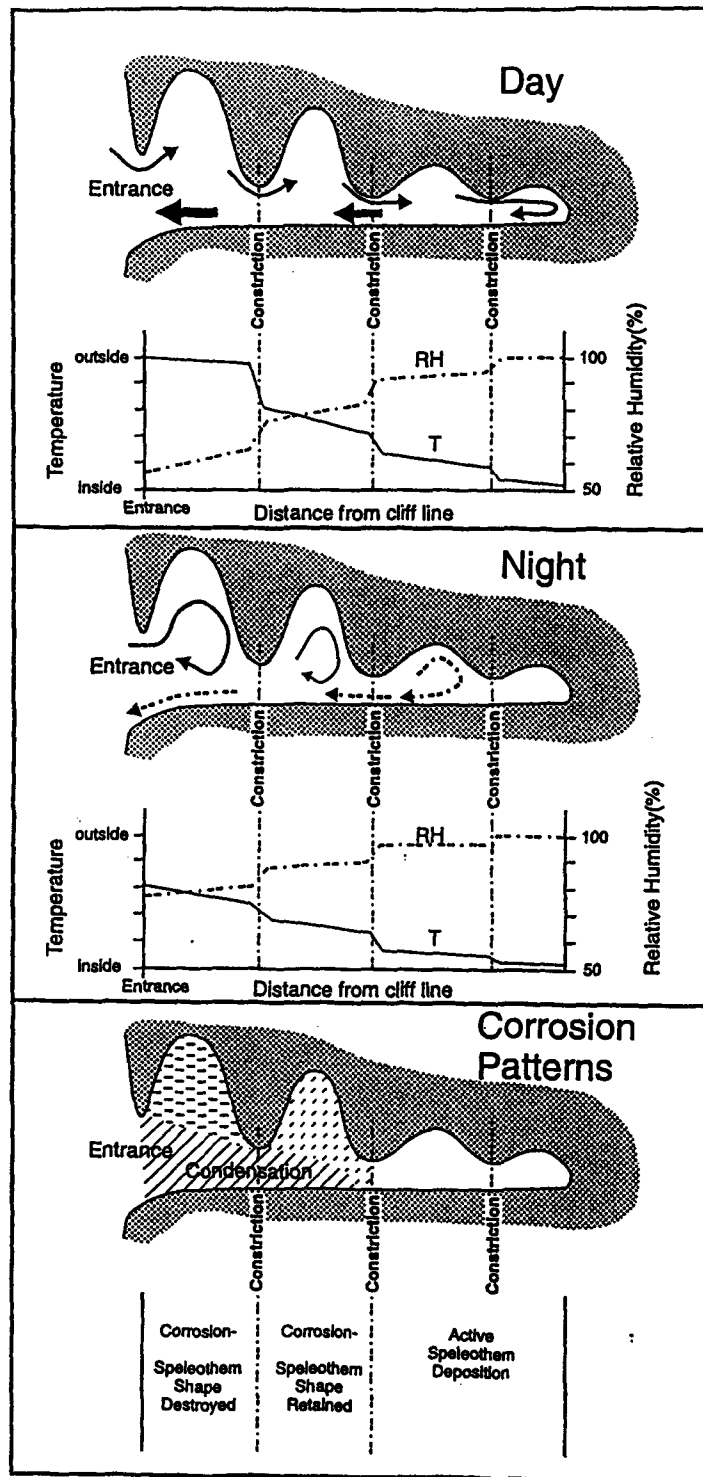


Fig. 5.15 Proposed model of condensation corrosion in coastal caves on small holokarstic oceanic islands with young rocks (Tarhule-Lips and Ford, 1998).

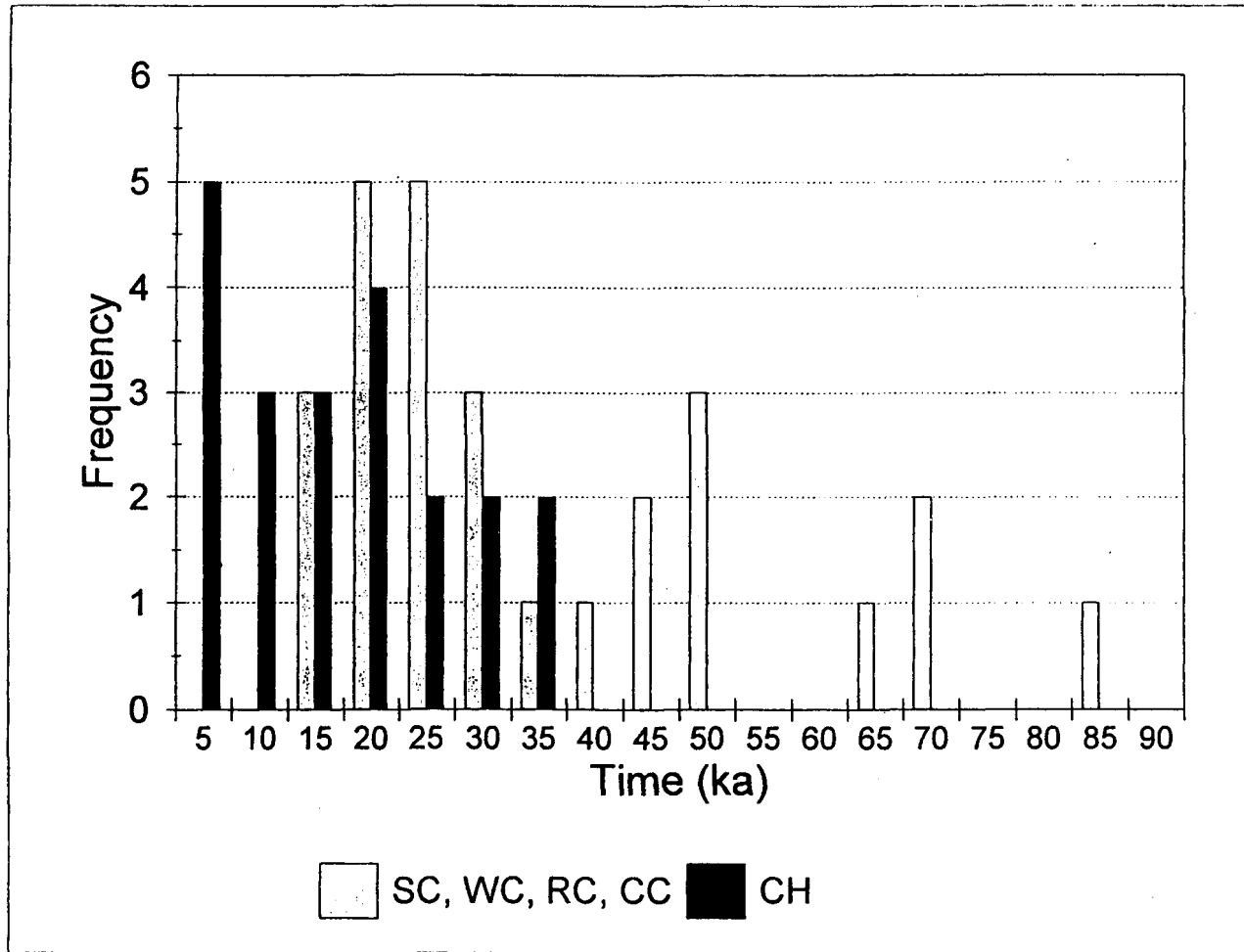


Fig. 5.16 Frequency distribution of estimated time (not necessarily continuous) required for the development of bell holes.

Table 5.1 Bell hole sizes reported in the literature.

Location	Author	Depth (m)	Diameter (m)
Trinidad	King-Webster and Kenny (1958)	0.91 - 1.82	0.45 - 0.76
Sarawak	Wilford (1966)	up to 1.82	0.15 - 0.76
Trobriand Islands	Ollier (1975)	-	up to 1
Belize	Miller (1981)	0.5 - 2	-
Bahamas	Lauritzen et al. (1997)	up to several meters	-
Isla de Mona	Dogwiler (1997, pers. comm.)	average: 0.31	average: 0.26
Cayman Brac	This study	0.17 - 5.68	0.25 - 1.30
	Lauritzen and Lundberg (in press)	typical: 0.40 - 0.80; but may be up to several meters	typical: 0.20 - 0.30
<i>ceiling pockets;</i> group 1: independent, without fissures	Slabe (1995)	small: 0.08 - 0.15 large: 0.15 - 0.75	0.08 - 0.15 0.30 - 1.50

Table 5.2 Maximum time required for bell hole development.

Cave	Bell Hole * (see Fig. 7)	Area (m <sup>2</sup> )	Volume (m <sup>3</sup> )	Time ** (ka)	
Skull Cave	1	0.38	0.20	22	
	2	0.50	0.30	25	
	3	0.38	0.39	42	
	4	1.33	2.55	80	
	5	0.38	0.45	48	
	10	0.38	0.15	16	
Walk-In Cave	1	0.50	0.28	23	
	2	0.64	0.64	42	
	3	0.79	0.52	28	
	4	0.79	0.31	16	
Rebecca's Cave	1	0.50	0.28	23	
	2	0.50	0.22	18	
	3	0.57	0.33	24	
	4	1.33	0.39	12	
	5	0.79	0.26	14	
	6	0.24	0.11	19	
Cross Island Road Cave	1	0.38	0.25	27	
	2	0.79	1.32	70	
	3	0.64	0.71	47	
	4	1.13	0.97	36	
	5	0.38	0.27	29	
	6	0.79	0.58	31	
	7	0.95	1.50	66	
	8	0.95	1.13	49	
	9	0.95	1.39	61	
	10	0.38	0.10	11	
	11	0.64	0.27	18	
Charlotte's Cave	1	0.33	0.11	14	
	2	0.64	0.27	17	
	3	0.33	0.13	17	
	4	0.07	0.05	29	
	5	0.10	0.05	23	
	6	0.13	0.03	8	
	7	0.07	0.02	11	
	8	0.20	0.02	5	
	9	0.10	0.05	20	
	10	0.16	0.03	8	
	13	0.20	0.13	27	
	14	0.07	0.02	11	
	15	0.07	0.01	6	
	17	0.13	0.10	33	
	18	0.20	0.15	31	
	19	0.20	0.09	19	
	20	0.28	0.16	23	
	21	0.05	0.00	2	
	22	0.07	0.01	3	
	23	0.07	0.01	3	
	24	0.07	0.01	4	
	<b>Maximum</b>		1.33	2.55	80
	<b>Minimum</b>		0.05	0.00	2
	<b>Average</b>		0.45	0.36	25

\* Compound bell holes for which the volume was estimated have been left out.

\*\* Time = V/(RR\*A), where RR = retreat rate = 24 mm/ka

# CHAPTER SIX

## Conclusions

### 6.1. *Major findings*

1. Karstification on Cayman Brac has occurred during periods of emergence extending from the Tertiary to the present. Today speleogenesis continues in the Pleistocene Ironshore Formation and in the submerged parts of the Tertiary Bluff Group.
2. Caves are found all over the island and at all elevations above sea level. Based on the latter, the caves were initially divided into two groups: Notch caves, located at or one - two metres above the Sangamon Notch (125 ka), and Upper caves, located at varying elevations more than two metres above the notch. This initial division can also be maintained when looking at morphology, age and speleothem abundance.
3. The morphology of the Notch caves accords to the flank margin model (Fig. 2.8): large entrance rooms along the cliffs with passages that end abruptly radiating towards the interior. The Upper caves on the other hand do not show such uniformity in their appearance. Their morphology is dominated by pre-existing

structures in the bedrock, such as vertical and horizontal fractures. They display three different patterns: (1) vertical joint type (e.g. First Cay Cave, Fig. 2.3; Northeast Cave 5); (2) low angle fissure type (e.g. Peter's Cave) and (3) flank margin type, not fracture-guided (e.g. Tibbetts Turn Cave, Fig. 2.9).

4. The Notch caves are much older than the marine Notch itself, which was formed during the last interglacial sea level high stand approximately 125 ka ago (Sangamonian or oxygen isotope stage 5e). Speleothem in two Notch caves were found to have grown well before the last interglacial, up to at least 350 ka. All Notch caves were likely formed at the same time, as indicated by their uniform elevation above the Notch and their comparable size and morphology. This formation took place during a relative sea level high stand 6 m above the notch, or 12 m above present sea level, at some period(s) between roughly 1400 and 400 ka.
5. The Upper caves are older than the Notch caves, and are believed to be late Tertiary to Early Quaternary in age. They most probably formed during several different speleogenetic episodes, as indicated by their varying elevations above the Notch.
6. Speleothem growth occurred when the caves were emerged. The Upper caves have a greater abundance of speleothem than the Notch caves, which is believed to result from the greater amount of time available for speleothem formation in these caves. Growth was discontinuous over time and growth hiatuses and periods of speleothem dissolution are observed in many speleothems. Today the majority of the speleothem have stopped growing and many are being dissolved.

7. The growth hiatuses were not found to be synchronous for all speleothem in all caves and do not appear to be related to the glacial-interglacial cyclic rhythm of the Quaternary.
8. Three types of speleothem dissolution have been identified in speleothem on Cayman Brac (Fig. 2.12):
  - i. Major - the speleothem has been extensively to largely eroded, such that its original depositional shape cannot be recognised. The deposits are preserved as remnants (mainly flowstone) within the curvilinear erosional facets in the walls or ceilings. They are often associated with breccia. In the facet, the transition between bedrock wall, speleothem and/or breccia is so smooth that it is not perceptible to the touch. The speleothem and/or breccia was seemingly attacked at the same time and rate as the bedrock in which it is located. There is no active growth of new calcite.
  - ii. Moderate - the dissolved speleothems still preserve their original shape but, on closer examination, have been reduced considerably in size. Dissolution has often taken place preferentially on one side of the speleothem but the dissolved faces are not necessarily congruous in the individual caves. Active growth has stopped.
  - iii. Minor - there is dissolution along selected faces or edges of the speleothems. The majority of them are still growing on all other parts of their surfaces today.

9. At present, growth cessation/dissolution is the result of changes in the microclimate of the cave in question rather than the general fluctuations of the regional climate. Although the past situation appears to be similar to the present, caution should be used in concluding that the present and past causes of speleothem dissolution/growth cessation are the same. If speleothems stopped growing in the past because of unfavourable microclimatic conditions inside the caves, then it would be unlikely they would restart growth at some later date because the inhibiting conditions (entrance zone and evaporitic) would still be unfavourable.
10. Effects of the growth hiatuses are also evident in the oxygen and carbon isotope records; values of the periods before and after a hiatus fall in statistically distinctly different groupings on a  $\delta^{13}\text{C}$  versus  $\delta^{18}\text{O}$  figure, indicating that the periods represent different microclimatic environments. If each hiatus represented a glacial period and the growth phases corresponded to interglacial periods (or *vice versa*), the isotopic values before and after that hiatus should indicate similar environments. This is clearly not the case, which supports the finding that periods of growth and growth cessation are independent of the glacial - interglacial cycling of the Quaternary.
11. Plotting the average values before and after hiatuses for all samples on one  $\delta^{13}\text{C}$  -  $\delta^{18}\text{O}$  figure establishes that they can be divided into two groupings that are statically significantly different from one another (t-test;  $\alpha = 0.01$ ; Fig. 3.15). These two groups can be characterized in terms of time, "young" (<120 ka) and "old" (>120

ka); or cave type, Notch and Upper caves; or location within the cave, entrance, mid-cave (RH > 80%; some diurnal temperature fluctuations) and deep cave (RH > 90%; stable temperature) location. The sample from Isla de Mona falls into the “young” group and displays the same characteristics: it was taken from a Notch cave at a mid-cave position and is less than 120 ka. At the mid-cave position evaporation will occur but the resulting kinetic effect is not sufficient to completely erase the climatic signal found in the isotopic records.

12. Modern calcite values for oxygen in the calcite were calculated from the drip water values and correspond with the speleothem values found during the previous interglacials and some glacials. This suggests that the climatic/environmental conditions have not changed considerably over time. They also show that there can be great inter-sample variation between different cave environments. It appears that a very thin roof and fast throughflow result in drip water oxygen compositions close to that of rain water and that evaporation also plays a role, though less than the throughflow effect in our case, resulting in higher  $\delta^{18}\text{O}$  values due to kinetic fractionation. Excluding the throughflow effect, there appears to be a decrease in the  $\delta^{18}\text{O}_w$  with increasing distance from the cliff and decreasing external climatic influence: -2.7 ‰VPDB at 3 m; about -3.8 ‰VPDB at 10 m and -5.1 ‰VPDB at 20 m. This distance/climatic influence effect is also reflected in the  $\delta^{18}\text{O}$  calculated for modern calcite (Table 3.3): -5.3, -6.5 and -7.6 ‰VPDB at 3, 10 and 20 m respectively.

13. The inter-sample variations calculated for modern calcite were more than 2 ‰. This helps to explain the great inter-sample variations found in the ancient speleothems, especially in the younger isotopic records. Supposing that the temperature and climatic conditions changed little in tropical marine regions over the Quaternary, the calculated modern day range of oxygen isotopic composition of calcite can be used as a basis for comparison with the speleothems.
14. The carbon records indicate that the climate over the period 450-120 ka has been relatively stable: tropical and wet, dominated by C<sub>3</sub> type plants. Since the last interglacial period the carbon record shows the same large fluctuations observed in the oxygen records which can be interpreted as changes between humid and desert like environments, dominated by C<sub>3</sub> or a combination of C<sub>4</sub> and CAM type plants respectively. However, such drastic change in climate has not been reported from other parts of the Caribbean and could be the result of more localised effects.
15. Based on measured present-day cave climates a model for condensation corrosion has been developed and is shown in Figure 4.12.
16. Calcite retreat rates due to condensation corrosion were determined with the aid of gypsum tablets and were estimated to be ~24 mm/ka. Theoretical rates calculated from the model by Buhmann and Dreybrodt (1985) were ~19 mm/ka. The close similarity between the measured and calculated values indicates that gypsum tablets can be used to estimate calcite retreat rates by condensation corrosion.
17. Condensation corrosion was also hypothesized to play a major role in the formation

of bell holes. These vertical cylinders in cave ceilings appear to have formed upwards and outwards in a subaerial environment. The outward expansion is slower than the upwards growth and appears to slow down when the bell holes becomes deeper. The dissolution by condensation corrosion appears to be aided by microbiological dissolution. Based on the calculated retreat rates for condensation corrosion, the deepest bell hole needed a maximum of 90 ka (not necessarily continuous) to form. The actual time of formation is likely much less because no account is taken of the microbiological activity.

## 6.2. *Future Research*

The thesis is composed of several different studies that approach the central theme from different angles and try to give an overview of the problem. Each individual study only scrapes the surface of its full potential and shows its usefulness and the need to explore it in more detail.

The stable isotope and dating study clearly reveals that climatic and environmental changes have taken place in the past 500 ka on Cayman Brac and that some of these are also visible on Isla de Mona. Especially the apparent climatic change around 120 ka needs further attention. Sampling of young samples from deep cave locations inside Upper caves, better dating of the existing young samples and more detailed isotope sampling are required.

To better understand the past, it is necessary to have a complete understanding of the present. Microclimatic investigations of more caves and of longer duration are needed

to do this and to verify the validity of the model of condensation corrosion proposed in Figure 4.12.

Concerning the intriguing ceiling morphologies called bell holes, rock samples and more detailed microclimatic analyses inside the bell holes are needed to verify the proposed mode of formation: a combination of condensation corrosion and microbiological activity.

As noted, it is necessary to address a problem from many different angles to obtain a more complete picture and to better study its general influence in caves on other oceanic islands in the Caribbean. This study is meant to give a first look at the role of subaerial dissolution in the speleogenesis of caves on small oceanic islands. It clearly shows that subaerial dissolution has occurred at different times in the past and is occurring at present. Further research should focus on the details and the many questions that this study has raised.